Some studies of magnetohydrodynamic oscillations of a rotating fluid

Khurana, K.K.

SOME STUDIES OF MAGNETOHYDRODYNAMIC OSCILLATIONS OF A ROTATING FLUID

by

K.K. Khurana

A thesis submitted for the degree of
Doctor of Philosophy at the University of Durham

Graduate Society

September, 1984

ABSTRACT

Some theoretical studies on the propagation of Rossby-MHD waves in homogeneous media and the reflection of Rossby-MHD and inertial-MHD waves at rigid boundaries are presented.

The evolution of an initial Rossby-MHD disturbance on a beta-plane is studied by the method of stationary phase in two dimensions. For positive β, long wavelength magnetic modes of this wave travel eastwards and propagate in a triangular region of the beta-plane. To an observer moving with the group velocity of a particular wave, its amplitude appears to diminish with time t as a function of t^{-1}.

The reflection of a Rossby-MHD wave by a conducting or insulating rigid boundary generates two reflected modes, one of which may be a non-propagating wave. The wavenumbers, group velocities, magnetic/kinetic energy ratios and energy densities of the incident and reflected waves are, in general, different. For waves of planetary dimensions, an eastwards travelling magnetic mode, on reflection from a N-S boundary, is transformed entirely into a long wavelength inertial mode and a large conversion of magnetic energy into kinetic energy is observed.

An inertial-MHD wave on reflection from a conducting or an insulating rigid boundary splits up into three reflected modes one of which is always a travelling magnetic mode. The wavenumbers, group velocities, magnetic to kinetic energy ratios and energy densities of the incident and reflected waves are not equal. Although, the reflection of any of these modes always generates a reflected magnetic mode, no travelling inertial modes may be generated for certain orientations of the boundary. In the long term this phenomenon will increase the share of the energy of the magnetic modes at the expense of the inertial modes.

PREFACE

Ever since 1954, when Lehnert recognised that rotation could split magnetohydrodynamic waves into fast and slow modes which possess unequal shares of kinetic and magnetic energies, a steady interest in the properties of these waves in rotating fluids has been evident in the literature. These waves are now frequently invoked in the dynamo models of the generation of planetary and stellar magnetic fields, and are suspected to cause the secular variations in the earth's magnetic field. This thesis is concerned with the long term propagation in homogeneous media and reflection at rigid boundaries of two classes of these waves, namely, the inertial-magnetohydrodynamic (IMHD) waves in infinite media and Rossby-magnetohydrodynamic waves which are associated with certain bounded media.

As the subject of MHD waves in rotating fluids is a relatively new branch of fluid dynamics, no systematic account of the generation, propagation, reflection and transmission of these waves in homogeneous and inhomogeneous media exists in the literature. Chapters 1 and 2 are meant to fill this lacuna and provide a general background to our work.

Rossby-magnetohydrodynamic waves were first introduced by Raymond Hide in 1966 to explain certain features of the secular variations of the geomagnetic field. In Chapter 3 we study the temporal and spatial evolution of an initial superposition of these waves by the method of stationary phase. By the help of analytical solutions and their numerical evaluation, a complete picture of the propagation of a Rossby-MHD wave packet on a beta-

plane is built. How such a disturbance in the toroidal magnetic field of a fluid body may influence its poloidal magnetic field is also discussed.

We revisit these two-dimensional Rossby-MHD waves in Chapter 4, where their reflection by rigid conducting and insulating boundaries is investigated. The wave equation and consequently the dispersion relation of these waves are of the fourth order in their independant variables, so no analytical or geometrical derivations of the characterstics of the reflected waves are possible. Instead a numerical approach is adopted to reveal the properties of the reflected waves. Proper boundary conditions to solve this problem are formulated in this Chapter and Appendix I. A novel finding of this analysis is that a magnetic mode can be partially or completely transformed into an inertial mode or vice-versa on reflection.

The experience gained from this Chapter is utilised in Chapter 5 in studying an even more complicated situation, namely, the reflection of three-dimensional inertial-MHD waves by conducting and insulating rigid boundaries. Once again because of the complexity of the governing equations, the approach is mainly numerical. It is shown that up to three reflected waves are generated which require three complex boundary conditions to solve the problem. Transformation of kinetic energy into magnetic energy and vice-versa is noted again, as in Chapter 4, for these waves, as well as the fact that multiple reflections of these waves may have the effect of increasing the share of the energy of magnetic modes at the expense of the inertial modes.

A summary of the present work and a few concluding remarks appear in chapter 6. Appendices I to III elaborate on some of the points made in chapters 3, 4 and 5. Appendix IV lists all the symbols used in this thesis. Copies of all the computer programs used in this thesis have been lodged with the Dept. of Geological Sciences and are available on request.

The work described in this thesis is guided by the central concept of a wave packet (also known as wave group), which travels at the group velocity of its constituent waves and carries the wave energy with it, whose theory for dispersive anisotropic waves, was so brilliantly formulated by M. J. Lighthill and G. B. Whitham in the late fifties and early sixties. The practical applications of our results to the earth's core-like fluid bodies are described in the relevant sections.

I would like to express my sense of deep gratitude to Professor M.H.P. Bott for constant encouragement and careful supervision of this work. I am very grateful to Dr. Raymond Hide (Meteorological Office, Bracknell) who was instrumental in shaping many of the ideas presented in this work. I have benefitted immensely from my frequent visits to his office for discussions on various aspects of this work, and from the use of his library which must be one of the finest collections of literature on Geophysical Fluid Dynamics in the land. Finally, I would like to thank my wife, Amber Khurana, for help in the typing and proof-reading of this thesis. During the tenure of this work, I was supported by a Commonwealth Universities' Scholarship.

CONTENTS

LIST OF FIGURES

CHAPTER ONE

SOME MAGNETOHYDRODYNAMIC WAVE SOLUTIONS AND THEIR SIGNIFICANCE TO THE EARTH'S MAGNETIC FIELD

1.1 BASIC EQUATIONS The dynamics of a conducting fluid permeated by a magnetic field is governed by the ordinary electromagnetic and hydrodynamic equations suitably modified to take into account the interaction between the fluid motion and the magnetic field. As one is dealing with fluid velocities it is necessary to define a frame of reference with respect to which the velocities are measured. With rotating fluid bodies like the Earth's core it is customary to choose a reference frame rotating with the body. For such a non-inertial frame Newton's law of motion applies only if we add two additional fictitious forces, namely the centrifugal and coriolis forces. Then the equation of motion of a volume element of fluid of density ρ moving with velocity $\bar{u}$ measured relative to a frame that rotates with instantaneous angular velocity $\bar{\Omega}$ is given by(Acheson and Hide,1973, Roberts,1967)

$$\rho\left(\frac{\partial \bar{u}}{\partial t} + (\bar{u}\cdot\nabla)\bar{u} + 2\bar{\Omega}\times\bar{u}\right) = -\nabla p' + \bar{J}\times\bar{B} + \bar{f} + \nu\nabla^2\bar{u} + \rho\,\bar{r}\times\frac{d\bar{\Omega}}{dt} \qquad \ldots(1.1)$$

Here the third term on LHS is the coriolis force. p is the non-hydrostatic pressure given by

$$\nabla p' = \nabla p - \rho\bar{g} \qquad \ldots(1.2)$$

where $\bar{g}$ is the acceleration due to gravity (which includes the

centrifugal term $-0.5|\bar{\Omega} \times \bar{r}|$, $\bar{r}$ being the distance vector from the origin to the fluid element. $\bar{J} \times \bar{B}$ represents the Lorentz force per unit volume where $\bar{J}$ and $\bar{B}$ are the electric current density and magnetic field. $\bar{f}$ describes any other forces such as buoyancy forces. The fourth term on RHS represents viscous forces arising from shear motion in the fluid where ν is the kinematic viscosity. The last term on RHS vanishes when $\bar{\Omega}$ is steady.

The equation of continuity is given by

$$\partial \rho / \partial t + (\bar{u} \cdot \nabla) \rho = - \rho \nabla \cdot \bar{u} \qquad \ldots(1.3)$$

The Maxwell's equations when the displacement current $\partial \bar{D} / \partial t$, is much smaller than the conduction current $\bar{J}$ are written as

$$\nabla \times \bar{B} = \mu \bar{J} \qquad \ldots(1.4)$$

$$\nabla \times \bar{E} = - \partial \bar{B} / \partial t \qquad \ldots(1.5)$$

$$\nabla \cdot \bar{B} = 0 \qquad \ldots(1.6)$$

$$\nabla \cdot \bar{D} = \phi \qquad \ldots(1.7)$$

where $D = \epsilon E$, ϕ is the electric charge density and μ & ϵ denote magnetic permeability and dielectric constant of the medium.

Equations (1.4) and (1.5) are Ampere's and Faraday's laws respectively. Equation (1.6) expresses the fact that the magnetic field is solenoidal whereas equation (1.7) relates the electric field to the volume density of electric charge, ϕ . The Maxwell's equations have been written here in their non-relativistic form as $\bar{\Omega} \times \bar{r} + \bar{u}$ is always much less than the velocity of light in

magnetohydrodynamics. Any electric charge moving with velocity $\bar{u}$ relative to a magnetic field $\bar{B}$ experiences a force $\bar{u}\times\bar{B}$ in addition to the electric field $\bar{E}$. Thus, if the conducting fluid satisfies Ohm's law, then

$$\bar{J} = \sigma (\bar{E} + \bar{u} \times \bar{B}) \qquad \ldots(1.8)$$

where σ is the conductivity of the fluid.

In magnetohydrodynamics, the electric part of the body force (which is of the order of $\epsilon_o E^2/d$ or $\epsilon_o B^2 u^2/d$, where d is a typical length scale of the system) is much smaller than the magnetic part (which is of the order of $B^2/\mu d$ and is thus c^2/u^2 times the electric part, where c is the velocity of light) and consequently the exact value of net charge distribution is of no concern to us. As a result equation (1.7) becomes redundant. Equations (1.1) to (1.6) then reduce to 14 scalar equations but involve 18 unknowns and thus need to be supplemented by more mathematical relations. These are provided by thermodynamic considerations. For example, a typical compressible fluid follows the perfect gas law: $p/(\rho T)$ = constant, where T is the temperature of the fluid. Now we can visualise two extreme situations to which the fluid may be subjected. One is the isentropic case, in which changes of the fluid state are so rapid that transport of heat can be altogether neglected and we can assume that the entropy per unit mass = $C_v \ln(p\rho^{-\gamma})$, (where C_v and C_p are the specific heat of the fluid at constant volume and pressure respectively and $\gamma = C_p/C_v$) remains constant.

Incompressible fluids can be further classified into

barotropic and baroclinic fluids. Barotropic incompressible fluids have uniform density and can not be subjected to a torque from the gravitational contribution to $\bar{f}$ in (1.1). Baroclinic fluids have non-uniform density and as a result of gravity tend to be stratified which gives rise to buoyancy forces. These forces exert a net torque on the fluid and it is not possible to maintain a hydrostatic equilibrium in their presence. Therefore baroclinic fluids can have hydrodynamic flow as a result of variations inside the fluid of temperature or chemical composition, whereas, to generate hydrodynamic flow in a barotropic fluid force will have to be applied at the bounding surfaces of the fluid.

In this work we will be dealing mainly with incompressible fluids, so that (1.2) reduces to

$$\nabla \cdot \bar{u} = 0 \qquad \ldots(1.9)$$

Equations (1.4),(1.5) and (1.8) can be combined into a single electrodynamic equation as follows. Substitute for $\bar{J}$ in (1.4) from (1.8) and operate with curl on both sides.

$$\nabla \times \nabla \times \bar{B} = \mu\sigma [\nabla \times \bar{E} + \nabla \times (\bar{u} \times \bar{B})] \qquad \ldots(1.10)$$

Eliminate $\bar{E}$ between (1.10) and (1.5) to obtain

$$\frac{\partial \bar{B}}{\partial t} = \nabla \times (\bar{u} \times \bar{B}) - \frac{1}{\mu\sigma} \nabla \times (\nabla \times \bar{B})$$

which by the help of (1.6) can be finally simplified to:

$$\frac{\partial \bar{B}}{\partial t} = \nabla \times (\bar{u} \times \bar{B}) + \eta \nabla^2 \bar{B} \qquad \ldots(1.11)$$

where $\eta = (\sigma\mu)^{-1}$ is defined as the magnetic diffusivity. In our work we will be concerned mainly with the situation $\sigma \longrightarrow \infty$, ie. the magnetic diffusivity of the fluid is very small and consequently the flux through each element moving with the fluid is constant (see eg. Cowling 1976 or Roberts 1967). This implies that the lines of force act as though they were 'frozen' with the medium and always move with it. For $\eta \rightarrow 0$, equation (1.11) reduces to

$$\partial\bar{B}/\partial t = \nabla\times(\bar{u}\times\bar{B}) \qquad \ldots(1.12)$$

1.2 ALFVEN WAVES In the absence of rotation and stratification and when the viscous effects are ignored the system defined by equations (1.1) and (1.12) can support only transverse waves, the so called magnetohydrodynamic or 'Alfven' waves, which travel along the magnetic lines of force. To study them in more detail let us consider a highly conducting fluid at rest in a uniform magnetic field $\bar{B}_0$. Assume that a small perturbation is imparted to the fluid and the velocity field becomes $\bar{u}$ while the total magnetic field (ambient field + field due to disturbance) is given by:

$$\bar{B} = \bar{B}_0 + \bar{b} = B_0\bar{k} + b\bar{n} \qquad \ldots(1.13)$$

Then equation (1.1) yields

$$\frac{\partial u}{\partial t} + (\bar{u}\cdot\nabla)\bar{u} = -\frac{1}{\rho}\nabla\left(p' + \bar{B}_0\cdot\bar{b}/\mu\right) + \frac{1}{\mu\rho}\bar{B}_0\cdot\nabla\bar{b} \qquad \ldots(1.14)$$

where second order terms in $\bar{b}$ have been neglected.
Taking the divergence of this equation and using equations (1.3) and (1.6), we find:

$$\nabla^2(p' + \bar{B}_0.\bar{b}/\mu) = 0 \qquad \ldots(1.15)$$

ie. $p' + \bar{B}_0.\bar{b}/\mu$ satisfies Laplace's equation. Now the only solution of (1.15) which is regular everywhere including infinity is $p + \bar{B}_0.\bar{b}$ = constant. Thus equation (1.14) reduces to:

$$\partial\bar{u}/\partial t + (\bar{u}.\nabla)\bar{u} = \bar{B}_0.\nabla\bar{b}/(\mu\rho) \qquad \ldots(1.16)$$

Similarly equation (1.12) yields

$$\partial\bar{b}/\partial t + (\bar{u}.\nabla)b = \bar{B}_0.\nabla u + \bar{b}.\nabla\bar{u} \qquad \ldots(1.17)$$

Now as $\nabla.\bar{B} = \nabla.\bar{u} = 0$,

$$\bar{b}.\nabla\bar{b} = \bar{u}.\nabla\bar{u} = \bar{b}.\nabla\bar{u} = \bar{u}.\nabla\bar{b} = 0$$

and $\bar{n}.\bar{k} = 0$ ie. $\bar{b}$ and $\bar{u}$ are transverse to $\bar{B}$.

Consequently equations (1.16) and (1.17) further reduce to:

$$\partial\bar{u}/\partial t = \bar{B}_0.\nabla\bar{b}/(\mu\rho) \qquad \ldots(1.18)$$

and $$\partial\bar{b}/\partial t = \bar{B}_0.\nabla\bar{u} \qquad \ldots(1.19)$$

Assume solutions of the form:

$$\bar{b} = B_0\,\bar{n}\,f[m(z \pm V_a t)] \qquad \ldots(1.20)$$

$$u = u_0\,\bar{n}\,f[m(z \pm V_a t)] \qquad \ldots(1.21)$$

Then it is immediately evident from equation (1.19) that

$$\bar{V}_a = \bar{u}_0 \qquad \ldots(1.22)$$

and when we substitute these solutions in equation (1.18), we

obtain: $\omega = (\bar{V}_a . \bar{m})$ where

$$V_a^2 = B_0^2/(\mu\rho) \qquad \ldots(1.23)$$

is the velocity of Alfven waves. Thus the phase velocity is independent of the frequency and hence the waves are not dispersive.

The average magnetic energy density associated with the wave motion is given by: $M = \langle b^2 \rangle /(2\mu)$ where $\langle\ \rangle$ denotes average over the period. Thus from equation (1.20):

$$M = 1/(2\mu)(B_0^2 f^2)/2 = B_0^2 f^2/(4\mu) \qquad \ldots(1.24)$$

which by the help of equations (1.23) and (1.22) is seen to be equal to $\rho u_0^2/4$ which is the average kinetic energy of the wave. Thus for Alfven waves there is an equipartitioning of energy between the magnetic and kinetic fields.

If we had included ν and η terms in equations (1.1) and (1.11), damped wave solutions will result and the energy of these Alfven waves will be dissipated in finite time; the rate of decay of each wave being proportional to the square of their wave numbers [see for example Roberts (1967) or Cowling (1976)].

Under conditions typical of the Earth's core (Hide,1970; Roberts and Soward, 1972) $\rho = 9.6 \times 10^3 kg/m^2$, $\mu = \mu_0 = 4\pi \times 10^{-7}$ henry/m and a strong basic toroidal magnetic field of strength 0.01 weber/m^2 (Hide 1966), the Alfven waves have a velocity of the order of 0.1 m/s. But see next section for the effect of rotation on these waves.

1.3 EFFECT OF ROTATION ON ALFVEN WAVES: INERTIAL MHD WAVES.

Assuming that the viscocity effects are negligible and $\bar{\Omega}$ is constant in time, equation (1.1) can be rewritten as

$$\rho\left(\frac{\partial \bar{u}}{\partial t} + (\bar{u}\cdot\nabla)\bar{u} + 2\bar{\Omega}\times\bar{u}\right) = -\nabla p + \bar{J}\times\bar{B} + \rho\bar{g} + \bar{f} \qquad \ldots(1.25)$$

For the sake of generality let us assume, in addition, that the fluid is stably stratified. In such a case one can assume the Boussinesq approximation to hold, according to which the basic rate of change of density is supposed to be so weak that the density may be treated as constant and replaced by its average value ρ_0 everywhere in equation (1.25) except in the buoyancy term $\bar{f}$.

Assume small scale perturbations of the form:

$$\rho = \rho_0(z) + \rho_1(x,y,z,t), \qquad \bar{u} = \bar{U}_0 + \bar{u}_1(x,y,z,t)$$

$$p = p_0(z) + p_1(x,y,z,t), \text{ and } \bar{B} = \bar{B}_0 + \bar{B}_1(x,y,z,t) \qquad \ldots(1.26)$$

where $\bar{U}_0 = 0$ and $\nabla p_0 = \bar{g}\rho_0$. Then equation (1.25) yields:

$$\frac{\partial \bar{u}}{\partial t} + 2\bar{\Omega}\times\bar{u}_1 = -\frac{1}{\rho_0}\nabla p_1 + \frac{(\nabla\times\bar{B}_1)\times\bar{B}_0}{\mu\rho_0} + \bar{g}\frac{\rho_1}{\rho_0} \qquad \ldots(1.27)$$

Similarly equation (1.3) yields

$$\nabla\cdot\bar{u}_1 = 0 \qquad \ldots(1.28)$$

and $$\partial\rho_1/\partial t + \omega_1\, d\rho_0/dz = 0 \qquad \ldots(1.29)$$

and from equation (1.6)

$$\nabla\cdot\bar{B}_1 = 0 \qquad \ldots(1.30)$$

The electrodynamic equation (1.12) linearises to

$$\partial \bar{B}_1/\partial t - (\bar{B}_0.\nabla)\bar{u}_1 = 0 \qquad \ldots(1.31)$$

We eliminate p_1, ρ_1, $\bar{B}_1$ in favour of $\bar{u}_1$. Operate on equation (1.27) by curl observing $\nabla.\bar{B}_1 = 0$ to obtain

$$\frac{\partial}{\partial t}(\nabla \times \bar{u}_1) + 2(\bar{\Omega}.\nabla)\bar{u}_1 = (\bar{B}_0.\nabla)(\nabla \times \bar{B}_1) + \nabla \times (\bar{g}\,\rho_1/\rho_0)$$

Take partial derivative with respect to time of both sides to find

$$\frac{\partial^2}{\partial t^2}(\nabla \times \bar{u}_1) + 2(\bar{\Omega}.\nabla)\frac{\partial \bar{u}_1}{\partial t} = (\bar{B}_0.\nabla)^2 \nabla \times \bar{u}_1 + \nabla \times (\bar{g}\frac{1}{\rho_0}\omega_1 \frac{d\rho_0}{dz}) \qquad \ldots(1.32)$$

where we used equations (1.29) and (1.31).

Now if we denote

$$\bar{N} = (\bar{g}/g)(g/\rho_0)(d\rho_0/dz) \qquad \ldots(1.33)$$

equation (1.32) transforms to

$$\left[\frac{\partial^2}{\partial t^2} - (\bar{V}_a.\nabla)^2\right]\nabla \times \bar{u}_1 - 2(\bar{\Omega}.\nabla)\frac{\partial \bar{u}_1}{\partial t} - \bar{N} \times \nabla(\bar{N}.\bar{u}_1) = 0 \qquad \ldots(1.34)$$

where V_a is given by equation (1.23).

Substitute a plane wave solution of the form:

$$\bar{u} = \bar{u}_0 \exp[i(\omega t - \bar{k}.\bar{r})] \qquad \ldots(1.35)$$

where $\bar{k} = (k,l,m)$ is the wave number vector, ω is the angular frequency and r is the distance vector, to obtain the dispersion relationship

$$\omega^2 \pm 2(\bar{\Omega}.\bar{K})\omega/|K| - (\bar{V}_a.\bar{K})^2 - (\bar{N} \times \bar{K})^2/K^2 = 0 \qquad \ldots(1.36)$$

which has solutions (Hide 1969)

$$\omega^2 = (\bar{V}_a \cdot \bar{K})^2 + \frac{1}{2}\left[\frac{(2\bar{\Omega}\cdot\bar{K})^2 + (\bar{N}\times\bar{K})^2}{K^2} \pm \left[\left(\frac{(\bar{N}\times\bar{K})^2 + 2(\bar{\Omega}\cdot\bar{K})^2}{K^2}\right)^2 + \frac{4(\bar{V}_a\cdot\bar{K})^2(2\bar{\Omega}\cdot\bar{K})^2}{K^2}\right]^{1/2}\right] \quad \ldots(1.37)$$

Clearly if $N^2 = g/\rho_0 * (d\rho_0/dz) > 0$, ω is always real and the density stratification remains stable. Once again due to equation (1.28), the particle displacements are transverse to the direction of phase velocity. Note that for $\bar{\Omega} = \bar{N} = 0$, ie., in the absence of rotation and stratification we once again obtain the non dispersive Alfven waves travelling with velocity $\bar{V}_a$. Whereas when $\bar{V}_a = \bar{N} = 0$, we have inertial waves (Batchelor, 1967; Greenspan, 1968) satisfying:

$$\omega^2 = (2\bar{\Omega}.\bar{K})^2/K^2 \quad \ldots(1.38)$$

whose energy is partitioned between particle displacement (kinetic energy) and rotation (due to coriolis force).
Similarly when stratification alone is present, only internal waves are possible (in which the buoyancy provides the restoring forces) (Lighthill 1978). The dispersion relationship being

$$\omega^2 = (\bar{N}\times\bar{K})^2/K^2 \quad \ldots(1.39)$$

We will concentrate here mainly on the case of Alfven waves effected only by rotation, (Lehnert, 1954; Chandrashekhar 1961), ie., $\bar{N} = 0$, for which equation (1.37) reduces to:

$$\omega_{\pm}^2 = (\bar{V}_a\cdot\bar{K})^2 + \frac{1}{2}\left[\frac{(2\bar{\Omega}\cdot\bar{K})^2}{K^2} \pm \left(\frac{(2\bar{\Omega}\cdot\bar{K})^4}{K^4} + \frac{4(\bar{V}_a\cdot\bar{K})^2(2\bar{\Omega}\cdot\bar{K})^2}{K^2}\right)^{1/2}\right] \quad (1.40)$$

where ω_+ denotes the solution of equation (1.40), when positive sign is taken in the expression and ω_- when the negative sign is

taken. It is evident from this equation that ω_+^2 increases, and ω_-^2 decreases monotonically with increasing $\bar{\Omega}$, though their product is independent of $\bar{\Omega}$, ie.,

$$\omega_+^2 \omega_-^2 = (\bar{V}_a.\bar{K})^4 \qquad ...(1.41)$$

We can infer from equation (1.31) that the ratio of magnetic to kinetic energy associated with any of these modes is given by

$$B_1^2/(2\mu)/(\tfrac{1}{2}\rho u^2) = (\bar{V}_a.\bar{K})^2/\omega_\pm^2 \qquad ...(1.42)$$

Thus for the mode corresponding to ω_+^2 for which $\omega_+^2 >> (\bar{V}_a.\bar{K})^2$ (see equation 1.40), most of its energy is in kinetic form and therefore it is commonly called an 'inertial mode' and will reduce to an inertial wave in the absence of a magnetic field. The other solution, for which $\omega_-^2 << (\bar{V}_a.\bar{K})^2$, is referred to as the magnetic mode (see Hide 1966) as most of the energy associated with this mode is in the form of a magnetic field. There is obviously no equipartioning of kinetic and magnetic energies as, eg., in Alfven waves and both modes are highly dispersive. These modes are alternatively known as fast (ω_+) and slow (ω_-) modes in keeping with their phase velocities. Under conditions typical of the earth's core V_a=0.1 m/s, $\bar{\Omega}$ = $7.3\text{X}10^{-5}$/s and thus for wavelengths of the order of several thousand kilometres (K = $2\text{X}10^{-6}$/m), the magnetic modes have oscillation periods, $2\pi/\omega_-$, of the order of $9\text{X}10^9$s (300 years) and a phase velocity, ω_-/K = $4.0\text{X}10^{-4}$ m/s (0.44 mm/sec). These values are of the same order of magnitude as encountered in the phenomenon of geomagnetic secular variations (with time scales of decades to

centuries and westward drifts of a few parts of a mm/sec.), a fact which led Hide(1966) and Braginsky(1967) to postulate that the geomagnetic secular variation may contain significant contributions from free hydromagnetic oscillations of the Earth's core. The oscillation periods of the inertial modes, on the other hand, are of the order of several hours to days which shows that they are unimportant in the phenomenon of geomagnetic secular variations.

Equation (1.40) can be written in a more useful form by scaling it with respect to time and length scales derived from $\bar{V}_a$ and $\bar{\Omega}$. If the wave vector $\bar{K}$ of a wave makes an angle ϕ with the rotation vector $\bar{\Omega}$ and an angle θ with the ambient magnetic field, B_0, it can be written as

$$\omega_{\pm}^2 = (V_a|K|\cos\theta)^2 + \frac{1}{2}\left[(2\Omega\cos\phi)^2 \pm \left[(2\Omega\cos\phi)^4 + 4(V_a|K|\cos\theta)^2(2\Omega\cos\phi)^2\right]^{1/2}\right] \quad \ldots(1.43)$$

Now if we express distances in V_a/Ω units and time in $1/\Omega$ units, equation (1.43) can be written in a form independent of Ω and V_a as

$$\omega_{\pm}^2 = (|K|\cos\theta)^2 + 0.5[(2\cos\phi)^2 \pm \{(2\cos\phi)^4 + 4(|K|\cos\theta)^2(2\cos\phi)^2\}^{1/2}] \quad \ldots(1.44)$$

1.4 ROSSBY-MAGNETOHYDRODYNAMIC WAVES: MHD WAVES IN A ROTATING THIN FLUID SHELL The oscillations studied above so far were those of an unbounded rotating fluid whereas in this secton we will concentrate on oscillations of bounded fluid bodies. We will study in particular the two dimensional oscillations of a

rotating incompressible thin spherical shell of highly conducting fluid which is in a quasi-geostrophic balance (Hide 1966). We shall later relate and link these findings to the quasi two dimensional wave motions between the sloping upper and lower boundaries of a rotating container (Pedlosky, 1971; Hide, 1977). We will also discuss the possibility of generalising the thin shell results to a thick shell and spell out the care necessary in interpreting these results.

Consider a thin shell with inner and outer radii a and b respectively with $b-a << b$ (Figure 1.1).In such a shell the fluid possesses little or no radial displacements, so only the local normal component of the shell's vorticity, $f=2\bar{\Omega}\sin\phi$, (where $\bar{\Omega}$ is the total angular velocity of the shell) is dynamically significant. In such a situation a local cartesian

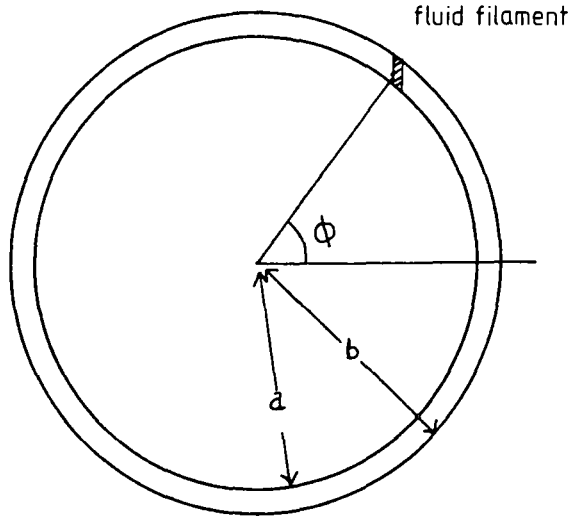

Figure 1.1 Showing the thin fluid shell geometry.

frame of axes centred at the latitude ϕ_0 of the region under consideration with X, Y and Z axes directed eastward, northward and upward respectively can be employed to describe horizontal coriolis accelerations if we take $\Omega \sin\phi$, the vertical component of the shell's angular velocity as the angular velocity of the fluid at latitude ϕ. The plane XY is equivalent to the Rossby-Haurwitz 'beta plane' (Rossby et. al., 1939) used in dynamical meteorology. This type of approximation expresses the effect of the shell's sphericity through the variation of the coriolis parameter, f, with latitude which can now be linearised about a mean latitude ϕ_0 as

$$f = f_0 + \beta y \qquad \ldots(1.45)$$

where $f_0 = 2\Omega \sin\phi_0$

and $\beta = 2\Omega\cos\phi_0/R$ $\qquad \ldots(1.46)$

R being the mean radius of the thin shell.

In such a system the equations of motions (1.1) become two-dimensional and can be written in component form as

$$\frac{Du}{Dt} - fv = -\frac{\partial}{\partial x}\left(p + \frac{B_z^2}{2\mu\rho}\right) - \frac{B_y}{\mu\rho}\left(\frac{\partial B_y}{\partial x} - \frac{\partial B_x}{\partial y}\right) \qquad \ldots(1.47)$$

$$\frac{Dv}{Dt} + fu = -\frac{\partial}{\partial y}\left(p + \frac{B_z^2}{2\mu\rho}\right) + \frac{B_x}{\mu\rho}\left(\frac{\partial B_y}{\partial x} - \frac{\partial B_x}{\partial y}\right) \qquad \ldots(1.48)$$

where u and v are the x and y components of the dynamic velocity, $\overline{B} = (B_x, B_y, B_z)$ is the ambient magnetic field. p is the local

pressure and other quantities are as defined earlier.

The continuity equation for velocity reduces to

$$\partial u/\partial x + \partial v/\partial y = 0 \qquad \ldots(1.49)$$

whereas the magnetic field satisfies a similar equation

$$\partial B_x/\partial x + \partial B_y/\partial y = 0 \qquad \ldots(1.50)$$

since B is solenoidal and we are working in a two-dimensional system in which all variations with respect to z are ignored.

Equation (1.12) with the help of (1.49) and (1.50) can be written in component form as

$$(\partial/\partial t + u\,\partial/\partial x + v\,\partial/\partial y)B_x = (B_x\partial/\partial x + B_y\partial/\partial y)u \qquad \ldots(1.51)$$

$$(\partial/\partial t + u\,\partial/\partial x + v\,\partial/\partial y)B_y = (B_x\partial/\partial x + B_y\partial/\partial Y)v \qquad \ldots(1.52)$$

and $$(\partial/\partial t + u\,\partial/\partial x + v\,\partial/\partial y)B_z = 0 \qquad \ldots(1.53)$$

Observe that B_z enters only one equation, (1.53), implying that any component of B perpendicular to the x-y plane is advected by the motion, though it does not contribute to the hydromagnetic forces. Therefore without any loss of generality we can restrict our attention to the case of uniform magnetic field whose lines of force are parallel to the xy plane. $[p + B_z{}^2/2(\mu\rho)]$ can be eliminated between equations (1.47) and (1.48) to obtain a modified vorticity equation given by

$$\frac{D\zeta}{Dt} + v\beta = \frac{1}{\mu\rho}\left(B_x\frac{\partial}{\partial x} + B_y\frac{\partial}{\partial y}\right)\left(\frac{\partial B_y}{\partial x} - \frac{\partial B_x}{\partial y}\right) \qquad \ldots(1.54)$$

Alternatively, this equation can be obtained directly from an extension of Ertel' potential vorticity theorem for the

hydromagnetic case as we will see later in this section.

Now assume small scale perturbations of the form

$$u = u_0 + u_1(x,y,t) \qquad v = v_0 + v_1(x,y,t)$$

$$B_x = B_{x0} + b_{x1}(x,y,t) \qquad B_y = B_{y0} + b_{y1}(x,y,t) \qquad \ldots(1.54)$$

$$B_z = B_{z0} + b_{z1}(x,y,t) \qquad p = p_0 + p_1(x,y,t)$$

in the velocity and magnetic components and consequently equations (1.47) to (1.53) linearise to:

$$\frac{Du_1}{Dt} - f v_1 = -\frac{\partial}{\partial x}\left(p_1 + \frac{B_{z0} b_{z1}}{\mu\rho}\right) - \frac{B_y}{\mu\rho}\left(\frac{\partial b_y}{\partial x} - \frac{\partial b_x}{\partial y}\right) \qquad \ldots(1.55)$$

$$\frac{Dv_1}{Dt} + f u = -\frac{\partial}{\partial y}\left(p_1 + \frac{B_{z0} b_{z1}}{\mu\rho}\right) + \frac{B_x}{\mu\rho}\left(\frac{\partial b_y}{\partial x} - \frac{\partial b_x}{\partial y}\right) \qquad \ldots(1.56)$$

$$\partial u_1/\partial x + \partial v_1/\partial y = 0 \qquad \ldots(1.57)$$

$$\partial b_{x1}/\partial x + \partial b_{y1}/\partial y = 0 \qquad \ldots(1.58)$$

$$\frac{Db_{x1}}{Dt} = B_0\left(\cos\theta\frac{\partial}{\partial x} + \sin\theta\frac{\partial}{\partial y}\right)u \qquad \ldots(1.59)$$

$$\frac{Db_{y1}}{Dt} = B_0\left(\cos\theta\frac{\partial}{\partial x} + \sin\theta\frac{\partial}{\partial y}\right)v \qquad \ldots(1.60)$$

and $$\frac{Db_{z1}}{Dt} = 0 \qquad \ldots(1.61)$$

where θ is the angle magnetic field makes with the x axis.

Eliminate $[p_1 + B_{z0}b_{z1}/(\mu\rho)]$ between equations (1.55) and (1.56) to get

$$\frac{D\zeta}{Dt} + v_1\beta = \frac{B_0}{\mu\rho}\left(\cos\theta\frac{\partial}{\partial x} + \sin\theta\frac{\partial}{\partial y}\right)\left(\frac{\partial b_{y1}}{\partial x} - \frac{\partial b_{x1}}{\partial y}\right) \qquad \ldots(1.62)$$

where $\zeta = \partial v_1/\partial x - \partial u_1/\partial y)$ ...(1.63)

Operate on this equation with D/Dt and use equations (1.59) and (1.60) to obtain

$$\left[\frac{D^2}{Dt^2} - V_a^2\left(\cos\theta\frac{\partial}{\partial x} + \sin\theta\frac{\partial}{\partial y}\right)^2\right]\zeta + \beta\frac{Dv_1}{Dt} = 0$$

Finally eliminate v_1 by the help of equations (1.63) to get the equation of vorticity

$$\left[\frac{D^2}{Dt^2} - V_a^2\left(\cos\theta\frac{\partial}{\partial x} + \sin\theta\frac{\partial}{\partial y}\right)^2\right]\nabla_H^2\zeta_1 + \beta\frac{D}{Dt}\frac{\partial\zeta_1}{\partial x} = 0 \qquad ...(1.64)$$

This equation admits plane wave solutions of the form

$$\zeta = \zeta_M \exp\{i(kx + ly - \omega t)\} \qquad ...(1.65)$$

whose substitution leads to the dispersion relation

$$\hat{\omega}^2 + \frac{\beta k\hat{\omega}}{k^2+l^2} - V_a^2(k\cos\theta + l\sin\theta)^2 = 0 \qquad ...(1.66)$$

where $\hat{\omega} = \omega - u_0 k$ ...(1.67)

and u_1, v_1, b_{x1} and b_{y1} can be obtained by the help of equations (1.57), (1.58), (1.59), (1.60) and (1.63) giving

$$u_1 = \frac{il}{k^2+l^2}\zeta_1 \qquad v_1 = \frac{-ik}{k^2+l^2}\zeta_1 \qquad ...(1.68)$$

$$b_{x1} = \frac{-i\beta_0 l(k\cos\theta + l\sin\theta)}{\hat{\omega}(k^2+l^2)}\zeta_1 \text{ and } b_{y1} = \frac{i\beta_0 k(k\cos\theta + l\sin\theta)}{\hat{\omega}(k^2+l^2)}\zeta_1 \qquad ...(1.69)$$

Equation (1.66) has two roots for each value of the wavenumber

$K = (k,l)$, which once again can be designated as inertial and magnetic depending on whether upper or lower sign is taken in the following equation

$$\omega_{i,m} = \frac{-\beta k}{2(k^2+l^2)}\left[1 \pm \left(1 + \left[\frac{2\nu_a(k^2+l^2)(k\cos\theta + l\sin\theta)}{k\beta}\right]^2\right)^{1/2}\right] \qquad \cdots(1.70)$$

We can see that $\omega_m << \omega_i$, ie., the time periods of magnetic modes are much longer than the inertial modes. We can also see that inertial modes always possess a negative (westward) phase velocity whereas magnetic modes always have positive (eastward) phase velocity.

Now we shall prove the dynamic equivalence of this system to another situation in which the fluid is bound between the upper and lower sloping walls of a rotating container (figure 1.2). The only assumption we need to make is that to a first approximation

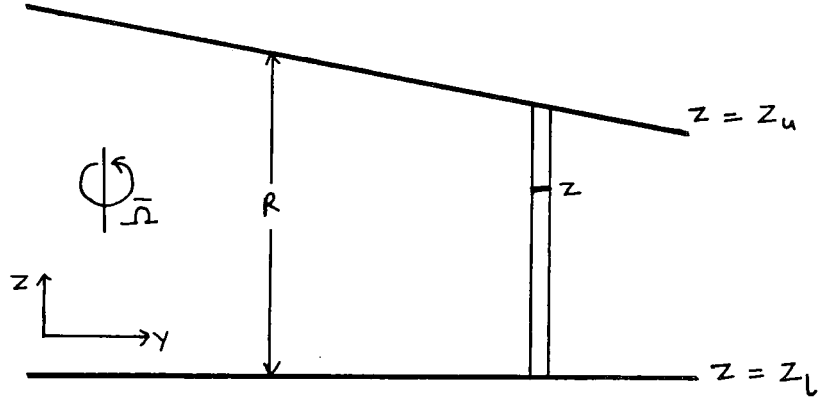

Figure 1.2 Geometry of a rotating container filled with conducting fluid.

the fluid motions are in a state of geostrophic balance. We shall make use of Hide's modified potential vorticity theorem (Hide 1983a, b, 1984) to derive the necessary equations. According to this theorem for an inviscid, perfectly conducting, rotating fluid

$$\frac{D}{Dt}\left[\bar{\omega}\cdot\nabla\wedge\right] = \nabla\wedge\cdot\nabla\times\left(\frac{\bar{J}\times\bar{B}}{\rho}\right) \qquad \ldots(1.71)$$

where $\bar{\omega}$ is the total vorticity of a fluid element ($= 2\Omega+\zeta$) and $\wedge$ is a Lagrangian invariant. ie.,

$$D\wedge/Dt = 0 \qquad \ldots(1.72)$$

For fluids roughly in geostrophic balance we can assume that axial filaments of the fluid retain their coherence. Thus we can define

$$\wedge = \frac{z - z_l}{z_u - z_l} \qquad \ldots(1.73)$$

where Z is the vertical co-ordinate of a specific point located on the fluid filament and Z_u and Z_l mark the vertical extent of the axial fluid filament (figure 1.2). Clearly $\wedge$ satisfies equation (1.72), as the ratio of the length of the lower part of the filament ($Z-Z_l$) to the total length of the filament remains constant because the fluid is mainly in geostrophic balance. Substitution of $\wedge$ in equation (1.71) gives:

$$\frac{D}{Dt}\left[\frac{2\Omega+\zeta}{z_u - z_l}\right] = \frac{1}{z_u - z_l}\left[\nabla\times\left(\frac{\bar{J}\times\bar{B}}{\rho}\right)\right]_z \qquad \ldots(1.74)$$

as $\zeta \ll \Omega$. Subscript z is used in the R.H.S term to denote its

vertical component. Noting that x and y components of $\bar{J} \times \bar{B}$ are

$$\frac{1}{\mu}\left[-\frac{1}{2}\frac{\partial B_z^2}{\partial x} - B_y\left(\frac{\partial B_y}{\partial x} - \frac{\partial B_x}{\partial y}\right)\right] \qquad \text{and}$$

$$\frac{1}{\mu}\left[-\frac{1}{2}\frac{\partial B_z^2}{\partial x} + B_x\left(\frac{\partial B_y}{\partial x} - \frac{\partial B_x}{\partial y}\right)\right]$$

Equation (1.74) can be written in an expanded form as

$$(z_4 - z_l)\left(\frac{\partial}{\partial t} + u\frac{\partial}{\partial x} + v\frac{\partial}{\partial y} + w\frac{\partial}{\partial z}\right)\left[\frac{2\Omega + \zeta}{z_4 - z_l}\right]$$

$$= \frac{1}{\mu\rho}\left(B_x\frac{\partial}{\partial x} + B_y\frac{\partial}{\partial y}\right)\left(\frac{\partial B_y}{\partial x} - \frac{\partial B_x}{\partial y}\right)$$

Axial coherence implies variations with respect to z axis are negligible. Therefore

$$\left(\frac{\partial}{\partial t} + u\frac{\partial}{\partial x} + v\frac{\partial}{\partial y}\right)\zeta + 2\Omega v\frac{d}{dy}\left(\frac{1}{z_4 - z_l}\right) = \frac{1}{\mu\rho}\left(B_x\frac{\partial}{\partial x} + B_y\frac{\partial}{\partial y}\right)\left(\frac{\partial B_y}{\partial x} - \frac{\partial B_x}{\partial y}\right)$$

ie.

$$\left(\frac{\partial}{\partial t} + u\frac{\partial}{\partial x} + v\frac{\partial}{\partial y}\right)\zeta + \beta v = \frac{1}{\mu\rho}\left(B_x\frac{\partial}{\partial x} + B_y\frac{\partial}{\partial y}\right)\left(\frac{\partial B_y}{\partial x} - \frac{\partial B_x}{\partial y}\right) \qquad \ldots(1.75)$$

where $\beta = 2\Omega d/dy[1/(Z_u - Z_1)] = -2\Omega d/dy[\ln(Z_u - Z_1)]$ $\qquad \ldots(1.76)$

Equation (1.75) is identical to the modified vorticity equation (1.54) which was derived with reference to a thin fluid shell, proving thereby the equivalence of these two systems, provided that we replace β $(= \partial f/\partial y)$ of the thin shell model with $-2\Omega d/dy[\ln(Z_u - Z_1)]$. This implies that in relation to figure (1.2) β is positive, and inertial Rossby waves will have a phase velocity in the direction of positive x axis (ie. pointing out of the paper) whereas magnetic modes possess phase velocities in the direction of the negative x axis. This may be rephrased as:

Rossby inertial waves propagate so that the deeper fluid is always on their left (figure 1.2), whereas magnetic modes propagate so that the deeper fluid always lies to their right. This is in agreement with the findings of the thin shell model in which the eastward propagating Rossby magnetic waves always have deeper fluid on their right (towards the equator), whereas Rossby inertial waves propagate westward so that the deeper fluid is on their left.

Before concluding this section we will rewrite the dispersion relation (1.66) in such a way that it becomes independent of V_a and β. This can be done by expressing length in units of $(V_a/\beta)^{1/2}$ and time in units of $(V_a\beta)^{-1/2}$ and equation (1.66) will reduce to:

$$\hat{\omega}^2 + k\hat{\omega}/(k^2+l^2) - (k\cos\theta + l\sin\theta)^2 = 0 \qquad ...(1.77)$$

Notice that in these units Alfven velocity assumes a value equal to unity and all other velocities are expressed as its multiples.

1.5 MAGNETOHYDRODYNAMIC WAVES IN A ROTATING THICK SHELL Now let us explore the possibility of generalising the above results of a thin shell model to a thick shell. Hide (1966) argued that for a thickshell for areas with latitudes greater than a certain latitude ϕ^* (see figure 1.3), β is, positive as in the case of a thin shell, as the fluid gets deeper when we move away from the rotation axis. But for the greater part of the shell below ϕ^* the fluid gets shallower as we move towards the equator and hence β should be negative. Hide (1966) thus argued that for this region the quantity $(\zeta+2\Omega)/[2(R+H)]$ will be conserved $[2(R+H)\sin\phi$ being

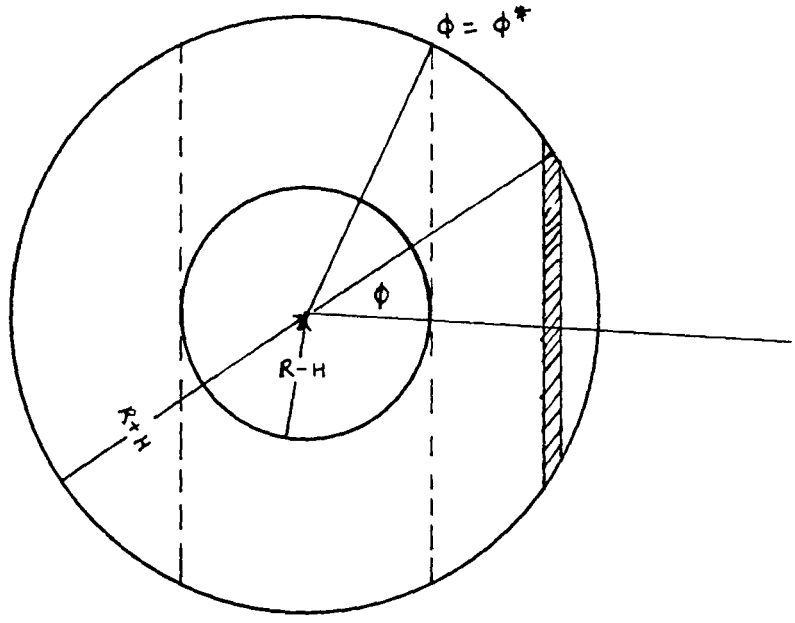

Figure 1.3 The thick shell geometry.

the thickness of the fluid filament in this region] and consequently β will be given by $-2\Omega\cos\phi^*/(R+H)$. In this way the magnetic Rossby waves will propagate westward for most part of the earth as indeed will be necessary to explain the westward drift (see section 1.6 below) of the Earth's magnetic field. A more careful analysis by Acheson (1978) on these lines while confirming these ideas suggests that indeed this will be the case if either the boundary slope is small or the waves have a very small wavelength in the (cylindrically) radial directon. This however is certainly not the case for a fluid shell like the Earth's outer core and thus the above conjecture still remains tentative. On the other hand some independent empirical evidence from laboratory experiments (Ibbetson and Philips 1967) in the absence of magnetic field certainly confirms Hide's ideas.

Fortunately some more rigorous analyses of these waves in spherical systems do exist. Stewartson (1967) studied the slow oscillations of a fluid in a spherical rotating shell in the presence of a uniform magnetic field and confirmed that in a thin shell the slow waves do propagate eastwards only. In addition Stewartson showed that certain principle modes, (which have radial velocity of the same sign for all radii) will also propagate eastwards even in a thick shell. The mathematical complexity of his model prevent him from relaxing this constraint on the radial velocity, so other non-principle modes with more general radial velocities may still propagate westwards in the case of a thick shell. Malkus (1967) studied these hydromagnetic oscillations in a full sphere with no inner boundary, for a basic

state of a uniform current parallel to the axis of rotation (or equivalently an azimuthal magnetic field B_0 proportional to r, the distance from the axis of rotation). Fortunately this choice of the basic state leads to a modified Poincare eigen value problem for the oscillations which have been extensively studied in other hydrodynamic situations. Then if one assumes wave solutions of the form

$$p = \tilde{p} \exp[i(m\phi - \omega t)] \qquad ...(1.78)$$

where ϕ is the azimuthal angle, it is seen that the eigen-values of the hydromagnetic waves can be obtained from those of the ordinary inertial waves (ω_0) for the same situation (but without a magnetic field) by the expression (Malkus 1967)

$$\omega^2 - \omega_0 \omega - m \frac{V_a^2}{a^2} \left(m + \frac{\omega_0}{\Omega} \right) = 0 \qquad ...(1.79)$$

where V_a is the Alfven velocity and a is the mean radius of the sphere. Thus the low frequency magnetic mode will be given by

$$\omega = -m \frac{V_a^2}{a^2} \left(\frac{m}{\omega_0} + \frac{1}{\Omega} \right)$$

ω_0 is always $\leq 2\Omega$ for inertial modes. On substituting the appropriate ω_0 for cellular two dimensional (ie no radial component) motions, it is seen (Wood 1977) that such modes propagate only eastwards whereas roughly as many three-dimensional modes travel westwards as eastwards. Malkus's study thus shows no preference for westwards propagating waves in a thick shell which compelled Acheson to consider some selection

mechanism by which one type of waves may be preferentially generated (Acheson 1971, 1972b, 1973).

1.6 THE EARTH'S CORE AND ITS MAGNETIC FIELD The applications of MHD wave theory to problems so far considered in this chapter and the rest of the thesis were made with a particular model, namely the earth's core, in mind. In this section we will broadly outline its structure and the main features of its magnetic field in order to appreciate the choice of various parameters (strong toroidal field, low magnetic diffusivity and viscosity over certain time scales etc.) made later in our work.

The earth's core consists of a liquid metallic outer shell of a radius of about 3485 kms and a solid inner core of a radius nearing 1227 kms. The core is believed to be composed mainly of iron with a little alloyed nickel and possibly certain light elements like Si, Fe or O (Bott 1982). The density of the outer core increases from 9970 kg m^{-3} at the core-mantle boundary to about 12120 kg m^{-3} near the inner core boundary where a sharp increase of 180 kg m^{-3} occurs. These densities should be compared with that of the mantle which is about 5500 kg m^{-3} at the core-mantle boundary. The estimates for electrical conductivity and viscosity are not so precise but values of $\sigma = 3X10^5$ mho/m and $10^{-7}m^2/s<\nu<10^2$ m^2/s (Roberts and Sowards 1972) for the outer core are often quoted. The outer core is, by general consensus, now believed to be the seat of the earth's magnetic field where new lines of force are created by a dynamo process (Bullard and Gellman, 1954; Herzenberg, 1958; Backus, 1958; Jacobs, 1963;

Soward and Roberts 1976) which converts the kinetic energy derived from convection (which in turn might have been caused by gravitational differentiation or thermal sources) into magnetic energy.

The earth's magnetic field can be, to a first approximation, described by the help of an eccentric dipole inclining at about 11^{0} to the axis of rotation with its centre displaced by about 300 kms towards Indonesia. Such a model will explain why the earth's magnetic field has roughly twice the intensity at the geomagnetic pole when compared with the intensity at the geomagnetic equator. However such an approximation leaves out most of the detail of the earth's magnetic field like the 'Siberian oval' seen in the declination maps or the South African anomaly best seen in the vertical intensity maps and further terms (quadrupoles, octupoles etc.) in this sequence of approximation will be required. This is best done by the help of spherical harmonic analysis of the main field and various coefficient sets for several epochs are available (Vestine et al, 1947; Bullard et al, 1950; Cain et al, 1967). An exhaustive compilation of the geomagnetic spherical harmonic coefficients from Gauss's original analysis to the present time can be found in Barraclough (1978). Spherical harmonic analysis can be used to separate the geomagnetic field of the earth's internal origin from that of the external sources. A study of the earth's magnetic field as obtained from data derived from magnetic observatories, satellite surveys and archeomagnetic & palaeomagnetic studies on human artifacts and rocks, reveals two

interesting phenomena. First, it is found that the earth's magnetic field has frequently reversed its polarity in the past. As magnetohydrodynamic equations admit solutions of either sign for $\bar{B}$, no mathematical problem is foreseen in obtaining a magnetic field of one or the other polarity from kinematic considerations; though exactly what causes these reversals is hard to pinpoint yet. Secondly, a study of the annual means of the earth's internal magnetic field shows major changes in its intensity and direction over time periods of decades to centuries. The maps of equal annual change of any element (isopors) at any epoch show focii which migrate slowly westwards at about 0.2 degree of latitude per year. This westward drift is seen to depend only marginally on the latitudinal position of these focii (Bullard et al 1950). When individual spherical harmonics are analysed, it is found (Hide 1966) that the westward drift of the dipole components is much less (typically one third) than that of the non-dipole field. Similarly the r.m.s. rate of change of the non-dipole field is about 2.5% of the total non-dipole field wheras the rate of change of dipolar field averages only 0.1% of the total.

So far two theories (Bullard et al, 1950; Hide, 1966) have been advanced to explain these features of the secular variation of the earth's magnetic field. Bullard argued that assuming that the individual fluid particles tend to conserve their angular momentum, any concomitant inward advective transfer of angular momentum associated with meridional flows will make the inner parts of the core to rotate more rapidly than the outer parts.

This angular velocity distribution can, however, be steady only if this inward transfer of the angular momentum is balanced by an outward transfer by some agency. Bullard showed that this can be achieved by electromagnetic forces. Thus if the earth's mantle is electromagnetically coupled with the core, except in a very thin boundary layer where viscosity will impede any motions, the outer parts of the core will move westward relative to the mantle carrying with it the minor features of the earth's magnetic field with it. The main difficulty with Bullard's theory is that his assumption that individual fluid particles conserve their angular momentum is generally not valid for a fast rotating system where a fluid column as a whole tends to conserve its angular momentum. Therefore such a system will not be able to sustain a continuous inwards transfer of the angular momentum as required in Bullard's theory.

Hide (1966) overcomes this problem by suggesting that the westward propagation of the secular variation is a manifestation of a wave motion which does not seriously affect the angular momentum of the system. Thus by the help of a β-plane approximation (see section 1.4 above), he was able to show that for an ambient magnetic field of 50 to 200 Oe Rossby-hydromagnetic waves will have the right wavelengths and periods to explain the observed secular variations in the earth's magnetic field (see his Table 2). As we have already discussed in sections 1.4 and 1.5, such waves will have group and phase velocities which are much lower than the Alfven velocity as will be required to explain westward drift velocities of only a

fraction of a mm/sec. The main controversy, however, is over the sign of the group velocities of these waves and theoretically many ways can be visualised (Hide, 1966; Malkus, 1967; Acheson, 1972b, 1973) by which the waves will selectively drift westwards.

CHAPTER TWO

A REVIEW OF PREVIOUS WORK ON WAVES AND INSTABILITIES IN CONDUCTING ROTATING FLUIDS

2.1. GENERAL A non-rotating homogeneous inviscid fluid can not provide any restoring forces to shear stresses and thus is incapable of supporting any shear waves. In addition, if the fluid is incompressible, no waves at all will be possible in it (apart from the surface waves due to gravity, which can exist only at a free boundary and do not interest us), and its steady motion will be completely and uniquely determined by a velocity potential Φ. However, when either a rotation is imparted to the fluid or if a magnetic field pervades the fluid, which is assumed to be conductive, a dramatic reversal of this conclusion results. In the case of rotation, transverse three-dimensional waves, the so called inertial waves, result, as was vividly demonstrated by Lord Kelvin (1877) through a series of experiments on rotating fluid-filled copper shells. In the latter case, one-dimensional transverse magnetohydrodynamic waves travelling in either directions of the magnetic field are possible, and were first postulated by Alfven (1942). The coriolis force provides the requisite restoring force for the inertial waves while Lorentz force balances the fluid motions in an Alfven wave. When both these phenomena are present simultaneously, two new types of hybrid waves, namely, the fast (inertial modes) and slow (magnetic modes) emerge (Lehnert 1954), and the stability of the

fluid to waves and instabilities becomes a very complex subject (Chandrashekhar 1960).

To put our own work in a proper perspective, we will review in the following sections the findings of the past and current research on the generation, propagation and reflection of these waves in homogeneous and inhomogeneous media and unbounded and bounded fluid bodies. No attempt is made to be exhaustive, and those works which are either directly relevant to our own work, or are fundamental to the understanding of this subject, receive most attention. A common thread running through this review and the rest of the thesis is that only those fluid motions which depart only slightly from a state of rapid uniform rotation are treated as these have most relevance to geophysical and astrophysical applications.

2.2. INERTIAL WAVES For a homogeneous, inviscid and uniformly rotating fluid in the absence of a magnetic field the equation of motion (Batchelor 1967, Pedlosky 1979) is given by

$$\rho\left[\frac{\partial \bar{u}}{\partial t} + (u\cdot\nabla)\bar{u} + 2\bar{\Omega}\times\bar{u}\right] = -\nabla p' \qquad \ldots(2.1)$$

where the notation is as in Chapter 1. To assess the relative importance of various terms in this equation, it is usual in the literature to make this equation non-dimensional by expressing distances in terms of L, a characteristic length scale of the fluid body, time in units of Ω^{-1}, velocities in terms of U, a characteristic magnitude of $\bar{u}$ and pressure in terms of $\rho\Omega UL$.

Then $$\frac{\partial \bar{u}}{\partial t} + \frac{2\bar{\Omega}\times\bar{u}}{|\Omega|} + \varepsilon(\bar{u}\cdot\nabla)\bar{u} = -\nabla p' \qquad \ldots(2.2)$$

where the quantity $\varepsilon = u/(\Omega L)$ is the 'Rossby number' of the flow and is a measure of the relative importance of inertial to coriolis force. For a fluid body in a state of almost rigid rotation, this number is very small and therefore the inertia terms are negligible, leaving us with

$$\frac{\partial \bar{u}}{\partial t} + \frac{2\bar{\Omega} \times \bar{u}}{|\bar{\Omega}|} = -\nabla p' \qquad \ldots(2.3)$$

With the help of the continuity equation, elimination of all other terms results in a single fourth order partial differential equation in p given by

$$\frac{\partial^2}{\partial t^2} \nabla^2 p + 4 \frac{\partial^2 p}{\partial z^2} = 0 \qquad \ldots(2.4)$$

named after Poincare who first formulated and obtained the solutions of the problem for pressure alone (Poincare 1910). A substitution of a standing wave solution of the form $p = p(x,y,z) \exp[-i\omega t]$, gives

$$\frac{\partial^2 p}{\partial x^2} + \frac{\partial^2 p}{\partial y^2} = \frac{4 - \omega^2}{\omega^2} \frac{\partial^2 p}{\partial z^2} \qquad \ldots(2.5)$$

which is elliptical for ω real when $\omega^2 > 4$ and has no non-zero solutions. It is hyperbolic for $\omega^2 < 4$ and can have wave solutions. Thus if

$$p(x,y,z) = A\exp[i(\bar{K}.\bar{X})]$$

(2.5) yields the dispersion relation for 'inertial waves'

$$\omega = 2K_z/|K| = 2\cos\theta \qquad \ldots(2.6)$$

where θ is the angle between K_z (which is assumed to be parallel

to $\bar{\Omega}$) and $\bar{K}$. The phase velocity of these waves is given by

$$C_p = 2K_z\bar{K}/K^3 \qquad \ldots(2.7)$$

and is proportional to the wavelength, $2\pi/K$, of the wave, implying that the waves are dispersive, the longest wavelengths being the fastest. The waves also propagate anisotropically; the higher the frequency of a wave, the more parallel to the z axis is its phase velocity. The energy of these waves is transported at the group velocity of the wave packet to which they belong (Greenspan 1968), as can be seen by an asymptotic approximation of an initial disturbance obtained preferably by the stationary phase method (Stewartson 1978). This group velocity is given by

$$\bar{C}_g = \nabla_k \omega = \nabla_k \left[\frac{2\hat{\Omega}\cdot\bar{K}}{|K|} \right] = \frac{2}{K^3}\left[\bar{K}\times(\hat{\Omega}\times\bar{K})\right] \qquad \ldots(2.8)$$

where $\hat{\Omega}$ is a unit vector in the direction of $\bar{\Omega}$. This equation shows that energy transport for these waves occurs perpendicular to the phase velocity. It is also evident that $\bar{C}_g$ vanishes if $\bar{\Omega}$ is parallel to $\bar{K}$, implying that no energy can normally be propagated in directions parallel and anti-parallel to the rotation axis. However, if the source of the disturbance is permanent, for example, a vibrating solid body moving with velocity $\bar{u}$ parallel to the rotation axis, it can cause disturbances which travel upstream of the object for long distances as well as form a well developed wake behind it (Nigam and Nigam 1962). The reasons for this exception are to be found in the effects of viscosity on the fluid and the near non-dispersive nature of waves travelling parallel to the rotation

axis (Stewartson 1978).

The reflection of these waves by rigid boundaries displays some remarkable properties. Phillips (1963) showed that the magnitudes of the incident and reflected wavenumbers are generally unequal and the incoming and reflected flux vectors make equal angles with Ω_p, the projection of $\bar{\Omega}$ in the plane formed by $\bar{K}$ and $\hat{n}$, the unit vector normal to the boundary. A forward reflection occurs when the angle α_1 between Ω_p and the incident flux vector is larger than the angle α_2 between Ω_p and the boundary. When the two angles are equal the reflected wave packet travels parallel to the wall and is absorbed quickly due to dissipative viscous processes. When $\alpha_2 > \alpha_1$, a backward reflection occurs. The energy density per unit volume of the wave is not conserved and waves which increase their wavelengths, as a consequence of reflection, have their energy densities reduced after reflection. When viscous effects are taken into account in the above equations, it can be shown that in an unbounded fluid these waves are damped with an exponential decay time $\tau = 1/\omega K^2$. The wave solutions are no longer purely harmonic, and linear superposition of different waves can be permitted only for small wavenumbers. Phillips (1963) also showed that in a viscous fluid the reflection coefficient equals $1-O(R^{1/2})$ where R is the wave Reynolds number $(=2\Omega/\nu K^2)$, and thus for waves reverberating in a region of characteristic size L, the fractional energy loss by viscous attenuation is of the order of $2\nu K^2 LK/\Omega$ which is much higher than the energy loss by reflection. Thus when the fluid is contained in a large container of arbitrary shape, the energy

interchange between various wavenumbers from repeated reflections can result in a statistical radiative equilibrium over the high wavenumbers.

Poincare's equation (2.4) does not admit cylindrical wave solutions (usually described in terms of Bessel's functions of the wavenumber of the wave) of the type invoked in non-dispersive wave theory to approximate the scattered waves arising from diffraction from uneven surfaces (Hurley 1970). This has some interesting implications for the reflection of inertial waves from uneven boundaries. Hurley (1970) shows that in the case of a forward reflection the diffracted waves give rise to a positive back-scatter of energy. When inertial waves are diffracted from a wedge, the diffracted waves are as important as the incident and reflected waves in a region of a quarter wavelength around the apex of the wedge. Baines (1971 a) found that the waves incident on a sinusoidally varying surface of small amplitude generate, in addition to the reflected wave, two new waves whose wavenumbers are the sum and difference, respectively, of the wavenumbers of the surface perturbations and the incident waves. In a subsequent paper, Baines (1971 b) showed that when an inertial wave is incident on a smooth bumpy surface in such a way that its ray is tangential to the surface at some point, diffraction takes place. However if the ray of the reflected wave is tangential to the surface, a 'split-reflection' takes place wherein in addition to the back reflected (diffracted) wave, two reflected waves are generated on either side of the diffracted wave.

2.2.1. The effect of stratification When the fluid is stably stratified, the action of buoyancy force speeds up the inertial waves to produce inertial-gravity waves which satisfy the dispersion relation

$$\omega^2 = \frac{(\bar{N}\times\bar{k})^2 + (2\bar{\Omega}\cdot\bar{k})^2}{\bar{k}^2} \qquad \ldots(2.9)$$

Unlike inertial waves, these waves can have angular frequencies larger than 2 . Here $\bar{N}$ is the Väisälä-Brunt frequency already defined in (1.33). If we assume that $\bar{N}$ and $\bar{\Omega}$ are parallel to the z axis, then the effect of stratification is to increase the horizontal group velocities of the inertial waves considerably without effecting their vertical component.

2.2.2. Inertial Waves in Bounded Media.

(a) Circular Cylinder. Imagine a rotating fluid- filled circular cylinder defined by ($0<r<a$, $0<z<1$) in the cylindrical coordinates (r,ϕ,z). To obtain inertial wave solutions in this situation we need to solve equation (2.3) in the cylindrical coordinate system under the boundary conditions

$$\bar{u} = 0 \text{ on } r = a, \text{ and } \partial p/\partial z = 0 \text{ at } z = 0,1.$$

Phillips (1960) and Stewartson (1959, 1978) showed that under these conditions (2.3) admits separable solutions of the form

$$P = J_{|m|}(\zeta r/a)\exp(im\phi)\cos m\pi z \qquad \ldots(2.10)$$

where $J_{|m|}$ is the Bessel function of order m. These solutions yield a dispersion relation

$$\omega^2 = 4/[(1+\zeta)/(n^2\pi^2a^2)$$

relating the 'cylindrical wavenumber' ζ with the frequency ω of the wave. The boundary conditions however stipulate that

$$\zeta \frac{d}{d\zeta} J_{|m|}(\zeta) - \frac{2m}{\omega} J_{|m|}(\zeta) = 0 \qquad \ldots(2.12)$$

Consequently ω is different for waves moving with the rotation ($m > 0$) when compared with the waves moving against it ($m < 0$).

(b) Inertial waves in spheres. If we transform the cylindrical coordinates (r,ϕ,z) to modified oblate spheroidal coordinates system by

$$r = \left(\frac{4}{4-\lambda^2} - \eta^2\right)^{1/2} (1-\mu^2)^{1/2}$$

$$\phi = \phi$$

and $z = [(4/\lambda^2)-1]^{1/2}\eta\mu$

where $\lambda^2 = (4-\omega^2)/\omega^2$

then (2.5) transforms into Laplace's equation in $(x,y,iz/\lambda)$ and admits separable solutions of the form (Greenspan 1968)

$$P = P_n^{|m|}(0.5(4-\lambda^2)^{1/2}\eta)\ P_n^{|m|}(\mu)\ \exp(im\phi) \qquad \ldots(2.13)$$

where $P_n^{|m|}$ is the associated Legendre function. These wave solutions yield

$$P_n^m(\lambda/2) = [(4-\lambda^2)/2m]\ d/d\lambda[P_n^{|m|}(\lambda/2)] \qquad \ldots(2.14)$$

Experimental confirmation of this relation for several modes has been obtained by Aldridge and Toomre (1967) who studied the

resonance peaks in the pressure response of a rotating fluid sphere to different forcing frequencies. Mathematical solutions similar to equations (2.13) and (2.14) for ellipsoidal containers have been obtained by Kudlick(1966).

2.3 ROSSBY WAVES Rossby waves (also known as planetary waves in dynamical meteorology) arise in rotating fluids whenever the total height of individual fluid filaments is constrained to change slowly in certain direction(s) by the geometry of the container. Two such examples are a sliced right circular cylinder whose sliced face slopes at an angle to the other face and a fluid-filled thin spherical shell. In the former geometry no geostrophic modes are possible and are in fact replaced by the Rossby waves with the consequence that these waves possess a net mean vorticity. For the fluid-filled shell, geostrophic modes are possible and actually contain all the net vorticity of the fluid whereas Rossby modes, though possible, have no net mean vorticity. Inertial waves are possible in both cases (though devoid of any mean vorticity) and these together with Rossby waves and the geostrophic modes can synthesize any initial velocity distribution. As already shown in chapter one both these situations can be described in cartesian co-ordinates by reference to a Beta plane. If we neglect the effect of magnetic field (ie $V_a = 0$) then the dispersion relationship for Rossby waves follows directly from equation (1.66) giving

$$\omega = -\beta k/(k^2+l^2) \qquad \ldots(2.15)$$

which shows that Rossby waves always have westward phase velocities though their group velocity

$$\partial\omega/\partial k = \beta(k^2-l^2)/(k^2+l^2)^2 \qquad \ldots(2.16)$$

$$\partial\omega/\partial l = \beta 2kl/(k^2+l^2)^2 \qquad \ldots(2.17)$$

can be westward or eastward depending on whether $l > k$ or $l < k$. Reflection of these waves at barriers displays many interesting oddities. Longuet-Higgins (1964a), for example, showed that on reflection the angles between the wall and the two wave vectors are not in general equal, but the group velocity vectors of the two waves are directed at equal angles to the wall. Pedlosky (1979) similarly showed that although the amplitudes of the incident and reflected waves are conserved, their energy densities are not conserved, even though the energy fluxes through and out of the wall are equal.

An interesting study of the evolution of Rossby waves from an initial disturbance is reported by Pedlosky (1979). He employed the method of stationary phase in one direction to study the form of a complicated initial disturbance after a long time, and showed that for large time t and large distance x from the source region, the dominant contribution to the disturbance comes from the wavenumbers in the original spectrum whose group velocities allow them to travel the distance x in time t. The stream function of the disturbance at (x,t) is actually given by

$$\phi_m(x,t) = \sum_{k_s} \frac{2A_m(k_s)}{\left(t\left|\frac{\partial^2\omega}{\partial k^2}(k_s)\right|\right)^{1/2}} \cos\left(k_s x - \omega(k_s)t - \frac{\pi}{4}\,\mathrm{sgn}\,\frac{\partial^2\omega}{\partial k^2}(k_s)\right) \qquad \ldots(2.18)$$

where $A_n(k_s)$ is the initial amplitude of the wavenumber k_s which forms a stationary phase at the region under study. Thus the disturbance diminishes like $t^{-1/2}$, though slightly modified by the dependence of k_s on x/t. Pedlosky also describes how this approximation fails at the extreme front of the wave disturbance where the wave amplitude decays more like $t^{-1/3}$. He also carried out the necessary modifications of (2.18) in terms of an Airy's function.

2.3.1. Rossby Waves in Spherical Shells The equation of motion (2.3) can be written in terms of a stream function ψ in spherical coordinates $(r,\theta,\phi,)$, (Longuet Higgins, 1964a), as

$$\frac{\partial}{\partial t}(\nabla^2\psi) + 2\Omega\frac{\partial\psi}{\partial\phi} = 0 \qquad \ldots(2.19)$$

This equation possesses separable solutions of the form

$$\psi = P_n^s(\cos\theta)\exp[is(\phi - \dot{\phi}t)]$$

where $P_n^s(\cos\theta)$ is the associated Legendre function of order n associated with zonal wavenumber s. The substitution of these solutions in (2.19) yields the dispersion relation

$$\dot{\phi} = -2\beta/[n(n+1)] \qquad \ldots(2.20)$$

The angular velocity $\dot{\phi}$ is the westward phase velocity we encountered in the β plane approximation. If we write $\beta = 2\Omega\sin\theta$ and observe that $|K|$ of the β plane approximation equals $n(n+1)\sin\theta$, we get

$\phi = -\beta/K^2$ which is the same as equation (2.15).

2.3.2. The Stability of Rossby Waves The problem of the long term stability of Rossby waves to other perturbations is of great importance to meteorologists as such instabilities are frequently responsible for the unpredictability of the atmosphere. Lorenz (1972) showed that zonal steady flows present with superposed neutral Rossby waves are unstable to further perturbations either when the perturbations have wavelengths exceeding that of the basic Rossby wave or if the basic wave is sufficiently strong. Gill (1974) generalised the work of Lorenz to wavenumbers in arbitrary direction and showed that the stability of a wave depends on: (1) a parameter $M = UK^2/\beta$, where U is the velocity amplitude of the planetary wave, and, (2) the direction of the wavenumber of the planetary waves. For large M, the β effect on the waves is small and the problem reduces to the Rayleigh problem for a sinusoidal velocity distribution. For small M, the disturbance is comprised of two waves which form a resonantly interacting triad with the basic wave (Longuet-Higgins and Gill 1967). Whatever is the value of M, the maximum rate of growth is of the order of UK. Gill also showed that for large M, the wavenumber of the secondary disturbance can lie in a large area of the wavenumber space with the most unstable disturbance having its wavenumber at right angles to the wavenumber of the basic wave. For small M, the wavenumber space from which the unstable disturbance can be chosen is considerably reduced and the choice of the most unstable wave depends only on

the orientation of the basic wave. Both Lorenz and Gill used a Fourier expansion to represent the perturbation, and they truncated the resulting infinite system of algebraic equations at the first approximation with the consequence that the results can only be described as qualitative. Coaker (1977) employed a third order Floquet system to describe exactly the normal modes and by the help of perturbation theory he was able to present the curves of marginal stability in the M, ξ space where ξ is the orientation of the Rossby wave on the β plane. Similar studies on the stability of Rossby waves on a full sphere are described by Hoskins (1973) and Baines (1976).

2.4. ALFVEN WAVES The basic idea behind the ability of conducting fluids to support transverse waves in the presence of magnetic field can be appreciated by expressing the Lorentz force $\bar{J} \times \bar{B}$ in terms of Maxwell's stresses. By the help of Ampere's Law we can write

$$\bar{J} \times \bar{B} = -\nabla(\bar{B}\cdot\bar{B}/2\mu) + \nabla\cdot(\bar{B}\bar{B}/\mu) \qquad \ldots(2.21)$$

where the last term denotes the divergence of a dyad. This equation means that the Lorentz force $\bar{J} \times \bar{B}$ is equivalent to a hydrostatic pressure $B^2/2\mu$ along with a tension $B^2/2\mu$ along the lines of force, or equivalently a tension $B^2/2\mu$ along the lines of force with an equal pressure in the transverse direction. It is this 'pseudo-rigidity' provided by the tension along the lines of force which enables the conducting fluid to support transverse wave motions. These waves were first predicted by Alfven (1942)

and confirmed experimentially by Lundquist(1949a,b) and Lehnert(1954b). They were immediately recognised as the primary vehicle by which magnetic disturbances could be carried over large distances in astrophysical and planetary bodies without serious attenuation by the 'skin effect' prevalent in solid conductors (Roberts 1954). The basic properties and dispersion relationship of these waves have already been described in section 1.2 and will not be repeated here.

2.4.1. Alfven Waves in Compressible Media: Magneto-acoustic waves. When the medium is compressible, its density ρ cannot be assumed to be constant in equation (1.14) and must be eliminated by employing a thermodynamic constraint of the form $p/p_0 = \gamma \rho/\rho_0$ in an adiabatic regime. Here p_0 and ρ_0 are now the mean pressure and density of the fluid and γ is the ratio of specific heats. The new system of equations can be shown [Herlofson (1950), Alfven and Falthammar (1963)] to possess transverse-longitudinal plane wave solutions satisfying the dispersion relationship

$$\omega^4 - \omega^2 k^2 (V_a^2 + C_s)^2 + C_s^2 V_a^2 k^4 \cos^2\phi = 0 \qquad \ldots(2.22)$$

where C_s in the speed of sound in the fluid and ϕ is the angle between the direction of the magnetic field and the wave vector. This equation has two real and positive roots for ω corresponding to two different wave propagation velocities. The mode with the slower phase velocity is normally called a modified hydromagnetic wave whereas the other mode whose velocity is near the sound velocity is called a modified sound wave. For $\phi = 0$, ie. when

the wave vector is in the direction of the magnetic field, the former mode takes the form of Alfven waves (pure transverse waves) whereas the latter mode simplifies to pure sound waves (longitudinal waves), and there is no interaction between the two types of waves. An interesting phenomenon associated with these waves is that of over-reflection at a vortex sheet (Acheson 1976), or by a finite magnetic-velocity shear (Eltayeb 1977) when reflection coefficients of greater than unity are obtained.

2.4.2 Reflection and Transmission of Alfven Waves When an Alfven wave encounters an interface between two fluid media with different values of Alfven velocities, the wave is partly reflected and partly transmitted through the second fluid (Walen 1944, 1946; Lundquist, 1952; Ferraro 1954). Following Ferraro and Plumpton (1961), consider the situation when an Alfven wave of frequency ω in a fluid travelling in the z direction (which implies B_0 is parallel to the z axis) meets an interface at z=0 between the two fluids. The magnetic fields of incoming, reflected and transmitted waves can be represented by

$$b_i = A_i \exp[i\omega(t-z/V_1)] \qquad ...(2.23)$$

$$b_r = A_r \exp[i\omega(t+z/V_1)] \qquad ...(2.24)$$

and $$b_t = A_t \exp[i\omega(t-z/V_2)] \qquad ...(2.25)$$

where V_1 and V_2 are the Alfven wave velocities in fluids 1 and 2. Then the fluid velocities associated with these waves are

$$v_i = -A_i(\mu/\rho_1)^{1/2}\exp[i\omega(t-z/V_1)] \quad \ldots(2.26)$$

$$v_r = A_r(\mu/\rho_1)^{1/2}\exp[i\omega(t+z/v_1)] \quad \ldots(2.27)$$

$$v_t = -A_t(\mu/\rho_2)^{1/2}\exp[i\omega(t-z/v_1)] \quad \ldots(2.28)$$

At the interface the tangential components of the magnetic field and the fluid velocity are continuous, implying

$$b_i + b_r = b_t \quad \ldots(2.29)$$

$$v_i + v_r = v_t \quad \ldots(2.30)$$

These boundary conditions and the above wave equations yield the following amplitude relations

$$A_r = \frac{(\mu_2\rho_2) - (\mu_1\rho_1)^{1/2}}{(\mu_2\rho_2) + (\mu_1\rho_1)^{1/2}} A_i \quad \ldots(2.31)$$

and

$$A_t = \frac{2(\mu_2\rho_2)}{(\mu_2\rho_2)^{1/2} + (\mu_1\rho_1)} A_i \quad \ldots(2.32)$$

Equations (2.31) and (2.32) also give the reflection and refraction coefficients of the wave for a reflection against a rigid conducting boundary on substituting $\rho_2 = \infty$ in these equations. Then it can be seen that $|A_r| = 1$, and $A_t = 0$ and the waves suffer a phase shift of π in the velocity though the magnetic field is unchanged. The extension of these results to compressible media is given by Simon (1958) and Williams (1960). Fejer (1963) discovered the phenomenon of over-reflection associated with the reflection of these waves in compressible

media at fluid velocity discontinuities (Vortex sheets) already mentioned in Section 2.4.1. Fejer also showed that in this situation a single type of incident wave can give rise to a single type of refracted wave only.

2.5. INERTIAL-MAGNETOHYDRODYNAMIC (IMHD) WAVES: When, in addition to a magnetic field, a conducting incompressible fluid is subjected to rotation, the fluid can support modified Alfven waves known as inertial-magnetohydrodynamics waves which can propagate across the magnetic lines of force. Depending on the type of their energy content, these waves are known as inertial (energy, mainly in kinetic form) or magnetic modes (energy, mainly magnetic). A detailed description of their propagational behaviour has already been given in Section 1.3. In the following sections, mainly the problem of the stability of these waves and their propagation in non-uniform magnetic fields and media are discussed. The author's own work on reflection of these waves by rigid boundaries is described in Chapter 5.

2.5.1. Stability of IMHD waves. Hesselman (1967) pointed out that if a single wave train interacts with two infinitesimal disturbances such that the three waves constitute a resonant triplet, then under certain conditions, the initial infinitesial disturbances may grow with time. Thus he proposed that any wave-train capable of undergoing resonant interaction will be intrinsically unstable. Such a phenomenon, by virtue of non-linear effects, will 'create' fresh waves from the background of other imperceptible waves by sharing the energy of the initial

waves. This will cause the wave spectrum to become broader and more complex as time passes. Dillon (1975) and Bland (1976) showed that a single hydromagnetic wave of arbitrary amplitude in a rotating infinite medium is a solution of the full non-linear basic equations. This, however, is not true of a superposition of waves if their amplitudes are high. At second order in wave amplitudes it is found that a continuous transfer of energy between modes is possible if the kinematic conditions for resonance

$$\omega_1 \pm \omega_2 \pm \omega_3 = 0$$

$$\bar{K}_1 \pm \bar{K}_2 \pm \bar{K}_3 = 0$$

are satisfied. Dillon (1975) showed that IMHD waves do satisfy these conditions in the rapid rotation limit, and can thus form resonant interaction triplets. Neither Dillon nor Bland have studied the behaviour of the individual waves in a triplet over time, mainly because of the enormous mathematical complexity of the problem, and more results are eagerly awaited.

2.5.2. IMHD Waves in a Non-Uniform Magnetic Field Consider a rotating, incompressible fluid pervaded by a basic magnetic field $\bar{B}_0 = [B_x(z), B_y(z), 0]$ whose magnitude and direction vary slowly along the z axis. Now if some IMHD waves of a narrow frequency and wavenumber band $(\omega, \omega+\Delta\omega)$, $(\bar{K}, \bar{K}+\Delta\bar{K})$ are generated in this fluid at some place, in a short time they will move away from the source of disturbance in an area where the magnetic field is different. As the waves propagate, their frequencies will remain

unaltered although their wavenumbers $\bar{K}$ will be affected. Owing to the dependence of $\bar{B}_0$ on z only, the wavenumber components k and l will also remain unaffected and the changes in K will be brought about only be changes in the wavenumber component m. Locally the dispersion relation [see (1.36)]

$$\omega^2 \pm (2\bar{\Omega}\cdot\bar{K})\omega/|K| - (\bar{V}_a\cdot\bar{K})^2 = 0 \qquad \ldots(2.33)$$

still holds if $\bar{V}_a$ is chosen appropriate to the local magnetic field. By an analysis similar to the one given in section (2.3), Acheson (1972a) showed that in this situation (and for $\bar{N}=0$) the partial differential equations (1.27) to (1.31) admit plane wave solutions of the form

$$w = \hat{w}\exp[i(Kx+ly-\omega t]$$

w is the z component of velocity and on elimination of all other variables this equation yield a dispersion relation

$$(P^2-R^2)\hat{w}'' + (R^2P'/P+PP'-2iRT)\hat{w}' + [T^2-P^2(K^2+l^2) + iRP'T/P]\hat{w} = 0 \qquad \ldots(2.34)$$

where accents denote differentiation with respect to z and

$$P(z) = (V_xK+V_yl)^2/\omega^2 - 1 \qquad \ldots(2.35)$$

$$R(z) = 2\Omega_z/\omega \qquad \ldots(2.36)$$

$$T(z) = 2(\Omega_xK+\Omega_yl)/\omega \qquad \ldots(2.37)$$

$$V_x(z) = B_x(z)/(\mu\rho)^{1/2} \qquad \ldots(2.38)$$

and $V_y(z) = B_y(z)/(\mu\rho)^{1/2}$ ...(2.39)

Equation (2.34) has a singularity at $z=z_c$ where the field $B_0(z)$ reaches a critical value for which $P^2=R^2$ ie.

$$[B_x(z_c)k+B_y(z_c)l]^2/(\mu\rho\omega^2) - 1 = \pm 2\Omega_z/\omega \quad ...(2.40)$$

or equivalently

$$[(\bar{V}_c.\bar{K})^2 - \omega^2]^2 = 4\omega^2\Omega_z^2 \quad ...(2.41)$$

where V_c is the Alfven velocity at Z_c. Such singularities at cetain critical levels or surfaces have been reported in many other linear systems [for example in internal gravity waves in a shear flow (Bretherton 1966, Booker and Bretherton 1967) or in magneto-acoustic waves in a shear flow (Eltayeb, 1977)] and usually take the form of an invisible barrier at which a wave packet is neither reflected nor transmitted but effectively loses its energy to the fluid there. This can be seen clearly if one expresses (2.33) in terms of a quadratic in m as

$$\{[(\bar{V}_a.\bar{K})^2-\omega^2]^2 - 4\omega^2\Omega_z^2\}m^2 - 8\omega^2\Omega_z(\Omega_x k+\Omega_y l)m + \{(k^2+l^2)[(\bar{V}_a.\bar{K})^2-\omega^2]^2 - 4\omega^2(\Omega_x k+\Omega_y l)^2\} = 0 \quad ..(2.42)$$

and obtains the larger of the two roots asymptotically as

$$m_1 = 8\omega^2\Omega_z(\Omega_x k+\Omega_y l)/\{[(\bar{V}_a.\bar{K})^2-\omega^2]^2 - 4\omega^2\Omega_z^2\} \quad ...(2.43)$$

by neglecting the last term in (2.42). To the first order $V_a = V_a(z_c) + (z-z_c)V_a'(z_c)$ and therefore the wavenumber component $|m_1|$ of the wave increases indefinitely as $(z-z_c)^{-1}$ near the critical level. Similarly by differentiating (2.33) with respect

to m, the asymptotic value of the group velocity at the critical level for this wave is (Acheson 1972a)

$$C_{gz} = \frac{-4\omega^2\Omega_z(\Omega_x k + \Omega_y l)}{4\omega m_1^2|\Omega_z|[(\bar{V}_c\cdot\bar{k})^2+\Omega_z]^{1/2}}\ sgn\left[\omega^2-(\bar{V}_c\cdot\bar{k})^2\right]$$

which tends to zero as $(z-z_c)^{-2}$ with the consequence that although the wave group is neither reflected nor transmitted, it never reaches the critical level in a finite time. A novel feature of Acheson's work is that only the mode with wavenumber component m, which approaches the critical level from a direction such that

$$Q(m_1) = C_{gz}\Omega_z[(\bar{V}_c\cdot\bar{k})^2-\omega^2](\Omega_x k+\Omega_y l)\omega \quad > 0$$

is effectively captured in the neighbourhood of this level whereas mode m_2 for which $Q(m_2) < 0$ is transmitted across the critical field line. Thus a critical level acts as a valve by effectively permitting the wave to penetrate it from one side only. Another noteworthy feature of Acheson's analysis is that it clearly demonstrates that the phenomenon of critical-layer absorption does not in general require the presence of a mean shear flow. The effects of such a phenomenon on the waves in the earth's core cannot be over stressed as the earth's magnetic field is believed to be fairly non-uniform in the radial direction. If Acheson's conjecture, that the westward drift in the secular variations of the earth's magnetic field is caused by retrogradely propagating unstable inertial-magnetohydrodynamic waves (Acheson, 1972b), is correct, then the earth's toroidal magnetic field will have to be non-uniform (starting at about 5

Gauss at the core-mantle boundary and increasing to about 100 Gauss in the deeper parts) to render instability to these waves and critical level phenomenon will play a vital role in the dynamics of the core.

2.5.3. Inertial-Hydromagnetic-Gravity Waves in Magnetic-Velocity Shears IMHD-Gravity waves (or MAC waves from Magnetic-Archimedean-Coriolis) also display the phenomenon of critical-layer absorption in varying backgrounds. (Rudraiah and Venkatachalappa 1972; Eltayeb 1977; El Sawi and Eltayeb 1978, 1981; Grimshaw 1980). Consider for example a basic state in which

$$\bar{u}_0 = U(z)\,\hat{x}, \qquad \bar{B}_0 = B(z)\,\hat{y} \qquad \ldots(2.44)$$

so that the basic fluid velocity and the magnetic field (which are assumed to be parallel to the x and y directions respectively) are sheared in the z direction. In this situation an IMHD-gravity wave will satisfy a wave equation of the form (Eltayeb, 1977)

$$a(z)w''(z) + 2b(z)w'(z) + c(z)w(z) = 0 \qquad \ldots(2.45)$$

where w is the component of velocity in the z direction and accents denote differentiation with respect to the argument

$$a(z) = \hat{\omega}^2 - l^2V_a^2 - 4\Omega^2\hat{\omega}^2/(\hat{\omega}^2 - l^2V_a^2) \qquad \ldots(2.46)$$

$$b(z) = -U'[-2i\Omega l + klV_a^2/\hat{\omega} + 4\Omega^2\hat{\omega}^3 k/(\omega^2 - l^2V_a^2)] - l^2V_aV_a'[1+4\Omega^2\hat{\omega}^2/(\hat{\omega}^2 - l^2V_a^2)] \qquad \ldots(2.47)$$

$$c(z) = U''[k(\hat{\omega}^2 - l^2 V_a^2/\hat{\omega} + 2i\Omega l] + 2k^2 U'^2 [2i\Omega l/(k\hat{\omega}) - l^2 V_a^2/\hat{\omega}^2]$$
$$-2l^2 V_a V_a' \, kU'/\hat{\omega}^2 - (\hat{\omega}^2 - l^2 V_a^2 - N^2)(k^2 + l^2) \quad \ldots(2.48)$$

$\hat{\omega}$, k, l are the frequency and the horizontal wavenumbers of the wave, respectively. Ω is the rotational velocity and $\bar{V}_a$ is the local Alfven velocity. The partial differential equation has a singularity at a(z) = 0, which from (2.46) occurs at $(\omega^2 - l^2 V_a^2)^2 = 4\Omega^2\omega^2$. As already discussed, these singularities are accompanied by the phenomenon of critical layer formation. Although both the magnetic field and the basic velocities vary continuously, locally the waves still satisfy the dispersion relationship

$$m^2 = \frac{(k^2+l^2)(\hat{\omega}^2 - l^2 V_a^2)(N^2 + l^2 V_a^2 - \hat{\omega}^2)}{(\hat{\omega}^2 - l^2 V_a^2) - 4\Omega^2\hat{\omega}^2} \quad \ldots(2.49)$$

and thus $m \longrightarrow \infty$ at critical levels as for IMHD waves. According to a criterion from McKenzie (1972), a critical level can exist only if the wave normal curve (basically the cross-section of the wave normal surface in the plane of propagation) possesses an asymptote in the direction in which the properties of the medium vary. When this criterion is applied to the present problem it can be shown that four asymptotes of this kind occur for every wave (Eltayeb 1977) and thus for every wave four critical levels can be defined where the wave will be highly attenuated. A useful concept in studying this phenomenon is that of a wave invariant, also known as wave action (Andrew and McIntyre, 1978) such as the vertical flux of angular momentum which is conserved everywhere along the basic shear except at critical levels where it jumps from one constant value to another. By the help of this quantity

it becomes possible to discriminate between real critical levels and pathological ones (e.g. at $\hat{\omega} = 0$, when k,l and $V_a \longrightarrow 0$ making a = 0), where no change occurs in the wave invariant. El Mekki and Eltayeb (1978) pointed out that critical levels will exist in the solar atmosphere as a consequence of the increase of the Alfven speed with height.

2.6. ROSSBY-MHD WAVES These very low frequency inertial magnetohydrodynamic waves which arise due to the combined effects of rotation and curvature of the fluid bodies on magnetohydrodynamic waves were first proposed by Hide (1966), and we have already dealt with their solutions and propagational properties at length in Section 1.4. Numerous other studies on the propagation and stability of these waves in homogeneous and in homogeneous basic states have appeared since, and are reviewed in this section.

Negi and Singh (1974) presented a similarity solution of the wave equation on the β plane given by Hide (1966). They first uncoupled the inertial modes by ignoring inertia terms in the equations of motion and derived a third order partial differential wave equation suitable for magnetic modes only in the form

$$\beta \frac{\partial b_y}{\partial t} + V_a^2 \nabla^2 \left(\frac{\partial b_y}{\partial x} \right) = 0 \qquad \ldots(2.50)$$

where b_y is the magnetic field of the wave in the N-S direction, and V_a is the Alfven speed. Then, by assuming that the fluid variables do not vary with respect to y (an assumption which, the

present author feels, is rather hard to justify), they approximate (2.50) to

$$\beta \frac{\partial b_y}{\partial t} + V_a^2 \frac{\partial^3 b_y}{\partial x^3} = 0 \qquad \ldots(2.51)$$

and show by the method of similarity that it has solutions given by

$$b_y = a (\sqrt{\beta V_a}\, t)^{-1/3} \, Ai\left[x/(3 V_a^2 t/\beta)^{1/3} \right] \qquad \ldots(2.52$$

which decay as $t^{-1/3}$. Superficially, this solution resembles one of the author's own solutions [see equation (3.66)] which was obtained by the method of stationary phase for waves trapped near a caustic. But whereas this solution is periodic elsewhere, Negi and Singh made the drastic assumption that $\partial/\partial y(u,v,b_x,b_y) = 0$ which by the continuity equations (1.57) and (1.58) results in $\partial/\partial x(u,b_x) = 0$ and restricts the solutions to those which will satisfy u = constant, and b_x = constant in the x-y plane. Perhaps not surprisingly they obtain only decaying solutions.

2.6.1. Stability of Rossby-MHD Waves An exhaustive study of the stability of Rossby-MHD waves on a β-plane was carried out by Bland (1976). He showed that the necessary (but not sufficient) conditions under which the primary wave is unstable to two other secondary disturbances are the same as the kinematic resonance conditions, that is

$$\omega_1 \pm \omega_2 \pm \omega_3 = 0$$

$$\bar{K}_1 \pm \bar{K}_2 \pm \bar{K}_3 = 0$$

and from a study of the dispersion relationship of these waves

this requires that in order, $(\omega_1, \bar{K}_1)$ be unstable to two infinitesimal disturbances, its wavenumber $\bar{K}_1$ should be intermediate to those of the perturbation waves, that is

$$|\bar{K}_2| \lesseqgtr |\bar{K}_1| \lesseqgtr |\bar{K}_3| \qquad \ldots(2.53)$$

This suggests that the energy does not 'cascade' to lower wave modes as in turbulence. Bland studied the amplitudes of the waves of an interacting triad over a time period by employing a two time technique. A fast time variable t describes the typical time periods of the waves whereas a slow time variable T is used to study the slowly varying wave amplitudes. By the help of non-linear analysis, Bland showed that the slowly varying amplitudes of the waves are governed by equations of the form

$$da_i/dT = C_{i+1}\, C_{i+2}\, a_{i+1}\, a_{i+2} \qquad i = 1,2,3 \qquad \ldots(2.54)$$

where a_i is the amplitude of the wave i and $C_{i+1}\ C_{i+2}$ is the interaction parameter which should not be equal to zero (dynamic condition of resonance) for an interacting triad. The total energy (kinetic plus magnetic) associated with the three waves remains constant. However, the individual waves do not conserve their energy and so kinetic and magnetic energies are continually redistributed amongst these waves. The solutions of the interaction equations (2.54) are periodic in time and can be expressed in terms of Jacobian elliptic functions. In a particular novel situation, Bland showed that the energy of a magnetic mode is lost to two inertial Rossby-MHD modes in such a way that although the total energy of the system remains

constant, its kinetic part of the energy increases at the expense of its magnetic energy. An analogous situation in which the magnetic mode increases its energy at the expense of the inertial modes is also possible.

2.6.2. Rossby-MHD Waves in Magnetic and Velocity Shears. The first attempt to generalise Hide's 1966 model to non-uniform magnetic fields was made by Suffolk and Allan (1969). While still employing the beta-plane model, they assumed in addition that the magnetic field was sheared in the y direction, that is

$$\bar{B}_0 = (B_0(y), 0, 0) \qquad \ldots(2.55)$$

The modified vorticity equation (1.54) can then be written as

$$\frac{\partial \zeta}{\partial t} + \beta v - \frac{B_0}{f} \frac{\partial j_z}{\partial x} = 0 \qquad \ldots(2.56)$$

where j_z is the disturbance in the z component of the current. Similarly the electrodynamic equations (2.51) and (2.52) can be combined into

$$\mu \frac{\partial j_z}{\partial t} - B_0 \frac{\partial \zeta}{\partial x} + 2B_0' \frac{\partial v}{\partial x} = 0 \qquad \ldots(2.57)$$

In addition we have

$$\zeta = \frac{\partial u}{\partial y} - \frac{\partial v}{\partial x} \qquad \ldots(2.58)$$

and $$\frac{\partial u}{\partial x} + \frac{\partial v}{\partial y} = 0 \qquad \ldots(2.59)$$

Suffolk and Allan then assume small amplitudeperturbations

$$F(\omega,k,l) = a \exp[i(k_x+ly-\omega t)] \qquad \ldots(2.60)$$

to all the four variables in the above equations and obtain the dispersion relationship

$$\omega^2 + \frac{\omega\beta k}{k^2+l^2} - k^2 V_a^2 + \frac{ik^2 l (V_a^2)'}{k^2+l^2} = 0 \qquad \ldots(2.61)$$

where V_a is the local Alfven velocity and accent denotes differentiation with respect to y. This dispersion relationship shows that except for $l = 0$, the frequencies always have a non zero imaginary part, suggesting that the waves are unstable, that is, their amplitudes increase or decrease with time. This is a highly unexpected result in comparison with the results of Acheson (1972) for propagation of IMHD waves in non-uniform magnetic fields (section 2.5.2). There is no evidence of instability due to the variations of the basic magnetic fields in any of the waves studied above. The author believes that this fallacy in Suffolk and Allan's analysis stems from the assumption that l, the wavenumber component in the y direction, is independent of y and thus constant in (2.60) and (2.61). Therefore any variations in V_a in (2.61) with distance will have to be compensated by changes in ω. This is not correct. A careful analysis of the kinematics of wavecrests in any inhomogeneous system (Lighthill, 1965, p13) reveals that energy in waves of a given frequency should remain always in the waves of the same frequency. As these waves propagate to a different region of space with a different basic state, their wavenumber components

in the direction of the basic change can be expected to change. Eltayeb and McKenzie (1977), in a similar study for Rossby-MHD waves in a magnetic and velocity shear, followed this principle and correctly deduced that the waves are stable and that a critical level should be observed for a wave of frequency (doppler shifted) at a place where

$$\hat{\omega}^2 = (\bar{V}_a.\bar{K})^2 \qquad \ldots(2.62)$$

and a reflection will occur where $L^2 = 0$.

In a 'jet-like' variation of $\bar{B}$ with latitude (that is $\bar{B}$ increases or decreases in strength on either side of the latitude under investigation) inertial modes will be trapped around the centre of the magnetic jet. When the variations in the basic state are abrupt, that is when $2\pi/l >> L$, where L is the length scale of the variation of the basic state, the treatment in terms of reflection and transmission through a current-vortex sheet is preferable. Eltayeb and McKenzie showed that when this sheet is parallel to the x axis, an over-reflexion can occur if

$$\hat{\omega}_1 \hat{\omega}_3 < 0$$

where $\hat{\omega}_1$ and $\hat{\omega}_3$ are the doppler shifted frequencies of the waves in medium 1 and 3. If we take medium 1 to be at rest so that $\hat{\omega}_1 = \omega$, then $\hat{\omega}_3$ will have to be negative for an over reflexion to occur, which is possible only if the jump in speed $|U_3|$ is greater that V_3, the Alfven speed in medium 3.

CHAPTER THREE

PROPAGATION OF ROSSBY-MAGNETOHYDRODYNAMIC WAVES GENERATED BY AN INITIAL DISTURBANCE

3.1 GENERAL A close examination of the dispersion relationship (1.66) for hydromagnetic Rossby waves (Hide 1966, Hide and Jones 1972) indicates that these waves are highly dispersive (ie. $\partial\omega/\partial k \neq$ constant, $\partial\omega/\partial l \neq$ constant) and anisotropic ($\partial\omega/\partial k \neq \partial\omega/\partial l$ in general) in their propagation. As a result they will not spread out isotropically from the source eg. as water waves in a pond do, and will not be expected to attenuate as a simple function of distance from the source region. The question we therefore ask ourselves is: How will an initial complicated disturbance generated by a source impulse in a localised region evolve in time and propagate away from the source region? Mathematically, we are concerned with an initial-value problem in which at time t=0, $\zeta(x,y,0) = \zeta_0(x,y)$ and we wish to calculate $\zeta(x,y,t)$ for large time t. We shall employ the method of stationary phase (Jeffreys and Jeffreys 1956, Lighthill 1965, 1978, Pedlosky 1979) to examine the asymptotic form of the initial disturbance for both large (x,y) and t. We shall work once again with the β plane approximation of the quasi-geostrophic fluid motions of a thin fluid shell or the fluid contained between the sloping walls of a container.

3.2 FORMULATION OF THE PROBLEM For small amplitude disturbances, the vorticity $\zeta(x,y,t)$ of an incompressible inviscid and highly conducting fluid on a β plane in the

presence of a uniform magnetic field B_0 is given by (see equation 1.64)

$$\left[\frac{d^2}{dt^2} - V_a^2\left(\cos\theta\frac{\partial}{\partial x} + \sin\theta\frac{\partial}{\partial y}\right)^2\right]\nabla_H^2\zeta + \beta\frac{d}{dt}\frac{\partial\zeta}{\partial x} = 0 \qquad \ldots(3.1)$$

In addition the components of fluid velocity (u,v) and magnetic field (b_x, b_y, b_z) of the disturbance satisfy the following differential equations (see section 1.4)

$$db_x/dt = B_0(\cos\theta\,\partial/\partial x + \sin\theta\,\partial/\partial y)u \qquad \ldots(3.2)$$

$$db_y/dt = B_0(\cos\theta\,\partial/\partial x + \sin\theta\,\partial/\partial y)v \qquad \ldots(3.3)$$

$$db_z/dt = 0 \qquad \ldots(3.4)$$

$$\partial b_x/\partial x + \partial b_y/\partial y = 0 \qquad \ldots(3.5)$$

and $$\partial u/\partial x + \partial v/\partial y = 0 \qquad \ldots(3.6)$$

where $$\zeta = \partial v/\partial x - \partial u/\partial y \qquad \ldots(3.7)$$

Now let us assume that a localised disturbance of arbitrary form is imparted to the fluid in the vicinity of x=0, y=0 at time t=0. By Fourier's theorem it will consist of many waves (the longest of which will have wavelengths of the order of the size of the source region), and therefore, the nature of propagation of this dispersive wave packet will be quite complex. For a short time after the disturbance is made, it will retain its initial basic form, though after a long time the disturbance would have spread over large distances and the wave propagation dynamics would have had sufficent time to contribute strongly to the waveform, dispersing waves of different wavenumbers in different

regions of the x-y plane. The essential dispersion relationship can be obtained by expressing equation (3.1) in the wave domain by the help of the Fourier transform.

Let us define the Fourier transform and its inverse for a function f(x,y,t) by

$$F(k,l,t) = \int_{-\infty}^{\infty}\int_{-\infty}^{\infty} \exp[i(kx+ly)]\, f(x,y,t)\, dx\, dy \qquad ...(3.8)$$

and $$f(x,y,t) = \frac{1}{(2\pi)^2}\int_{-\infty}^{\infty}\int_{-\infty}^{\infty} \exp[i(kx+ly)]\, F(k,l,t)\, dk\, dl \qquad ...(3.9)$$

where k and l are the wavenumbers of the function F in x and y directions, respectively. Then the Fourier transformation of the L.H.S. of equation (3.1) yields

$$-(k^2+l^2)\left[\frac{\partial^2}{\partial t^2} + V_a^2(k\cos\theta + l\sin\theta)^2\right]\mathfrak{F}(k,l,t) + \beta\frac{\partial}{\partial t} ik\,\mathfrak{F}(k,l,t) = 0$$

where it has been assumed that the perturbations in the fluid motion are small and the basic fluid velocity is zero. ie.

$$\partial/\partial t = d/dt$$

or $$\frac{\partial^2\mathfrak{F}(k,l,t)}{\partial t^2} - i\beta\frac{k}{k^2+l^2}\frac{\partial\mathfrak{F}(k,l,t)}{\partial t} + V_a^2 k^2\mathfrak{F}(k,l,t) = 0 \qquad ...(3.10)$$

if we assume that $\theta = 0$, ie. the basic magnetic field is latitudinal. Equation (3.10) will possess solutions of the form

$$\mathfrak{F}(k,l,t) = A(k,l)\exp[-i\omega(k,l)t] \qquad ...(3.11)$$

which when substituted in equation (3.10) yields the desired dispersion relationship

$$\omega^2 + \beta k/(k^2+l^2)\omega - V_a{}^2k^2 = 0 \qquad \ldots(3.12)$$

which as we can see is identical to the one given by Hide(1966). The two roots of ω correspond to inertial and magnetic modes of oscillation of plane waves and are given by

$$\omega_{i,m} = \frac{-\beta k}{2(k^2+l^2)}\left[1 \pm \left(1 + (2V_a(k^2+l^2))^2\right)^{1/2}\right] \qquad \ldots(3.13)$$

depending on whether the positive or the negative sign is taken.

Now let us try to obtain a complete solution for $\mathfrak{z}(x,y,t)$ under the initial condition

$$\mathfrak{z}(x,y,o) = \mathfrak{z}_0(x,y) \qquad (3.14)$$

This initial waveform of the disturbance can be decomposed into an infinite numbers of waves each given by

$$\mathfrak{z}(k,l,0) = \int_{-\infty}^{\infty}\int_{-\infty}^{\infty}\mathfrak{z}(x,y,0)\exp[i(kx+ly)]dx\,dy \qquad \ldots(3.15)$$

Substitution of this initial condition in equation (3.11) shows

$$A(k,l) = \mathfrak{z}(k,l,0) = \int_{-\infty}^{\infty}\int_{-\infty}^{\infty}\mathfrak{z}(x,y,0)\exp[i(kx+ly)]dx\,dy \qquad \ldots(3.16)$$

The disturbance thus consists of an infinite Fourier superposition of plane waves of form (3.11) each with a different wavenumber K(k,l) and oscillating with frequency $\omega(k,l)$ which is determined by equation (3.13). The amplitude of each mode is given completely by equation (3.16). Therefore, our complete solution can be written as

$$\mathfrak{z}(x,y,t) = 1/(2\pi)^2\int_{-\infty}^{\infty}\int_{-\infty}^{\infty}A(k,l)\exp[i(kx+ly-\omega t)dk\,dl \qquad \ldots(3.17)$$

3.3 THE ASYMPTOTIC EVALUATION OF THE WAVE INTEGRAL To evaluate $\zeta(x,y,t)$, we shall examine its asymptotic form for large t by the method of stationary phase. For the sake of brevity, only a basic description of the method outlining the physical reasoning behind the asymptotic approximation will be presented here, though more rigorous derivations can be seen in Jeffreys and Jeffreys (1956) or Lighthill (1978). The basic idea is that as $t \to \infty$, with x/t, y/t fixed, the phase Φ of the exponential term in equation (3.17) is a rapidly fluctuating function of k and l (Pedlosky 1979), ie for large t the function

$$\Phi = t\, g(k,l) = t[(x/t)k + (y/t)l - \omega(k,l)] \qquad \ldots(3.18)$$

changes by large amounts for very small variations of k and l as

$$\partial\Phi/\partial k = t(x/t - \partial\omega/\partial k) \qquad \ldots(3.19)$$

and $$\partial\Phi/\partial l = t(y/t - \partial\omega/\partial l), \qquad \ldots(3.20)$$

become very large. Thus as t increases both the real and imaginary parts of $\exp[i(kx+ly-\omega t)]$ oscillate more and more widely between plus and minus one. One can envisage a situation in which finally for a very large t, the contribution to the integral (3.17) from one value of K(k,l) will be cancelled by a neighbouring value of K(k,l) for which the phase has advanced by π. This will be possible of course only if A(k,l) is asmoothly varying function of k and l, and is thus nearly the same for both values of K(k,l). This type of behaviour can be expected to occur for all values of K(k,l) except for those values $K(k_s,l_s)$ for which the phase Φ is stationary ie. $\partial\Phi/\partial k = 0$ and $\partial\Phi/\partial l = 0$,

which as can be seen from equations (3.19) and (3.20) occur at points where

$$x/t = \partial\omega/\partial k\ (k_s,l_s) \quad \text{and} \quad y/t = \partial\omega/\partial l\ (k_s,l_s) \qquad ...(3.21)$$

Therefore, the main contribution to the integral of equation (3.17) will arise from the neighbourhood of those wavenumbers which satisfy equations (3.21). Equations (3.21) have a simple interpretation. After a large lapse of time after the initial disturbance, the main contribution to $\zeta(x,y,t)$ at a point (x,y) comes from only those wavenumbers whose group velocity ($\partial\omega/\partial k$, $\partial\omega/\partial l$) has allowed them to travel a distance x in the east and y in the north direction from the point of disturbance at x=y=0 in this time t. Thus at any large time, relations (3.21) can be employed to map the location of the dominant wavenumbers $K(k_s,l_s)$ at each point on the x,y plane.

Now, in the tiny interval around $K(k_s,l_s)$, $\omega(k,l)$ can be expanded to second order by the help of Taylor's theorem giving

$$\omega(k,l) = \omega(k_s,l_s) + (k-k_s)\frac{\partial\omega}{\partial k}(k_s,l_s) + (l-l_s)\frac{\partial\omega}{\partial l}(k_s,l_s) + \frac{1}{2}\left[\frac{\partial^2\omega}{\partial k^2}(k_s,l_s)(k-k_s)^2 + \frac{\partial^2\omega}{\partial l^2}(k_s,l_s)(l-l_s)^2 + 2(k-k_s)(l-l_s)\frac{\partial^2\omega}{\partial k\,\partial l}(k_s,l_s)\right] \qquad ...(3.22)$$

so that

$$kx+ly-\omega t = \left[k_s x + l_s y - \omega(k_s,l_s)t\right] + \left[x - \frac{\partial\omega}{\partial k}(k_s,l_s)t\right](k-k_s) + \left[y - \frac{\partial\omega}{\partial l}(k_s,l_s)t\right](l-l_s) - \frac{t}{2}\left[\frac{\partial^2\omega}{\partial k^2}(k_s,l_s)(k-k_s)^2 + \frac{\partial^2\omega}{\partial l^2}(k_s,l_s)(l-l_s)^2 + 2\frac{\partial^2\omega}{\partial k\,\partial l}(k_s,l_s)(k-k_s)(l-l_s)\right] \qquad ...(3.23)$$

The second and third terms in this equation vanish by virtue of stationary phase relations (3.21). Thus for large t, the integral (3.17) can be approximated by

$$\zeta(x,y,t) = \frac{1}{4\pi^2} \int_{l_s-\Delta}^{l_s+\Delta} \int_{k_s-\Delta}^{k_s+\Delta} A(k,l)\ \exp\left[i(k_s x + l_s y - \omega(k_s,l_s)t\right] \times$$

$$\exp\left[\frac{-it}{2}\left(\frac{\partial^2\omega}{\partial k^2}(k_s,l_s)(k-k_s)^2 + \frac{\partial^2\omega}{\partial l^2}(k_s,l_s)(l-l_s)^2 + 2(k-k_s)(l-l_s)\frac{\partial^2\omega}{\partial k\,\partial l}(k_s,l_s)\right)\right] dk\,dl \quad \ldots(3.24)$$

where 2Δ is the tiny interval around k_s and l_s in which the phase of $\zeta(x,y,t)$ can be termed stationary. In this interval $A(k,l)$ can be replaced by its mean value $A(k_s,l_s)$ as it is a smooth function of k and l. Thus

$$\zeta(x,y,t) = \frac{1}{4\pi^2} A(k_s,l_s)\ \exp\left[i(k_s x + l_s y - \omega(k_s,l_s)t\right] \times$$

$$\int_{l_s-\Delta}^{l_s+\Delta} \int_{k_s-\Delta}^{k_s+\Delta} \exp\left[\frac{-it}{2}\left(\frac{\partial^2\omega}{\partial k^2}(k_s,l_s)(k-k_s)^2 + \frac{\partial^2\omega}{\partial l^2}(k_s,l_s)(l-l_s)^2 + 2(k-k_s)(l-l_s)\frac{\partial^2\omega}{\partial k\,\partial l}(k_s,l_s)\right)\right] dk\,dl \quad \ldots(3.25)$$

The final result is independent of the size of Δ as long as it is small. Now introduce

$$P = [t/2\ \partial^2\omega/\partial k^2\ (k_s,l_s)\ \mathrm{sgn}(\partial^2\omega/\partial k^2\ (k_s,l_s))]^{1/2}(k-k_s) \quad \ldots(3.26)$$

$$Q = [t/2\ \partial^2\omega/\partial l^2\ (k_s,l_s)\ \mathrm{sgn}(\partial^2\omega/\partial l^2\ (k_s,l_s))]^{1/2}(l-l_s) \quad \ldots(3.27)$$

in equation (3.25) which becomes

$$\zeta(x,y,t) = \frac{1}{4\pi^2} \exp\left[i(k_s x + l_s y - \omega(k_s,l_s)t)\right] A(k_s,l_s) \times$$

$$\frac{1}{N} \int_{-Q_s}^{Q_s} \int_{-P_s}^{P_s} \exp\left[i\left(P^2\,\mathrm{sgn}\frac{\partial^2\omega}{\partial k^2}(k_s,l_s) + Q^2\,\mathrm{sgn}\left(\frac{\partial^2\omega}{\partial l^2}(k_s,l_s) + 2mPQ\right)\right] dP\,dQ \quad \ldots(3.28)$$

where $\mathrm{sgn}\frac{\partial^2\omega}{\partial k^2}(k_s,l_s) = \begin{cases} +1 & \text{if } \frac{\partial^2\omega}{\partial k^2}(k_s,l_s) > 0 \\ -1 & \text{if } \frac{\partial^2\omega}{\partial k^2}(k_s,l_s) < 0 \end{cases}$

$$P_s = \Delta[t/2\ |\partial^2\omega/\partial k^2\ (k_s,l_s)|]^{1/2} \quad \ldots(3.29)$$

$$Q_s = \Delta\,[t/2\,|\partial^2\omega/\partial l^2\ (k_s,l_s)|]^{1/2} \qquad \ldots(3.30)$$

$$m = \frac{\partial^2\omega}{\partial k\,\partial l}(k_s,l_s) \Big/ \left(\left|\frac{\partial^2\omega}{\partial k^2}(k_s,l_s)\,\frac{\partial^2\omega}{\partial l^2}(k_s,l_s)\right| \right)^{1/2}$$

and $N = t/2[\,|\partial^2\omega/\partial k^2\ (k_s,l_s)\ \partial^2\omega/\partial l^2\ (k_s,l_s)|]^{1/2}$

As $t \to \infty$, $P_s \to \infty$ and $Q_s \to \infty$ and (3.28) reduces to a definite integral.

Now, noting from Gradshteyn and Ryzhik (1965) p.397

$$\int_0^\infty \sin(ax^2+2bx+c)dx = 0.5(\pi/a)^{1/2}\ \sin[\pi/4 + (ac-b^2)/a],\quad a > 0$$

and $$\int_0^\infty \cos(ax^2+2bx+c)dx = 0.5(\pi/a)^{1/2}\ \cos[\pi/4 + (ac-b^2)/a],\quad a > 0$$

the inner integral in equation (3.28) reduces to

$$\sqrt{\pi}\ \exp i\left[\frac{\pi}{4} + Q^2\left(\frac{\operatorname{sgn}\frac{\partial^2\omega}{\partial k^2}(k_s,l_s)\ \operatorname{sgn}\frac{\partial^2\omega}{\partial l^2}(k_s,l_s) - 4m^2}{\operatorname{sgn}\ \frac{\partial^2\omega}{\partial k^2}(k_s,l_s)}\right)\right].$$

Also note that $\int_0^\infty \sin(ax^2)dx = \int_0^\infty \cos(ax^2)dx = 0.5[\pi/2a]^{1/2},\quad a > 0$

(Gradshteyn and Ryzhik (1965) p.395

and the integral (3.28) simplifies to

$$\zeta(x,y,t) = \sum_{k_s,l_s} \frac{1}{2\pi}\ t\left[\left|\frac{\partial^2\omega}{\partial k^2}(k_s,l_s)\frac{\partial^2\omega}{\partial l^2}(k_s,l_s) - \left(\frac{\partial^2\omega}{\partial k\,\partial l}(k_s,l_s)\right)^2\right|\right]^{1/2} \frac{A(k_s,l_s)}{\exp i[k_s x + l_s y - \omega t - \phi]} \qquad \ldots(3.31)$$

where contributions from all stationary phases are to be summed

and $$\Phi = \frac{\pi}{4}\operatorname{sgn}\frac{\partial^2\omega}{\partial k^2}(k_s,l_s) + \frac{\pi}{4}\operatorname{sgn}\left[\frac{\partial^2\omega}{\partial l^2}(k_s,l_s) - m^2\ \operatorname{sgn}\frac{\partial^2\omega}{\partial k^2}(k_s,l_s)\right] \qquad \ldots(3.32)$$

Thus $\phi = \pi/2, -\pi/2$ or 0, as the integral is evaluated over a maximum, minimum or a saddle point of ω.

It appears from equation (3.31) that the wave amplitude diminishes like $(t)^{-1}$, which is not strictly true since $\omega(k_s, l_s)$ and hence its first and second derivatives are all complicated functions of x/t and y/t by virtue of (3.21). [But see the discussion following equation (3.33).] To calculate the denominator and the exponential terms of equation (3.31), we need to obtain k_s and l_s in terms of x/t and y/t. This mapping can be done by inverting the equations (3.21), where the required values of functions $\partial\omega/\partial k\ (k_s, l_s)$ and $\partial\omega/\partial l\ (k_s, l_s)$ can be obtained by differentiating the dispersion relationship (3.13) w.r.t. k and l, respectively. However, it will be seen that the expressions for $\partial\omega/\partial k\ (k_s, l_s)$ and $\partial\omega/\partial l\ (k_s, l_s)$ are highly non-linear functions of k_s and l_s, and it will thus be impossible to obtain analytical solutions of k_s and l_s in terms of x/t and y/t. We can overcome this difficulty by studying the phenomenon separately for small and large wavenumber limits.

3.3.1 <u>The small wavenumber limit.</u> For most wavesof planetary dimensions wavenumber $|K| = (k^2+l^2)^{1/2} << (\beta/2V_a)^{1/2}$ and as a result equations (3.13) can be simplified by the help of binomial expansion to

$$\omega_i \simeq -\beta k/(k^2+l^2) \qquad \ldots(3.33)$$

$$\omega_m \simeq (V_a^2/\beta)\, k(k^2+l^2) \qquad \ldots(3.34)$$

Equation (3.33) is the well known dispersion relationship for

ordinary Rossby waves to which our inertial modes reduce to, in the small wavenumber approximation. We will not investigate these modes any further as they have already been the subject of similar investigations by other fluid dynamicists (see eg. Pedlosky 1979 p.130-144.)

The frequency of the magnetic modes is a straight forward function of wavenumbers k and l in the small wave number limit. Differentiate (3.34) w.r.t. k and l to obtain

$$\partial\omega/\partial k\ (k_s,l_s) = x/t = (V_a^2/\beta)\ (3k_s^2+l_s^2) \qquad ...(3.35)$$

and $$\partial\omega/\partial l\ (k_s,l_s) = y/t = (2V_a^2/\beta)\ k_s l_s \qquad ...(3.36)$$

These expressions can be easily inverted to obtain k_s and l_s as functions of x/t and y/t, which are now given by

$$k_s = \frac{1}{\sqrt{12}} \left(\frac{\beta}{V_a^2}\right)^{1/2} \left[\left(\frac{x}{t} + \sqrt{3}\frac{y}{t}\right)^{1/2} \pm \left(\frac{x}{t} - \sqrt{3}\frac{y}{t}\right)^{1/2} \right] \qquad ...(3.37)$$

$$l_s = \frac{1}{2}\left(\frac{\beta}{V_a^2}\right)^{1/2} \left[\left(\frac{x}{t} + \sqrt{3}\frac{y}{t}\right)^{1/2} \mp \left(\frac{x}{t} - \sqrt{3}\frac{y}{t}\right)^{1/2} \right] \qquad ...(3.38)$$

where the negative sign is to be taken in l_s when positive sign is taken for k_s and vice-versa. Thus there is a kind of inverse relationship between wavenumbers k_s and l_s; l_s being small when k_s is large and k_s is small when l_s is large. Clearly two wave solutions are possible for each positive value of x (if β is positive), thus the waves propagate only in those two quadrants where x is positive. Further no solutions occur for k_s and l_s outside the region defined by $x \geq \sqrt{3}\,|y|$ (see figure 3.1). For every point inside this region we obtain two waves, whose

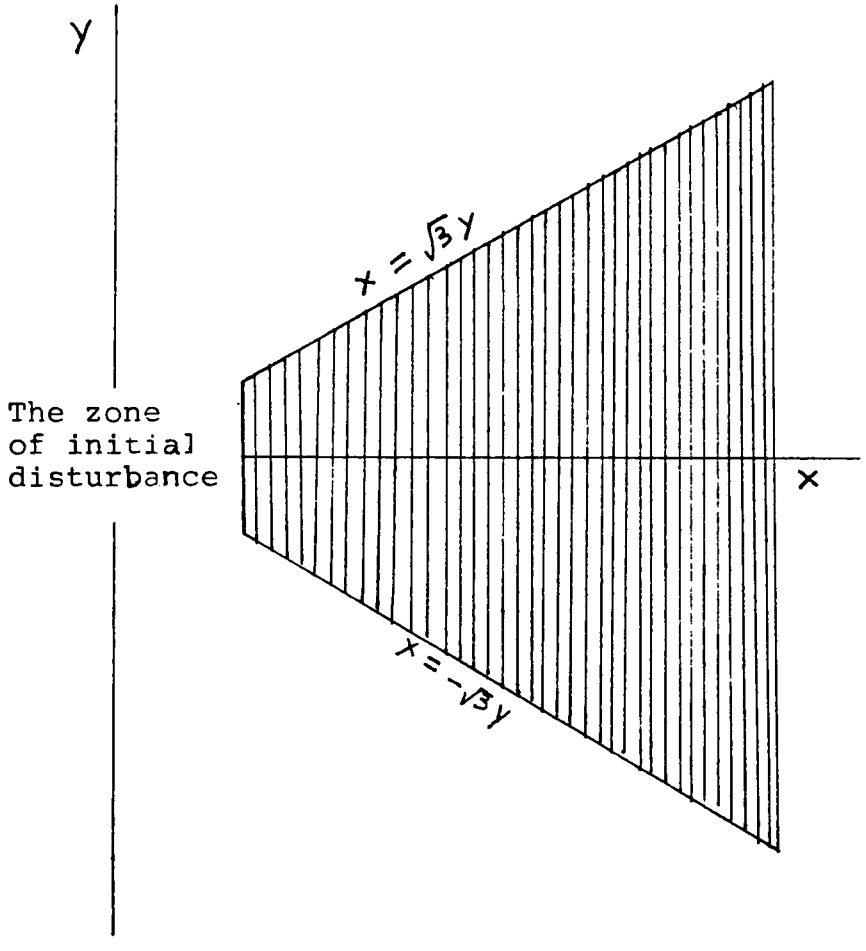

Figure 3.1 The solutions for stationary phases $\Phi(k_s, l_s)$ are possible only in the shaded region encosed by the lines $x=\sqrt{3}y$ and $x=-\sqrt{3}y$. Each of these lines marks a caustic characterised by the presence of two waves on one side and none on the other.

wavenumbers form two stationary points each (one for positive and one for negative wavenumber) which contribute dominantly to $\zeta(x,y,t)$ at that point. Figures 3.2 and 3.3 show them as contours of constant k_s and l_s, respectively, on the x/t, y/t plane.

Also $$\partial^2\omega/\partial k^2\ (k_s,l_s) = [6V_a{}^2/\beta\ ]k_s \qquad ...(3.39)$$

$$\partial^2\omega/\partial l^2\ (k_s,l_s) = [2V_a{}^2/\beta\ ]k_s \qquad ...(3.40)$$

and $$\partial^2\omega/\partial k\partial l\ (k_s,l_s) = [2V_a{}^2/\beta\ ]l_s \qquad ...(3.41)$$

which when substituted in (3.31), simplify it to

$$\zeta(x,y,t) = \sum_{k_s,l_s} \frac{\beta}{4\pi V_a{}^2} \frac{A(k_s,l_s)}{t\sqrt{3k_s^2-l_s^2}} \exp\left[i(k_s x + l_s y - \omega(k_s,l_s)t - \phi\right] \qquad ...(3.42)$$

Substitute for k_s and l_s in the denominator of this equation from (3.37) and (3.38) to obtain

$$\zeta(x,y,t) = \sum_{k_s,l_s} \frac{\sqrt{\beta}}{4\pi V_a} \frac{A(k_s,l_s)}{t\left[\left(\frac{x}{t}\right)^2 - 3\left(\frac{y}{t}\right)^2\right]^{1/4}} \exp\left[i(k_s x + l_s y - \omega(k_s,l_s)t - \phi_1)\right] \qquad ...(3.43)$$

where $\phi_1 = \pi/2$ when both k_s and l_s are either +ve or -ve.

$\phi_1 = -\pi/2$ when only one out of k_s and l_s is positive.

This solution indicates that an observer following a wave by travelling with its group velocity (x/t,y/t) will find its local vorticity diminishing slowly with time as a function of t^{-1}. If on the other hand the observer was tracking a particular crest which moves with the local phase velocity, he will find its amplitude diminish in a far more complicated manner. This rather slow rate of reduction in the amplitude of the wavepacket is not surprising as the waves fill a limited region of the x-y plane as

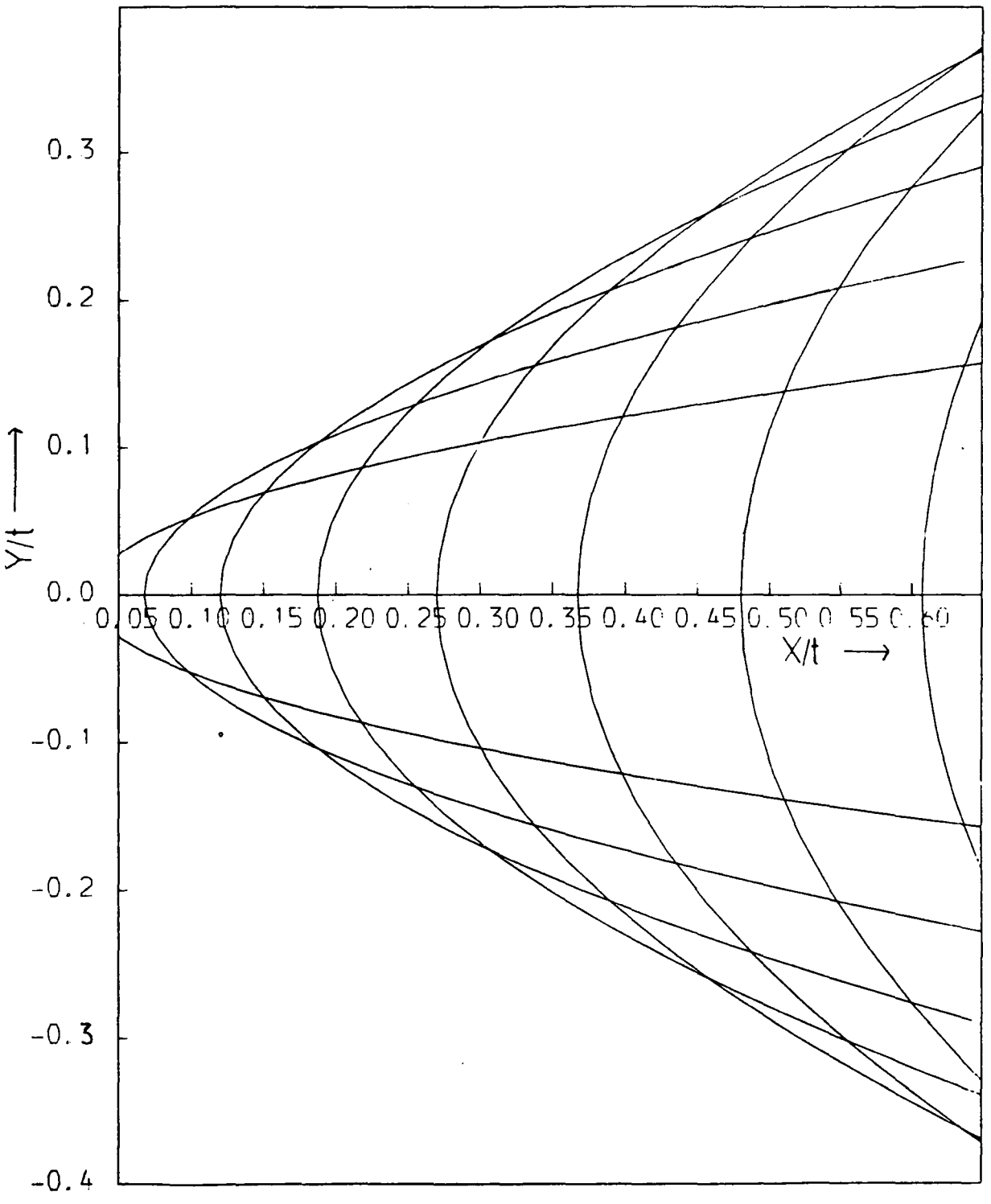

Figure 3.2 Contours of k_s on x-y plane. For any fixed value of x/t, y/t, there are two waves which have stationary phases. Contour interval = $0.05\sqrt{\beta}/V_a$.

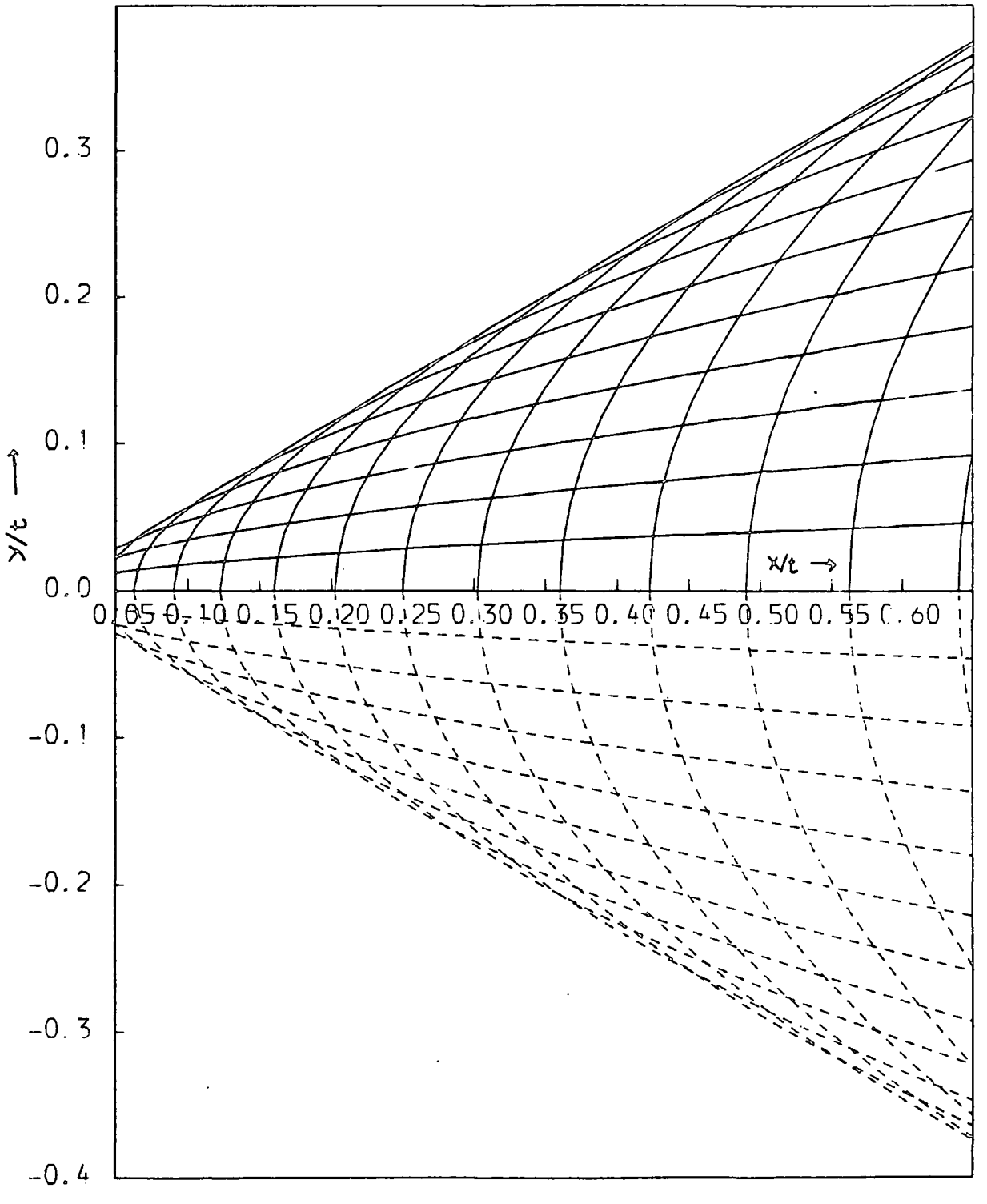

Figure 3.3 Contours of l_s on x-y plane. Out of the two l wavenumbers which form stationary phases at any place, the larger one pairs with the smaller k_s of figure 3.2 and vice-versa. Broken contours are negative. Contour interval = $0.05\sqrt{\beta}/V_a$.

they propagate. Waves with large wavenumbers are found the farthest from the source area at any time and have their energies diminished at rates that are rather larger than those of lower wavenumbers, as the presence of a term involving velocities in the denominator of equation (3.43) points out. This behaviour occurs because shorter waves disperse far more rapidly than the longer waves as can be seen from equations (3.35) and (3.36). Once $\zeta(x,y,t)$ is known, other variables associated with the disturbance like the local velocity fields $u(x,y,t)$ and $v(x,y,t)$, the horizontal magnetic field components $b_x(x,y,t)$ and $b_y(x,y,t)$ and their temporal variations ($\partial b_x/\partial t$ and $\partial b_y/\partial t$) are calculated as follows: Fourier transform equations (3.2), (3.3), (3.6) and (3.7), observing that $e = 0$, to get

$$\partial b_x(k,l,t)/\partial t = iB_0 ku(k,l,t) \qquad ...(3.44)$$

$$\partial b_y(k,l,t)/\partial t = iB_0 kv(k,l,t) \qquad ...(3.45)$$

$$iku(k,l,t) + ikv(k,l,t) = 0 \qquad ...(3.46)$$

and $$\zeta(k,l,t) = ikv(k,l,t) - ilu(k,l,t) \qquad ...(3.47)$$

Eliminate v between equations (3.46) and (3.47) to obtain

$$u(k,l,t) = il/(k^2+l^2)\ \zeta(k,l,t) \qquad ...(3.48)$$

similarly $$v(k,l,t) = -ik/(k^2+l^2)\ \zeta(k,l,t) \qquad ...(3.49)$$

Then from equations (3.44) and (3.45)

$$\partial b_x(k,l,t)/\partial t = -B_0 kl/(k^2+l^2)\ \zeta(k,l,t) \qquad ...(3.50)$$

and $\partial b_y(k,l,t)/\partial t = B_0k^2/(k^2+l^2)\ \zeta(k,l,t)$ ...(3.51)

The last two equations are integrated with respect to time to get

$$b_x(k,l,t) = -iB_0kl/[\omega(k^2+l^2)]\ \zeta(k,l,t) \quad ...(3.52)$$

$$b_y(k,l,t) = iB_0k^2/[\omega(k^2+l^2)]\ \zeta(k,l,t) \quad ...(3.53)$$

where use was made of equation (3.11)

Equations (3.48) to (3.53) can be inverse transformed to obtain the various quantities on L.H.S. of these equations in space domain. eg.

$$u(x,y,t) = \int_{-\infty}^{\infty}\int_{-\infty}^{\infty} il/(k^2+l^2)\ \zeta(k,l,t)\ \exp[i(kx+ly)]dk\ dl$$

$$= \int_{-\infty}^{\infty}\int_{-\infty}^{\infty} il/(k^2+l^2)\ A(k,l)\ \exp[i(kx+ly-\omega t)]dk\ dl \quad \text{[from (3.11)]}$$

$$= \frac{1}{(2\pi)^2}\int_{-\infty}^{\infty}\int_{-\infty}^{\infty} A'(k.l)\ \exp[i(kx+ly-\omega t)]dk\ dl \quad ...(3.54)$$

where $A'(k,l) = il/(k^2+l^2)\ A(k,l)$ is a smoothly varying function of k and l and represents the initial amplitude of u(k,l) in terms of the amplitude of $\zeta(k,l)$.

Equation (3.54) is of the same form as (3.17) and is integrated as above to yield

$$u(x,y,t) = \sum_{k_s,l_s} \frac{c}{4\pi}\frac{l_s}{k_s^2+l_s^2}\ \frac{A(k_s,l_s)}{t\sqrt{3k_s^2-l_s^2}}\ \exp\left[i(k_sx+l_sy-\omega(k_s,l_s)-\phi+\frac{\pi}{2}\right] \quad ...(3.55)$$

$$v(x,y,t) = \sum_{k_s,l_s} \frac{c}{4\pi}\frac{k_s}{k_s^2+l_s^2}\ \frac{A(k_s,l_s)}{t\sqrt{3k_s^2-l_s^2}}\ \exp\left[i(k_sx+l_sy-\omega(k_s,l_s)-\phi-\frac{\pi}{2}\right] \quad ...(3.56)$$

$$\frac{\partial b_x(x,y,t)}{\partial t} = \sum_{k_s,l_s} \frac{-c}{4\pi} \frac{B_0 k_s l_s}{k_s^2 + l_s^2} \frac{A(k_s,l_s)}{t\sqrt{3k_s^2 - l_s^2}} \exp\left[i(k_s x + l_s y - \omega(k_s,l_s)t - \phi)\right] \quad \ldots(3.57)$$

$$\frac{\partial b_y(x,y,t)}{\partial t} = \sum_{k_s,l_s} \frac{c}{4\pi} \frac{B_0 k_s^2}{k_s^2 + l_s^2} \frac{A(k_s,l_s)}{t\sqrt{3k_s^2 - l_s^2}} \exp\left[i(k_s x + l_s y - \omega(k_s,l_s)t - \phi)\right] \quad \ldots(3.58)$$

$$b_x(x,y,t) = \sum_{k_s,l_s} \frac{c}{4\pi\omega(k_s,l_s)} \frac{B_0 k_s l_s}{(k_s^2 + l_s^2)} \frac{A(k_s,l_s)}{t\sqrt{3k_s^2 - l_s^2}} \exp\left[i(k_s x + l_s y - \omega(k_s,l_s)t - \phi + \tfrac{\pi}{2})\right] \quad \ldots(3.59)$$

$$b_y(x,y,t) = \sum_{k_s,l_s} \frac{-c}{4\pi\omega(k_s,l_s)} \frac{B_0 k_s^2}{(k_s^2 + l_s^2)} \frac{A(k_s,l_s)}{t\sqrt{3k_s^2 - l_s^2}} \exp\left[i(k_s x + l_s y - \omega(k_s,l_s)t - \phi + \tfrac{\pi}{2})\right] \quad \ldots(3.60)$$

where $c = \beta/V_a^2$

So far we have confined our attention to the region enclosed by the lines $x = \pm\sqrt{3}\ y$. All the above asymptotic approximations clearly break down at the boundary of this region and beyond as $3k_s^2 - l_s^2 \longrightarrow 0$ along this boundary. Such a boundary is called a 'caustic' (Lighthill 1978) and it separates a region of complicated wave pattern formed by the interference of two groups of waves of nearly equal wavenumbers from a neighbouring region marked by the absence of any waves.

To see why such a breakdown occurs and to produce a 'healed' version of these functions near a caustic, let us return to equation (3.22) and rewrite it in a new frame of local axes in which the tensor T formed by the second derivatives (w.r.t. the wavenumbers) of ω has only diagonal elements. ie. if we denote

the wavenumbers in the new frame of axes by k' and l' then

$\partial^2\omega/(\partial k'\,\partial l') = \partial^2\omega/(\partial l'\,\partial k') = 0$ and we get

$$\omega(k',l') = \omega(k'_s,l'_s) + (k'-k'_s)\frac{\partial\omega}{\partial k'}(k'_s,l'_s) + (l'-l'_s)\frac{\partial\omega}{\partial l'}(k'_s,l'_s)$$

$$+\frac{1}{2}\left[(k'-k'_s)^2\frac{\partial^2\omega}{\partial k'^2}(k'_s,l'_s) + (l'-l'_s)\frac{\partial^2\omega}{\partial l'^2}(k'_s,l'_s)\right] \qquad \ldots(3.61)$$

In this system of co-ordinates the integral (3.24) splits into a product of two Gaussian integrals and can be simplified (Lighthill 1960, 1978) to

$$\zeta(x',y',t) = \frac{A(k'_s,l'_s)}{2\pi t}\exp\left[i(k'_s x' + l'_s y' - \omega(k'_s,l'_s) - \phi')\right]\frac{1}{\left[\frac{\partial^2\omega}{\partial k'^2}(k'_s,l'_s)\frac{\partial^2\omega}{\partial l'^2}(k'_s,l'_s)\right]} \qquad \ldots(3.62)$$

where x' y' is the new system of space co-ordinates and ϕ' the phase of the wave = $\pi/4[\mathrm{sgn}(\partial^2\omega/\partial k'^2) + \mathrm{sgn}(\partial^2\omega/\partial l'^2)]$. This new system of co-ordinates can be obtained by rotating the old frame of axes by $\pi/6$ in the clockwise direction. Now near the caustic, the denominator of equation (3.62) vanishes, implying that one of the diagonal elements of the tensor T must itself be zero. For our choice of new axes, it is $\partial^2\omega/\partial l'^2$, which means that $\partial\omega/\partial l'$, the group velocity of the wave at the caustic has reached an extremum in the direction of y' (actual calculations show that it is minimum there) and thus there are no neighbouring waves with which these waves can share a stationary phase. This is the reason why these approximations fail. Near the caustic we will now need to expand $\omega(k',l')$ to the third order terms in l'. ie.

$$\omega(k',l') = \omega(k'_c,l'_c) + (k'-k'_c)\frac{\partial\omega}{\partial k'}(k'_c,l'_c) + (l'-l'_c)\frac{\partial\omega}{\partial l'}(k'_c,l'_c)$$

$$+\frac{1}{2}\left[(k'-k'_c)^2\frac{\partial^2\omega}{\partial k'^2}(k'_c,l'_c)\right] - \frac{1}{6}(l'-l'_c)^3\frac{\partial^3\omega}{\partial l'^3}(k'_c,l'_c)$$

when $\omega(k',l')$ is substituted in the integral (3.24), it reduces $\mathfrak{Z}(x',y',t)$ to a product of a Gaussian integral in k' and an Airy's integral in l' ie

$$\mathfrak{Z}(x',y',t) = \frac{A(k_c',l_c')}{2\pi^2} \exp\left[i(k_c'x'+l_c'y'-\omega(k_c',l_c')\right] \int_{-\infty}^{\infty} \exp\left[\frac{it}{2}[k'-k_c']^2 \frac{\partial^2\omega}{\partial k'^2}(k_c',l_c')\right] dk' \times$$

$$\int_{-\infty}^{\infty} \exp\left[it(l'-l_c')\left(x'-\frac{\partial\omega}{\partial l'}(k_c',l_c')\right) + \frac{1}{6}(l'-l_c')^3 \frac{\partial^3\omega}{\partial l'^3}(k_c',l_c')\right] dl' \qquad (3.63)$$

We have already dealt with the Gaussian integral above and the second integral can be evaluated by the help of the integral relation

$$\int_0^{\infty} \cos(ak^3+bk)dk = \pi/(3a)^{1/3} \quad A_i[(3a)^{-1/3}b)] \qquad ...(3.64)$$

where $A_i(x)$ is the tabulated Airy function which satisfies the differential equation

$$d^2A_i(x)/dx^2 - xA_i(x)=0 \qquad ...(3.65)$$

and decays exponentially for positive arguements and oscillates for negative arguements.

This results in an expression which is a product of an ordinary stationary phase expression in variable k' and an Airy integral term in l',

$$\mathfrak{Z}(x,y,t) = 2A(k_c',l_c')\left[\frac{1}{2\pi|t\frac{\partial^2\omega}{\partial k'^2}(k_c',l_c')|}\right]^{1/2} \exp\left[i\frac{\pi}{4}\,\mathrm{sgn}\frac{\partial^2\omega}{\partial k'^2}(k_c',l_c')\right] \times$$

$$\frac{1}{\left[\frac{t}{2}\frac{\partial^3\omega}{\partial l'^3}(k_c',l_c')\right]^{1/3}} A_i\left[\frac{t\frac{\partial\omega}{\partial l'}(k_c',l_c')-y'}{(\frac{1}{2}t\frac{\partial^3\omega}{\partial l'^3}(k_c',l_c'))^{1/3}}\right] \exp\left[i(\omega(k_c',l_c')t-k_c'x'-l_c'y')\right] \qquad ...(3.66)$$

Other quantities (u, v, b_x, b_y, $\partial b_x/\partial t$, $\partial b_y/\partial t$) are also calculated by following the same procedure; though the actual expressions for these functions will not be reproduced here.

3.3.2 The large wave number limit. For very short Rossby-MHD waves, the dispersion relationship (3.13) can again be simplified considerably. Especially if $|K| = \sqrt{k^2+l^2} >> \sqrt{\beta/2V_a}$, then $2V_a(K^2+l^2)/\beta$ is much larger than unity and (3.13) yields

$$\omega_{i,m} = \pm V_a k \qquad \ldots(3.67)$$

which is the phase velocity equation of ordinary Alfven waves propagating non-dispersively ($\partial\omega/\partial k = \omega/k$ = constant) in either direction of the magnetic field with velocities equal to V_a. (Observe, however, that due to Taylor-Proudman constraint for barotropic fluids in geostrophic equilibrium, the fluid columns move as coherent units and thus waves are not strictly one-dimensional). Alfven waves do not have any velocity component in the y (north) direction ($\partial\omega/\partial l = 0$), and will therefore be found immediately to the east or the west of the source. The method of stationary phase is inapplicable (and unnecessary) for these waves as the second derivatives of ω are zero for such waves. As Alfven waves are non-dispersive, an initial envelope of these waves will be expected to travel along the magnetic lines of force without any attenuation of its constituent waves and will thus propagate for long distances with no changes in its initial shape.

3.4 A FEW SYNTHETIC EXAMPLES The above discussion suggests that from a highly localised source region of magnetic waves, the waves that leave that area first are the Alfven waves. As Alfven waves travel without spreading their energies in large areas, they will be observed at long distances from the source until they either lose their energy by the combined dissipative effect of the viscocity and finite electrical conductivity of the fluid or are reflected by a boundary. Immediately following the waves and filling much larger areas will be the magnetic Rossby waves of intermediate frequencies which will in turn be followed by the slowest waves of all, the large wavelength magnetic Rossby waves spreading their energy gradually over larger and larger areas. Most of the observable planetary MHD. waves will fall under this last category, which we will now study in greater detail by the help of a few examples.

Before we can actually calculate the perturbations associated with a propagating disturbance we still need to answer one crucial question. In deriving the asymptotic form of the Fourier wave integral, we have so far implicitly assumed that 't' is large. We will have to give a more precise meaning to this statement to avoid incurring large errors. We can see that the main source of error in the asymptotic approximation of the integral (3.17) will come from the neglect of higher order terms in the Taylor's series expansion of ω around $\omega(k_s,l_s)$. Whitham (1974) shows that for one dimensional waves, when the Taylor's series expansion of ω includes terms up to the 4th order, the method of stationary phase provides an additional term in the asymptotic

approximation, which can be written as a factor

$$1 - \frac{i}{t|\omega''|}\left(\frac{5}{24}\frac{\omega'''^2}{\omega''^2} - \frac{1}{8}\frac{\omega''''}{\omega''}\right)$$

('/' denotes derivative w.r.t. k)

multiplying the terms of the second order approximation. When appropriate substitutions are made for these derivatives from the above equations, this factor simplifies to

$$1 - 0.035/(t\omega) = 1 - 0.005\ T/t$$

where T is the typical time period of the waves. Thus when $t \simeq T$, there will be less than half a percent of error due to neglect of the 4th order term in the asymptotic approximation. Thus in all our calculations t has been chosen to be of the same order as the typical time period of the wave we are studying. The time periods of the waves in turn are derived from the dispersion relation and from the length scale prescribed in the initial condition.

Figure (3.4) shows the field of local vorticity $\zeta(x,y,t)$ associated with the propagating disturbance, calculated in the small wavenumber limit. As expected, the disturbance associated with the magnetic Rossby waves propagates only in the positive x quadrants and is confined mainly in the region enclosed by the lines $x = \pm\sqrt{3}y$. Inside this region the function is calculated by the help of equation (3.43) whereas equation (3.66) involving Airy's function was employed for the rest of the map. The initial disturbance was assumed to have a constant amplitude for all wavenumbers $|K| < 2\pi/\lambda$, λ being the spatial dimension of the initial disturbance.The amplitude of any other wave with wavelength $> \lambda$ was truncated by an exponential factor whose

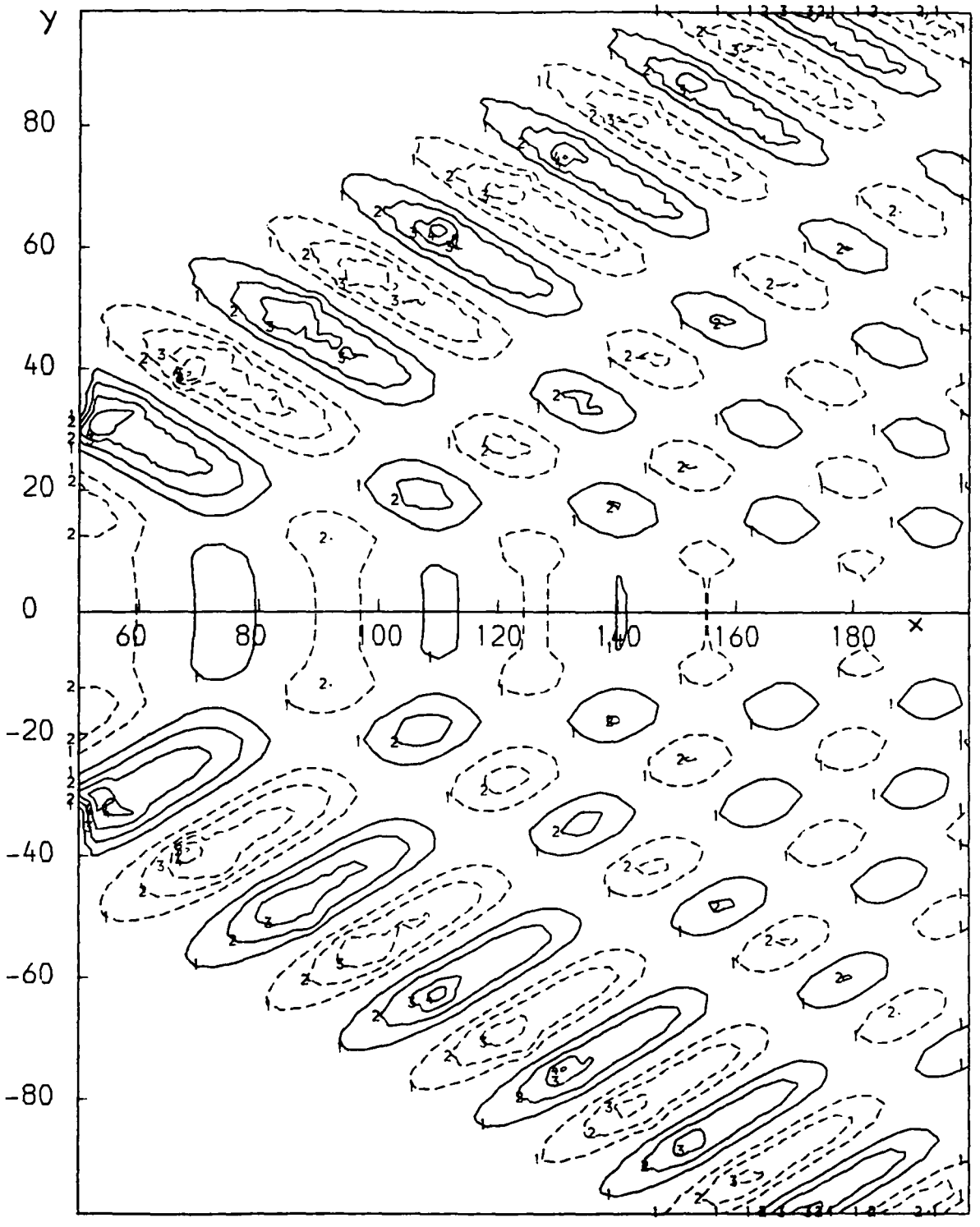

Figure 3.4 Vorticity field $\zeta(x,y,t)$ associated with the propagating waves caused by an initial disturbance. Contour interval is arbitrary. Positive contours in this and subsequent figures are drawn in solid lines whereas negative contours are shown in broken lines. The distances are in units of $(V_a/\beta)^{1/2}$ and $t = 1000(V_a/\beta)^{-1/2}$ units.

arguement is given by $[(T-T_\lambda)/T_\lambda]^2$, (T is the time period of the wave in question and T_λ is the time period of the wave whose wavelength is λ). In addition we assumed that the initial disturbance is symmetric about both the axes and as a result $A(k,l) = A^*(k,l)$, where * denotes complex conjugate, which implies that the imaginary part of the initial amplitude should be taken as zero. The highest values of disturbance in the vorticity field of figure 3.4 occur near the caustic and tend to dominate the amplitude of the wave train. Figures 3.5 and 3.6 show the x and y components of fluid velocity associated with the propagating disturbance which present a very similar picture, except that the contours of v(x,y,t) tend to form concentric circles around the zone of initial disturbance. We should, however, mention that the fields u and v plotted here are not unique, as any velocity field $u(u_1,v_1)$, whose vorticity $\zeta(x,y) = \partial v_1/\partial x - \partial u_1/\partial y = 0$, can be added to our velocities with impunity. If on the other hand, we can specify in the beginning that the original disturbance was purely rotational in character, then the above interpretation is certainly correct and the only one that is possible. Figures 3.7 and 3.8 show the x and y magnetic field components of the disturbance which can be seen to decay rapidly for the shorter waves in the front, though the temporal variations of these field ($= \partial b_x/\partial t$ and $\partial b_y/\partial t$, figures 3.9 and 3.10) remain comparable in amplitude for faster and slower waves.

If we apply the results of this section to the case of the earth's core keeping in mind the caution that should be exercised

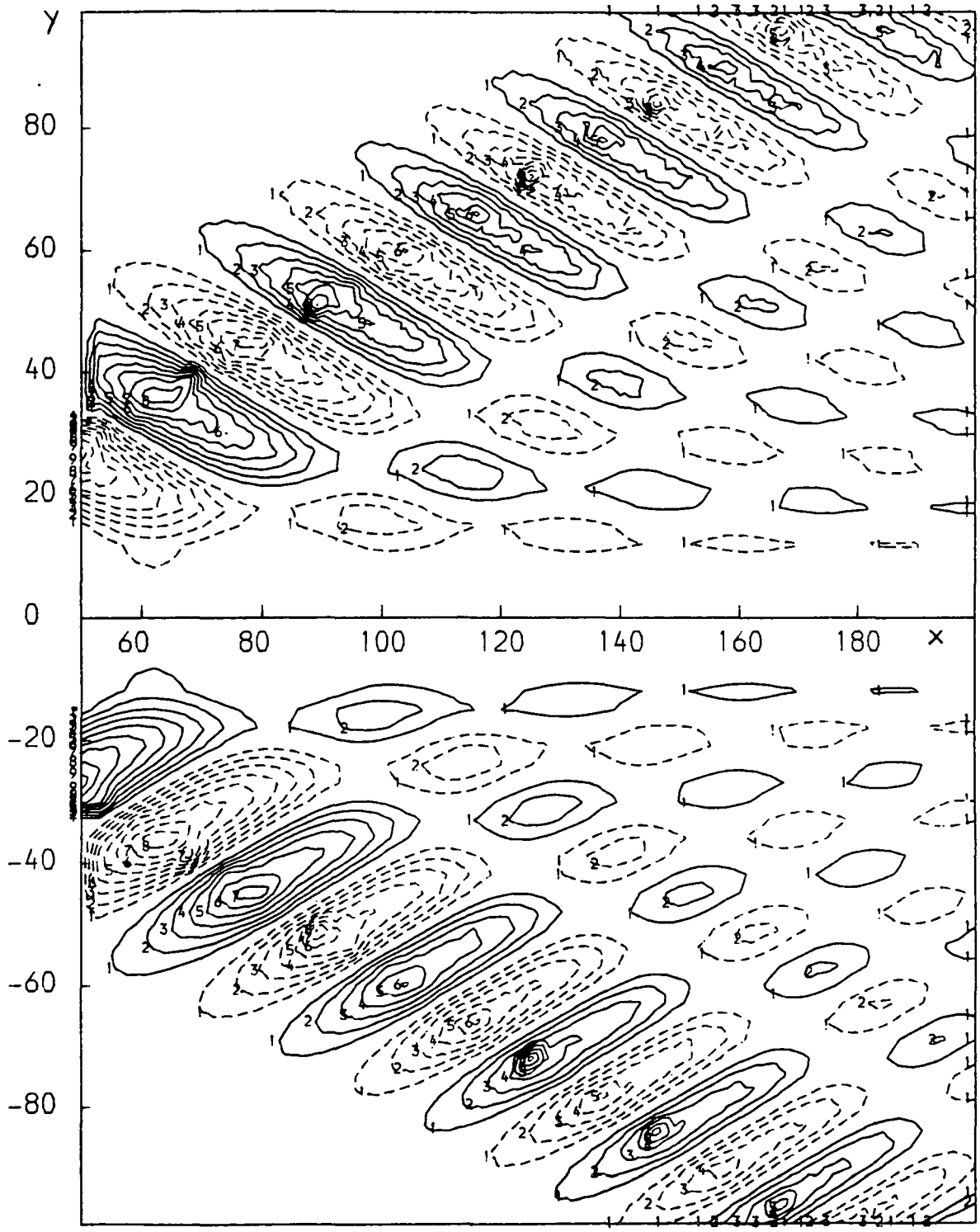

Figure 3.5 u(x,y,t), the x-component of fluid velocity associated with the propagating disturbance. For other details see figure 3.4. Contour interval arbitrary.

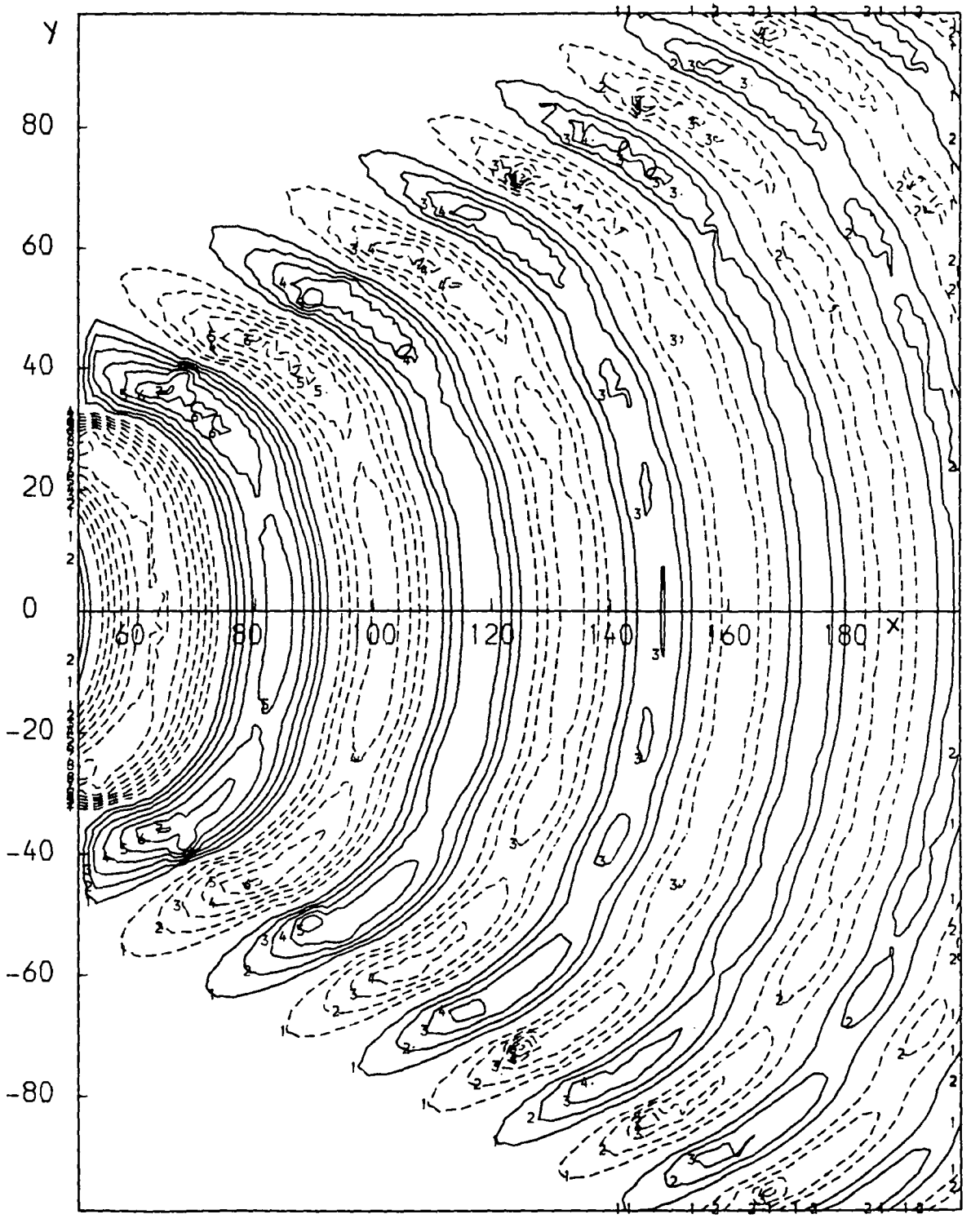

Figure 3.6 v(x,y,t), the y-component of fluid velocity associated with the propagating disturbance. For other details see figure 3.4. Contour interval arbitrary.

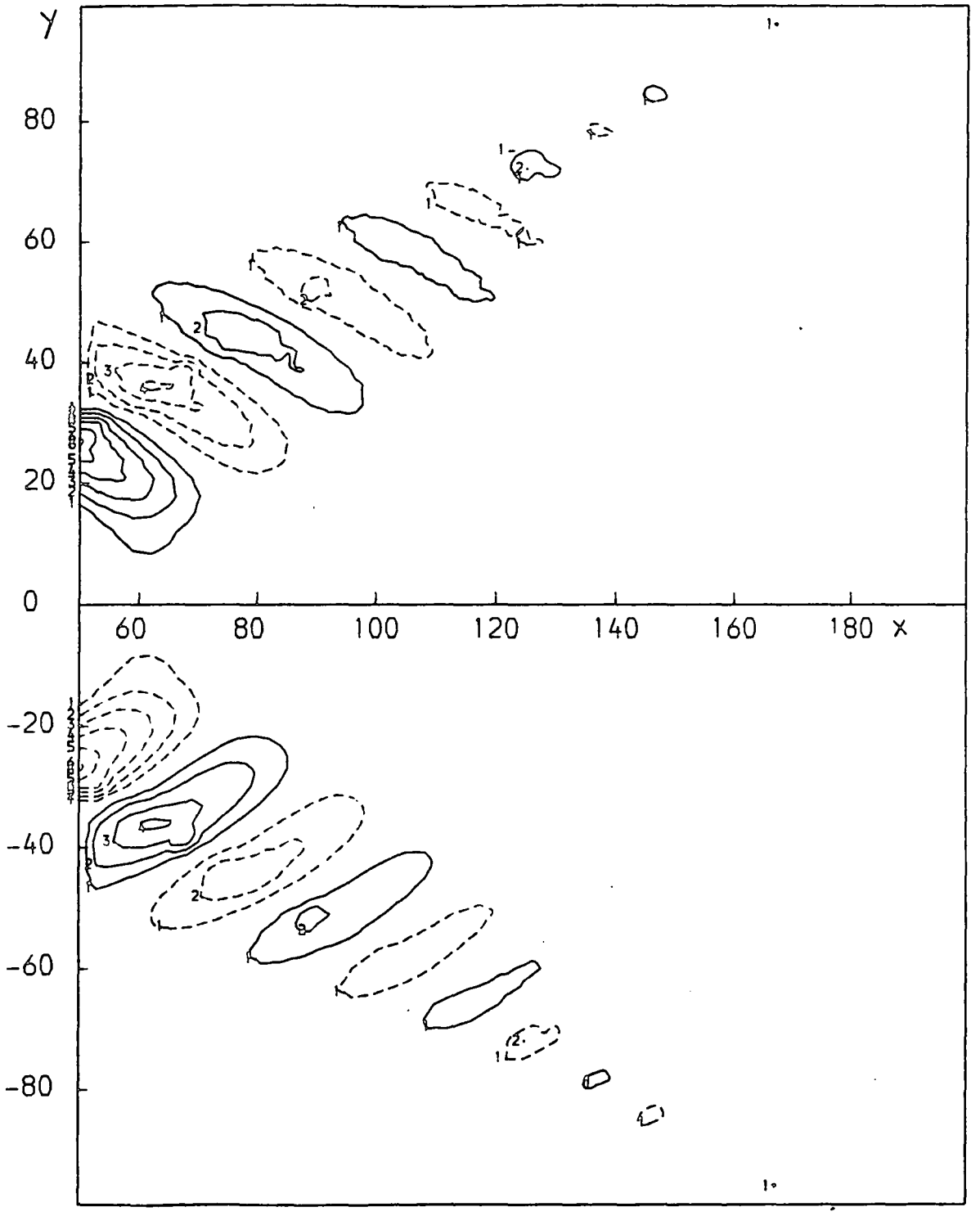

Figure 3.7 $b_x(x,y,t)$, the x component of the magnetic field associated with the propagating disturbance. For other details see figure 3.4. Contour interval arbitrary.

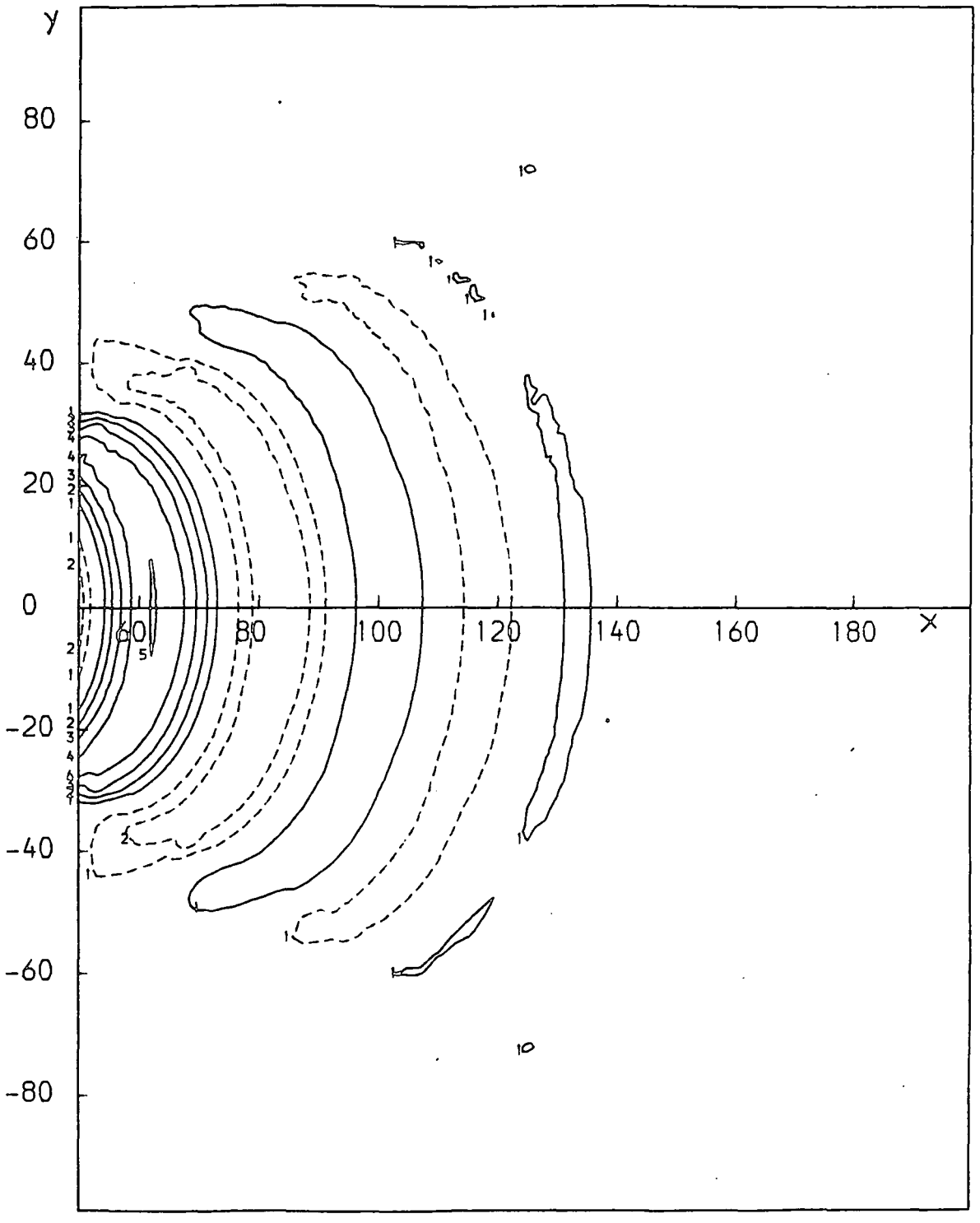

Figure 3.8 $b_x(x,y,t)$, the y component of the magnetic field associated with the propagating disturbance. For other details see figure 3.4. Contour interval arbitrary.

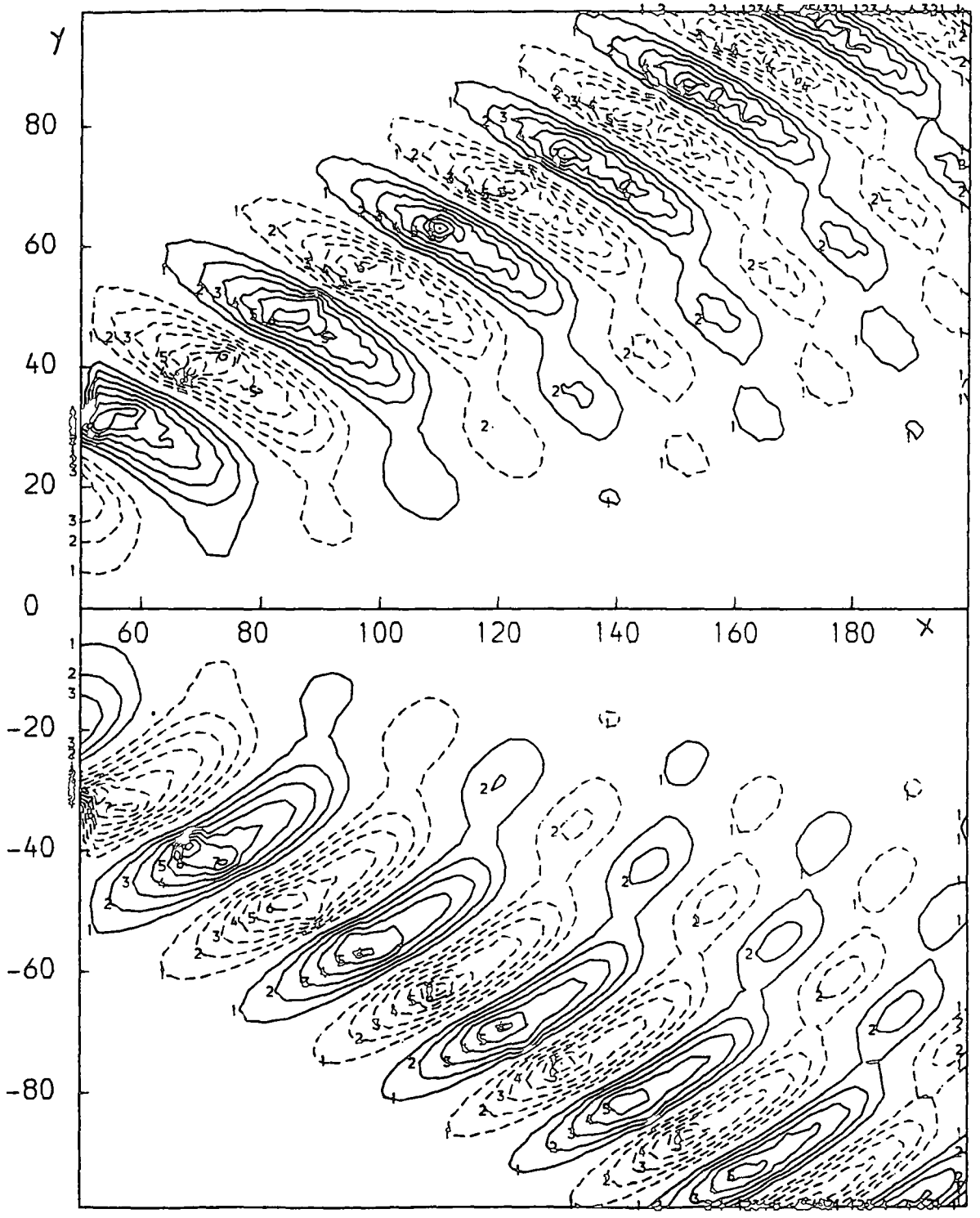

Figure 3.9 $\partial b_x(x,y,t)/\partial t$, the temporal variations of b_x, associated with the propagating disturbance. For other details see figure 3.4. Contour interval arbitrary.

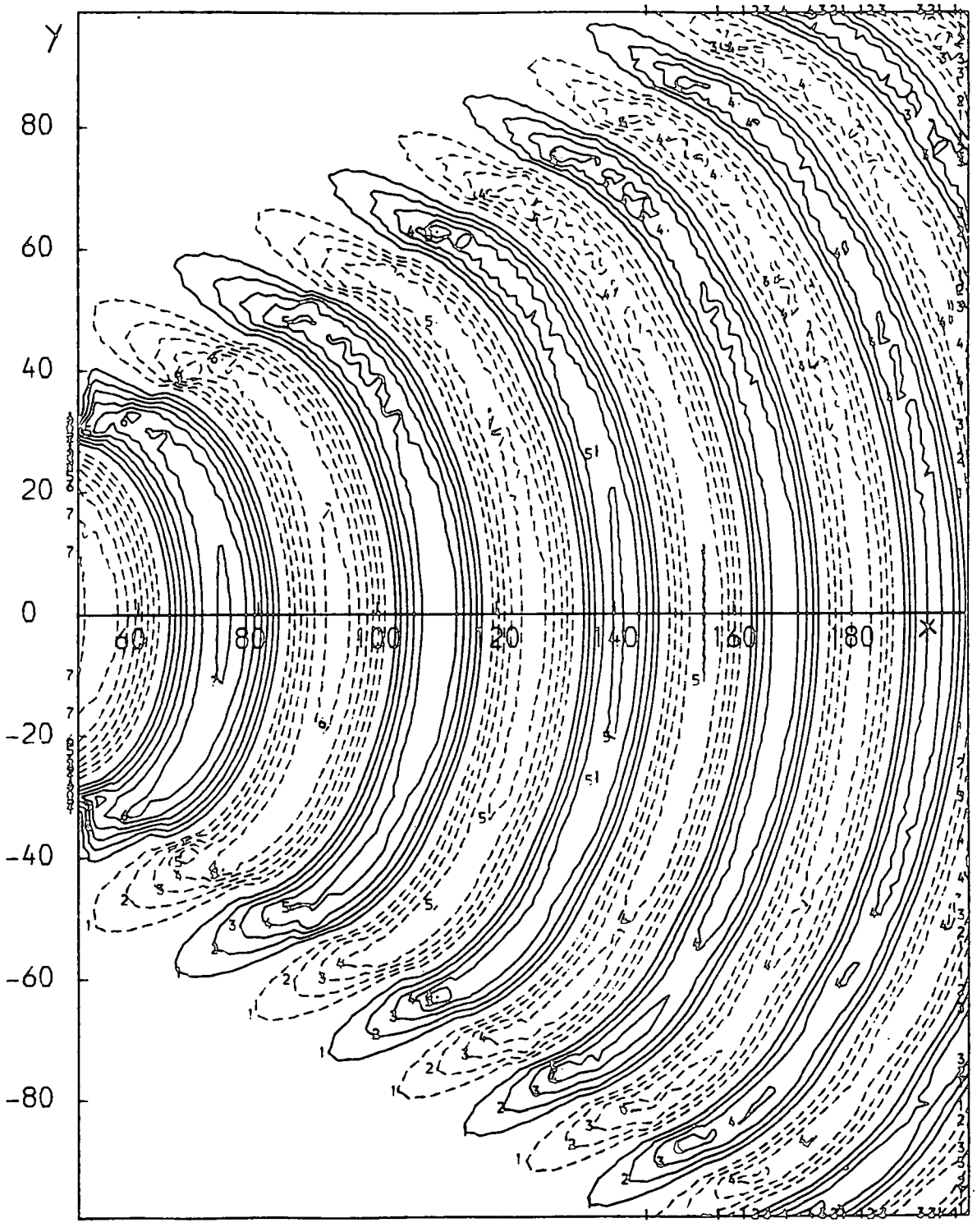

Figure 3.10 $\partial b_y(x,y,t)/\partial t$, the temporal variation of b_y, associated with the propagating disturbance. For other details see figure 3.4. Contour interval arbitrary.

while applying the results of a β plane model to a thick shell (see sections 1.4 and 1.5), for a basic latitude $\phi_o = 34^o$ we can take $\beta = -3.4X10^{-11}m^{-1}s^{-1}$ (Hide 1966 and equation 1.76) and for a basic toroidal magnetic field of strength 50 Oersteds, V_a = 0.05m/sec. Then each unit of distance displayed on these maps $\simeq$ 36 kms. and the unit of time $\simeq$ 9 days. Then the perturbations have length scales of many hundred kilometers and time periods of the order of several decades.

3.5 PERTURBATIONS IN THE VERTICAL COMPONENT OF THE MAGNETIC FIELD

So far we have taken $\overline{B}_0$, the ambient magnetic field to be uniform in all directions and as a consequence b_z satisfies an equation of the form (3.4) and thus does not in any way contribute to the dynamics of the system. The magnetic disturbances in this type of system can not be observed from outside as there is no outward component of b associated with the disturbance. This is analogous to the situation in the earth's core in which the perturbation of toroidal magnetic field can not produce disturbances in the radial direction directly. However if a non-uniform poloidal field B_p ($\partial B_p/\partial\theta \neq 0$, $\partial B_p/\partial\phi \neq 0$) is present along with the toroidal field, then it will be convected by the fluid motions associated with the original perturbations and its radial component can be easily distorted. If we carry this analogy to our β plane model we could then assume the vertical component of the ambient magnetic field in such a way that

$$\partial B_z/\partial x \neq 0 \text{ and } \partial B_z/\partial y \neq 0 \qquad \ldots(3.68)$$

Though still $\partial B_x/\partial x + \partial B_y/\partial y = -\partial B_z/\partial z = 0$. Once again the total magnetic field (ambient+perturbations) will satisfy the equation

$$d[(B_z + b_z)]/dt = 0 \qquad ...(3.69)$$

which can now be linearised to

$$\partial b_z/\partial t + u\partial B_z/\partial x + v\partial B_z/\partial y = 0 \qquad ...(3.70)$$

Thus, though the vertical component of the total magnetic field still does not contribute to any hydromagnetic forces, it can now act as a tracer of the fluid motions by displaying temporal perturbations which are proportional to its gradient in the direction of the perturbed fluid velocity (ie. $\partial b_z/\partial t = u.\nabla B_z$). When equation (3.70) is integrated with respect to time we obtain

$$b_z(x,y,t) = a(x,y,t)\ \partial B_z/\partial x + b(x,y,t)\ \partial B_z/\partial y \qquad ...(3.71)$$

where a and b are the fluid displacements at any point (x,y) in the E-W and N-S directions, respectively, at time t.

We have calculated these fluid displacements for the initial value problem of the previous section and are shown in figures 3.11 and 3.12. Now, say for example, we assume that $\partial B_z/\partial x = 0$, ie the vertical component of the impressed magnetic field is uniform in the E-W direction and $\partial B_z/\partial y$ = constant (=c say) ie B_z varies linearly with latitude, then by virtue of equation (3.71)

$$b_z(x,y,t) = c\ b(x,y,t) \qquad ...(3.72)$$

and the contours of fluid displacements of figure 3.12 will be directly proportional to the variations in the vertical component of the magnetic field.

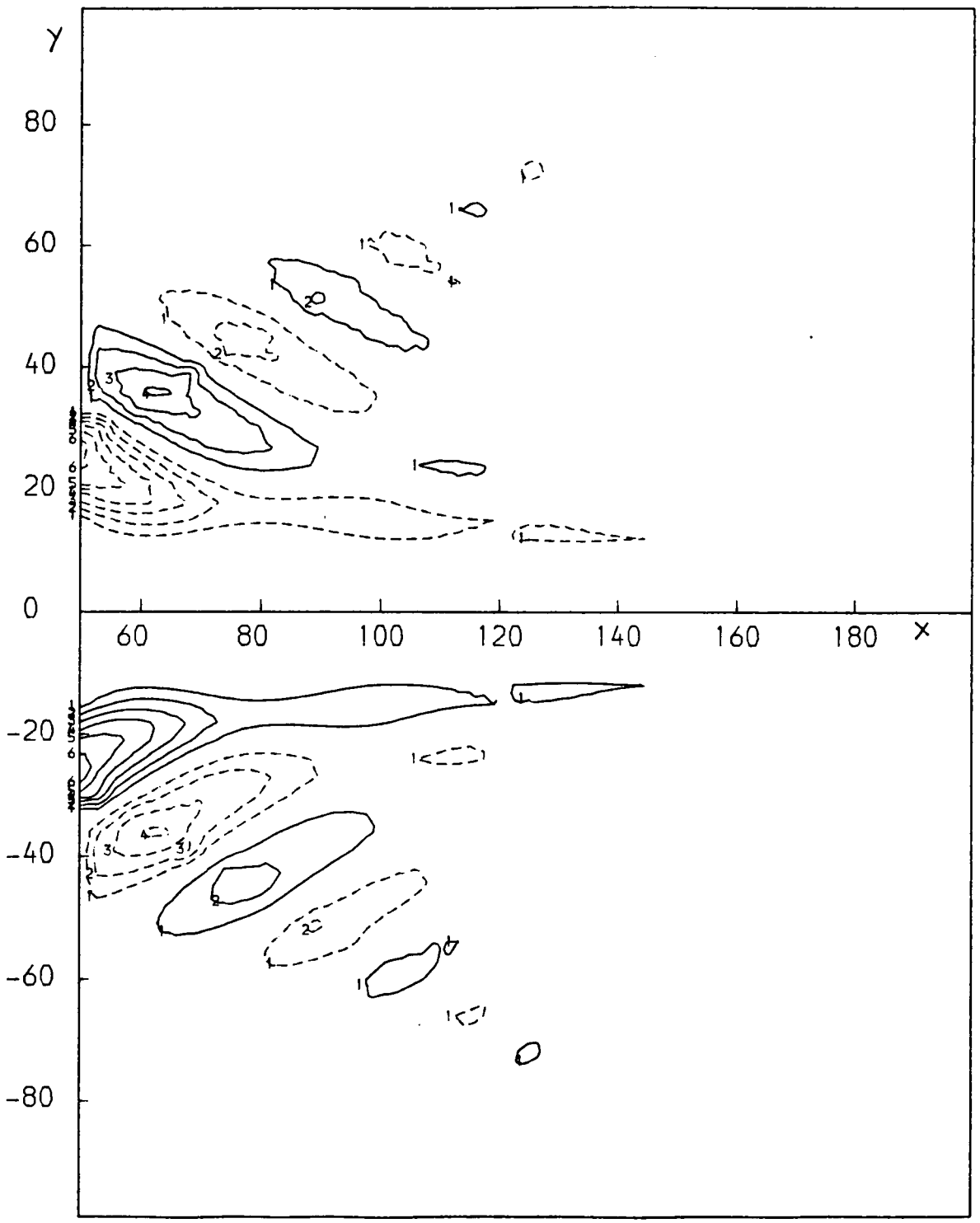

Figure 3.11 a(x,y,t), the x component of the fluid displacement vector associated with the propagating disturbance. For other details see figure 3.4. Contour interval arbitrary.

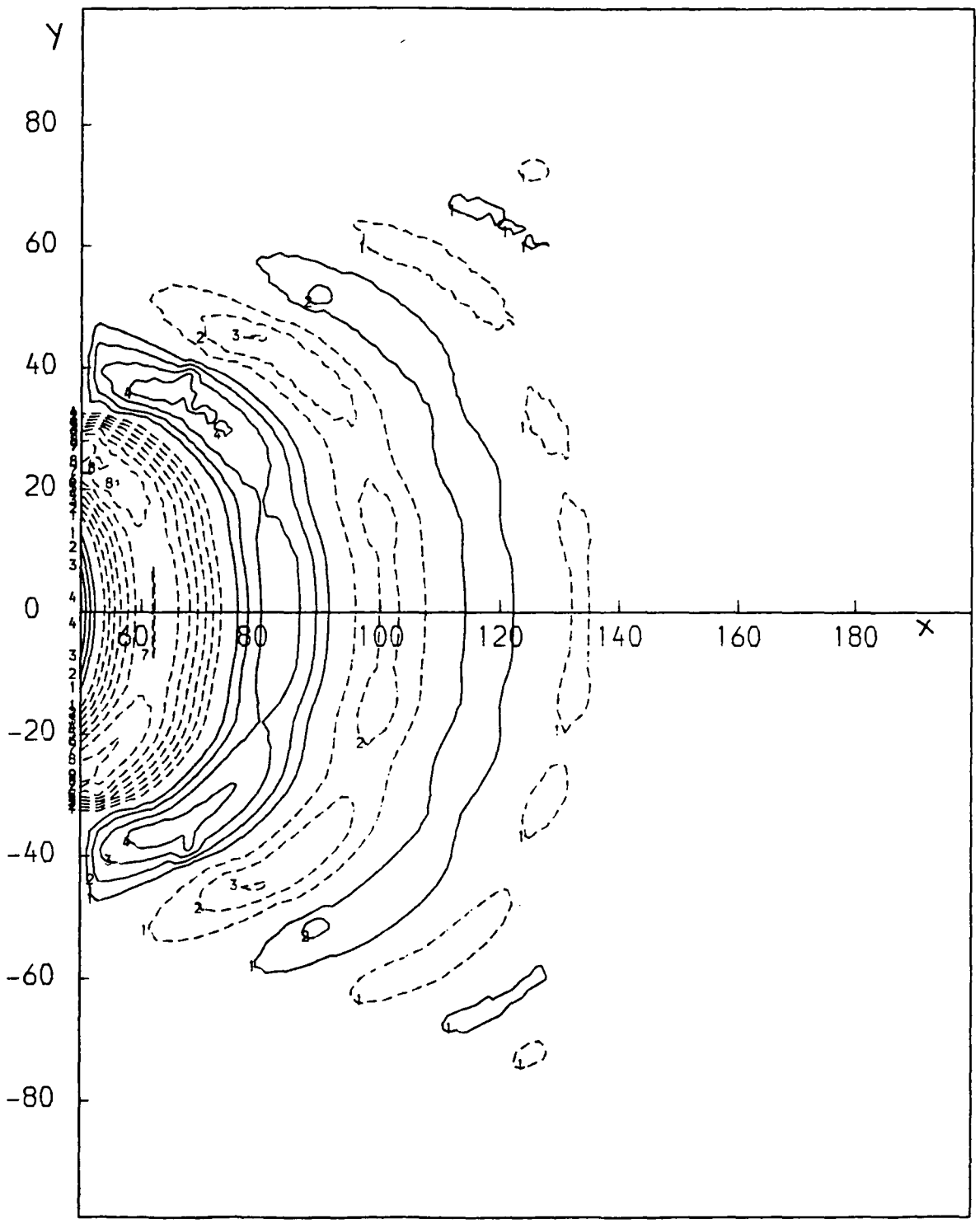

Figure 3.12 b(x,y,t), the y component of the fluid displacement vector associated with the propagating disturbance. For other details see figure 3.4. Contour interval arbitrary.

CHAPTER FOUR

THE REFLECTION OF ROSSBY-MAGNETOHYDRODYNAMIC WAVES AT A RIGID BOUNDARY

4.1 GENERAL A good illustration of how a magnetic Rossby-MHD wave may convert its magnetic energy to kinetic form and thus transform completely or partially into one or more inertial Rossby-MHD waves is provided by the case study of the reflection of a magnetic Rossby wave by a rigid boundary. Such reflections will obviously be important in the studies of all bounded fluid bodies approximately in geostrophic equilibrium. Although, in the following sections, the dissipative effects of viscosity and finite conductivity of the fluid and the boundary will be neglected, they will certainly be important in studies involving multiple reflections, especially of short waves, which will decay in a finite time. In this work we will essentially make use of the concept of a wave packet which is assumed to travel at the group velocity of its constituent waves (see eg. Whitham, 1960, 1965; Lighthill, 1965, 1978), to understand the ongoing process of reflection of waves by insulating and conducting rigid boundaries. In some respects this investigation extends the work of Longuet-Higgins (1964a,b) and Pedlosky (1979) for ordinary Rossby waves. We shall once again assume a beta-plane configuration.

4.2 Formulation of the problem Consider figure 4.1 in which the ray of a wave packet of magnetic Rossby waves is incident upon a N-S boundary and makes an angle α_1 to the x-axis. For the wave to

truly approach this boundary, its group velocity and consequently its energy flux will have to be directed towards the boundary. We also assume that $\bar{B}_0$, the basic toroidal magnetic field is azimuthal ie. parallel to x-axis. The vorticity

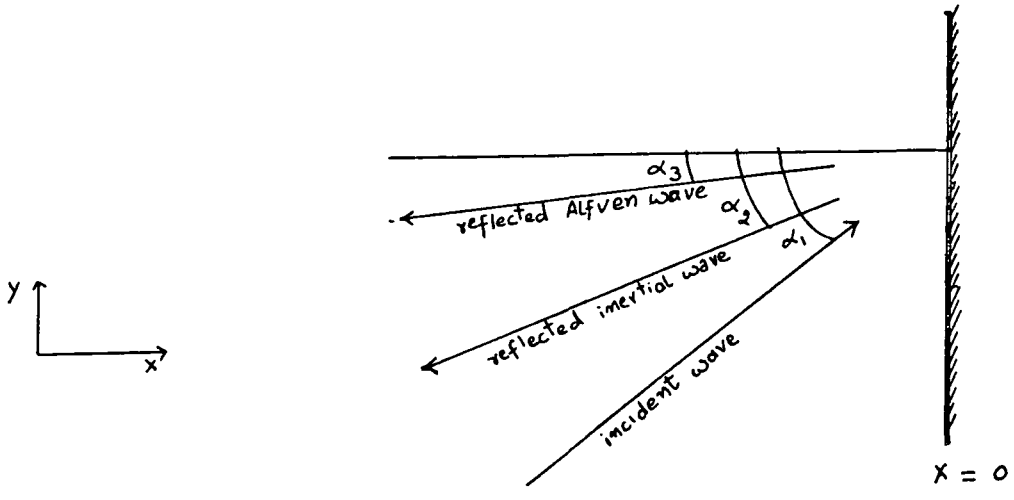

Figure 4.1 Reflection of a hydromagnetic wave packet by a rigid boundary

function ζ for any incident plane wave with wave numbers k_1 and l_1 and frequency ω_1 can be written (see equation 1.65) as

$$\zeta_1 = A_1 \exp[i(k_1 x + l_1 y - \omega_1 t)] \qquad ...(4.1)$$

where ω_1, k_1 and l_1 satisfy the dispersion equation

$$\omega^2 + \omega\beta k/(k^2+l^2) - k^2 V_a^2 = 0 \qquad ...(4.2)$$

The presence of the rigid boundary will produce one or more reflected waves (we shall ascertain their number later) each of which can in turn be described by

$$\zeta_r = A_r \exp[i(k_r x + l_r y - \omega_r t) \qquad ...(4.3)$$

and will also satisfy the dispersion relationship (4.2). Following Hide (1966) and equation (1.68), the E-W component of the fluid velocity associated with the wave (4.1) can be written as

$$u_1 = il_1/(k_1^2+l_1^2)\ A_1 \exp[i(k_1x + l_1y - \omega_1 t)]$$

We can write similar equations corresponding to all the reflected waves described by equation (4.3). Now the E-W velocity of the fluid should vanish at the boundary. ie. at x = 0

$$u_1 + \sum_r u_r = \frac{il_1}{k_1^2+l_1^2} A_1 \exp\left[i(l_1y-\omega_1 t)\right] + \sum_r \frac{il_r}{k_r^2+l_r^2} A_r \exp\left[i(l_r y-\omega_r t)\right] = 0 \qquad \ldots(4.4)$$

The only way equation (4.4) can hold for all t is that $\omega_1 = \omega_2 = \omega_3 = \omega_r = \omega$ (say) which implies that the frequencies of all the reflected waves are equal to the frequency of the incident wave. Also if relation (4.4) is true for all y then $l_1 = l_2 = l_3 = l_r = l$ (say), ie. the projection of the wavenumber parallel to the boundary is also preserved under reflection.

To gain a clear understanding of the situation let us turn to equation (4.2) and rewrite it in units of $(V_a/\beta)^{1/2}$ for distance and $(V_a\beta)^{-1/2}$ (see equation 1.77) for time.

$$\omega^2 + k\omega/(k^2+l^2) - k^2 = 0 \qquad \ldots(4.5)$$

which can be arranged as a quartic in k as

$$k^4 + (l^2-\omega^2)k^2 - k\omega - \omega^2 l^2 = 0 \qquad \ldots(4.6)$$

As ω and l remain unaffected by the process of reflection equation (4.6) associates 4 values of k (say k_1, k_2, k_3 and k_4)

with each of these ω and l. It is impossible to extract the roots of equation (4.6) analytically but we can readily deduce the size and nature of these roots from the 'normal curves' which are contour maps of frequency ω in the (k,l) plane. Hide and Jones (1972) published an exhaustive numerical study of the dispersion relationship (4.5) and figure (4.2) here has been reproduced from their work.

It can be seen from these normal curves that if is greater than a critical frequency ω^* and $l<<l^*(\omega)$, for each set of ω and l, we can assign 4 different values to k as already suggested by equation (4.6). It can also be seen that two of these wavenumbers [corresponding to the largest negative root ($=k_3$ say) and the root with the smallest absolute value ($=k_2$ say)] are associated with waves which have westward group velocities (ie. $\partial\omega/\partial k < 0$ which means that the gradients of the normal curves of these waves are in the direction of negative x-axis) while the other two wavenumbers ($=k_1$ the only positive root of the equation and k_4, the remaining root) belong to eastward travelling waves. But as the reflected waves can have only westward (ie. pointing away from the boundary) group velocities at x = 0, we are forced to conclude that the amplitude of the wave corresponding to k_4 must be zero and thus at the most two reflected waves can be generated.

To see whether these reflected waves are magnetic or inertial in their behaviour, we shall look at the magnetic and kinetic energy contents of these waves. To do this first obtain a simple equation of the form

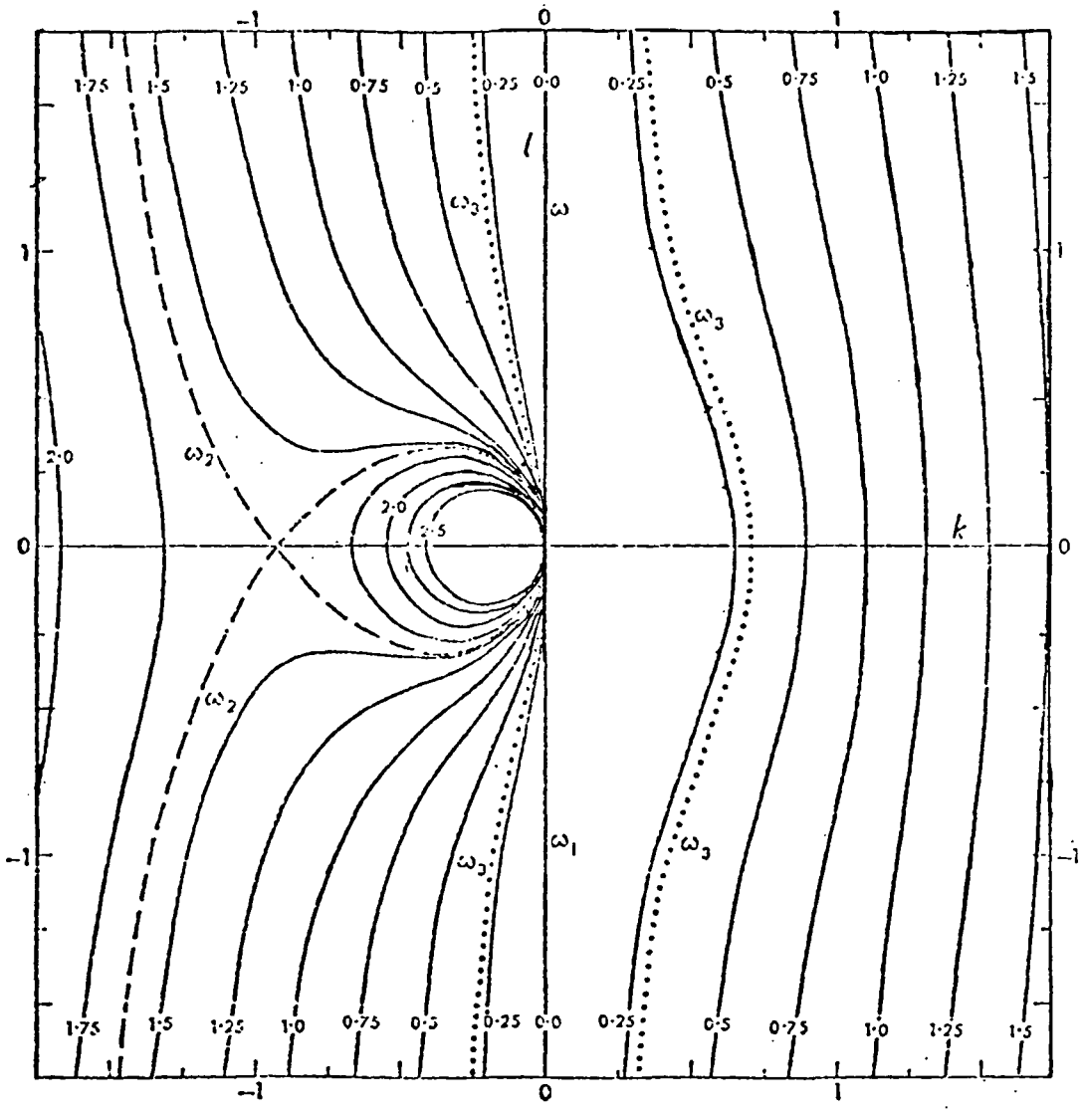

FIGURE 4.2 Normal curves for the case $\theta = 0$ (i.e. magnetic field parallel to x-axis)

$\omega_1 = 0$, $\omega_2 = 1.6119$, $\omega_3 = 0.2929$

$$\frac{\frac{1}{2}\mu^{-1}(b_x^2+b_y^2)}{\frac{1}{2}\rho(u^2+v^2)} = \frac{B_0^2}{\mu\rho}\frac{k^2}{\omega^2} = V_a^2\frac{k^2}{\omega^2} \qquad \ldots(4.7)$$

by a little manipulation of equations (1.59) and (1.60) and considering that $\Theta = 0$.

The left hand side of this equation represents the ratio of the magnetic energy of a wave of frequency ω and x-wavenumber k, to its kinetic energy. Write this equation in new units of distance and time as

$$\frac{\frac{1}{2}\mu^{-1}(b_x^2+b_y^2)}{\frac{1}{2}\rho(u^2+v^2)} = \frac{k^2}{\omega^2} \qquad \ldots(4.8)$$

This equation states that for any wave for which in the normalised units $k >> \omega$, its energy will be mainly magnetic, whereas the waves with $\omega >> k$ are mainly inertial. Waves with $\omega \simeq k$ are marked by the equipartitioning of magnetic and kinetic energies and thus represent Alfven waves unaffected by rotation. A cursory examination of the normal curves shows that by this criterion one of the waves (k_2) is an inertial Rossby wave while the wave represented by k_3 is mainly Alfven, though its kinetic energy is slightly larger than its magnetic energy.

Thus in the light of discussion we can say that a magnetic Rossby wave represented by equation (4.1) produces on reflection, an inertial Rossby-MHD waves and an Alfven wave which can be described by

$$\mathcal{P}_2 = A_2 \exp[i(k_2x + ly - \omega t)] \qquad \ldots(4.9)$$

and $$\psi_3 = A_3 \exp[i(k_3 x + ly - \omega t)] \qquad \ldots(4.10)$$

The boundary condition (4.4) then simplifies to

$$\frac{A_1}{k_1^2+l^2} + \frac{A_2}{k_2^2+l^2} + \frac{A_3}{k_3^2+l^2} = 0 \qquad \ldots(4.11)$$

where l, k_1, k_2, k_3, A_1 and consequently A_2 and A_3 are all real.

A very different picture of the situation emerges when the frequency of the wave is less than a critical frequency ω^* or when $l > l^*(\omega)$, as is the case with most of the hydromagnetic planetary waves found in nature. In such a situation equation (4.8) will have only two real roots of k (Hide and Jones 1972); a fact also evident from a consideration of the normal curves of figure of 4.2. In this case root k_3 becomes complex which signifies the presence of a 'non-propagating' or leaking type of mode at the boundary. These modes continually radiate energy into the surrounding medium and thus attenuate as they travel away from the boundary. Such waves cannot penetrate deeply into the media and can thus exist only at the boundary. The total energy associated with these modes is negligible and they often arise as a consequence of a phase shift in the reflected waves. (See Pilant1979 p.163, or Officer 1974 p.201 for examples of similar leaking modes in the case of elastic waves). To obtain the amplitudes A_2 and A_3 of the reflected (or leaking) waves, we shall presently study the two cases in detail separately.

4.2.1 Case 1. The frequency of the incident wave is large ie. $\omega \geqslant \omega^*$ and $l \leq l^*(\omega)$

The boundary condition (4.11) alone is not sufficient to

determine the amplitudes of the two reflected waves relative to the incident wave. Therefore we shall introduce the second boundary condition, namely, the continuity of the normal component of the magnetic field across the boundary. If b_{x1}, b_{x2} and b_{x3} denote the x components of the incident magnetic Rossby wave, reflected long wave inertial Rossby wave and reflected Alfven wave, then

$$[b_{x1} + b_{x2} + b_{x3}]_1 = [B_x]_2 \qquad ...(4.12)$$

where points [1] and [2] are situated very close to each other in the fluid and the rigid boundary respectively and $[B_x]_2$ is the value of the x component of the magnetic field in the boundary at point [2].

Now depending on the conductivity of the rigid boundary two further cases arise.

Case 1.A Boundary has infinite conductivity.

The electromagnetic skin depth is zero for a solid perfect conductor and consequently no time varying field penetrates its boundary. Therefore $[B_x]_2 = 0$ and equation (4.12) reduces to: (see Stewartson 1956 and 1957 for the range of applicability of such an assumption)

$$b_{x1} + b_{x2} + b_{x3} = 0 \quad \text{at the boundary} \qquad ...(4.13)$$

Notice that as we are dealing with an inviscid and perfectly conducting fluid there are no boundary conditions on the tangential components of velocity and magnetic field and hence we

cannot rule out the possibility of both vortex and current sheets existing at the interface (Shercliff 1965).

Thus by the help of equations (1.69) and (4.13)

$$k_1A_1/(k_1^2+l^2) + k_2A_2/(k_2^2+l^2) + k_3A_3/(k_3^2+l^2) = 0 \qquad ...(4.14)$$

By eliminating A_3 between (4.11) and (4.14) we obtain

$$\frac{k_1-k_3}{k_1^2+l^2}A_1 + \frac{k_2-k_3}{k_2^2+l^2}A_2 = 0$$

or
$$A_2 = -\left[\frac{k_1-k_3}{k_2-k_3}\right]\frac{k_2^2+l^2}{k_1^2+l^2}A_1 \qquad ...(4.15)$$

Similarly eliminate A_2 from (4.11) and (4.14) to get

$$A_3 = \frac{k_1-k_2}{k_2-k_3}\frac{k_3^2+l^2}{k_1^2+l^2}A_1 \qquad ...(4.16)$$

Thus we can obtain the amplitudes of the reflected waves relative to the amplitude of the incident wave from (4.15) and (4.16) if we have a knowledge of k of the incident and reflected waves. These can be obtained from (4.6) by employing some numerical root solving techniques like the Newton-Ralphson algorithm (see eg. Hilderbrand 1974 p. 575). In this work we: (a) first of all extracted two real roots k_i, k_j numerically, (b) divided (4.8) by $k-k_i$ and $k-k_j$ respectively to obtain a quadratic equation in k which (c) was solved exactly for the remaining two roots which can be real or complex.

Case 1.B The boundary is a perfect insulator.

This corresponds to a more realistic case. For example the earth's mantle may be treated as an insulating boundary as the

time scales involved are very large. Stewartson (1960, also see Roberts 1967, p.26 and Shercliff 1965,p.132) shows that for a fluid of conductivity σ and kinematic viscosity ν in contact with a fixed solid insulator, any jump in the tangential component of the magnetic field is related to the jump in the tangential component of the fluid velocity by the relation

$$\Delta B_s = \mu (\rho \sigma \nu)^{1/2} v_s$$

provided a strong component of magnetic field exists in the normal direction. This relation suggests that in the limit of $\nu \to 0$ and $\sigma \to \infty$, only one of the two boundary sheets ie. current or vortex sheets can exist. In fluids of importance in terrestial or planetary context $\nu\sigma$ is invariably very small and therefore $B_s = 0$. [Note that these results were derived for a non-rotating steady fluid. In appendix I it is shown that as long as $\omega < \Omega$, these conclusions are valid in planetary contexts even for large rotation.] Thus both of the magnetic field components will be continuous across the interface and inside the insulating boundary the magnetic field can be expressed by a potential field ϕ. ie.

$$\bar{b} = \nabla \phi \qquad \text{(inside the boundary)} \qquad \ldots(4.17)$$

Now div $\bar{b} = 0$. Therefore $\nabla^2 \phi = 0$.

This equation has solutions of the form

$$\phi = A \exp(ily - lx) \qquad \ldots(4.18)$$

which when substituted in equation (4.17) yields

$$b_x = -l\phi \quad \text{and} \quad b_y = il\phi$$

ie. $$b_x = ib_y \text{ for } x \geq 0 \qquad \ldots(4.19)$$

Then at x=0, the continuity of magnetic field implies

$$\frac{k_1 - il}{k_1^2 + l^2} k_1 A_1 + \frac{k_2 - il}{k_2^2 + l^2} k_2 A_2 + \frac{k_3 - il}{k_3^2 + l^2} k_3 A_3 = 0 \qquad \ldots(4.20)$$

which with the boundary condition (4.11) gives

$$A_2 = -A_1 \frac{k_2^2 + l^2}{k_1^2 + l^2} \frac{k_1^2 - k_3^2 - il(k_1 - k_3)}{k_2^2 - k_3^2 - il(k_2 - k_3)} \qquad \ldots(4.21)$$

and

$$A_3 = A_1 \frac{k_3^2 + l^2}{k_1^2 + l^2} \frac{k_1^2 - k_2^2 - il(k_1 - k_3)}{k_3^2 - k_2^2 - il(k_3 - k_2)} \qquad \ldots(4.22)$$

Both A_2 and A_3 have imaginary parts indicating that the reflected waves suffer phase shifts. If we denote these phase shifts by ϵ_2 and ϵ_3 respectively then the complex amplitudes can be written as

$$A_2 = |A_2| \exp(i\epsilon_2) \quad \text{and} \quad A_3 = |A_3| \exp(i\epsilon_3)$$

where

$$|A_2| = \frac{A_1}{(k_2 + k_3)^2 + l^2} \frac{k_2^2 + l^2}{k_1^2 + l^2} \frac{k_1 - k_3}{k_2 - k_3} \times \left[\left[(k_1 + k_3)(k_2 + k_3) - l^2 \right]^2 + l^2 (k_1 + k_2 + 2k_3)^2 \right]^{1/2} \qquad \ldots(4.23)$$

$$\epsilon_2 = \tan^{-1} \frac{l(k_1 + k_2 + 2k_3)}{l^2 - (k_1 + k_3)(k_2 + k_3)} \qquad \ldots(4.24)$$

$$A_3 = \frac{A_1}{(k_2 + k_3)^2 + l^2} \frac{k_3^2 + l^2}{k_1^2 + l^2} \frac{k_1 - k_2}{k_3 - k_2} \times \left[\left[(k_1 + k_2)(k_2 + k_3) - l^2 \right]^2 + l^2 (k_1 + k_3 + 2k_2)^2 \right]^{1/2} \qquad \ldots(4.25)$$

and $$\epsilon_3 = \tan^{-1} \frac{l(k_1 + k_3 + 2k_2)}{l^2 - (k_1 + k_2)(k_2 + k_3)} \qquad \ldots(4.26)$$

Note that in this case, though a vortex sheet is permitted, no current sheet can exist at the interface.

Case 2. The frequency of the incident wave is small. $\omega < \omega^*$ OR $l > l^*(\omega)$

As already mentioned, k_3 becomes complex in this case and consequently $\mathfrak{H}_3$ (see equation (4.10)) decays exponentially as this mode moves away from x=0. The necessary electromagnetic boundary condition is again specified by the conductivity of the rigid boundary. Let us first assume a perfectly conducting boundary.

Case 2.A The rigid boundary has infinite conductivity.

Equation (4.13) supplies the necessary boundary condition and A_2 can be obtained from equation (4.15) by replacing k_3 by R+iI in it. As A_1, l, k_1 and k_2 are all real quantities this equation shows that A_2 becomes complex. This is possible only if the wave 2 emerges with a phase shift after reflection.

Then if $A_2 = |A_2| \exp(i\epsilon_2)$

$$|A_2| = \frac{[(k_1-R)(R-k_2)-I^2]^2 + I^2(k_1-k_2)^2}{(R-k_2)^2 + I^2} \qquad \ldots(4.27)$$

$$\epsilon_2 = \tan^{-1} \frac{I(k_1-k_2)}{(k_1-R)(R-k_2)-I^2} \qquad \ldots(4.28)$$

A_3 can be obtained from (4.16) by replacing k_3 by R+iI but the mean value of the amplitude associated with $\mathfrak{H}_3$ ($=A_3\exp(ix)$, remembering that x is negative in the fluid) averaged over many

wavelengths is infinitesimal.

CASE 2.B The boundary is a perfect insulator.

In this case the electromagnetic boundary condition is given by equation (4.20) in which k_3 should be replaced by R+iI. Then A_2 can be obtained from equation (4.21) as

$$A_2 = -A_1 \frac{k_2 + l^2}{k_1^2 + l^2} \quad \frac{k_1^2 - R^2 + I^2 - Il + i(Rl - 2IR - k_1 l)}{k_2^2 - R^2 + I^2 - Il + i(Rl - 2IR - k_2 l)} \qquad \ldots(4.29)$$

It is a simple matter to extract $|A_2|$ and ϵ_2 from this equation, though the exact expressions are very long and will not be reproduced here. A_3 once again has a zero averaged value as its amplitude decays exponentially in the x direction.

4.3 A NUMERICAL STUDY OF THE PROCESS OF REFLECTION.

In the following pages a numerical investigation of the process of reflection carried out for a wide range of incident waves (from small to large frequencies and wavelengths) is reported. Figure 4.3(a) which is based on equation (4.6) illustrates graphically the relationship between k_1 and the x-wavenumbers of the reflected waves over a large range of frequencies ω. l, the y-wavenumber is unchanged for reflected waves and is held constant at l=0.05. It is immediately evident from this diagram that for $\omega \leq \omega^*$, only one reflected wave which has $k_2 << k_1$ is produced. For $\omega > \omega^*$, another reflected wave corresponding to k_3 is generated amd again we can see that $k_3 < k_1$, indicating that the reflected waves are of much longer wavelengths. Figure 4.3b shows the relationship between k_1 and k_2

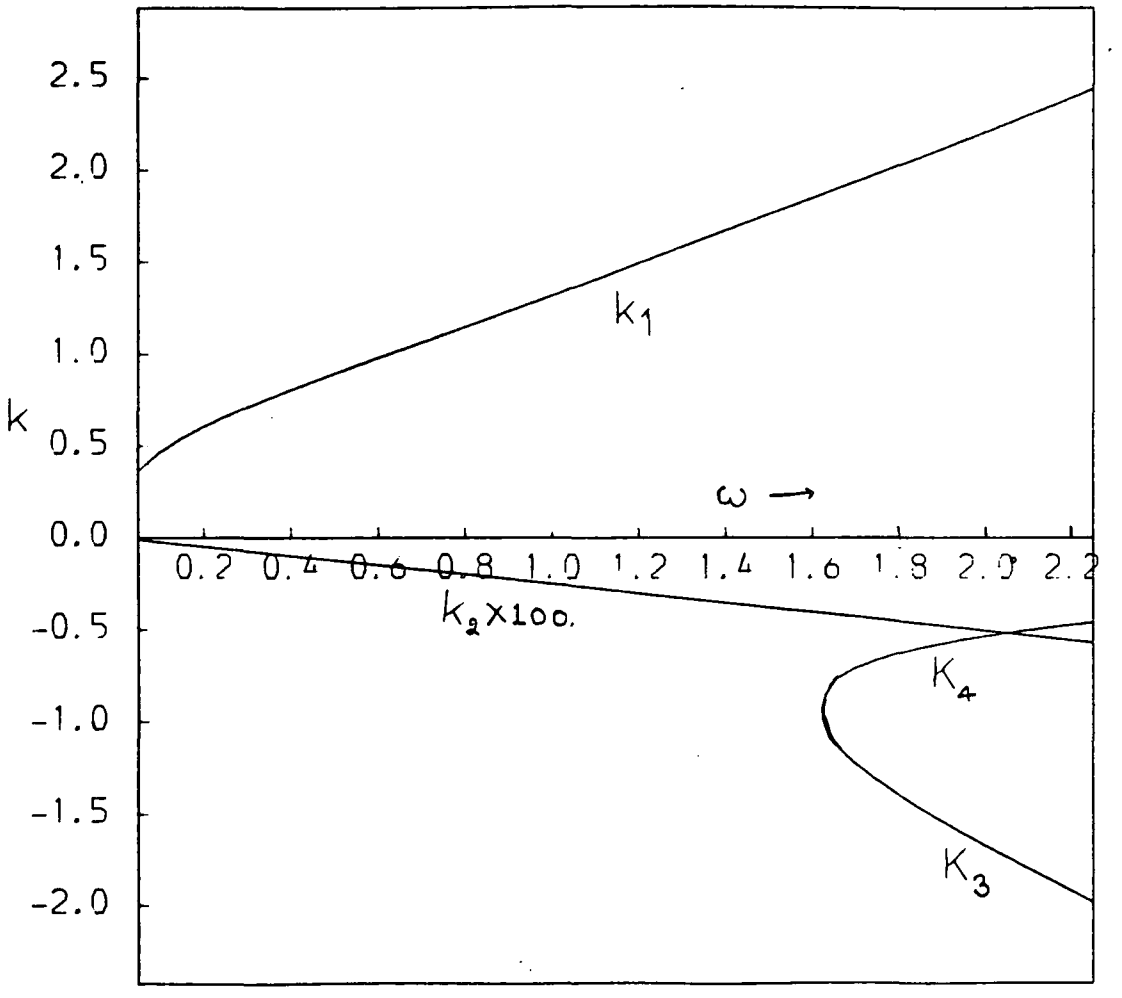

FIGURE 4.3(a) The incident and reflected x wavenumbers as functions of frequency. l is constant at 0.05. Note that k_2 has been multiplied by 100.0 to enable it to be plotted on the same graph.

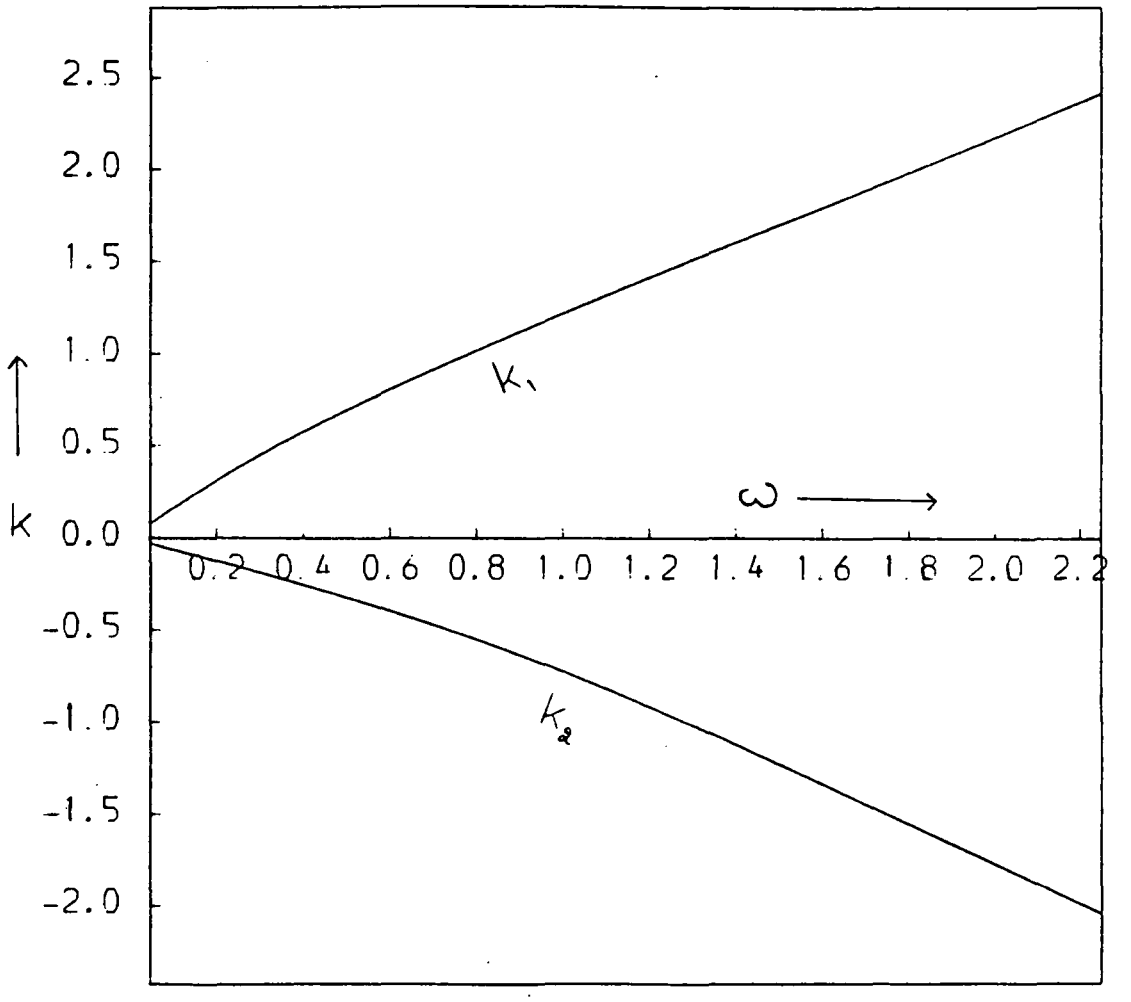

FIGURE 4.3(b) The incident and reflected wave numbers as functions of frequency. $l = 1.0$. k_3 and k_4 are imaginary for all ω.

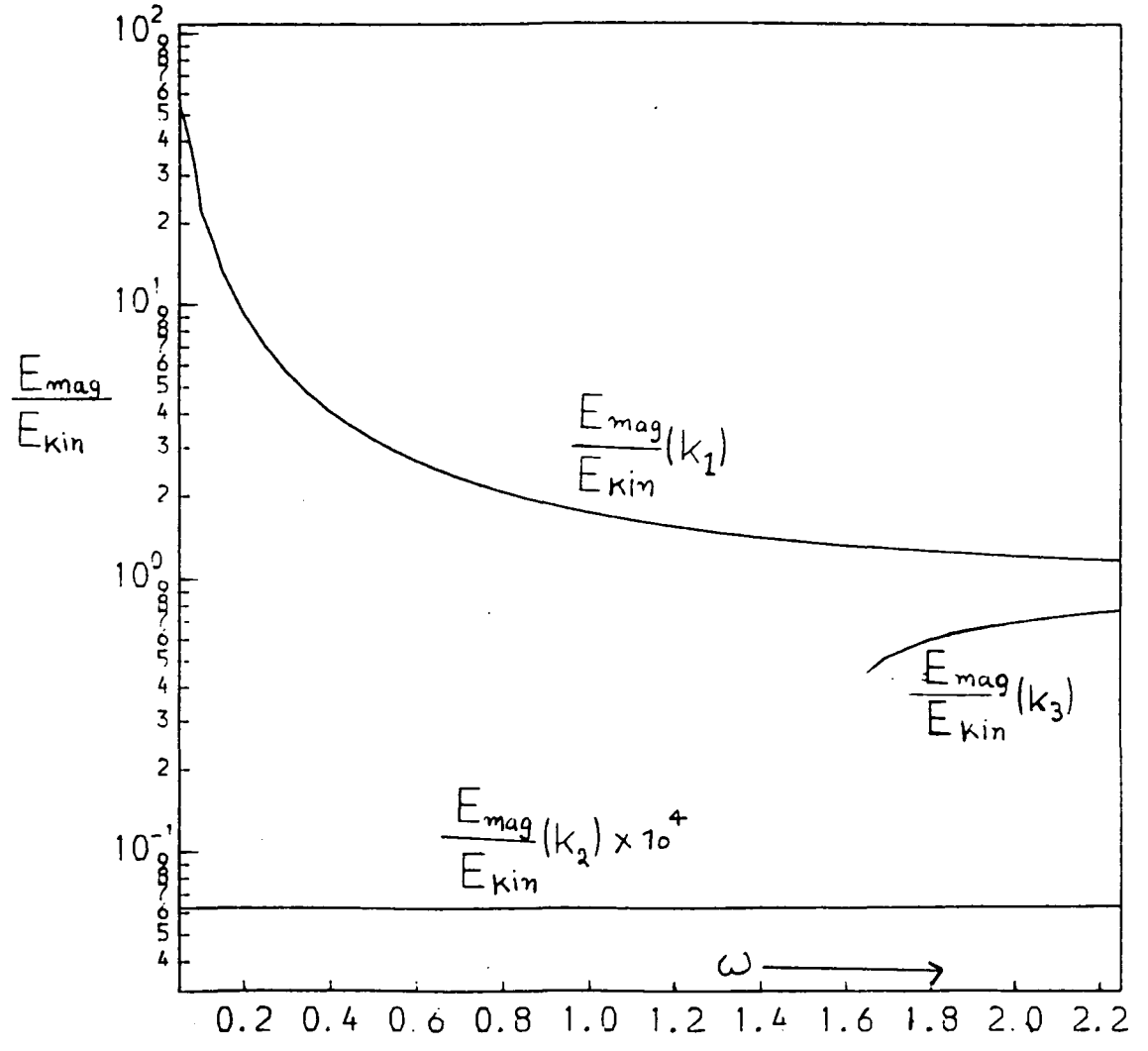

FIGURE 4.4(a)The plots of magnetic/kinetic energy ratios for incident and reflected waves vs ω. l=0.05.

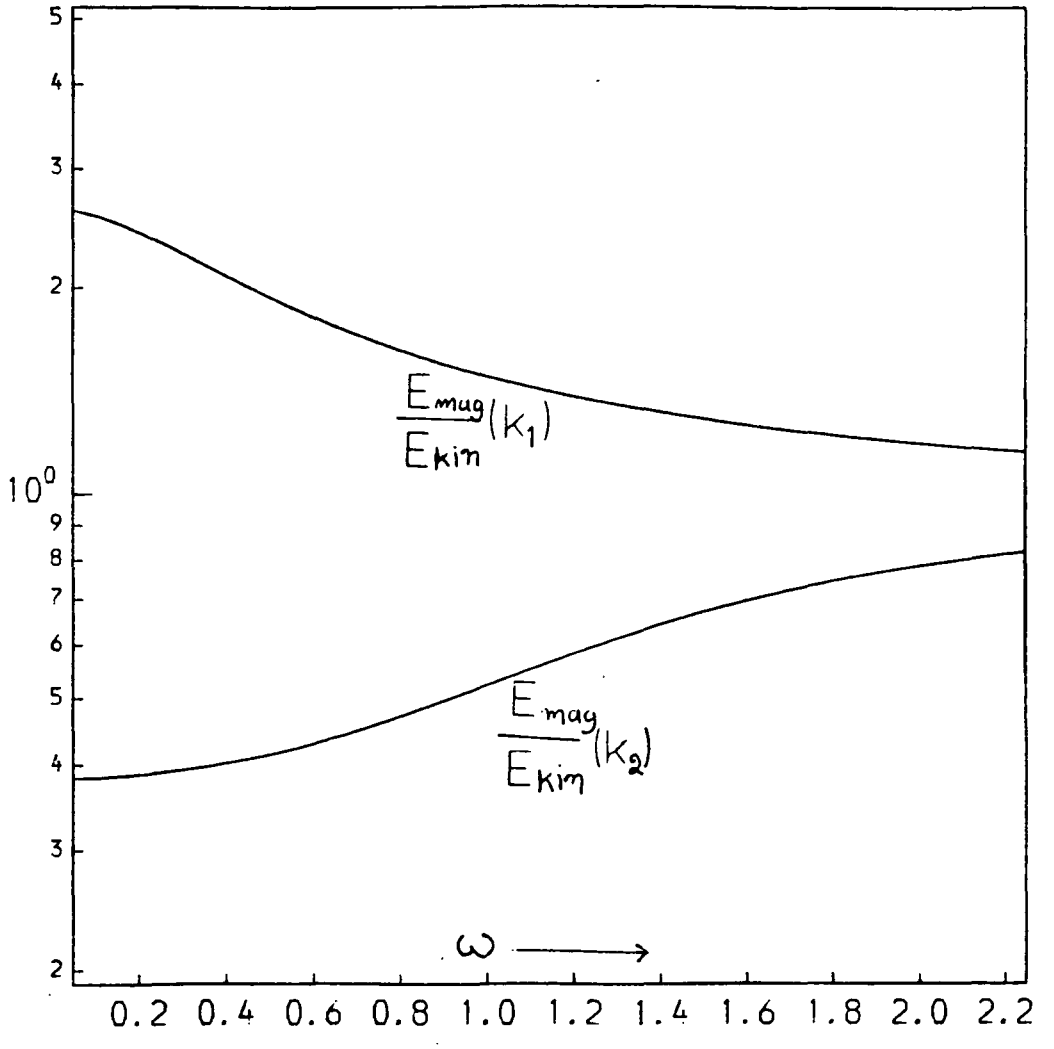

Figure 4.4(b) Same as figure 4.4(a) except l = 1.0.

for the case l=1.0. Similar remarks as above apply to this figure except for the fact that k_3 and k_4 are complex for all ω.

Once we know the exact values of the wavenumbers and the frequencies of the incident and reflected waves, we can determine the relative contents of magnetic and kinetic energies of each of these waves by the help of equation (4.7). These have been plotted in figure 4.4(a) for waves with l=0.05 and confirm that $E_{mag}/E_{kin}\ (k_2) << E_{mag}/E_{kin}\ (k_1)$ demonstrating once again that wave 2 represents an inertial Rossby-MHD wave. Thus for low frequencies (most planetary waves have $\omega << 0.2$ and $K << 0.4$ in these dimensionless units), there is a major conversion of magnetic energy into kinetic form as a consequence of reflection at a N-S boundary. Wave 3 is generated only when the incident wave has a very high frequency. At such high frequencies the incident magnetic wave is essentially an Alfven wave which is unaffected by rotation as is evident from its magnetic to kinetic energy ratio which is O(1). Then wave 3 is also an Alfven wave though $E_{mag}/E_{kin}(k_3) < E_{mag}/E_{kin}(k_1)$. Figure 4.4(b) shows these ratio plots for waves with l=1.0. Once again similar inferences can be drawn except that only one wave is generated after reflection.

The E-W and N-S group velocities of a wave i (i = 1,2,3) can be obtained from (4.5) by differentiating it w.r.t. k or l.

$$C_{gx}(k_i) = \frac{\partial \omega}{\partial k_i} = \frac{1}{\left(2\omega + \frac{k_i}{k_i^2 + l^2}\right)} \left[2k_i - \frac{\omega(l^2 - k_i^2)}{(k_i^2 + l^2)^2} \right] \qquad \ldots(4.30)$$

$$C_{gy}(k_i) = \frac{\partial \omega}{\partial l} = \frac{1}{\left(2\omega + \frac{k_i}{k_i^2 + l^2}\right)} \left[\frac{2\omega k_i l}{(k_i^2 + l^2)^2}\right] \qquad \ldots(4.31)$$

The group velocities so determined are shown in figures 4.5 to 4.7. It is clearly evident from these figures that for all ω, the group velocities of wave 2 are much larger than the group velocities of waves 1 and 3. At higher frequencies waves 1 and 3 have group velocities which are representative of Alfven waves. Further the E-W component of the group velocity of wave 1 is positive which confirms that it is an eastward propagating wave whereas the x components of group velocity of wave 3 is negative which shows that it is an inertial Rossby-MHD wave moving away from the boundary as we stressed earlier.

As the group velocities of the reflected inertial waves are considerably larger than that of the incident wave we would intuitively expect these reflected waves to have much lower energy densities. The average energy density of a hydromagnetic wave j is given by (Acheson and Hide 1973)

$$\langle E_j \rangle = \langle 0.5(u_j^2 + v_j^2) + 0.5(b_{xj}^2 + b_{yj}^2)/(\mu\rho) \qquad \ldots(4.32)$$

where u_j, v_j are the x and y components of the kinematic fluid velocity associated with the wave and b_{xj} and b_{yj} are the x and y components of magnetic field perturbation. $\langle\ \rangle$ denotes average over a period.

Now from Hide(1966) and equations (1.68) and (1.69)

$$u_j = il/(k_j^2 + l^2)\,\zeta_j \qquad \ldots(4.33A)$$

$$v_j = -ik_j/(k_j^2 + l^2)\,\zeta_j \qquad \ldots(4.33B)$$

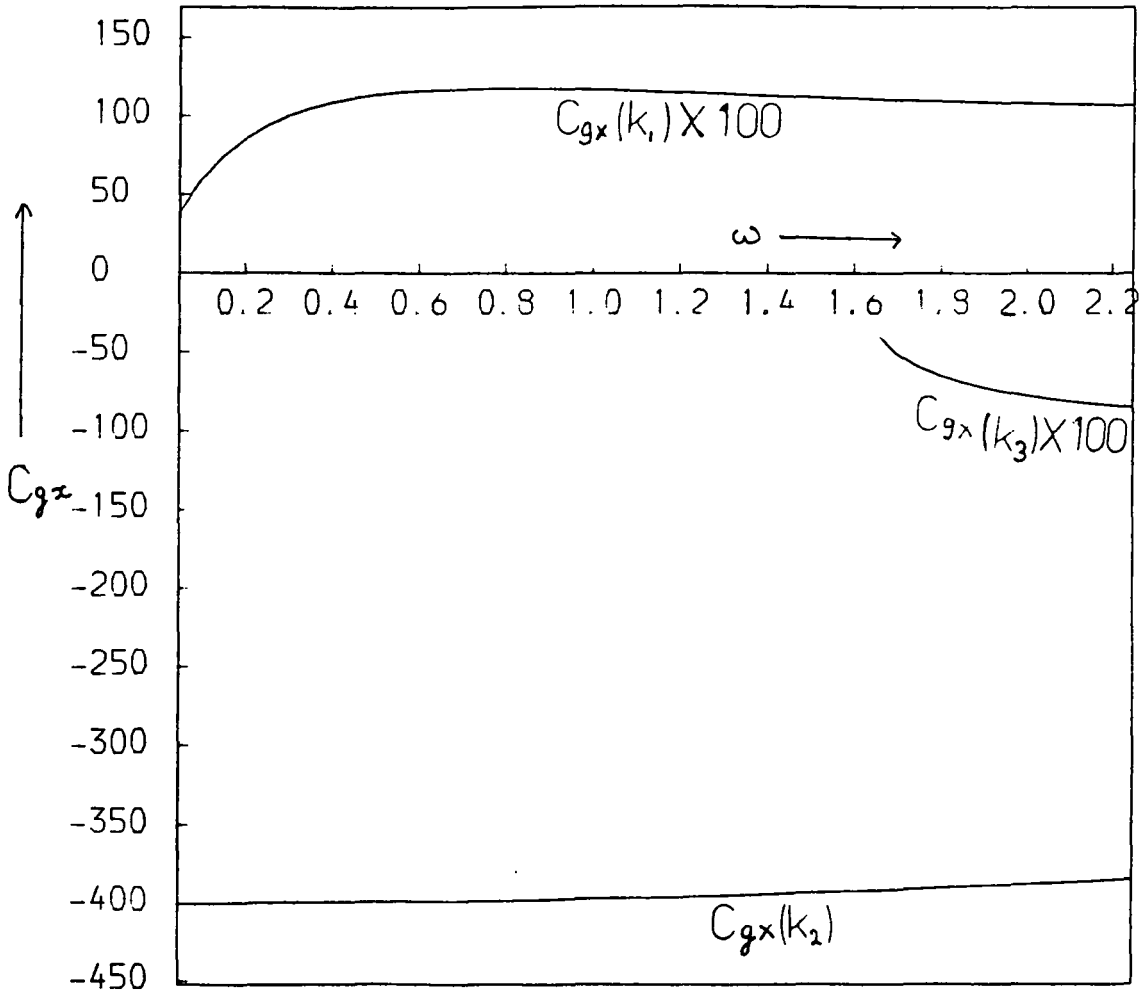

FIGURE 4.5(a) The E-W components of the group velocities of the incident and reflected waves. Note that for $\omega<1.6119$ $C_{gx}(k_3) = 0.0$. $l=0.05$.

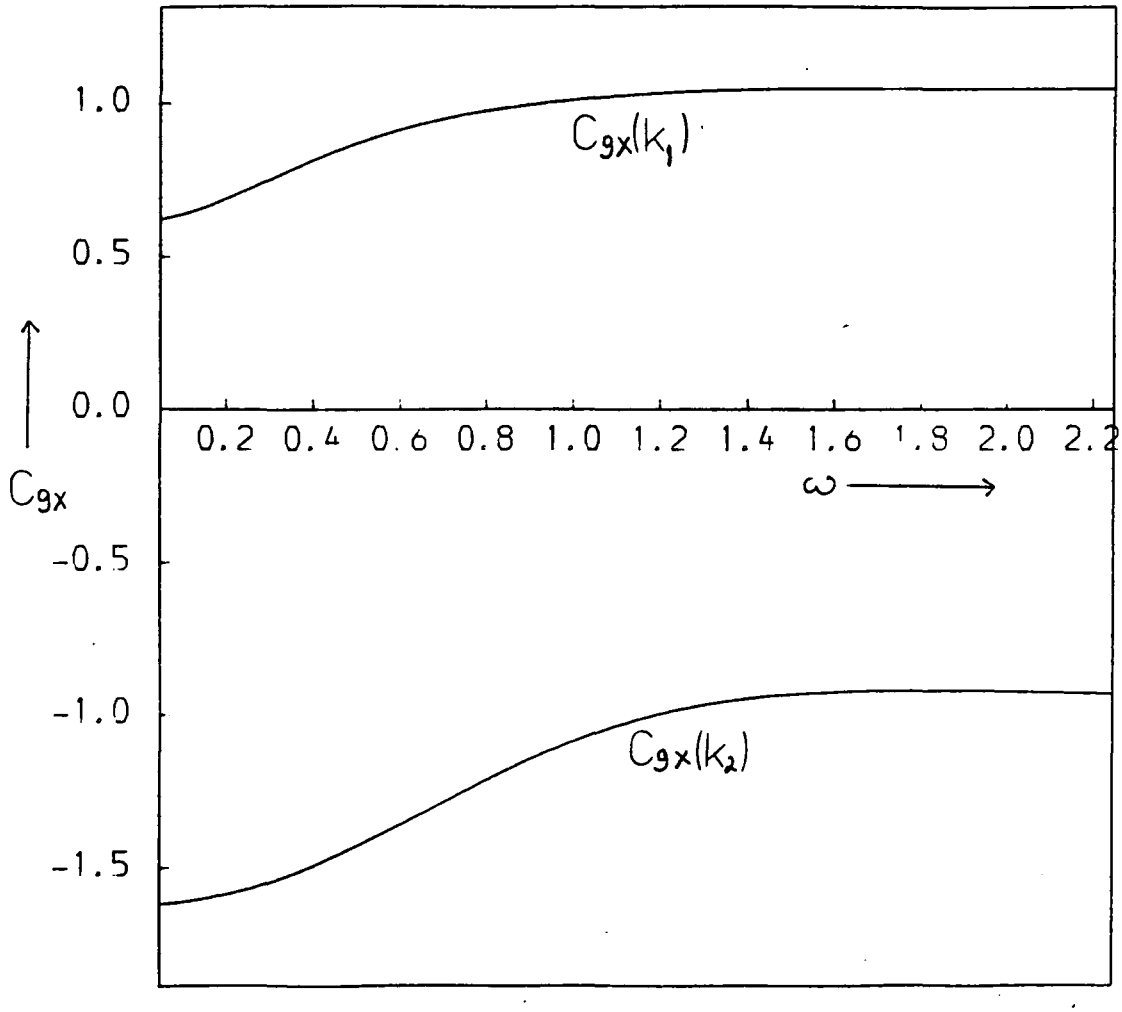

FIGURE 4.5(b) Same as figure 4.5(a) except l=1.0

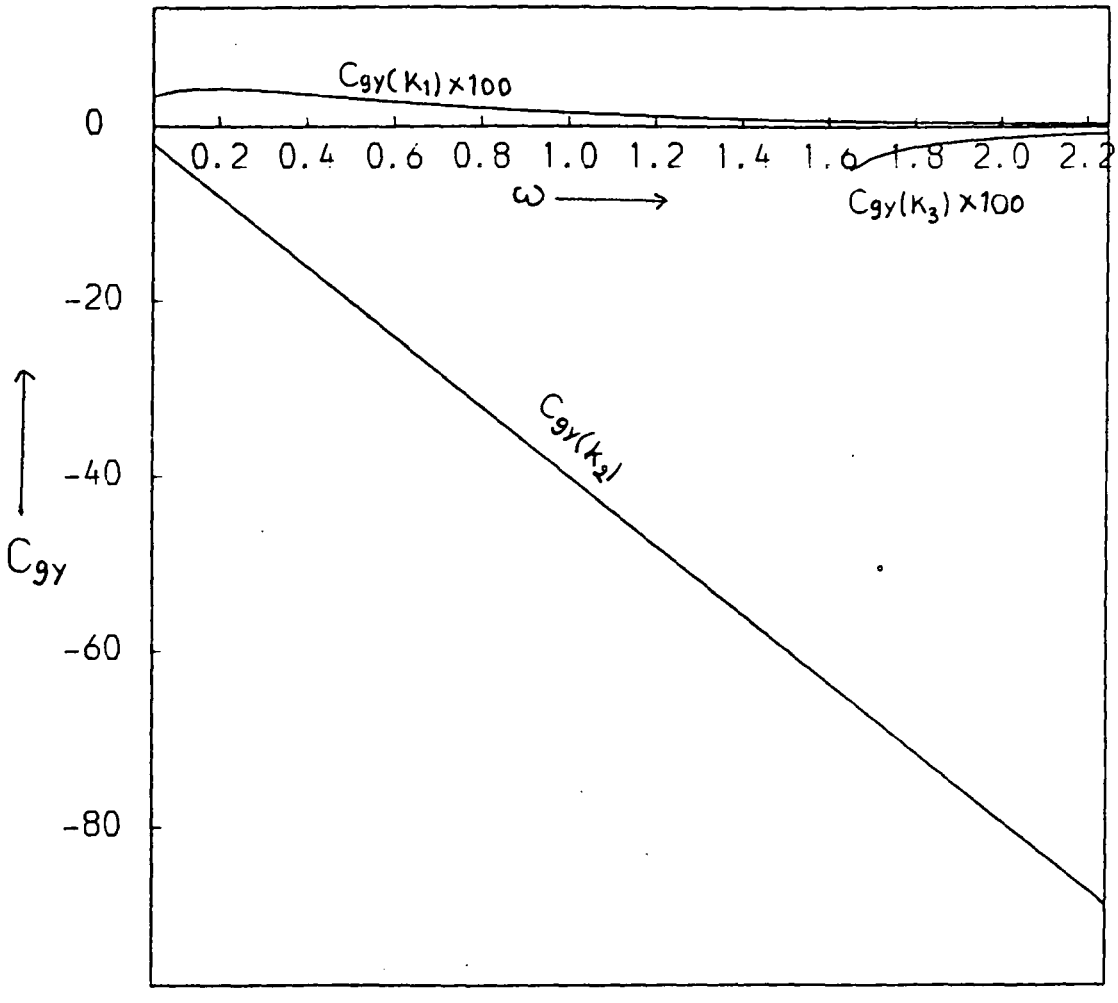

FIGURE 4.6(a)The N-S group velocities of the incident and reflected waves. For $\omega < 1.6119$ $C_{gy}(k_3) = 0$. l=.05

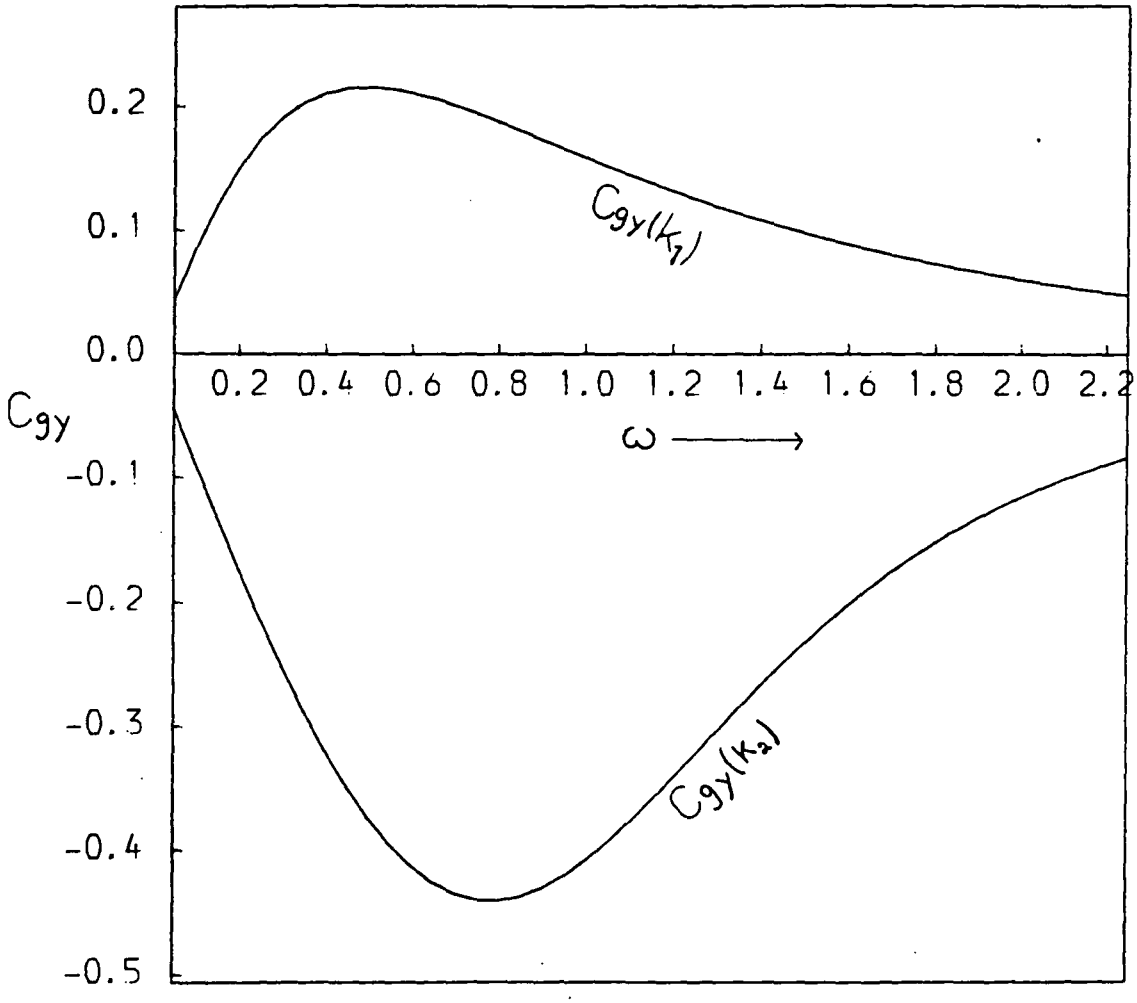

FIGURE 4.6(b) Same as figure 4.6(a) except 1 = 1.0.

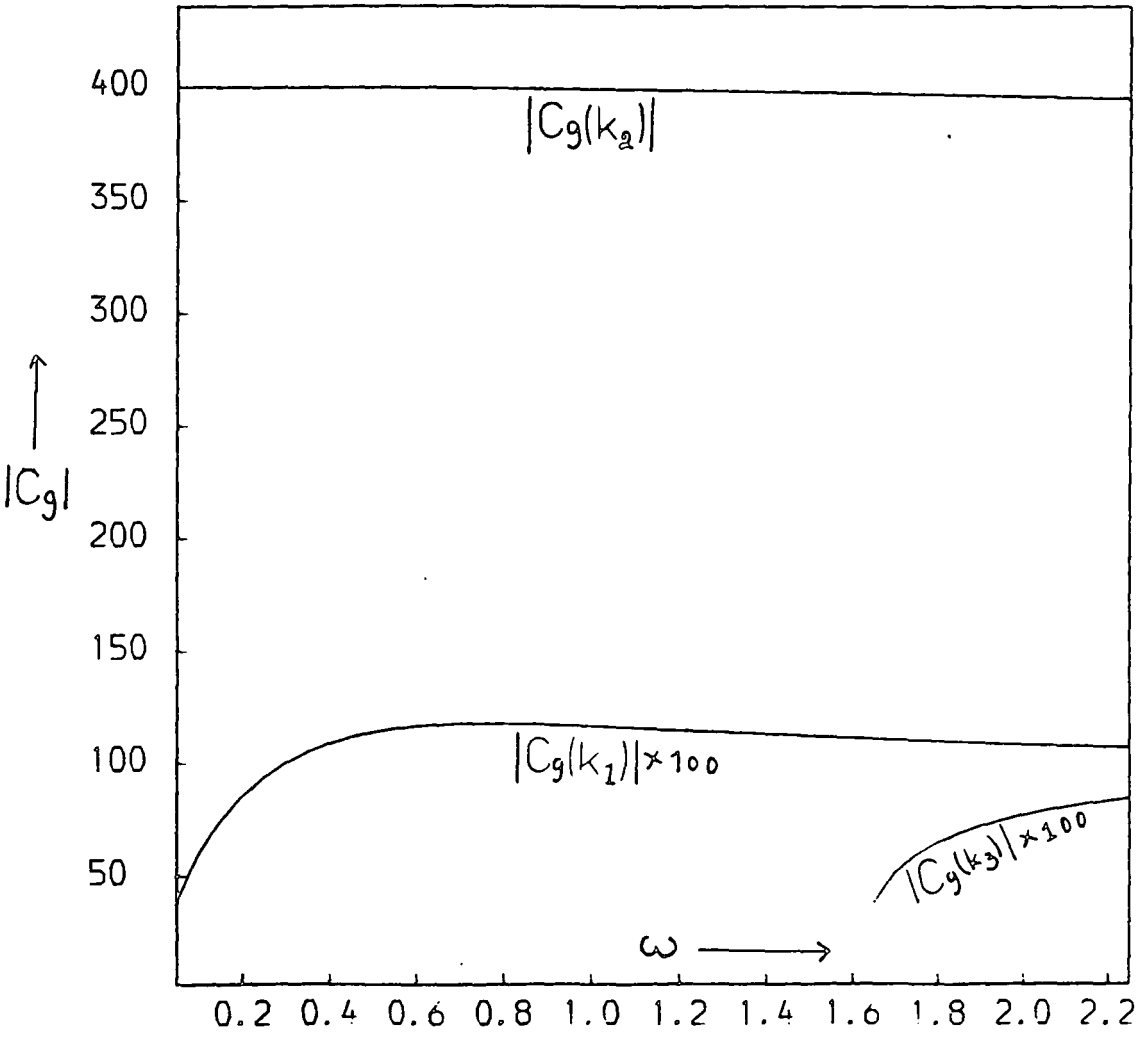

FIGURE 4.7(a)The group velocity $|C_g|$ of the incident and reflected waves. For $\omega < 1.6119$, $C_g(k_3) = 0.1 = 0.05$

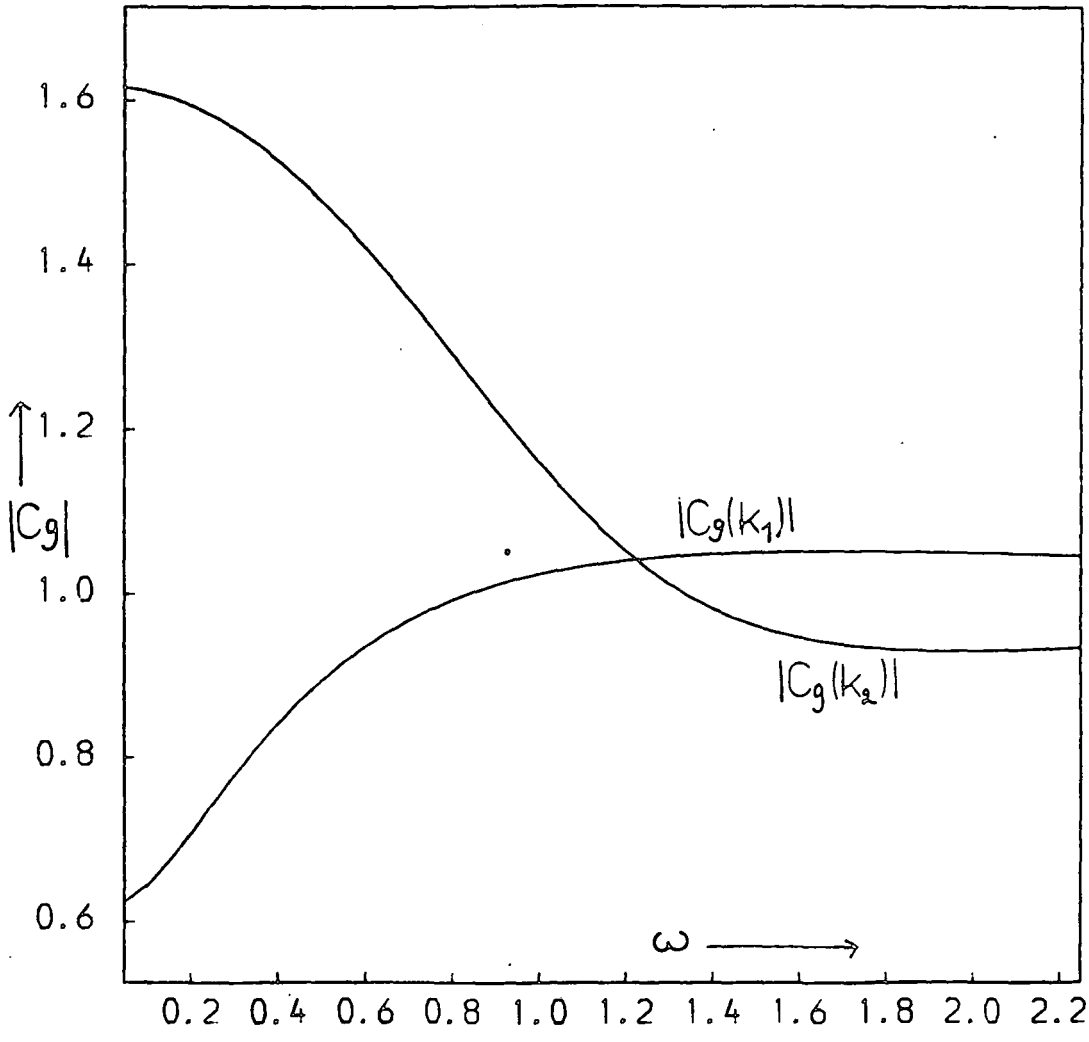

FIGURE 4.7(b) The group velocity $|C_g|$ of the incident and reflected waves for the case $l = 1.0$ $|C_g(k_3)|$ is zero throughout.

$$b_{xj} = -iB_0 k_j l/[\omega(k_j^2+l^2)]\,\mathfrak{b}_j \qquad \ldots(4.33C)$$

and $$b_{yj} = iB_0 k_j^2/[\omega(k_j^2+l^2)]\,\mathfrak{b}_j \qquad \ldots(4.33D)$$

Thus from (4.32)

$$\langle E_j \rangle = \frac{1}{2}\,\frac{\omega^2 + k_j^2 V_a^2}{\omega^2(k_j^2+l^2)}\,|\mathfrak{b}_j|$$

which can be written in terms of the amplitudes as

$$\langle E_j \rangle = \frac{1}{4}\,\frac{\omega^2 + k_j^2}{\omega^2(k_j^2+l^2)}\,A_j^2 \qquad \ldots(4.34)$$

where A_j is given by one of (4.1), (4.15), (4.16), (4.21), (4.22), (4.23) or (4.24) and observe that V_a is unity in our units.

One can easily appreciate from figure 4.8(a) which has been drawn for the case of reflection of a magnetic wave by a conducting boundary that the energy density of the incident magnetic wave far exceeds that of the inertial wave. At higher frequencies an Alfven wave is also generated whose energy density is marginally smaller than that of the incident wave. Contrast this with the reflection at an insulating boundary (Figure 4.8c) where the energy density of the returning Alfven wave is actually larger than that of the incident wave. Thus at higher frequencies we can expect an insulator to return more energy in the form of an Alfven wave than a conductor. Figures 4.8(b) and 4.8(d) are identical to each other (as one would expect, because all the incident energy returns in the same reflected form in both the cases), though the differences of energy densities between the

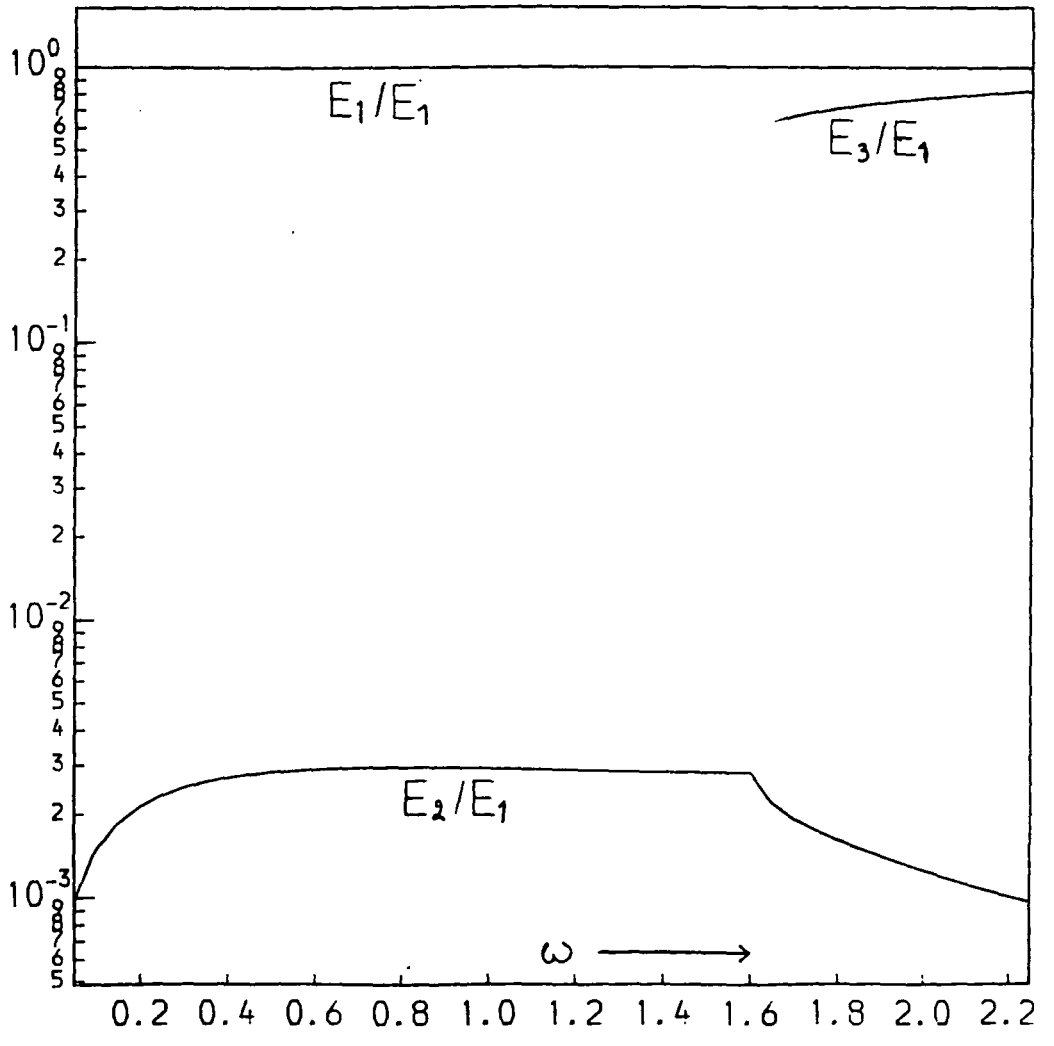

FIGURE 4.8(a) The energy densities of the incident and reflected waves as functions of frequency. l = 0.05. The wave is incident on a perfectly conducting boundary.

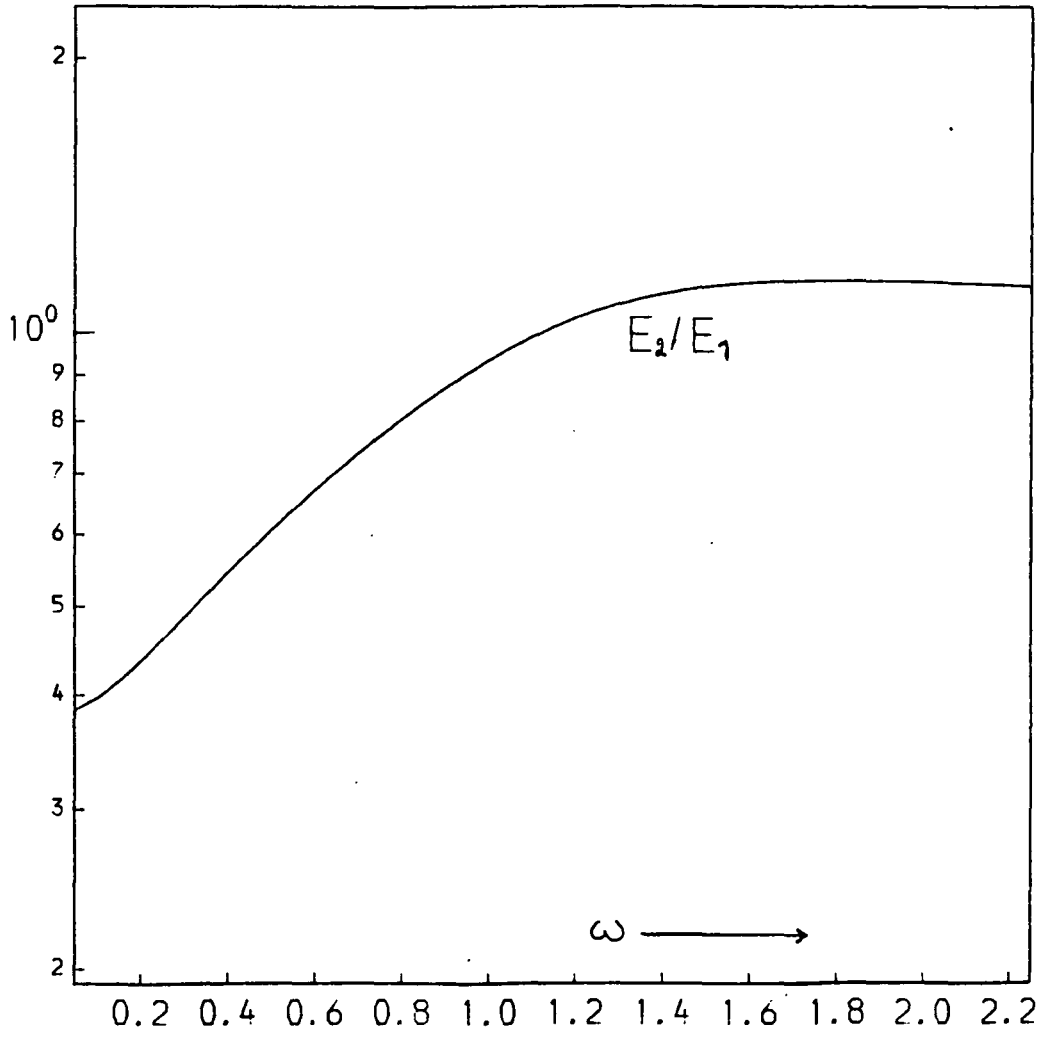

FIGURE 4.8(b) Same as figure 4.8(a) except l = 1.0

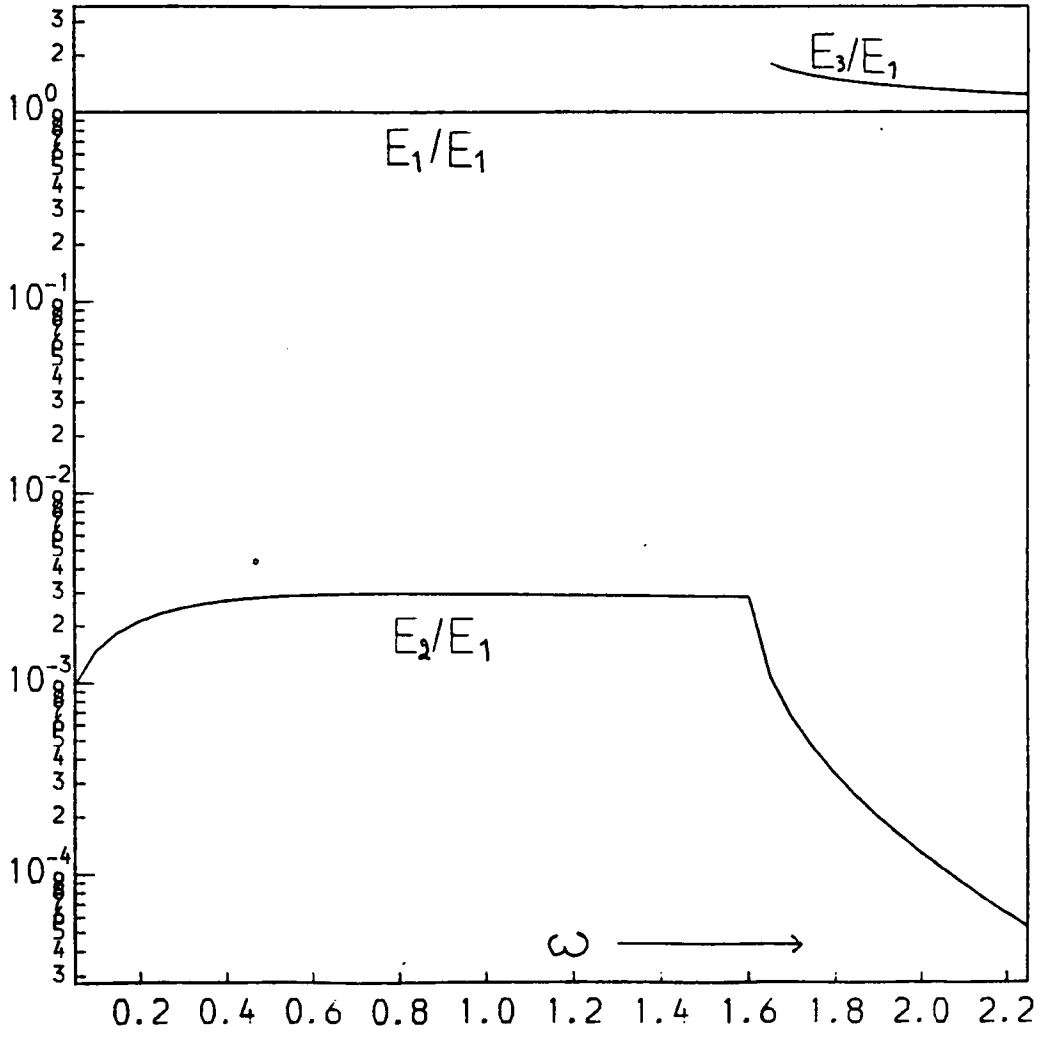

Figure 4.8(c) The energy densities of the incident and reflected waves when the wave is incident on an insulating boundary. l = 0.05.

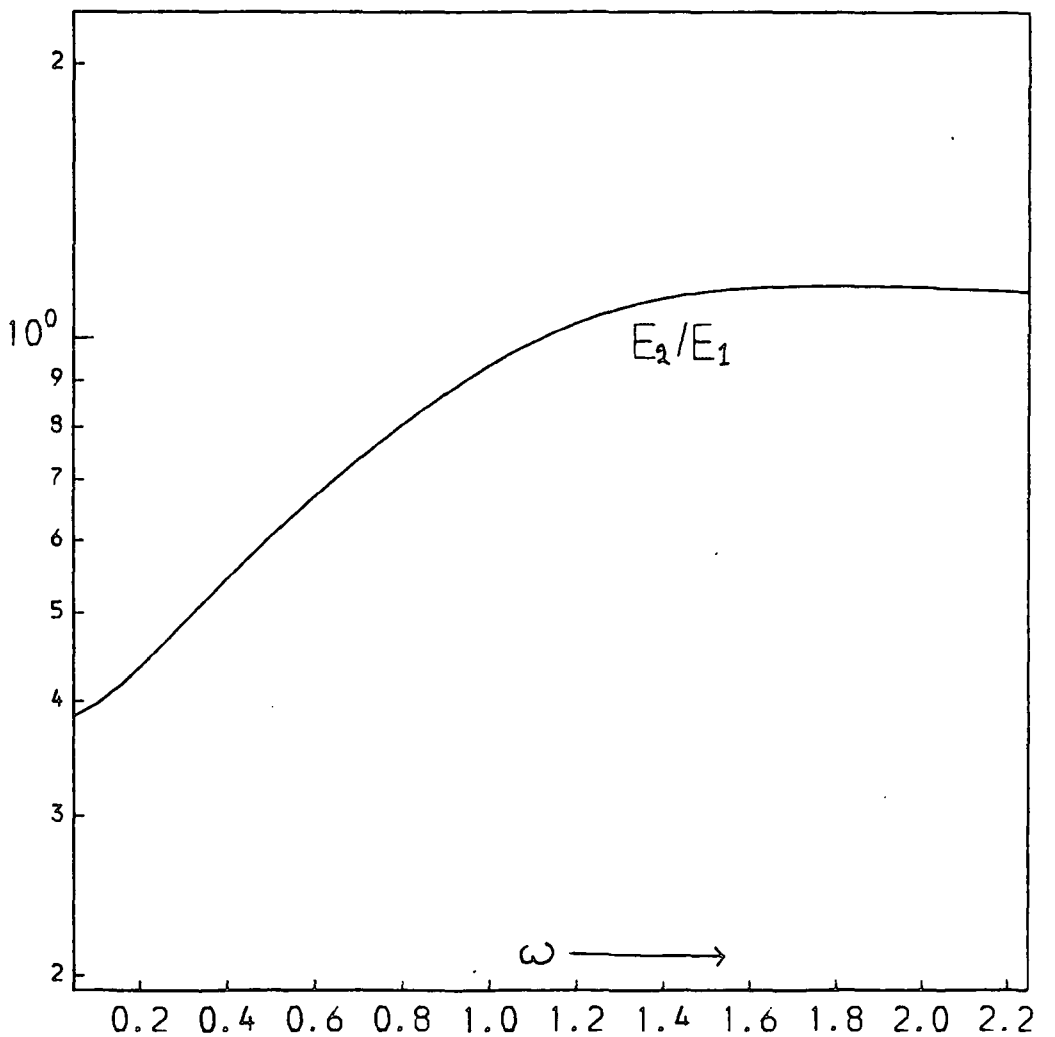

Figure 4.8(d) Same as figure 4.8(b) except l = 1.0.

incident and reflected wave are not so dramatic. The reflected waves are never in phase with the incident wave as can be seen from figures 4.9 (a), (b), (c) and (d); the conducting boundary in general producing larger phase differences between the incident and reflected waves.

Though the energy densities of the reflected inertial waves are much smaller than that of the incident wave one would expect the flux of energy to remain constant for incoming and outgoing waves. The energy flux through a unit area of the rigid boundary is given by (for the justification of this choice, of the definition of energy flux, see Appendix II.)

$$F_j = E_j . C_{gj} \cos(\alpha_j) \qquad \ldots(4.35)$$

where α_j is the angle of incidence or reflection measured anti-clockwise from the normal to the boundary. It will be given by

$$\alpha_j = \mathrm{TAN}^{-1}(C_{gy} / C_{gx}) \qquad \ldots(4.36)$$

Figures 4.10 (a) and (b) graphically illustrate the relationship between the angles of incidence and reflection for a wide range of wave frequencies. It can be seen that both the incident and reflected wave packets make very small angles to the x-axis and thus propagate, for the range of frequencies studied, almost parallel to the x-axis. At low frequency limit the incident wave can be seen to fall far more obliquely on the rigid boundary than the emerging reflected inertial wave which would imply that the width of the wave packet increases as a result of reflection. Figures 4.11 to 4.13 show the x and y components and total energy

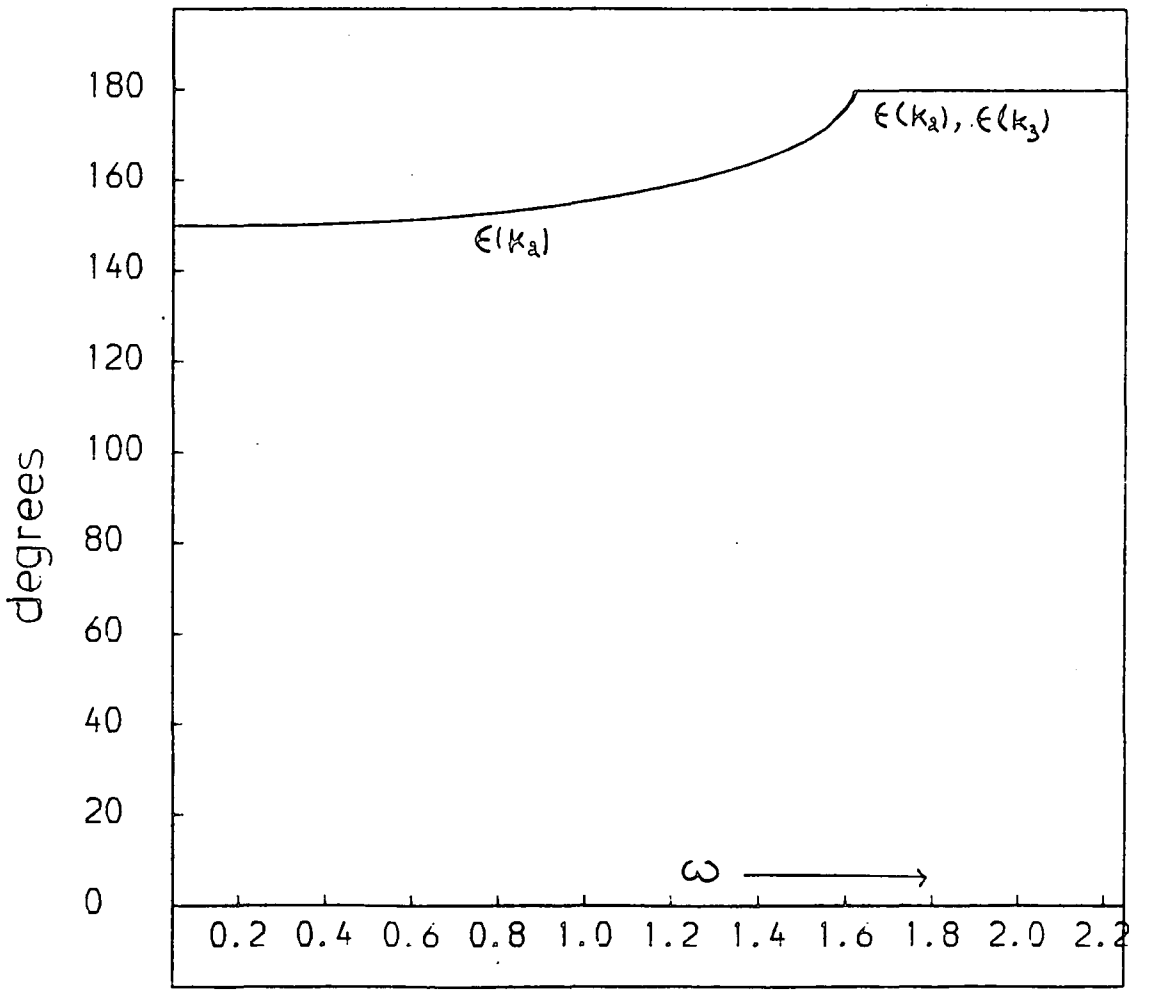

Figure 4.9(a)The phases of the incident and reflected waves for the case of reflection from a conducting body. $l = 0.05$.

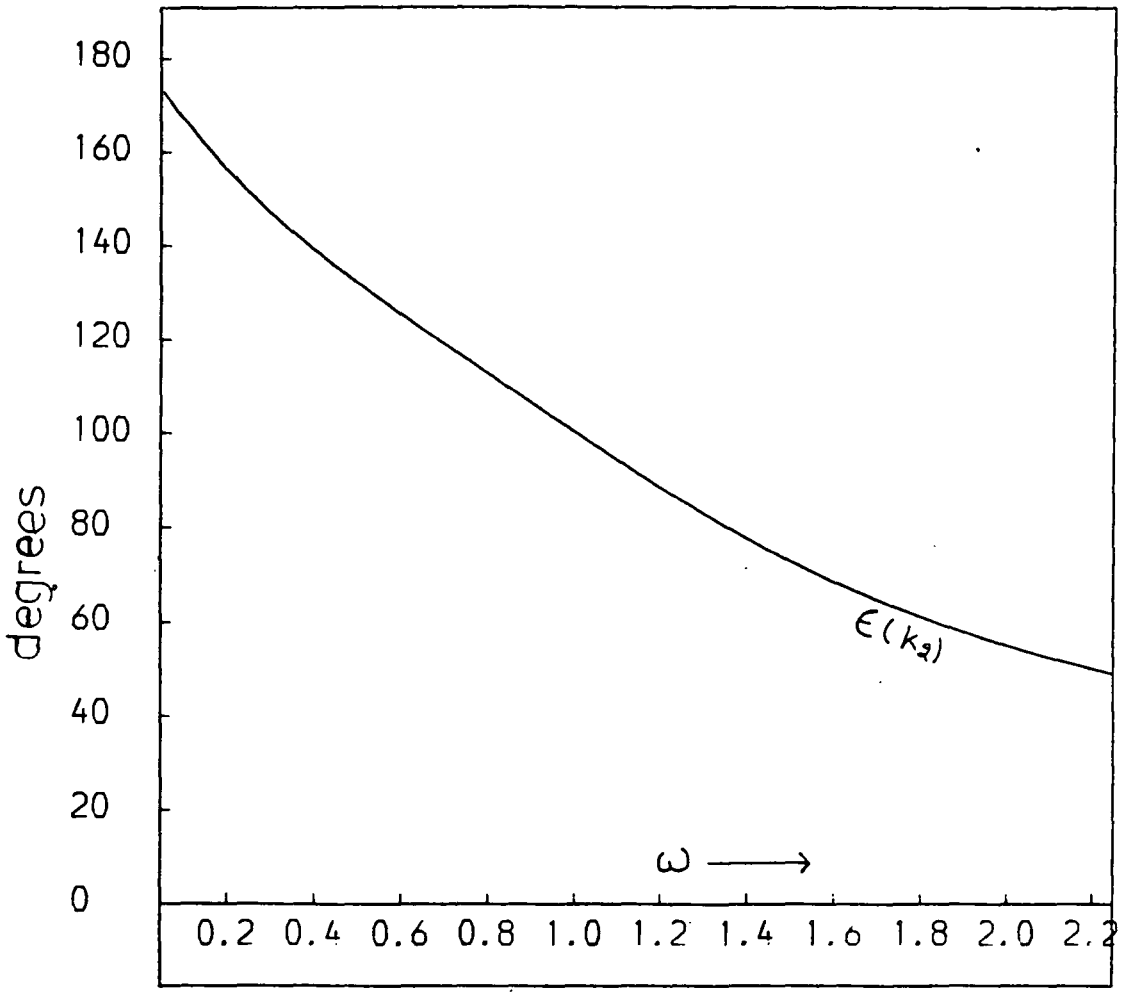

Figure 4.9(b) Same as 4.9(a) except l = 1.0.

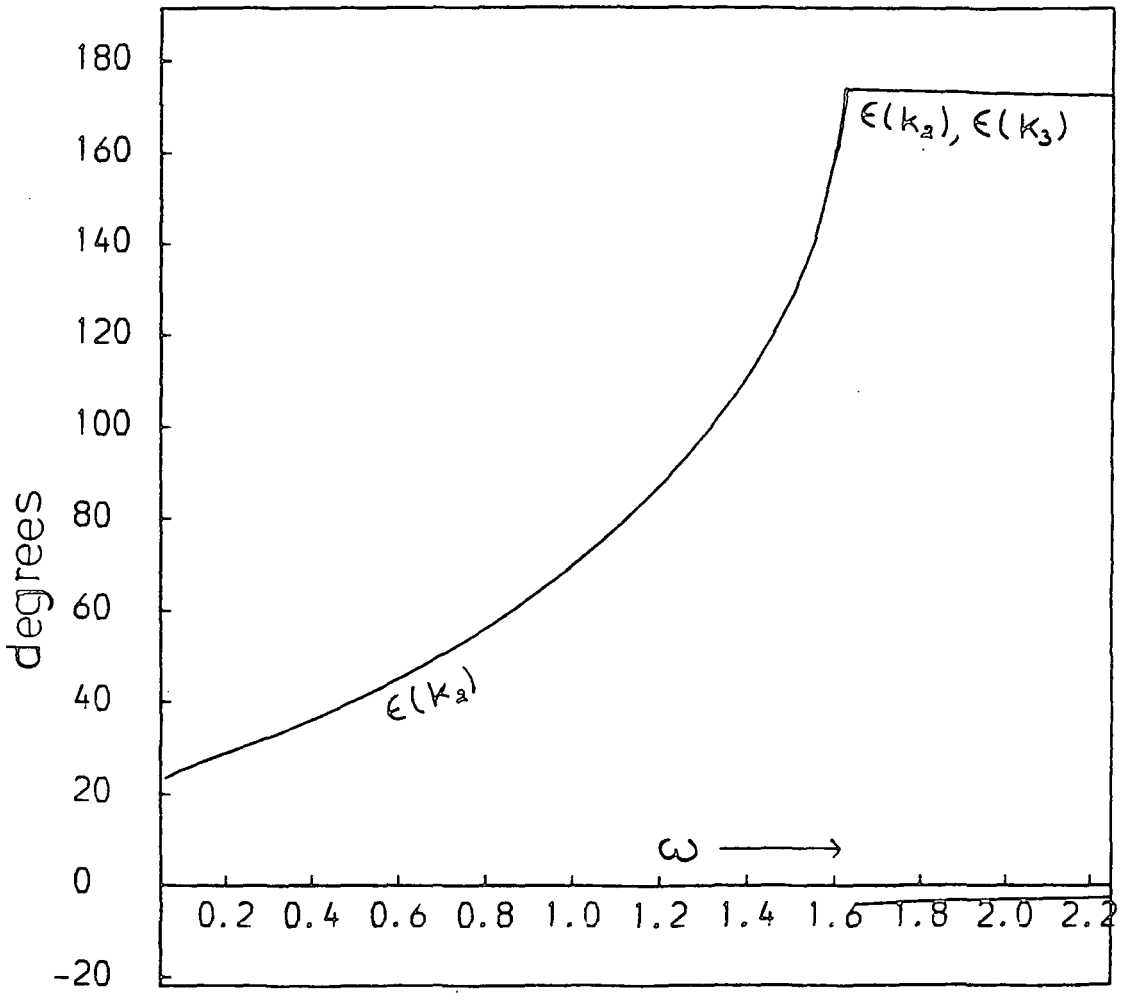

Figure 4.9(c) The phase angles of incident and reflected waves for the case of reflection from an insulating boundary. $l = 0.05$.

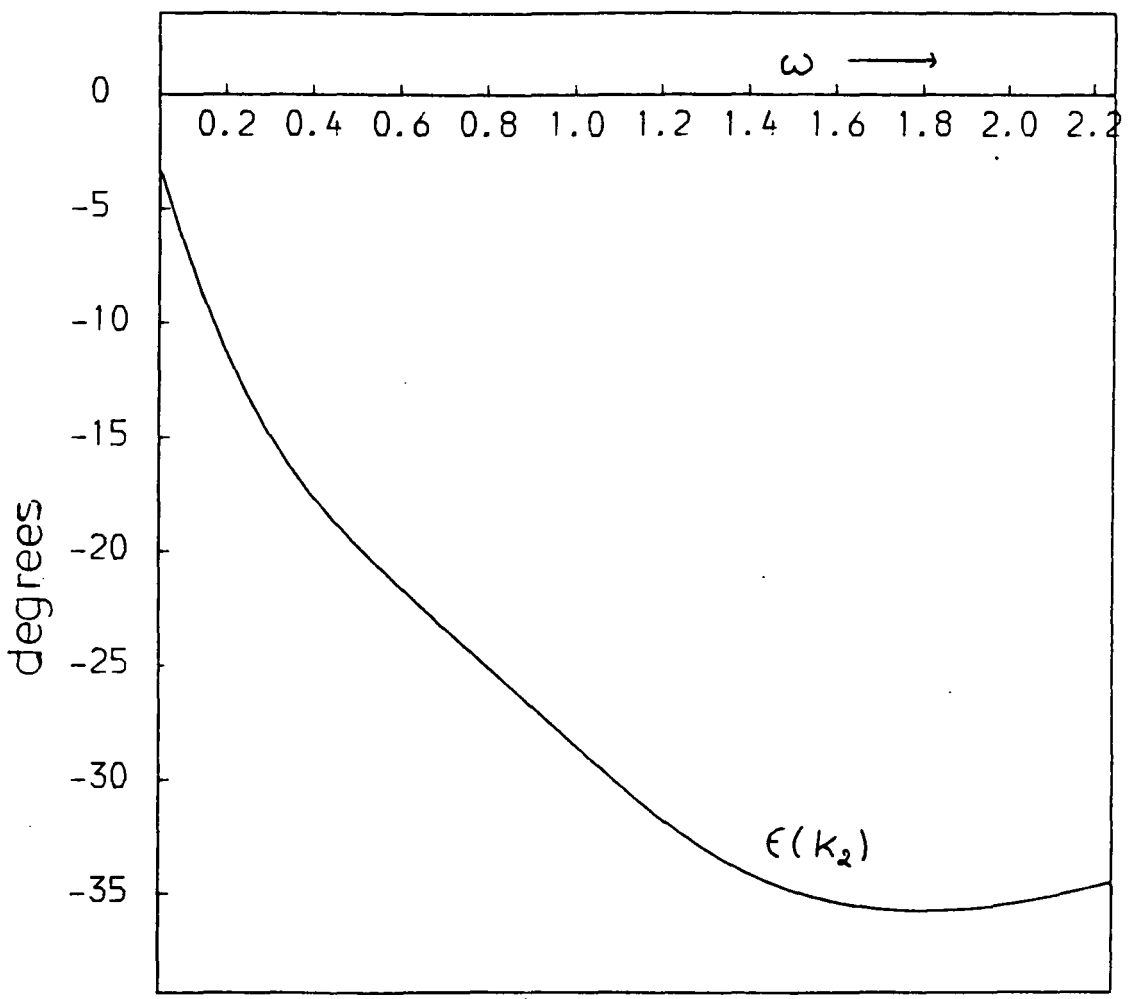

Figure 4.9(d) Same as figure 4.9(C) except 1 = 1.0

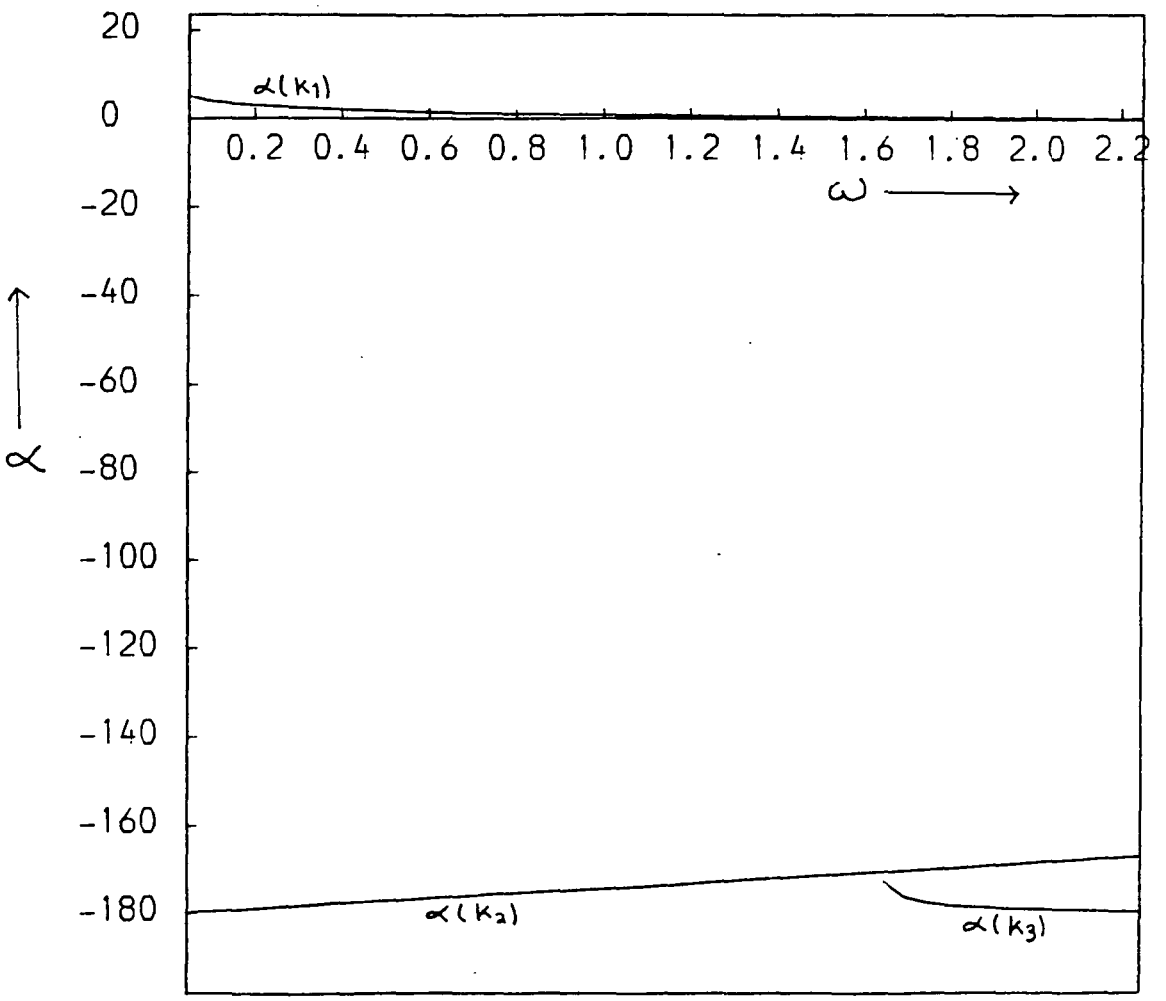

FIGURE 4.10(a) Showing the relationship between the angles of incidence and reflection for the three waves. Note that for very small ω the reflected fast wave returns almost parallel to the x-axis. $l = 0.05$

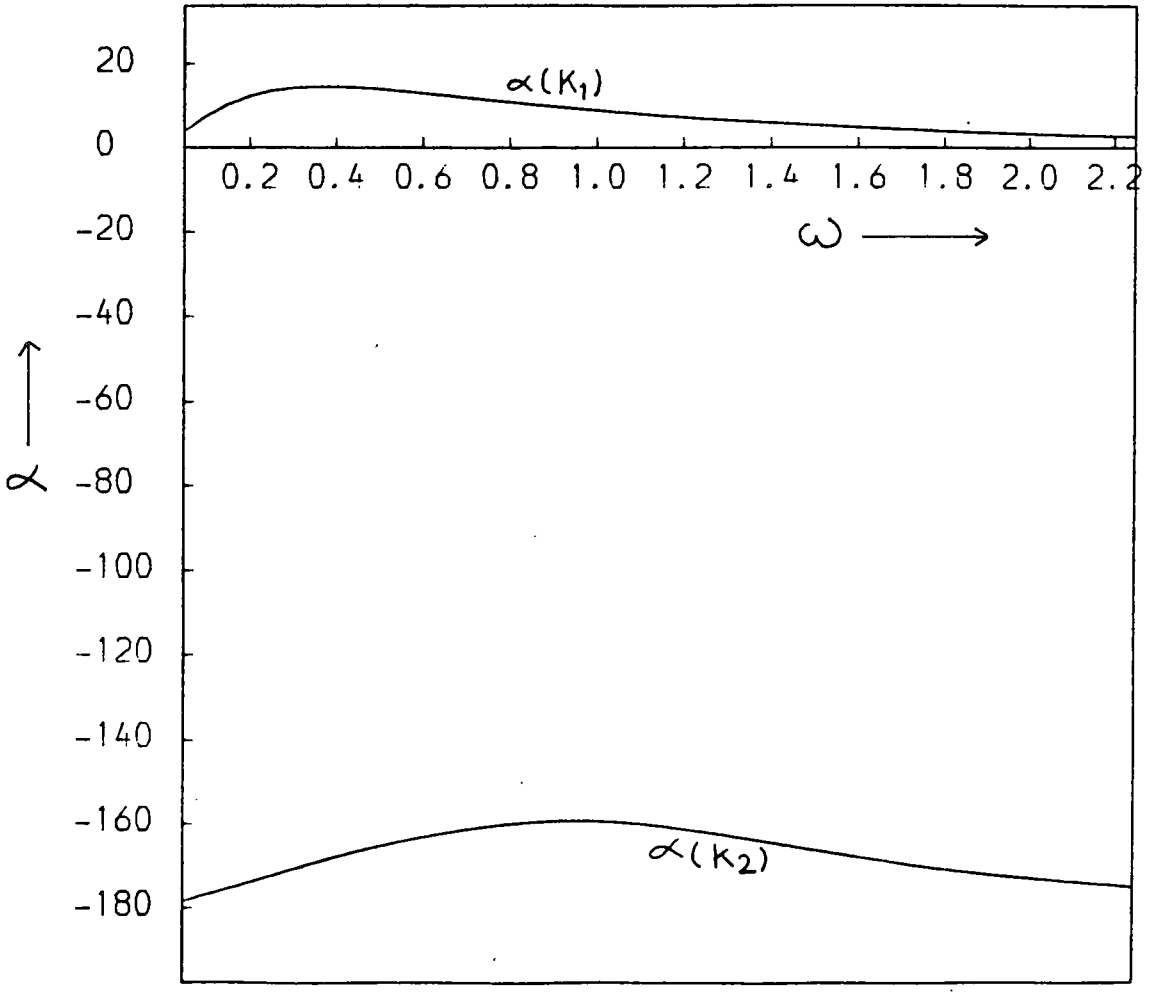

FIGURE 4.10(b) Same as figure 4.10(a) except l = 1.0

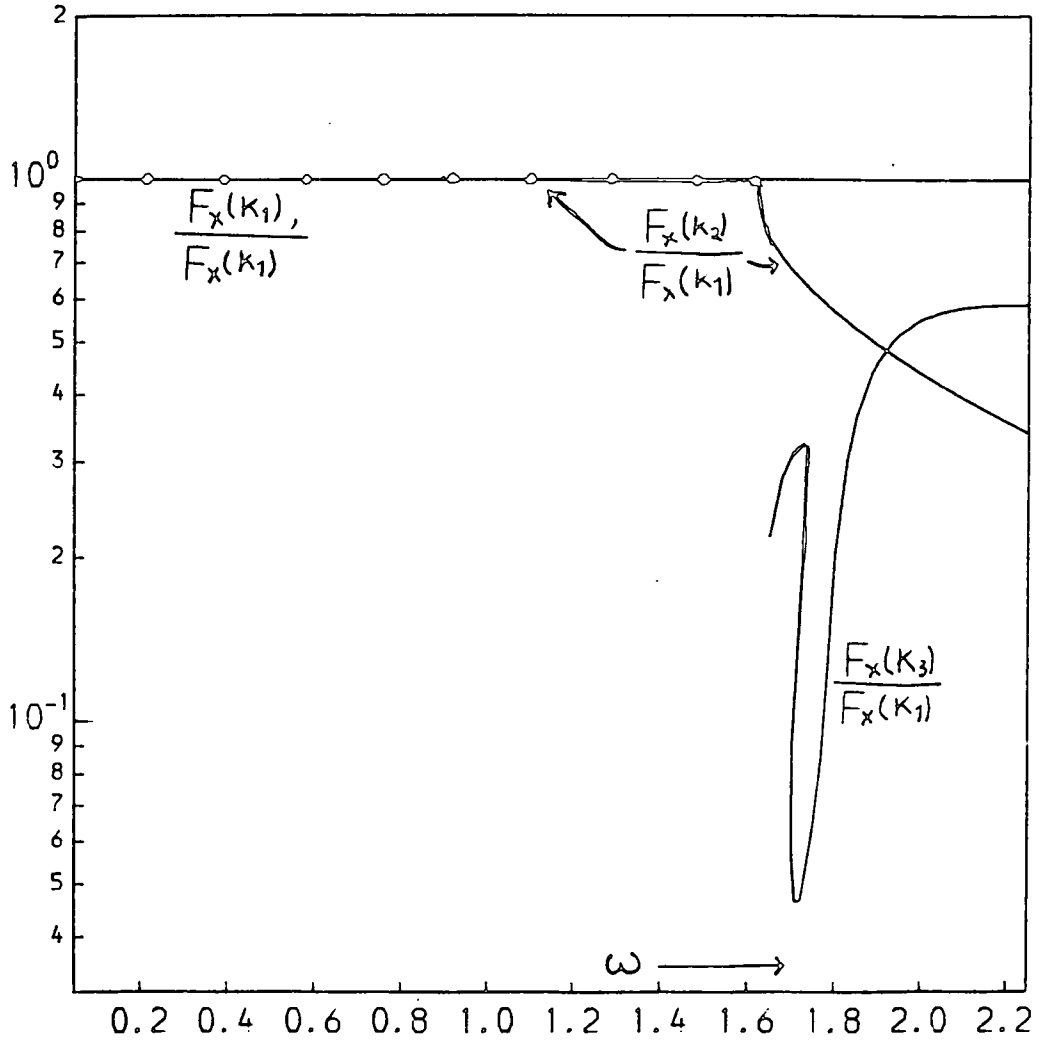

FIGURE 4.11(a) The x component of the flux of energy for the incident and reflected waves. $l = 0.05$ $F_x(k_2)$ is shown by solid circles. The reflecting boundary was assigned infinite conductivity.

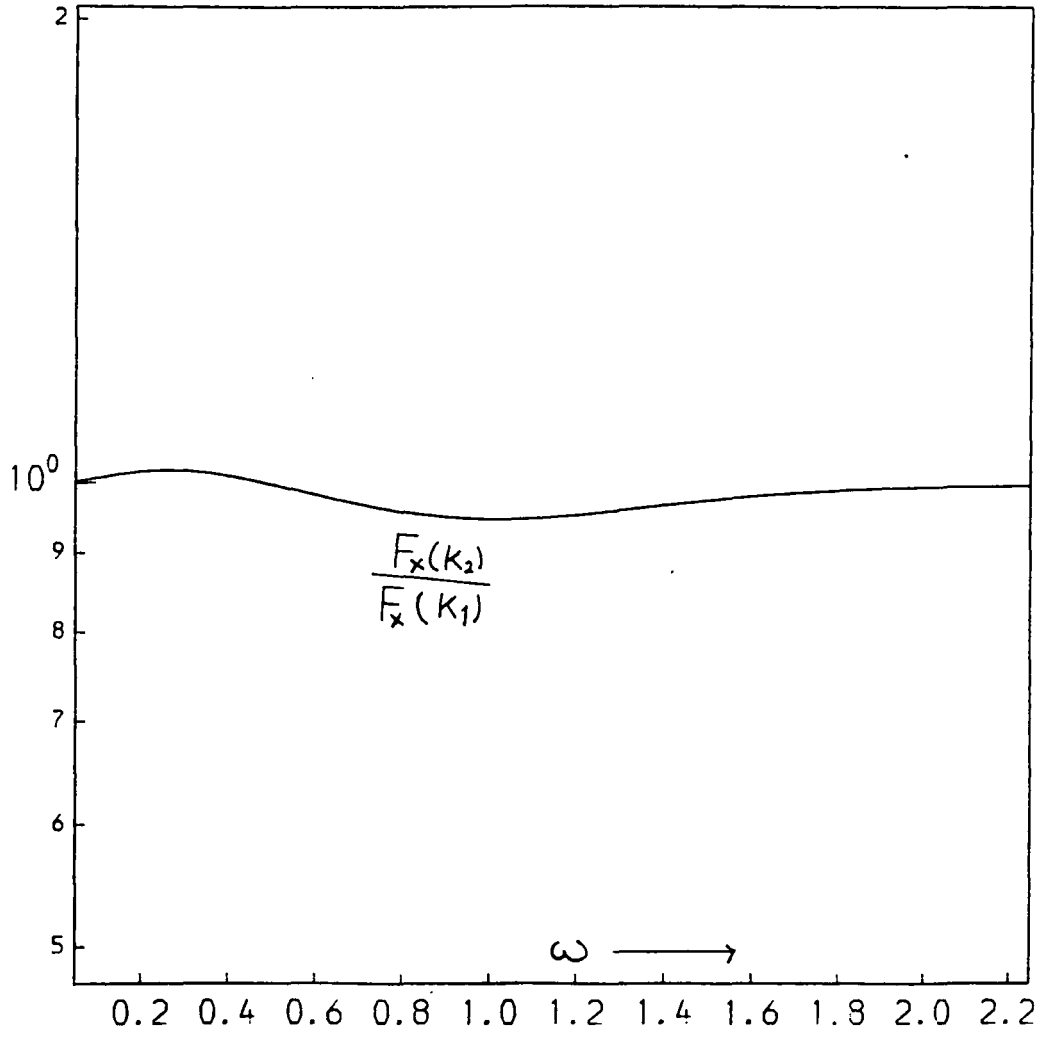

Figure 4.11(b) Same as figure 4.11(a) except l = 1.0.

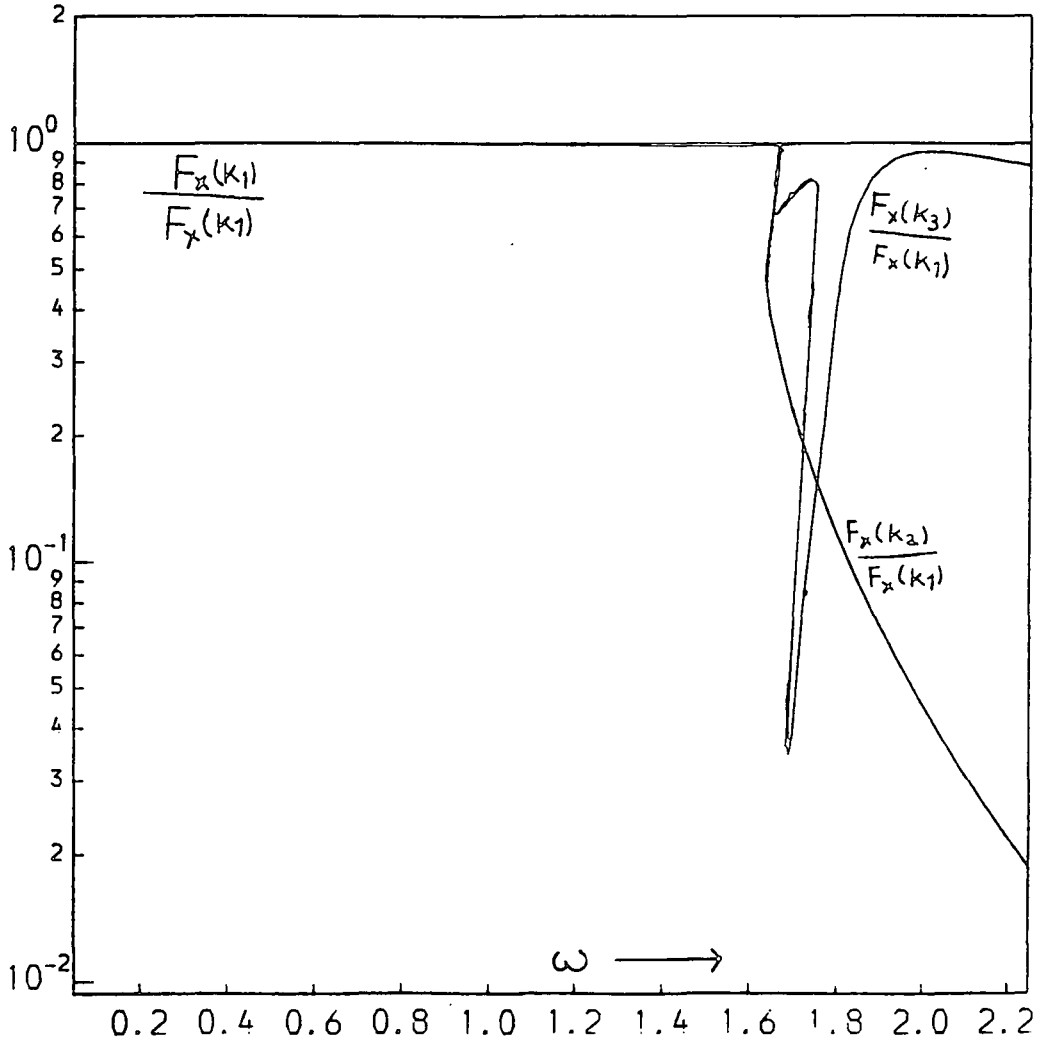

Figure 4.11(c) The x component of the flux of energy for the incident and reflected waves. l = 0.05 and the reflecting boundary is highly insulating.

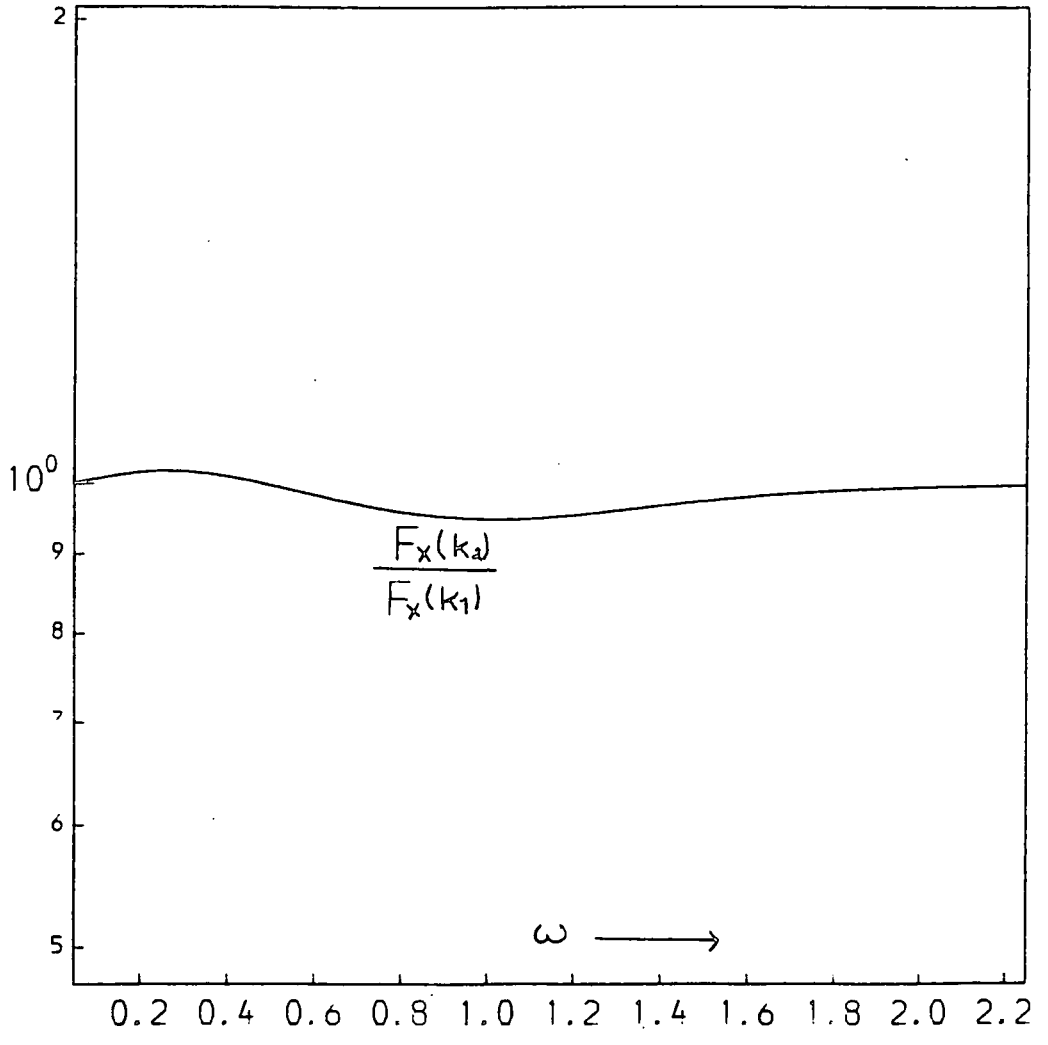

FIGURE 4.11(d) Same as figure 4.11(c) except l = 1.0

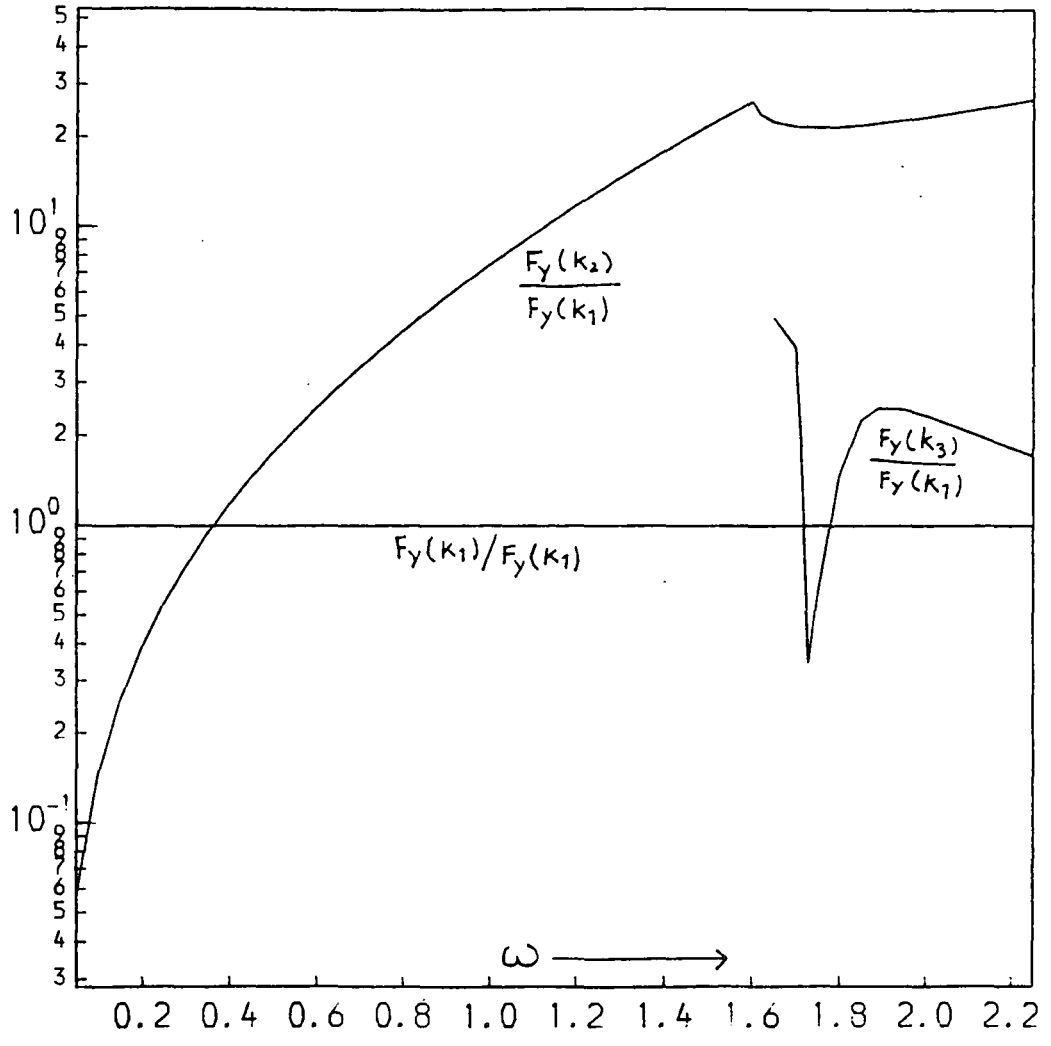

FIGURE 4.12(a) The y component of the flux of energy for the three waves. l = 0.05. The reflecting boundary is highly conducting.

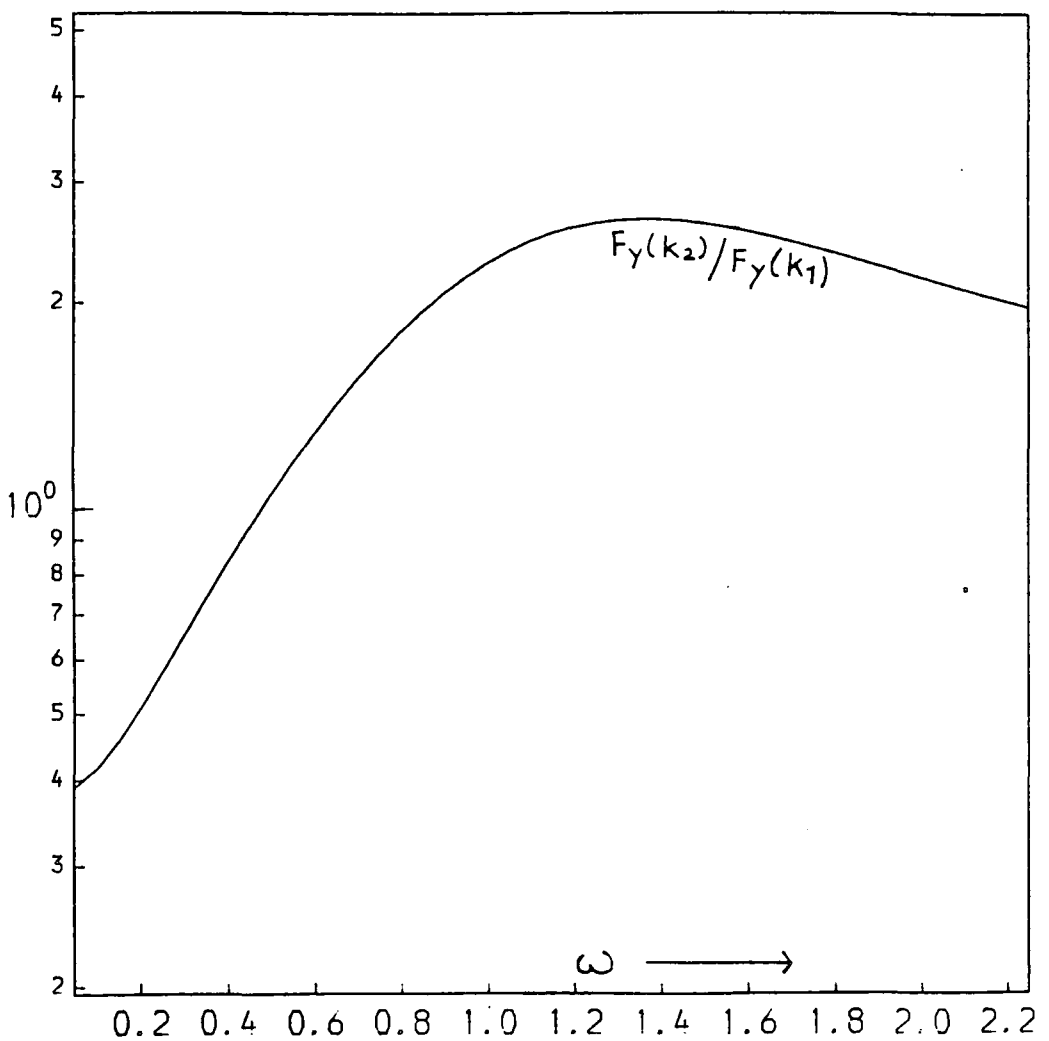

FIGURE 4.12(b) Same as figure 4.12(a) except l = 1.0

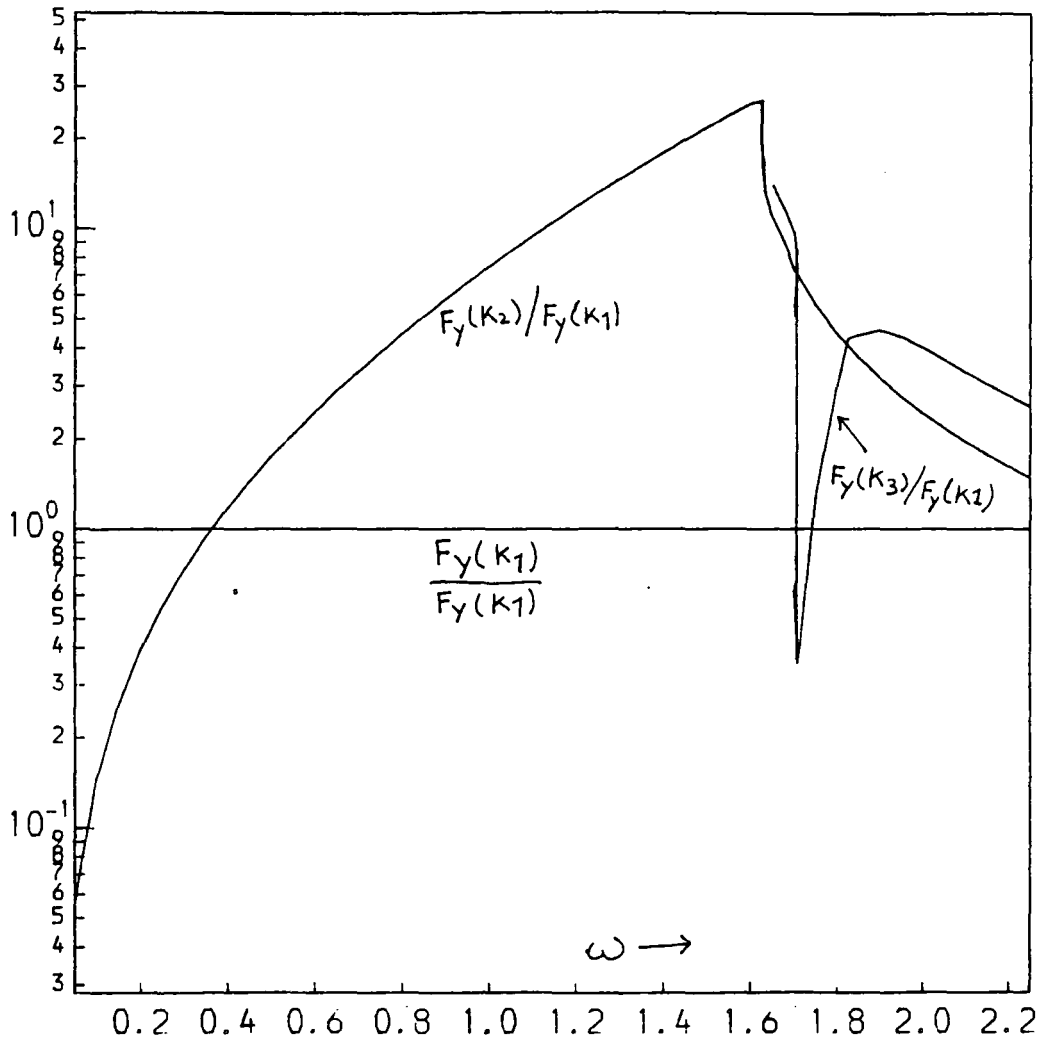

Figure 4.12(c) The y component of the flux of energy through a unit area of the reflecting boundary for the three waves. l = 0.05. Boundary, insulating.

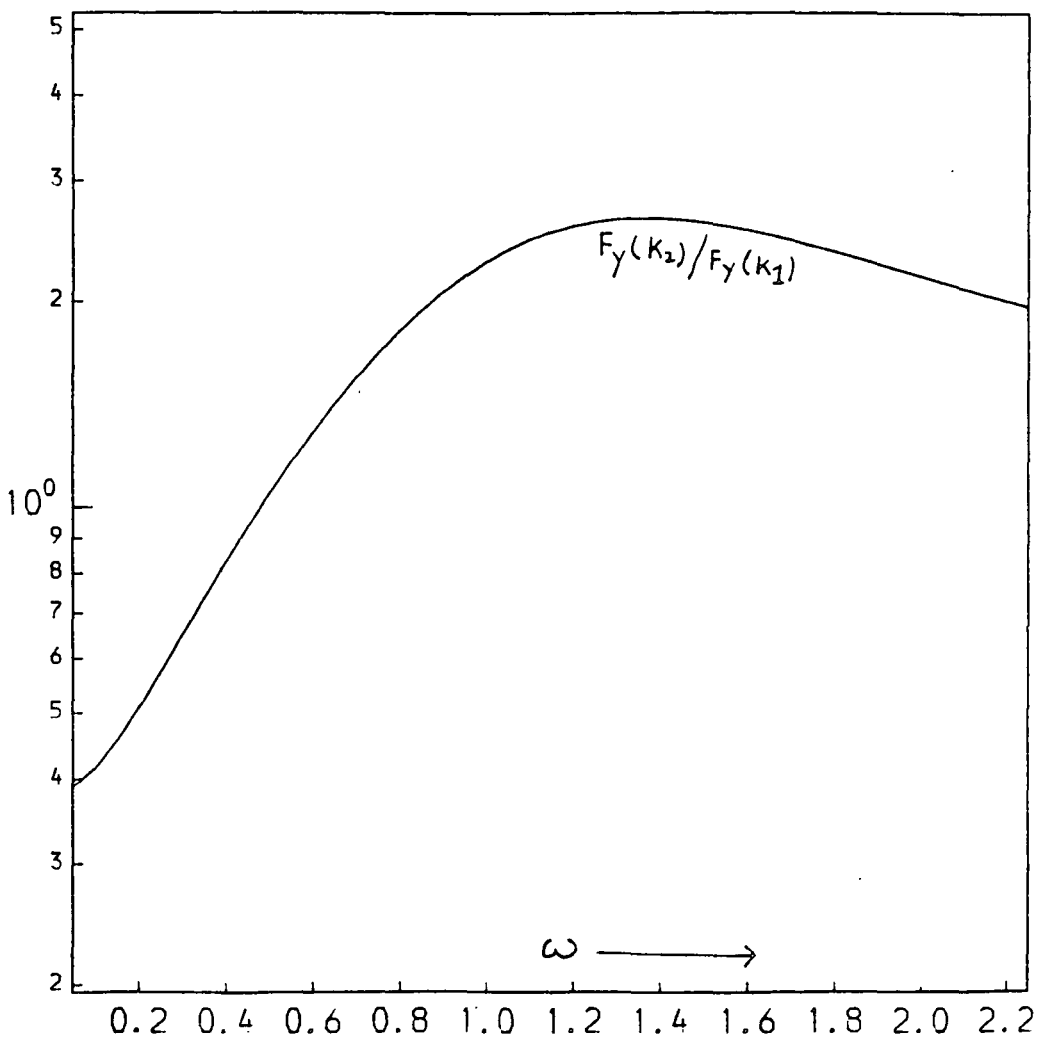

Figure 4.12(d) Same as figure 4.12(c) except l = 1.0.

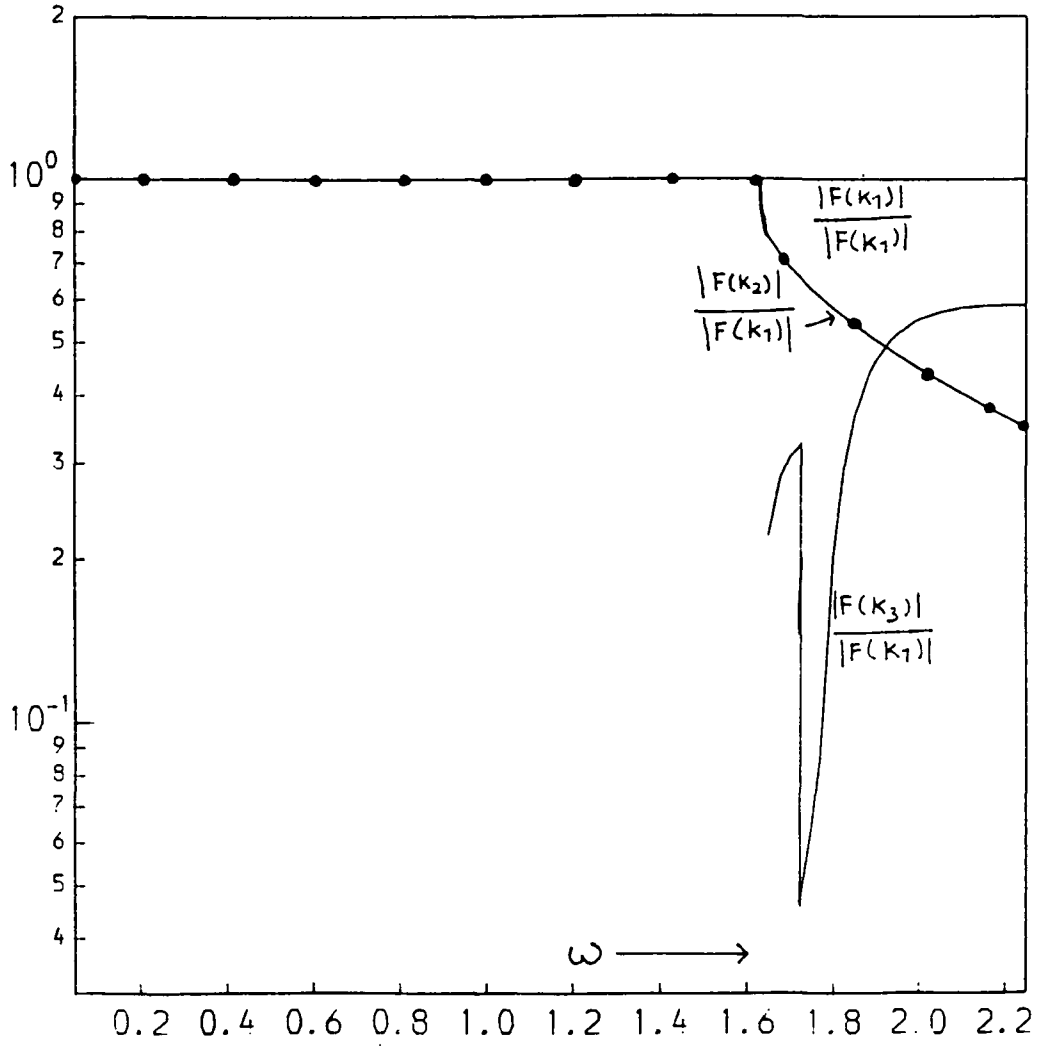

FIGURE 4.13(a) The flux F(k) of energy for the incident and reflected waves. The F(k) curve is shown by solid circles. The case of conducting boundary.

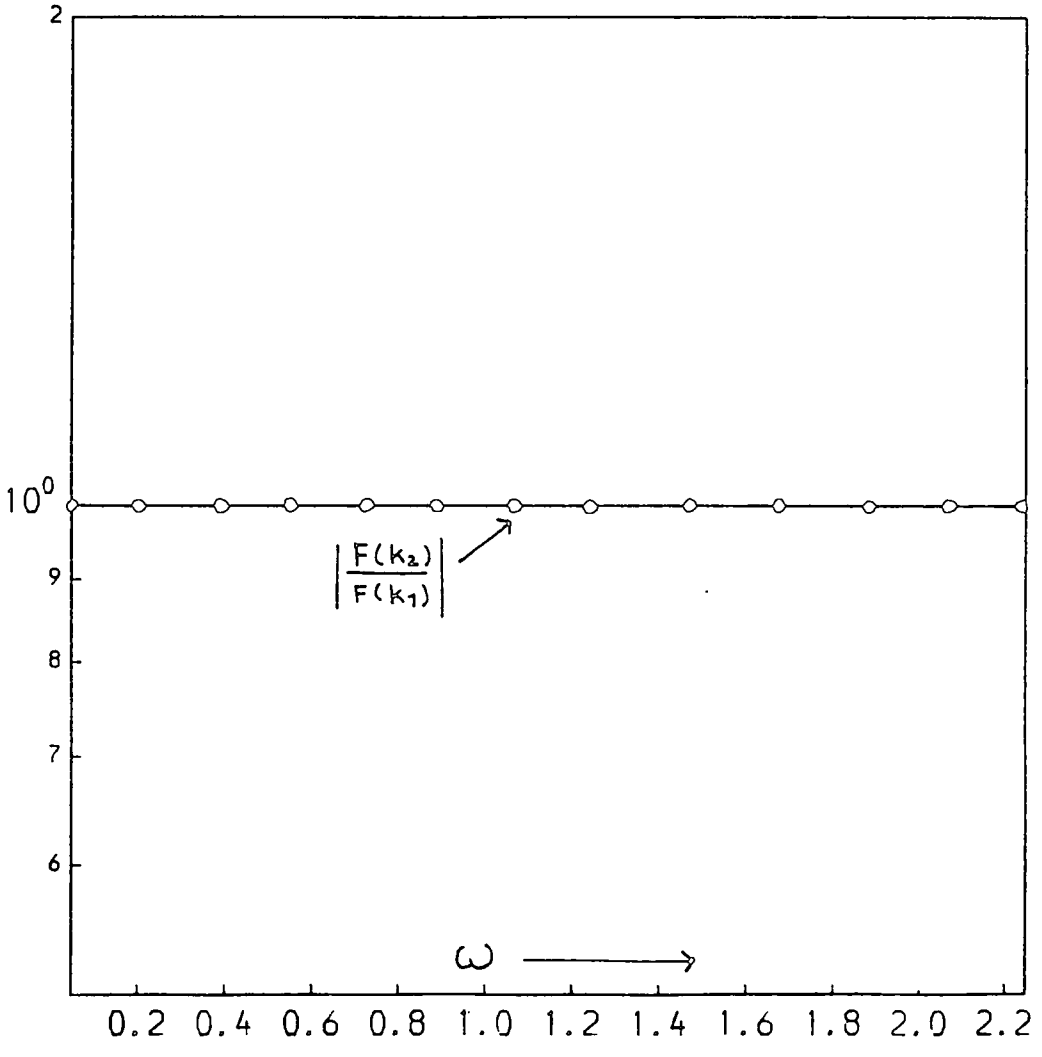

FIGURE 4.13(b) Same as figure 4.13(a) except l = 1.0

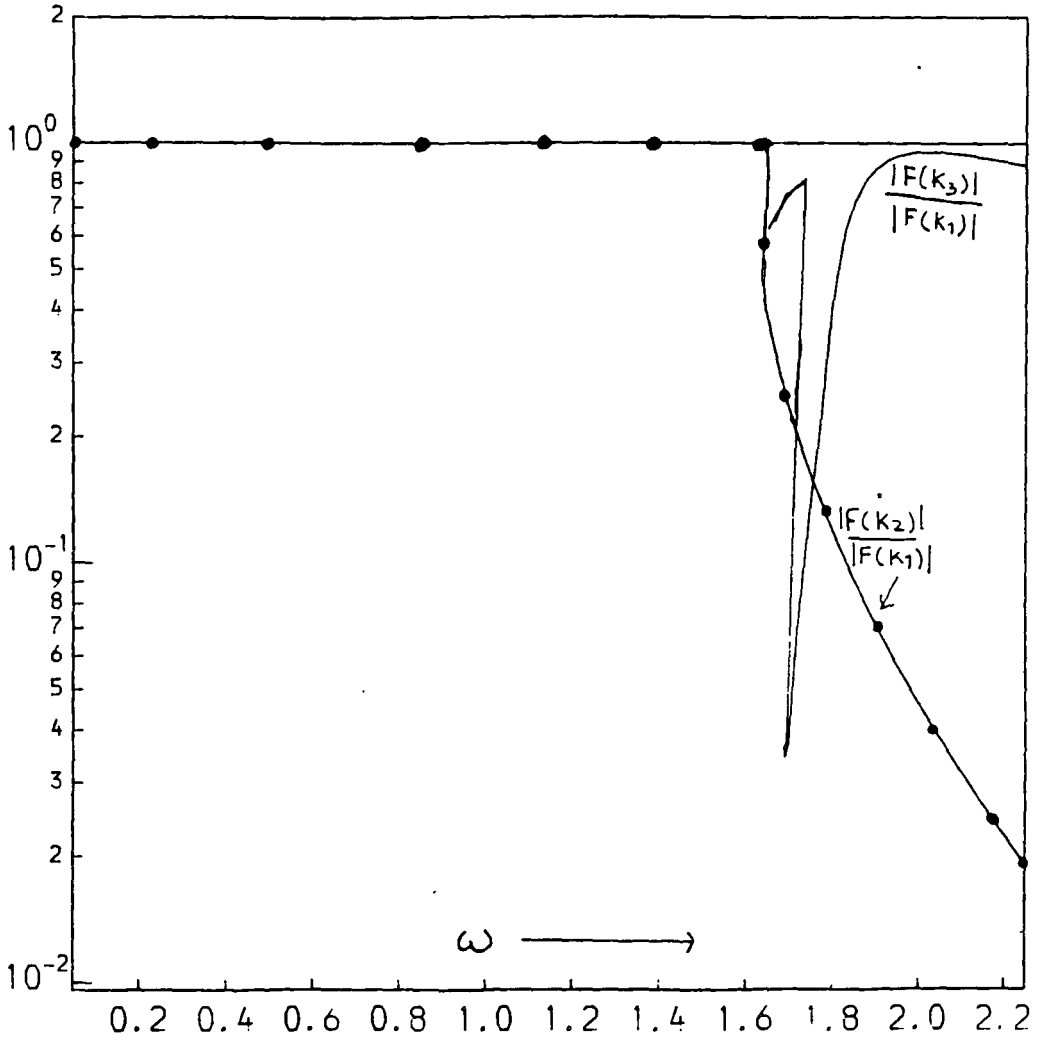

Figure 4.13(c) The flux $|F(k)|$ of energy carried through a unit area of the insulating boundary by the three waves. $F(k_2)$ is shown in solid circles. l = 0.05.

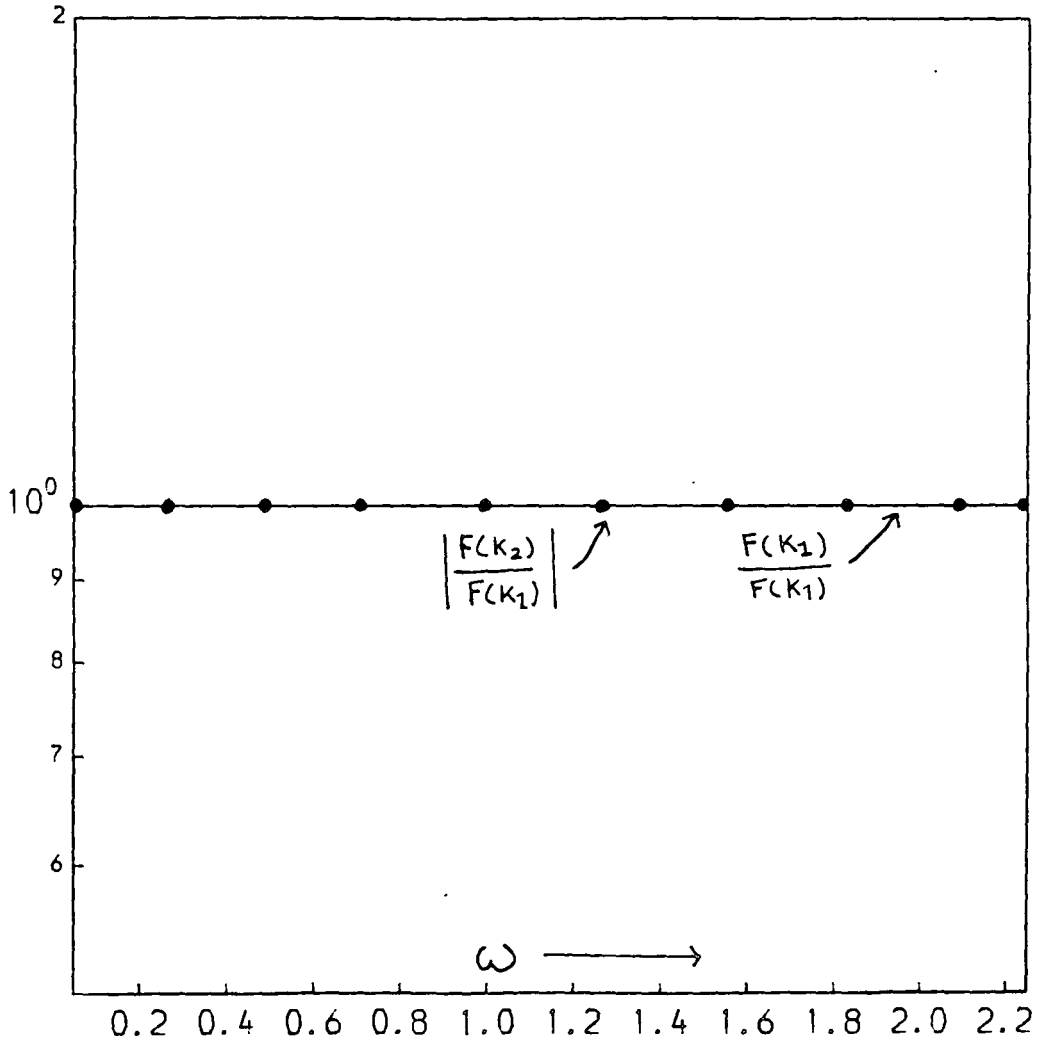

Figure 4.13(d) Same as figure 4.13(c) except 1 = 1.0.

flux passing through a unit area of the boundary for incoming and outgoing waves. Though the individual components of the flux are not conserved the total outgoing flux of energy contained in waves 2 and 3 is equal to the flux of energy provided by the incident wave (see figures 4.13 (a), (b), (c) and (d)) vindicating that the total energy of the waves is conserved.

To sum up, when a low frequency magnetic Rossby wave packet propagating eastwards encounters a N-S boundary, it is reflected back as a phase shifted faster inertial wave packet. Since the group velocity of the wave packet increases as a consequence of reflection, it will have its length stretched along the ray and because the reflected wave packet emerges almost parallel to the normal to the boundary it will have its width (as measured in the direction perpendicular to ray path) slightly enlarged. As a consequence its energy density will be considerably reduced, though the total energy of the wave packet is conserved by reflection. A wave packet consisting of higher frequencies will produce on reflection an additional Alfven wave packet whose group velocity and energy density are comparable to that of the incident wave packet and which manages to capture a larger share of the energy (and almost all the energy when the reflector is highly insulating) from the incident wave packet.

We can mention here in the passing that a complementary process of reflection will occur when an Inertial Rossby-MHD wave encounters a rigid boundary situated at the eastern end of the fluid body. This time the reflection will produce two westward travelling waves whose properties can be evaluated by treating 2

as the incident and 1 and 3 as the reflected waves.

4.4 THE REFLECTION BY AN E-W BOUNDARY

The process of reflection is a function of the orientation of the rigid boundary. The special case of a boundary parallel to the x-axis (see figure 4.14) can be studied by the same method of analysis as above. Once again the frequency and the wave vector parallel to the boundary are preserved implying that ω and k are the same for incident and reflected waves. A simple study of figure 4.2 then shows that wavenumber 1 undergoes only a change of sign, so that the mode, wavelength, group velocity and thus the energy density of the waves are unaffected by reflection.

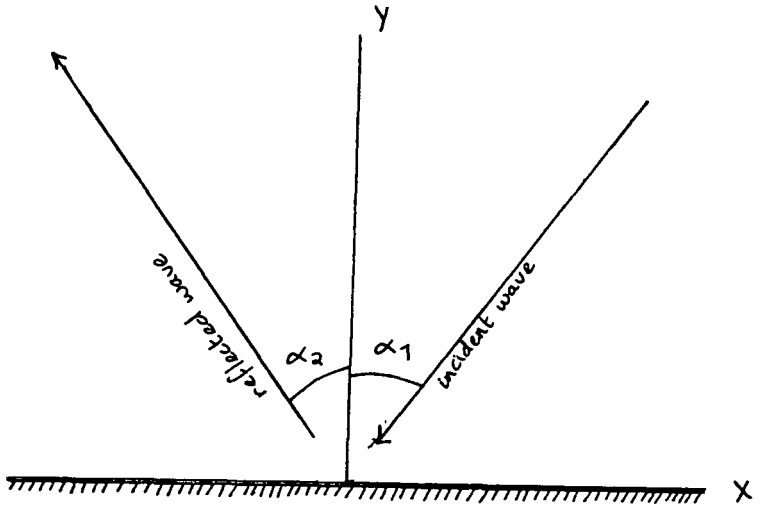

Figure 4.14 The reflection of the hydromagnetic wave packet at an E-W boundary

Another property of the process of reflection in this special

case is that the angle of incidence of the wave packet equals the angle of reflection ie. the wave reflection obeys Snell's law.

In general, when the direction of the rigid boundary is intermediate to these two special orientations we have studied, the reflection of a magnetic (or inertial) Rossby-MHD wave packet will produce both magnetic and inertial wave packets simultaneously whose energies can be determined by the above approach.

CHAPTER FIVE

THE REFLECTION OF INERTIAL-MAGNETOHYDRODYNAMIC WAVES AT RIGID BOUNDARIES

5.1 GENERAL Ordinary inertial waves and Alfven waves which can be regarded, respectively, as the rotation dominant and magnetic field dominant cases of inertial-magnetohydrodynamic (IMHD) waves possess many remarkable propagational and reflection properties. Inertial waves are highly dispersive and anisotropic and are reflected by boundaries in such a way that the incoming and reflected flux vectors make equal angles with Ω_p, the projection of the rotation vector in the plane occupied by the normal to the boundary and the wave vector. The wavenumbers of the incident and reflected waves are in general unequal; though the frequency is conserved. [See e.g. section 2.2 or Phillips (1963)]. Alfven waves on the other hand are non-dispersive and are reflected by rigid boundaries without change of wave amplitude, wavenumber, frequency or phase of the associated magnetic field (though the velocity has its phase reversed) and return in the direction of the magnetic lines of force [See e.g. Walen (1944, 1946), Lundquist (1952), Ferraro and Plumpton (1961), Alfven and Falthammar (1963), Roberts (1967)]. When both rotation and magnetic field are important, from our experience of the last chapter, we can expect more than one wave to be generated by the reflection of an IMHD wave at a rigid boundary and in many situations a major conversion of kinetic energy into magnetic

energy or vice versa. Such studies are crucial in the determination of the effect of boundaries on the exchange of energy between different wavenumbers (Phillips 1963) and the dynamo action associated with random IMHD waves (Moffatt 1970).

5.2 FORMULATION OF THE PROBLEM Consider a plane boundary which passes through a point $p(p_1,p_2,p_3)$ and has an outward normal given by $\hat{n} = (n_x,n_y,n_z)$. The boundary can be represented by

$$\hat{n}.\bar{X} = \hat{n}.\bar{p} \qquad ...(5.1)$$

where p is the position vector defined by p and $\bar{X} = (x,y,z)$. For a wave to be truly incident on this boundary its group velocity will have to be such that

$$\bar{C}_g.\hat{n} \geqslant 0 \qquad ...(5.2)$$

Let us define the z axis of our rectangular system of co-ordinates in the direction of the rotation vector $\bar{\Omega}$ and because we are mainly interested in the geophysical applications of our results we assume a strong basic magnetic field in the x direction which on a local scale simulates the earth's toroidal magnetic field. Once again we assume that the fluid is highly conducting, inviscid, incompressible and rotating rapidly and is thus able to support plane IMHD waves of the form

$$\bar{u} = \bar{A} \exp[i(\bar{K}.\bar{X} - \omega t)] \qquad ...(5.3)$$

where $\bar{u}$ is the local velocity = (u,v,w), $\bar{K}$ = (k,l,m) is the wavenumber of the wave and ω is its frequency. The dispersion relation (1.36) [noting that $\bar{N} = 0$ in our case] for these waves can then be written as

$$\omega^2 \pm 2\Omega m\omega/(k^2+l^2+m^2)^{1/2} - V_a{}^2k^2 = 0 \qquad \ldots(5.4)$$

If we express distances in units of V_a/Ω and time in units of $1/\Omega$, this equation can then be non-dimensionalised to

$$\omega^2 \pm 2m\omega/(k^2+l^2+m^2)^{1/2} - k^2 = 0 \qquad \ldots(5.5)$$

It is a simple matter to show by the help of the continuity equation (1.28), Gauss's Law (1.30) and the wave equation (1.34) (when $\bar{N} = 0$) that the components u and v of the local velocity u in these units can be represented in terms of w as

$$u = \left(\frac{-(k^2-\omega^2)mk + 2il m\omega}{(k^2-\omega^2)(k^2+l^2)}\right)w \qquad \ldots(5.6)$$

and

$$v = \left(\frac{-(k^2-\omega^2)ml - 2ikm\omega}{(k^2-\omega^2)(k^2+l^2)}\right)w \qquad \ldots(5.7)$$

Similarly, the electrodynamic equation (1.31) can be manipulated to yield the magnetic field components b_x, b_y, b_z in terms of u, v and w.

$$b_x = -ku/\omega \qquad \ldots(5.8)$$

$$b_y = -kv/\omega \qquad \ldots(5.9)$$

and

$$b_z = -kw/\omega \qquad \ldots(5.10)$$

Let us assign the subscript '1' to quantities associated with the incident wave so that

$$u = A_1 \exp[i(\bar{K}_1.\bar{X} - \omega_1 t)] \qquad ...(5.11)$$

where $\bar{K}_1$ and ω_1 are the wavenumber and frequency of the incident wave and $\bar{X}$ is the position vector. The presence of the rigid boundary will produce one or more reflected waves each of which can be described by

$$\bar{u}_r = \bar{A}_r \exp[i(\bar{K}_r.\bar{X} - \omega_r t)] \qquad ...(5.12)$$

and satisfies the dispersion relation (5.5).

Now the mechanical boundary condition at the wall requires that the normal component of velocity should vanish at the boundary. ie.

$$\bar{u}.\hat{n} = [\bar{u}_1 + \sum_r \bar{u}_r\ ].\hat{n} = 0 \text{ at the boundary} \qquad ...(5.13)$$

As the origin of the co-ordinate system is at our disposal, we can choose it in such a way that it lies somewhere on the boundary. Hence $\hat{n}.p = 0$ and the boundary can be defined by

$$\hat{n}.\bar{X} = 0 \qquad ...(5.14)$$

Let us decompose each of the $\bar{K}$ into two vectors $\bar{K}_n$ and $\bar{K}_t$ which are, respectively, normal and parallel to the boundary ie

$$\bar{K}_j = K_{nj}\,\hat{n} + \bar{K}_{tj} \qquad ...(5.15)$$

Hence, as a consequence of (5.14) our boundary condition (5.13) specifies that

$$\bar{A}_1.\hat{n} \exp[i(\bar{K}_{t1}.\bar{X} - \omega_1 t)] + \sum_r \bar{A}_r.\hat{n} \exp[i(\bar{K}_{tr}.\bar{X} - \omega_r t)] = 0 \qquad ...(5.16)$$

and since this condition holds at any time and at any point on

the plane, the frequencies and the tangential wavenumbers of incident and reflected waves must be identical. ie

$$\omega_1 = \omega_2 = \omega_r = \omega \text{ (say)} \qquad \ldots(5.17)$$

and $$\bar{K}_{t1} = \bar{K}_{t2} = \bar{K}_{tr} = \bar{K}_t \text{ (say)} \qquad \ldots(5.18)$$

Once we know the frequency and the tangential component of the wavenumbers of all the reflected waves, their normal components can be obtained from the dispersion relation (5.5). To this end substitute for $\bar{K}$ from (5.15) into this relation and rearrange after a little mathematical manipulation, to find a sixth order polynomial in K_n ie

$$C_0 K_n^6 + C_1 K_n^5 + C_2 K_n^4 + C_3 K_n^3 + C_4 K_n^2 + C_5 K_n + C_6 = 0 \qquad \ldots(5.19)$$

where $C_0 = n_x^4$

$$C_1 = 4n_x^3 K_{tx}$$

$$C_2 = n_x^4 |K_t| + 6n_x^2 (K_{tx})^2 - 2\omega^2 n_x^2$$

$$C_3 = 4n_x^3 K_{tx} |K_t|^2 + 4(K_{tx})^3 n_x - 4\omega^2 n_x K_{tx}$$

$$C_4 = 6n_x^2 (K_{tx})^2 |K_t|^2 - 2\omega^2 n_x^2 |K_t|^2 + \omega^4 + (K_{tx})^4 - 2\omega^2 (K_{tx})^2 - 4\omega^2 n_z^2$$

$$C_5 = |K_t|^2 [4(K_{tx})^3 n_x - 4\omega^2 n_x K_{tx}] - 8\omega^2 n_z K_{tz}$$

$$C_6 = |K_t|^2 [\omega^4 + (K_{tx})^4 - 2\omega^2 (K_{tx})^2] - 4\omega^2 (K_{tz})^2$$

Here K_{tx} and K_{tz} are the components of $\bar{K}_t$ in the direction of the

magnetic field (which is parallel to x axis) and rotation axis (parallel to z axis) respectively. This polynomial has six roots of K_n, each of which when combined with $\bar{K}_t$ yields one of the six wavenumbers that are possible which have the same frequency and tangential component and satisfy dispersion relation (5.5). Clearly one of these wavenumbers belongs to the initial incident wave we started with and the other five will belong to the reflected waves. However, if the group velocity of a wave j, represented by any of these wavenumbers is such that

$$\bar{C}_{gj}.\hat{n} \gtrless 0 \qquad (5.20)$$

ie its group velocity is towards the boundary, its amplitude will have to be equal to zero, because no wave can propagate across the rigid boundary. However, the analytical extraction of the roots of the polynomial (5.19) is impossible and therefore we cannot analytically ascertain the number of waves that have the right group velocity. Fortunately this can be easily judged from the appropriate normal curves for these waves which are the contours of ω drawn in the wavenumber (k,l,m) space. Figures 5.1(a) to (f) based on equation (5.5) show such curves for inertial modes [corresponding to positive sign in (5.5)] in solid lines and for magnetic modes [negative sign in (5.5)] in broken lines. Figures 5.1 (a) to (c) have been drawn for certain fixed values of l and are particularly useful for studying reflections from boundaries which are parallel to y axis [as wavenumber l is conserved for reflections by such boundaries as in these diagrams), whereas Figures 5.1 (d) to (e) show normal curves for certain fixed values of m and are best suited to investigate

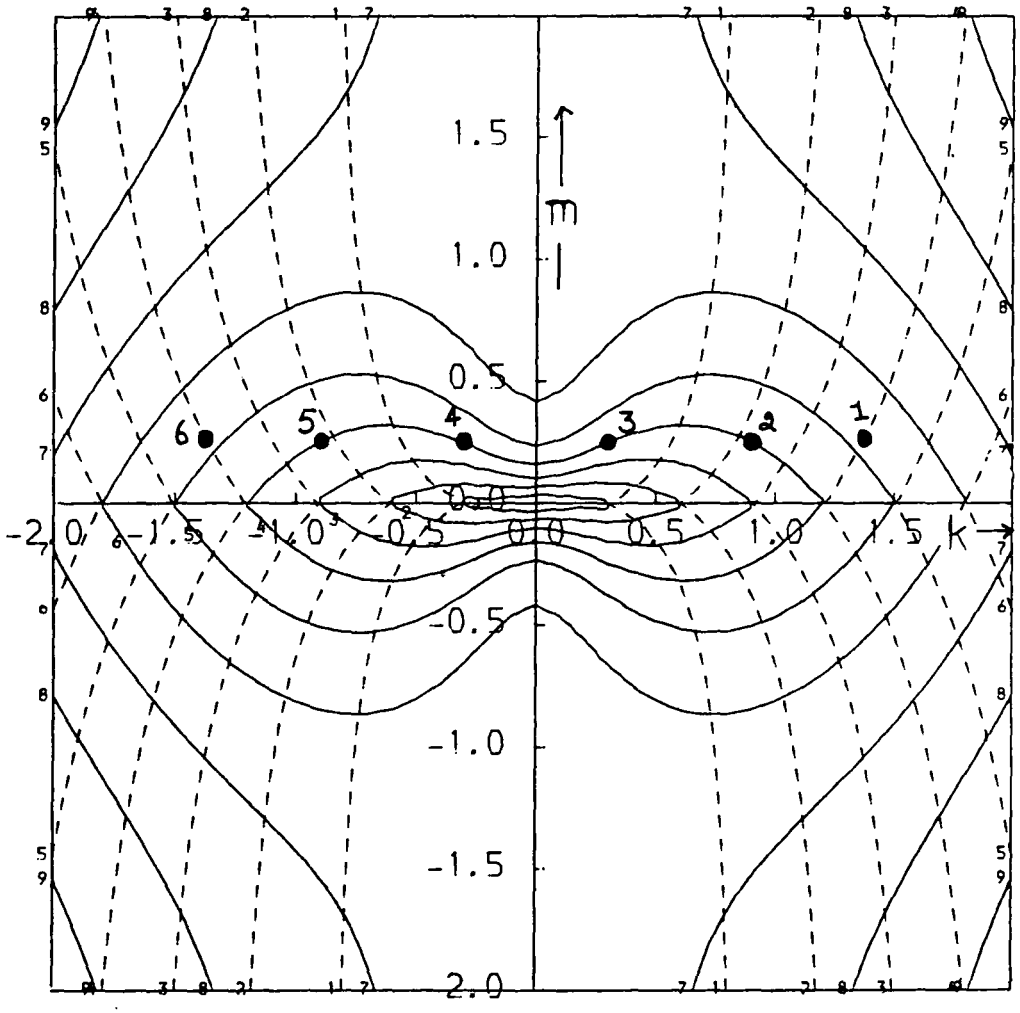

Figure 5.1(a) Normal curves for IMHD waves for which l = 0.2 [see equation (5.5)]. The curves for inertial modes are drawn in solid lines whereas for magnetic modes they are in broken line. All quantities are in normalised units. The contour interval for these ω curves is 0.3 units.

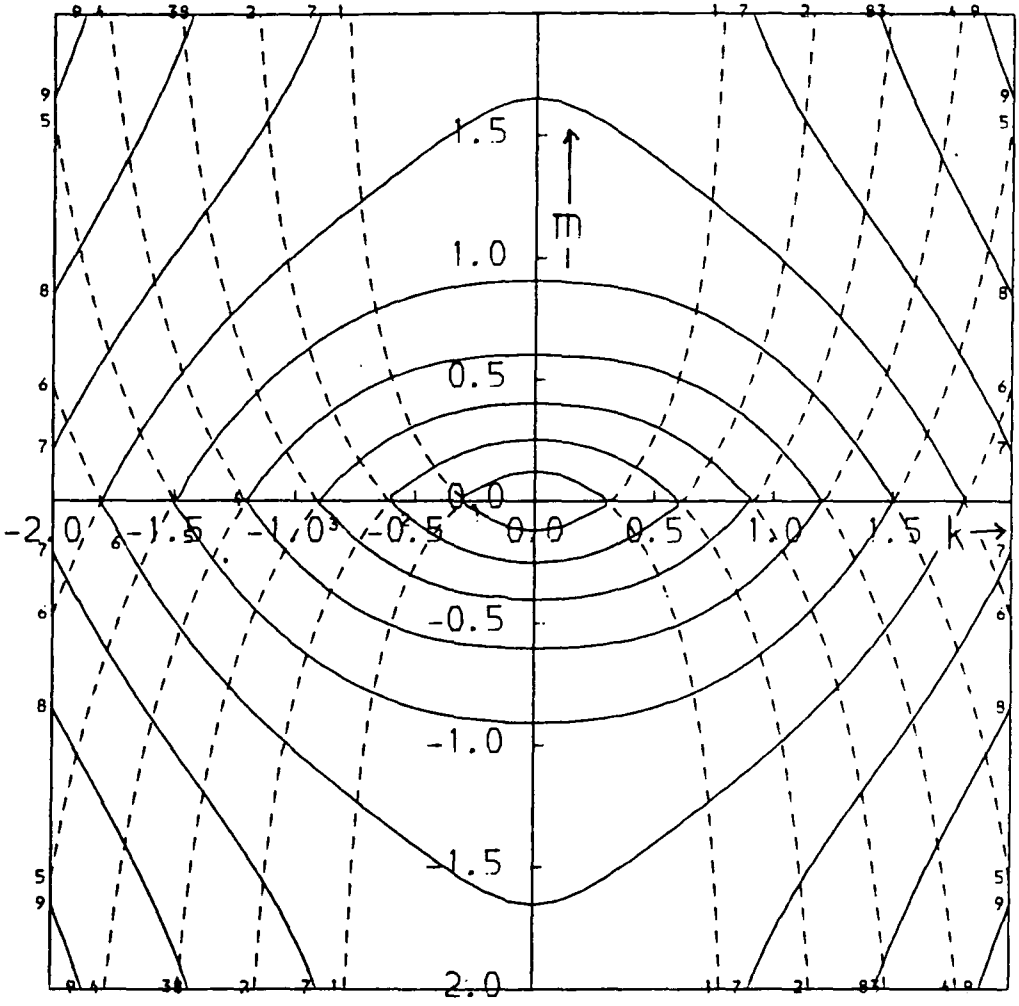

Figure 5.1(b) Same as Figure 5.1(a) except l = 0.8 units for these curves.

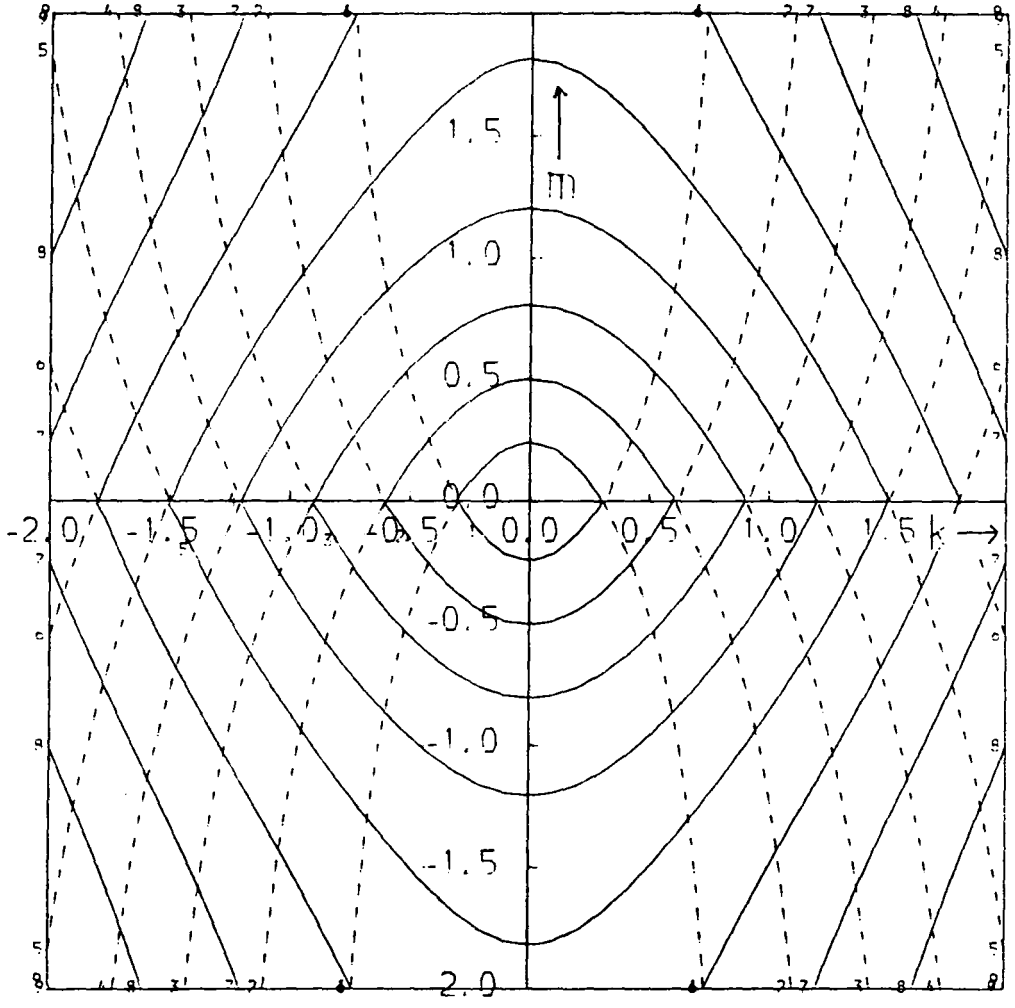

Figure 5.1(c) Same as Figure 5.1(a) except 1 = 1.6 units for these curves.

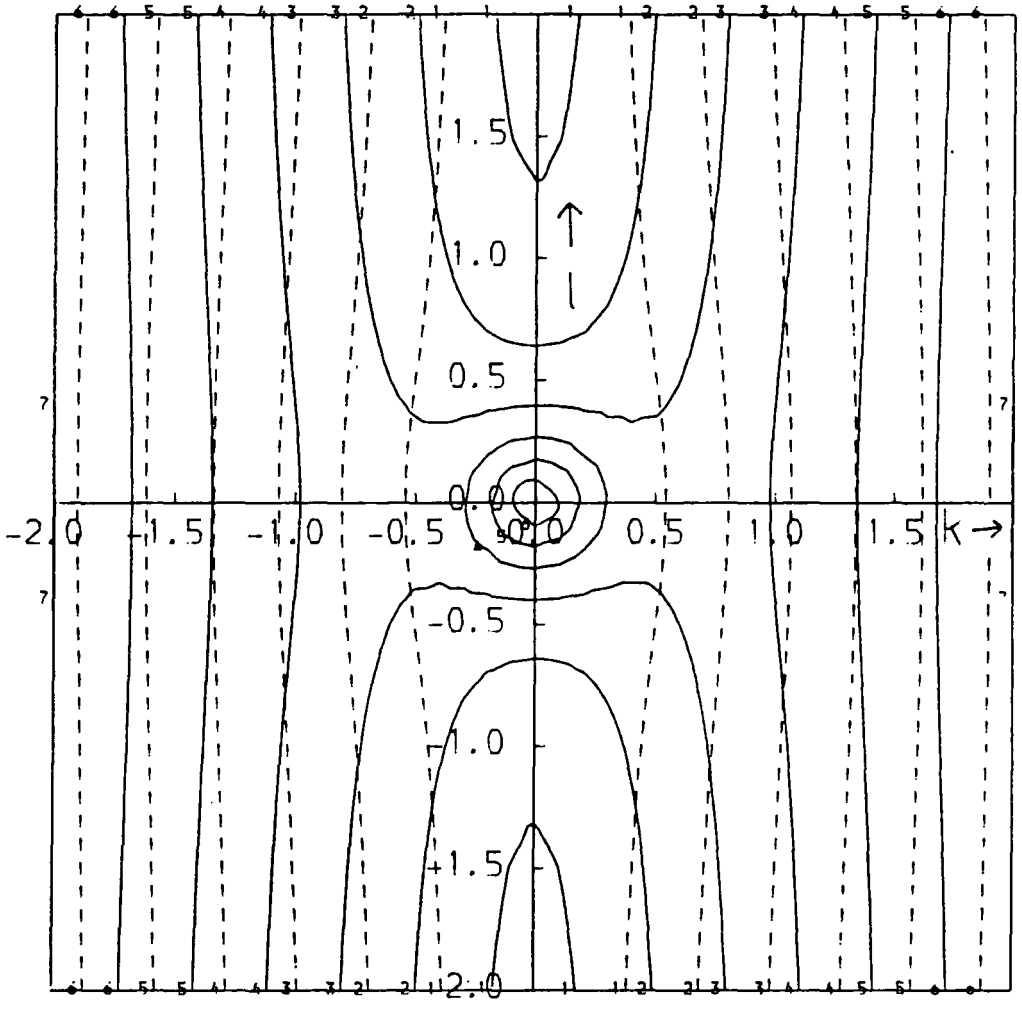

Figure 5.1(d) Normal curves for IMHD waves for which m = 1.2 normalised units. The curves for inertial modes are in solid lines whereas magnetic modes are in broken lines. The contours are drawn for a frequency interval of 0.3 units.

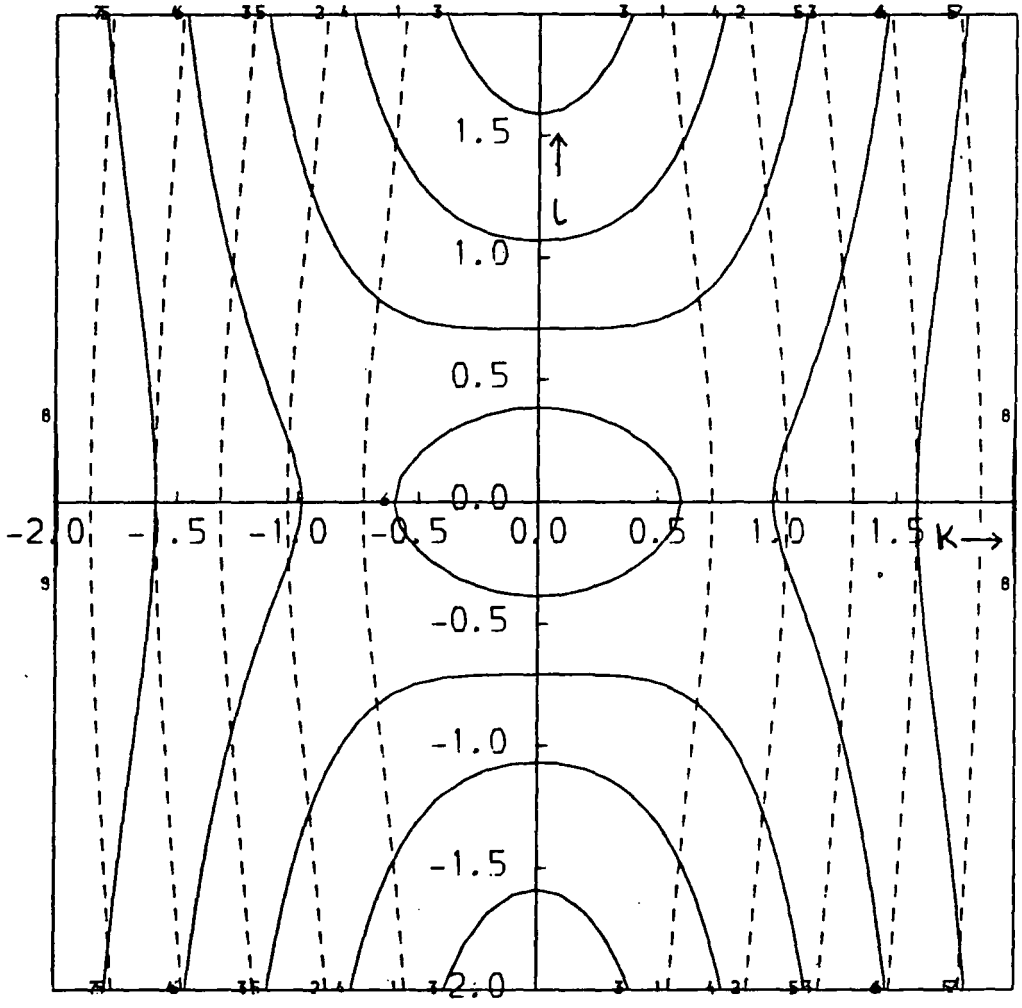

Figure 5.1(e) Same as Figure 5.1(d) except m = 0.8 units for these curves.

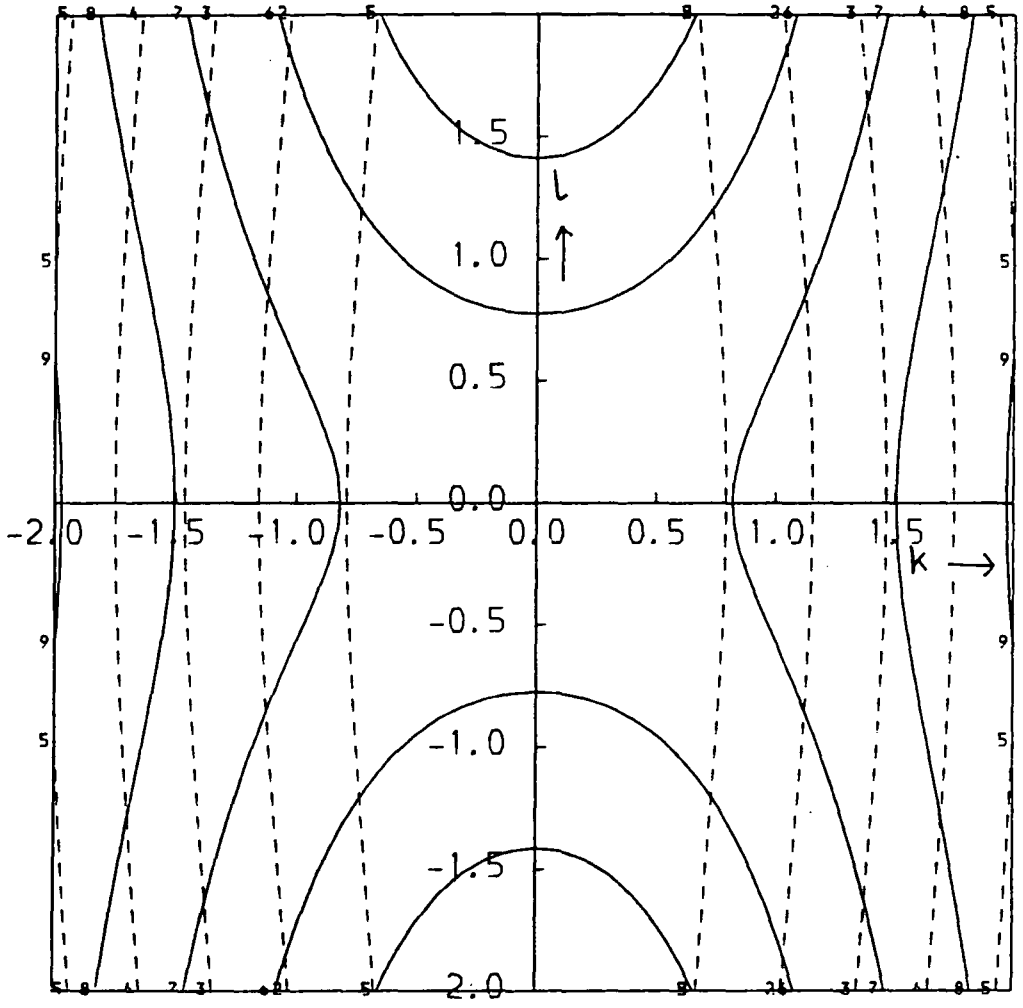

Figure 5.1(f) Same as Figure 5.1(d) except m = 1.6 units for these curves.

reflections from vertical boundaries (though the orientation can be arbitrary). A cursory glance at these figures reveals that for any fixed wavenumber $\bar{K}(k,l,m)$ an inertial mode has a much higher frequency than its magnetic counterpart. In addition the group velocity $\bar{C}_g = (\partial\omega/\partial k, \partial\omega/\partial l, \partial\omega/\partial m)$ [whose rough measure for any wavenumber $\bar{K}$ in these diagrams is the density of ω contours around that wavenumber] of magnetic modes is much smaller than those of the inertial modes.

To illustrate the use of these diagrams let's assume a magnetic IMHD mode with wavenumber $\bar{K}$=(1.4, 0.2, 0.2) and frequency ω = 1.2 (all quantities are in normalised units) incident on the boundary x = c, where c is a positive constant. This mode is marked by point 1 on diagram 5.1(a). Now from our discussion above we know that after reflection, the frequency of the wave and the tangential components of its wavenumbers are conserved. Therefore, ω = 1.2 l = 0.2 and m = 0.2 for all the reflected waves. In addition to point 1, five more wavenumbers satisfy these criteria and are marked 2 to 6 on this figure. Out of these, waves 2 and 4 clearly have group velocities whose normal components are towards the boundary. This leaves us with waves 3, 5 (which are inertial modes) and 6 (which is magnetic) only, which can be generated by a reflection. One can repeat this exercise for any other orientations or for any other set of wavenumbers and always arrive at the conclusion that, atbest, three reflected waves can be generated. For certain combinations of wavenumbers and frequencies one of the roots of (5.19) can become complex and will mark the presence of a non-propagating

leaking mode at the boundary. In that situation only two travelling waves will be generated upon reflection. A similar study of Figure 5.1(d) shows that on reflection from a vertical boundary which is normal to the magnetic field lines, an inertial IMHD mode splits into two inertial and a magnetic mode. However under the same conditions a low frequency magnetic mode will produce only one reflected wave which will again be magnetic. A reflection from an x-x' boundary produces only one reflected wave of finite wavenumber (the other two roots become infinite) which is of the same type as the incident wave.

If the plane boundary is not tangential to y and z axes, wavenumber components l and m of the reflected waves will also suffer change and clearly diagrams of Figure 5.1 cannot be used satisfactorily for such cases. Therefore, in order to gain a better qualitative knowledge of the wavenumbers of reflected waves we propose the use of 'normal surfaces' which are surfaces of constant ω in the three dimensional wave number space (with k and l horizontal and m vertical). Figures 5.2(a) and (b) show two such surfaces on which frequency has constant values of 0.2 and 1.2 respectively, the latter diagram being the relevant one for the example we have been studying. The six points of intersection of the line l=0.2, m=0.2 with this surface will represent the required wavenumbers. Clearly, we can use the same diagram for any orientation or inclination of the boundary now; each time the points of intersection of this surface with the line drawn through the incident wavenumber in the direction of the normal (to the boundary) representing the required wavenumbers. However,

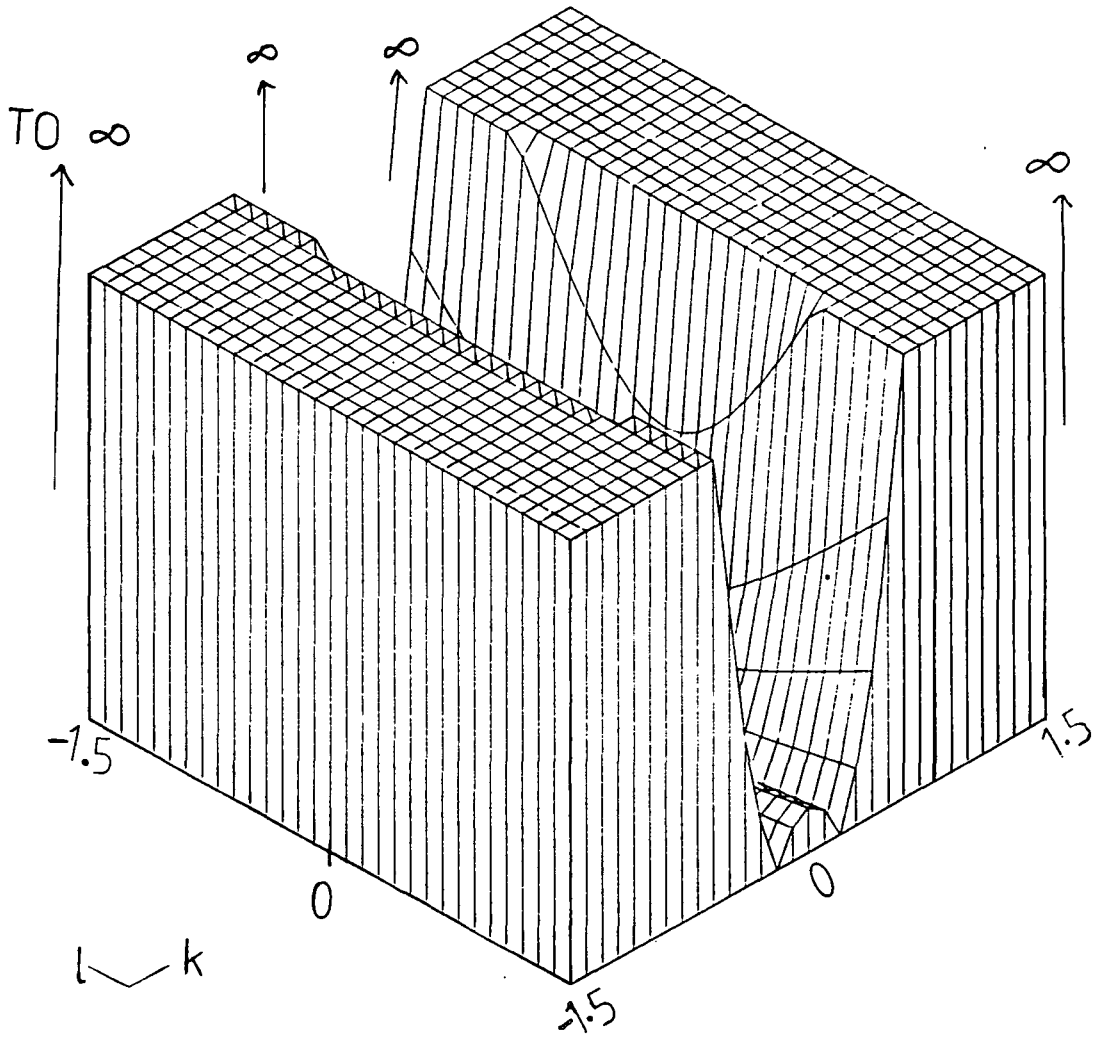

Figure 5.2(a) The normal surface for IMHD waves with frequency $\omega = 0.2$. This surface represents all the possible IMHD waves whose frequency is 0.2 units.

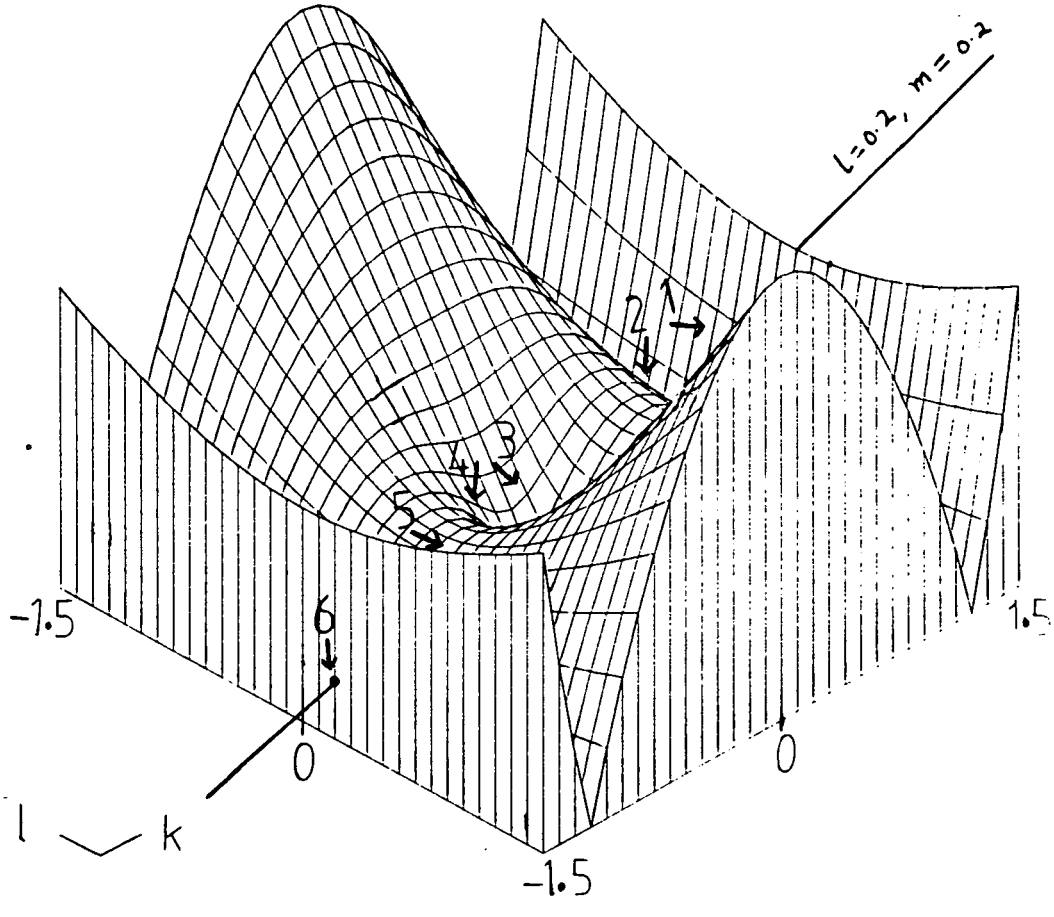

Figure 5.2(b) The normal surface $\omega = 1.2$ in the k,l,m space. Notice the six intersections of the line l = 0.2, m = 0.2, with this surface. All quantities are in normalised units.

this generalisation has been obtained at a cost; now, no information can be obtained about the group velocities of the waves as the location of the neighbouring normal surface is not known.

In our work we have adopted a numerical approach to obtain the wavenumbers and group velocities of the reflected waves. If the orientation of the boundary is known, $\hat{n}$ (the unit normal to the boundary) can be calculated easily and from a knowledge of the wavenumber of the incident wave $\bar{K}_t$ can also be calculated. Then if we substitute for $\bar{K}_t$, $\hat{n}$ and ω in equation (5.19), we can obtain a sixth order polynomial in K_n whose coefficients are known. We then employ an efficient root solving computer routine (see eg. Conte and Boor pp.110-124) to extract all the real and complex roots of this polynomial. Finally we obtain the required wavenumbers by adding the tangential components to these by the help of (5.15). To obtain the components of group velocity of any wave (ω ,k,l,m) first obtain the inertial and magnetic modes of ω from (5.5) in the form

$$\omega_i = \mp\, m/(k^2+l^2+m^2)^{1/2} \pm [m^2/(k^2+l^2+m^2) + k^2]^{1/2} \quad ...(5.21)$$

and $$\omega_m = \mp\, m/(k^2+l^2+m^2)^{1/2} \mp [m^2/(k^2+l^2+m^2) + k^2]^{1/2} \quad ...(5.22)$$

If we specify in addition that ω_i and ω_m are always positive then

$$\omega_i = |m|/(k^2+l^2+m^2)^{1/2} + [m^2/(k^2+l^2+m^2) + k^2]^{1/2} \quad ...(5.23)$$

and $$\omega_m = -|m|/(k^2+l^2+m^2)^{1/2} + [m^2/(k^2+l^2+m^2) + k^2]^{1/2} \quad ...(5.24)$$

These are then differentiated w.r.t. k, l and m to yield

$$C_{gx} = \frac{\partial \omega_{i,m}}{\partial k} = \frac{\mp |m| k}{(k^2+l^2+m^2)^{3/2}} + k\left(\frac{m^2}{k^2+l^2+m^2} + k^2\right)^{-1/2}\left(1 - \frac{m^2}{(k^2+l^2+m^2)^2}\right) \quad \ldots(5.25)$$

$$C_{gy} = \frac{\partial \omega_{i,m}}{\partial l} = \mp \frac{|m| l}{(k^2+l^2+m^2)^{3/2}} + l\left(\frac{m^2}{k^2+l^2+m^2} + k^2\right)^{-1/2}\left(-\frac{m^2}{(k^2+l^2+m^2)^2}\right) \quad \ldots(5.26)$$

$$\text{and } C_{gz} = \frac{\partial \omega_{i,m}}{\partial m} = \pm \operatorname{sgn}(m) \frac{k^2+l^2}{(k^2+l^2+m^2)^{3/2}} + m\left(\frac{m^2}{(k^2+l^2+m^2)} + k^2\right)^{-1/2}\left(\frac{k^2+l^2}{(k^2+l^2+m^2)^2}\right) \quad \ldots(5.27)$$

where upper sign is taken for inertial modes and lower sign for magnetic modes and sgn(m) is 1 when m is positive and -1 when it is negative.

Thus by the help of these equations we calculate the vectors $\bar{C}_{gj}$s and by the help of criterion (5.20) we reject two of the unwanted roots and arrange the remaining three wavenumbers in such a way that wavenumber $\bar{K}_4$ represents the magnetic mode (ie. the ratio of its magnetic to kinetic energy is greater than unity which from (1.42) stipulates that $|k/\omega| > 1$ for this mode) and $\bar{K}_2$ and $\bar{K}_3$ represent the small and large wavenumber inertial waves, respectively.

With the above discussion in mind the incident and the three reflected waves can be expressed by

$$\bar{u}_1 = \bar{A}_1 \exp[i(\bar{K}_1.\bar{X} - \omega t)] \quad \ldots(5.28)$$

$$\bar{u}_2 = \bar{A}_2 \exp[i(\bar{K}_2.\bar{X} - \omega t)] \quad \ldots(5.29)$$

$$\bar{u}_3 = \bar{A}_3 \exp[i(\bar{K}_3.\bar{X} - \omega t)] \quad ...(5.30)$$

and $$\bar{u}_4 = \bar{A}_4 \exp[i(\bar{K}_4.\bar{X} - \omega t)] \quad ...(5.31)$$

where $\bar{A}_1$ is known and our task is to calculate $\bar{A}_2, \bar{A}_3$ and $\bar{A}_4$. In addition we have the boundary condition

$$\bar{A}_1.\hat{n} + \bar{A}_2.\hat{n} + \bar{A}_3.\hat{n} + \bar{A}_4.\hat{n} = 0 \quad ...(5.32)$$

Note however that if any component of $\bar{A}_j$ (say = A_j, the amplitude of w_j) is known the other two are automatically defined by (5.6) and (5.7). As the origin of the time scale is at our disposal we can assume that A_1 (the amplitude of w_1 that is) is real implying that its phase is zero. The reflected waves can, however, suffer phase shifts so that A_2, A_3 and A_4 will in general have imaginary parts. This leaves us with three complex unknowns and only one complex equation (5.32). The additional constraints are provided by the electromagnetic boundary conditions and constraints imposed on the tangential components of the velocity. Once again we consider the cases of reflection by infinitely conducting and insulating boundaries separately.

5.2.1 Reflection by a highly conducting rigid boundary This type of situation arises when the conductivity of the boundary is much larger than the fluid (as for example in some laboratory experiments). Strictly speaking, the effects of ohmic dissipation will be significant in the fluid though no significant energy loss occurs due to the process of reflection itself. As the electromagnetic skin depth is zero for a solid perfect conductor, the normal component of the magnetic field should become zero at

the boundary. ie

$$\bar{b}_1.\hat{n} + \bar{b}_2.\hat{n} + \bar{b}_3.\hat{n} + \bar{b}_4.\hat{n} = 0 \qquad \ldots(5.33)$$

which by the help of equations (5.6) to (5.10) can be reduced to

$$k_1\,\bar{A}_1.\hat{n} + k_2\,\bar{A}_2.\hat{n} + k_3\,\bar{A}_3.\hat{n} + k_4\,\bar{A}_4.\hat{n} = 0 \qquad \ldots(5.34)$$

The assumption of this less than perfect conductivity for the fluid automatically excludes the possibility of a current sheet forming at the boundary. Similarly if we assign a finite viscosity to the fluid, we will also rule out the formation of a vortex sheet at the boundary and consequently the tangential components of the velocity will also be zero at the boundary. ie

$$\bar{A}_1.\hat{t} + \bar{A}_2.\hat{t} + \bar{A}_3.\hat{t} + \bar{A}_4.\hat{t} = 0 \qquad \ldots(5.35)$$

where $\hat{t}$ is a unit vector in the plane of the boundary. In Appendix III we employ equations (5.32),(5.34) and (5.35) in their vector component form to generate a six by six matrix which can be inverted to obtain the real and imaginary parts of $\bar{A}_2$,$\bar{A}_3$ and $\bar{A}_4$.

5.2.2 Reflection by an insulating rigid boundary The case of the Earth's core mantle is best treated under this condition (Acheson and Hide 1973). For terrestrial conditions the factor $\nu\sigma$ is very small and therefore the jump in the tangential componet of the magnetic field will be infinitesimal (see Appendix I for detailed discussion of the electrodynamic boundary conditions when $\nu \to 0$, $\sigma \to \infty$, $\omega \neq 0$ and $\bar{\Omega} \neq 0$). Thus the magnetic

fields will be continuous across the interface and is expressible in terms of a potential ϕ inside the boundary ie.

$$\bar{b} = \bar{b}_1 + \bar{b}_2 + \bar{b}_3 + \bar{b}_4 = \nabla\phi \quad \text{(inside the boundary)} \quad ...(5.36)$$

As $\nabla.b = 0$, therefore $\nabla^2\phi = 0$ inside the boundary.

This equation has solutions of the form

$$\phi = \underline{\Phi} \exp[i(K_{t1}t_1+K_{t2}t_2) - (K_{t1}^2+ K_{t2}^2)^{1/2} r] \quad ...(5.37)$$

where t_1,t_2 and r define a rectangular co-ordinate system and K_{t1} and K_{t2} are the wavenumbers in the direction of t_1 and t_2. Let us assume r to be in the direction of the normal to the boundary so that t_1 and t_2 describe two orthogonal co-ordinates in the plane of the boundary. Then from (5.37)

$$b_{t1} = iK_{t1}\phi \quad ...(5.38)$$

$$b_{t2} = iK_{t2}\phi \quad ...(5.39)$$

and $$b_n = b_r = -(K_{t1}^2 + K_{t2}^2)^{1/2}\phi \quad ...(5.40)$$

We can derive two local boundary conditions on the magnetic field from the above three equations. For example

$$b_{t1}/b_{t2} = K_{t1}/K_{t2} \quad \text{ie.} \quad K_{t2}b_{t1} - K_{t1}b_{t2} = 0 \quad ...(5.41)$$

and $$b_{t1}/b_n = -iK_{t1}/|K_t| \quad \text{or} \quad |K_t|\, b_{t1} + iK_{t1}b_n = 0 \quad ...(5.42)$$

which, by the help of equation (5.36) and equations (5.8) to (5.10), are written in their expanded form as

$$K_{t2}[k_1\bar{A}_1.\hat{t}_1 + k_2\bar{A}_2.\hat{t}_1 + k_3\bar{A}_3.\hat{t}_1 + k_4\bar{A}_4.\hat{t}_1] -$$
$$K_{t1}[k_1\bar{A}_1.\hat{t}_2 + k_2\bar{A}_2.\hat{t}_2 + k_3\bar{A}_3.\hat{t}_2 + k_4\bar{A}_4.\hat{t}_2] = 0 \quad ...(5.43)$$

and $|K_t|[k_1\bar{A}_1.\hat{t}_1 + k_2\bar{A}_2.\hat{t}_1 + k_3\bar{A}_3.\hat{t}_1 + k_4\bar{A}_4.\hat{t}_1] -$

$$iK_{t1}[k_1\bar{A}_1.\hat{n} + k_2\bar{A}_2.\hat{n} + k_3\bar{A}_3.\hat{n} + k_4\bar{A}_4.\hat{n}] = 0 \quad \ldots(5.44)$$

where $\hat{t}_1$,$\hat{t}_2$ and $\hat{n}$ are unit vectors in the directions of t_1,t_2 and r, respectively. In Appendix III we employ equations (5.32), (5.43) and (5.44) in their expanded form to obtain six linear equations in as many unknowns. We also describe there, the necessary modifications to these equations when the wavenumber of one of the waves becomes complex. These equations are then solved for the real and imaginary parts of the amplitudes of the reflected waves.

5.3 A NUMERICAL STUDY OF THE PROCESS OF REFLECTION In this section we report the results of a few numerical investigations of the process of reflection of IMHD waves by rigid boundaries. We study in detail the reflection of two waves, one an inertial mode with frequency = 1.21 normalised units and wavenumber = (1.0, 0.2, 0.2) and the other a magnetic mode with frequency = 0.012 units and wavenumber = (0.1, 0.05, 0.05) by conducting and insulating boundaries at various orientations and inclinations.

5.3.1 Wave 1. Reflection of an inertial mode This moderate frequency inertial mode travels with a group velocity of 1.345 units. [All the quantities are in normalised units, therefore velocities are in units of Alfven velocity.] The group velocity vector of this wave makes angles $C_{g\phi} = -3.15^{\circ}$ with the x axis (ie. the horizontal component of the group velocity of the wave lies in the positive x, negative y quadrant) and $C_{g\theta} = 55^{\circ}$ with

the horizontal (ie. the vertical component of the wave's group velocity is upwards). To cover most of the interesting possibilities we will first present this wave with boundaries of common inclination for a wide range of orientations (ie. n_θ = constant, n_ϕ = variable, where $\hat{n} = (1, n_\theta, n_\phi)$ is the unit normal of the boundary) and next with boundaries with a fixed orientation in the x-y plane for a wide range of inclinations (ie. n_θ = variable, n_ϕ = constant).

We choose $n_\theta = C_{g\theta} = 55^\circ$ for our first case and study the reflection of this wave for n_ϕ ranging from $C_{g\phi} - \pi/2$ to $C_{g\phi} + \pi/2$. Notice that outside this range, the group velocity of the incident wave has no component towards the boundary so that no reflections are possible. From our results it is seen that for this inclination the incident wave produces only two reflected waves for each reflection over the entire range of n_ϕ. Figure5.3 shows the wavenumbers $|K|$ of the incident (thick line) and the reflected waves plotted against n_ϕ, where it can be seen that $|K_4| > |K_1|$ and $|K_4| > |K_3|$ and $|K_3| = O(|K_1|)$, suggesting that $\bar{K}_3$ is an inertial mode whereas $\bar{K}_4$ represents a magnetic mode. This conjecture is confirmed by Figure 5.4 [based on equation (1.42)] where we plot magnetic to kinetic energy ratios of all these modes. The magnetic energy of the wave represented by $\bar{K}_4$ is seen here to be many times that of its kinetic energy whereas mode $\bar{K}_3$ has most of its energy in kinetic form. The nature of these modes (ie. whether they are inertial or magnetic) is also reflected in their group velocities $|\bar{C}_g|$ shown in Figure 5.5 [see equations (5.25) to (5.27)] where it is seen that the group velocity of the

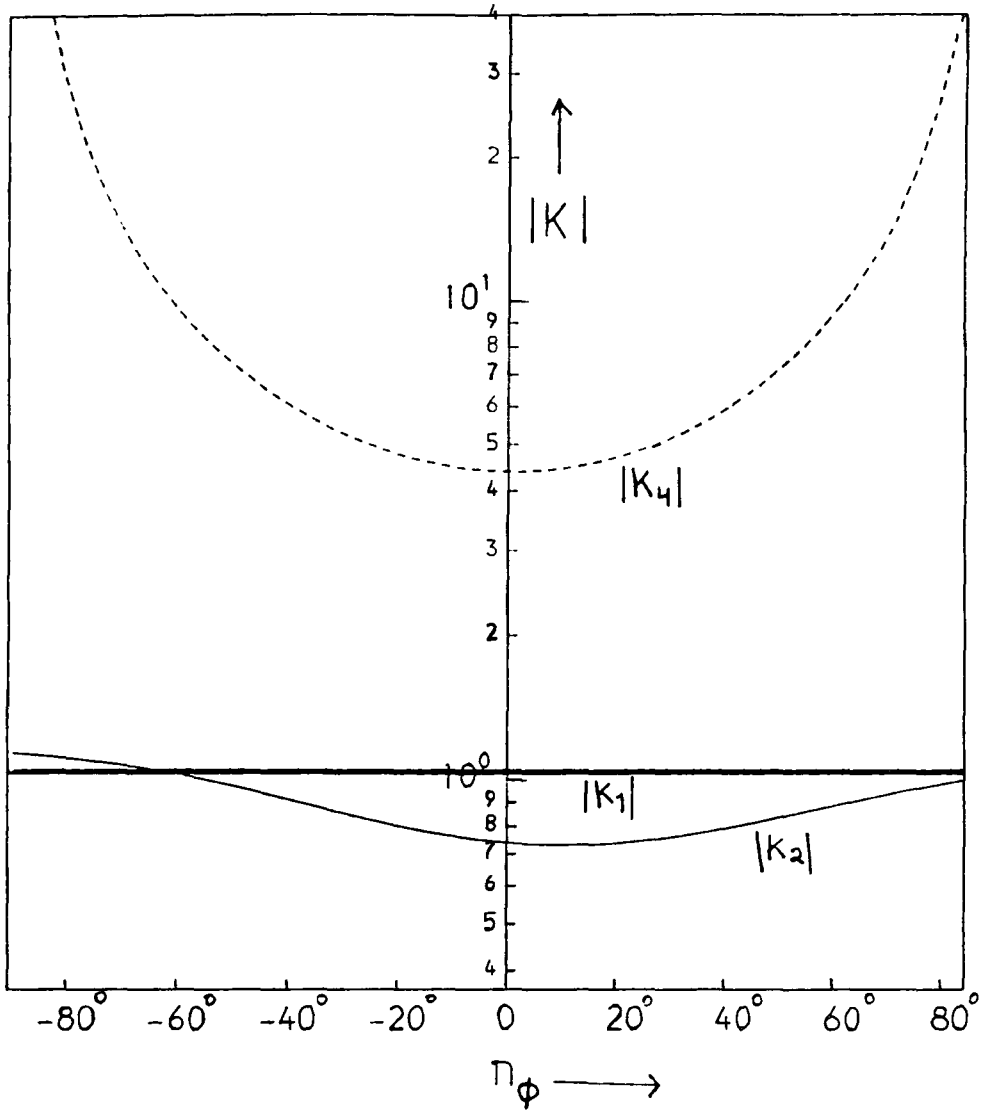

Figure 5.3 The wavenumbers K of the incident and reflected waves as functions of n_ϕ. K_2 is complex for the complete range of orientations shown here. The incident wave quanities in this and subsequent plots are shown in thick lines and the reflected magnetic modes are in broken lines. Solid lines represent inertial modes. All quantities here and later are in normalised units. ω = 1.21 units for all these waves and $n_\theta = 55^\circ$.

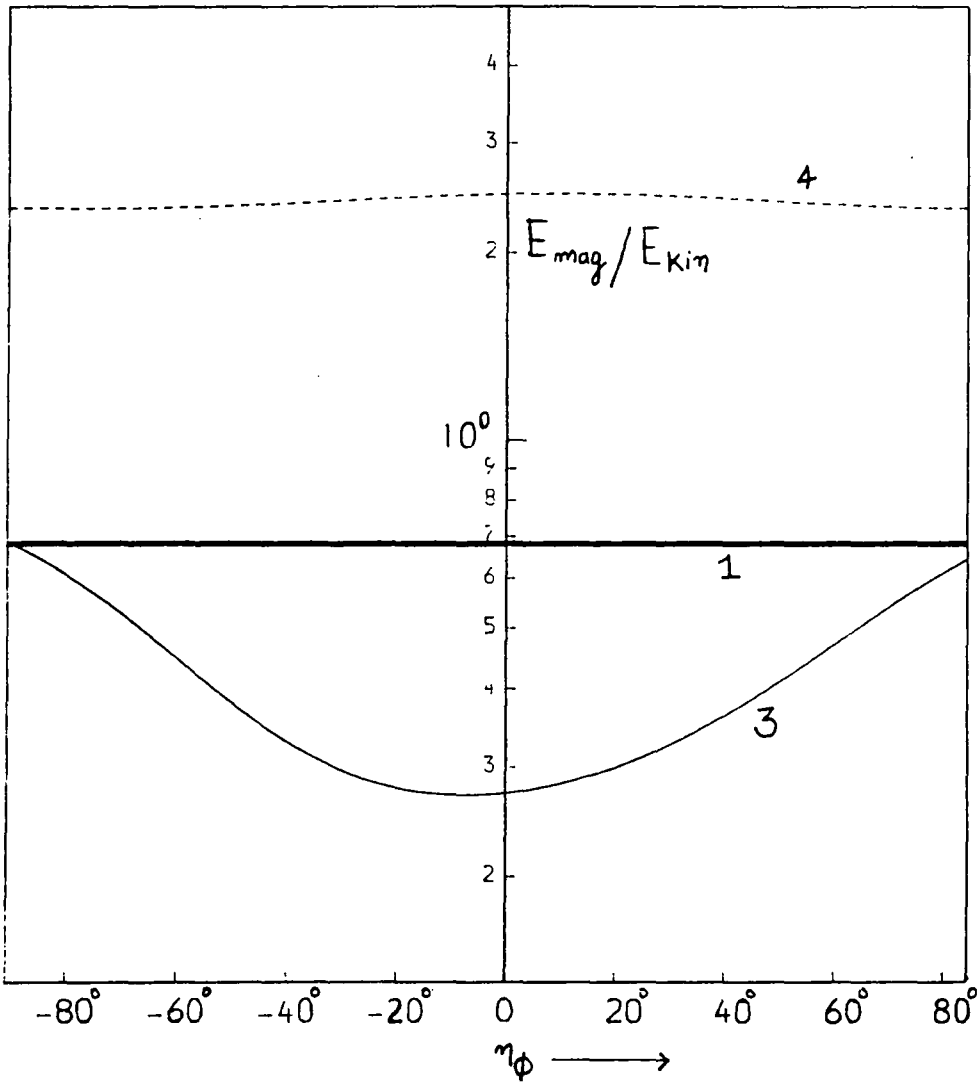

Figure 5.4 The magnetic to kinetic energy ratios of the incident and reflected waves as functions of n_ϕ. Notice the large magnetic energies of wave 4 compared to that of wave 3. ω = 1.21 units for all these waves and $n_\theta = 55^0$.

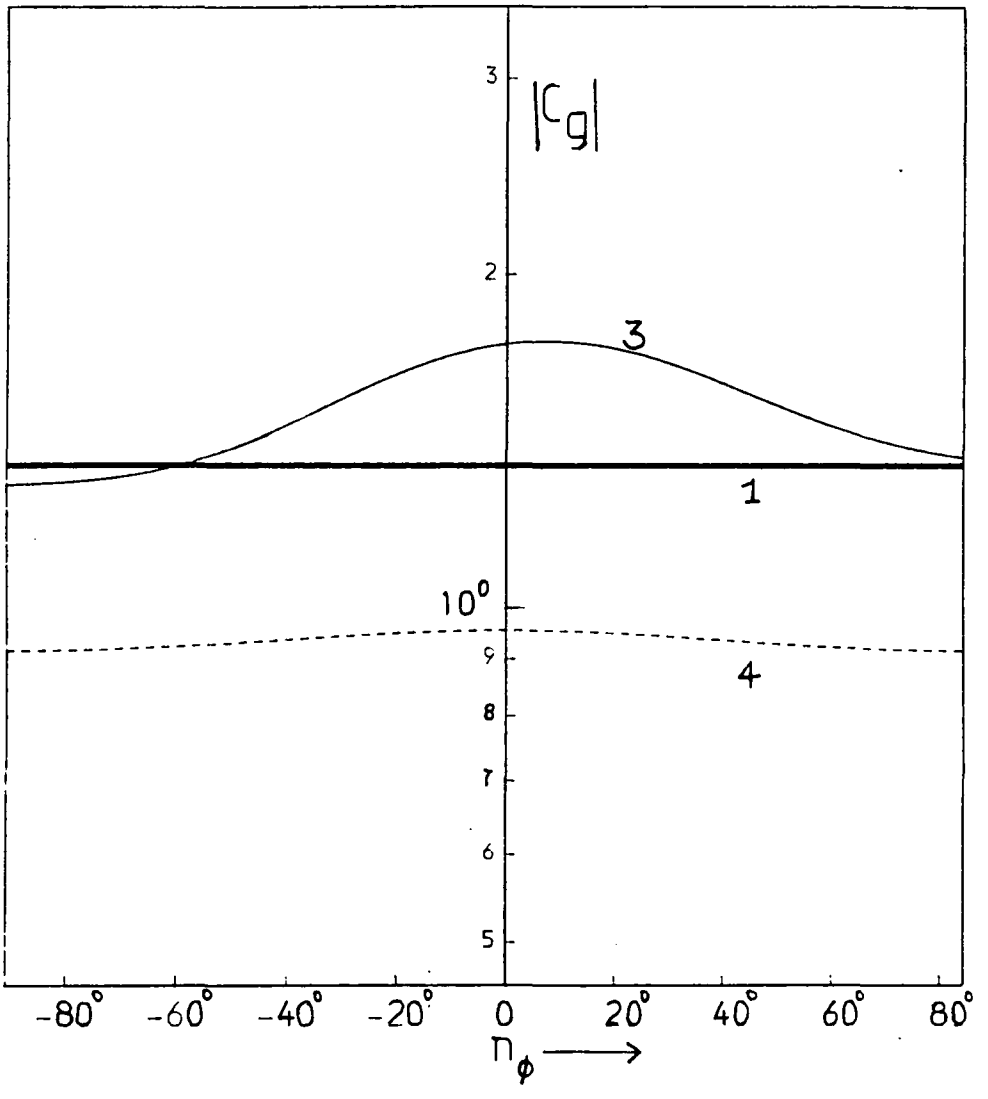

Figure 5.5 The group velocities |Cg| of incident and reflected waves as functions of n_ϕ. Magnetic mode 4 has much smaller group velocities than the inertial modes 1 and 3. The velocities are in normalised units. ω = 1.21 units for all these waves and $n_\theta = 55^\circ$.

magnetic mode $\bar{K}_4$ is less than the Alfven velocity (of unity) for the entire range shown, though both the incident wave and mode 3 have group velocities larger than unity. For certain values of $\hat{n} = (l, n_\theta, n_\phi)$, one of the reflected waves may emerge parallel to the boundary with the consequence that due to the dissipative action of viscosity its energy will be quickly absorbed by the boundary. Such a situation does occur for magnetic modes when the boundary is parallel to x axis ie. $n_\phi = \pi/2$ where C_{gn} the normal component of its group velocity becomes zero, as shown in Figure 5.6.

For dispersive waves, the amplitude of a wave is not a good indicator of the energy content of the wave. For example a magnetic IMHD wave and an inertial IMHD wave of the same velocity amplitude and frequency do not have equal energies. The function of the amplitude for a dispersive wave is best carried out by its 'average energy density', which for IMHD waves (see Acheson and Hide 1973) can be expressed by

$$E_j = 0.5 < \bar{u}_j . \bar{u}_j > + 0.5 < \bar{b}_j . \bar{b}_j > /(\mu\rho) \qquad \ldots(5.45)$$

where $< >$ denotes average over a period. By the help of equations (5.3) and (5.6) to (5.10), we can obtain

$$E_j = \frac{1}{2}\left(\frac{k_j^2 + l_j^2 + m_j^2}{k_j^2 + l_j^2}\right)\left(\frac{\omega_j^2 + k_j^2}{\omega_j^2}\right) A_j \qquad \ldots(5.46)$$

where A_j is the amplitude of the vertical component of the fluid velocity associated with the wave j. These energy densities for our case study obtained from the numerically computed amplitudes

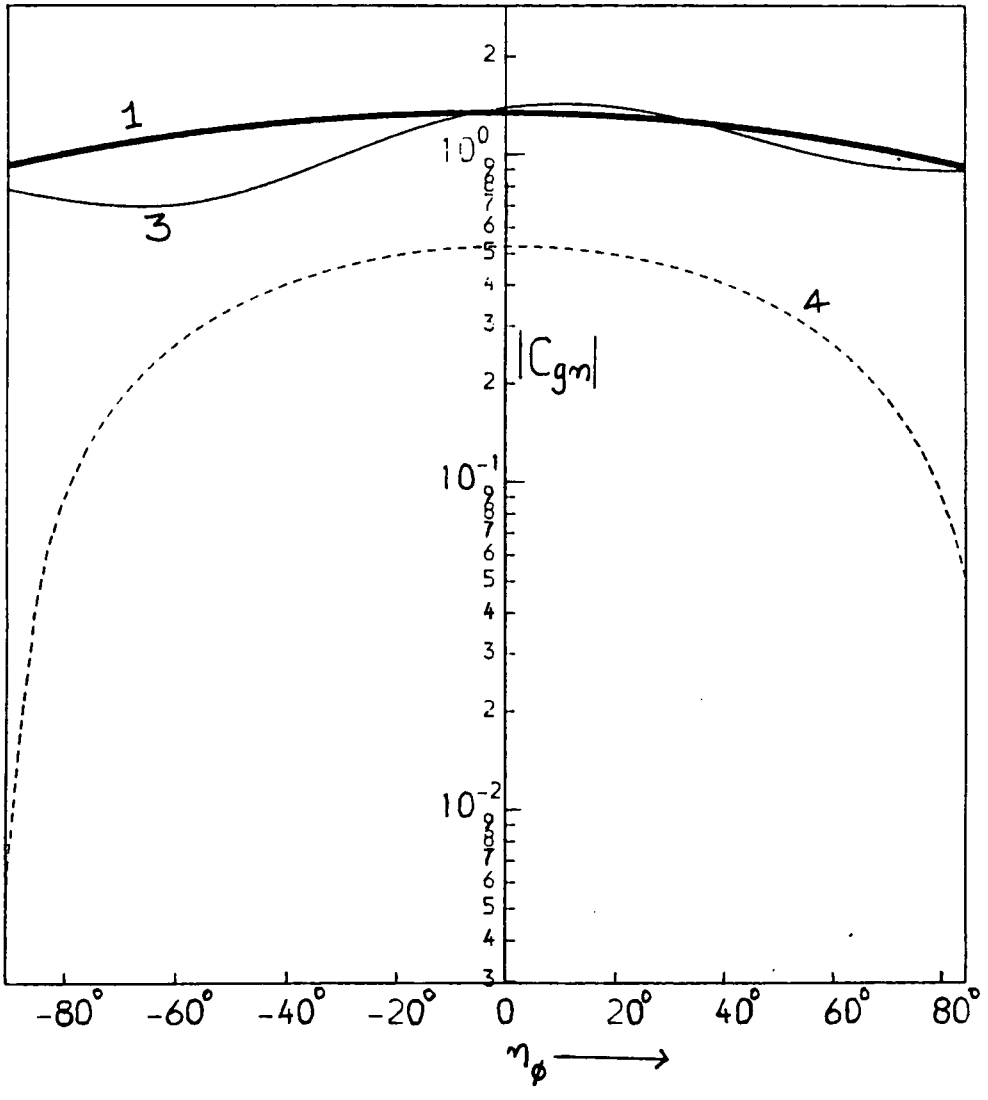

Figure 5.6 The components of group velocities normal to the plane of the rigid boundary for incident and reflected waves shown as function of n_ϕ. ω = 1.21 units for all these waves and $\eta_\theta = 55^\circ$.

(see Appendix III) are shown in Figures 5.7(a) and (b) for conducting and insulating boundaries, respectively. Notice that though the energy densities of the reflected inertial modes is of the same order as the incident wave in both these cases the energy density of the magnetic mode is distinctly higher for reflections from conducting boundaries as compared to reflections from insulating boundaries. As the time over which the reflected waves are generated is the same for all the reflected waves, waves that have group velocities larger than the incident wave will have the lengths of their wave packets stretched, whereas slower reflected waves will have the lengths of their wavepackets reduced. In addition the emerging wavepackets do not make the same angle with the boundary and hence will have their widths either enlarged or decreased depending on whether they emerge in a direction more normal or parallel (compared with the direction of the incident wave packet) to the boundary.

The measure of the total energy content of a wave packet is provided by its energy flux vector defined as

$$\bar{F}_j = \bar{E}_j . \bar{C}_{gj} \qquad \ldots(5.47)$$

From energy conservation considerations, we will expect the energy flux of the incoming wave to equal the flux of the outgoing wave. If we concentrate on a unit area of the boundary this condition implies that the flux per unit area through and out of this boundary should be equal. ie.

$$F_1 \cos\alpha_1 = \sum_r F_r \cos\alpha_r \qquad \ldots(5.48)$$

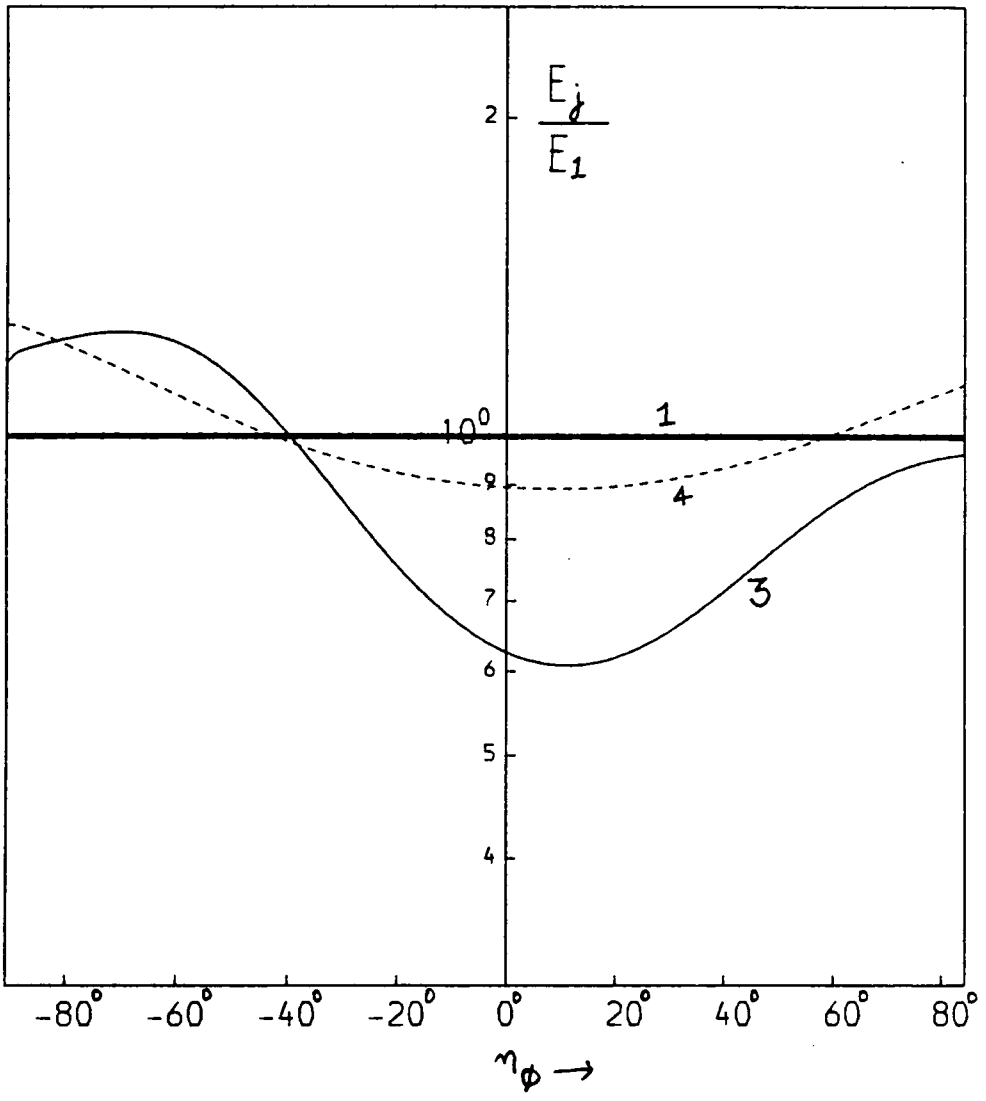

Figure 5.7(a) The average energy densities of the incident and reflected waves as function of n_ϕ for a conducting boundary. All of these energy densities are expressed here as fractions of the energy density of the incident wave. ω = 1.21 units for all these waves and $\eta_\theta = 55^\circ$.

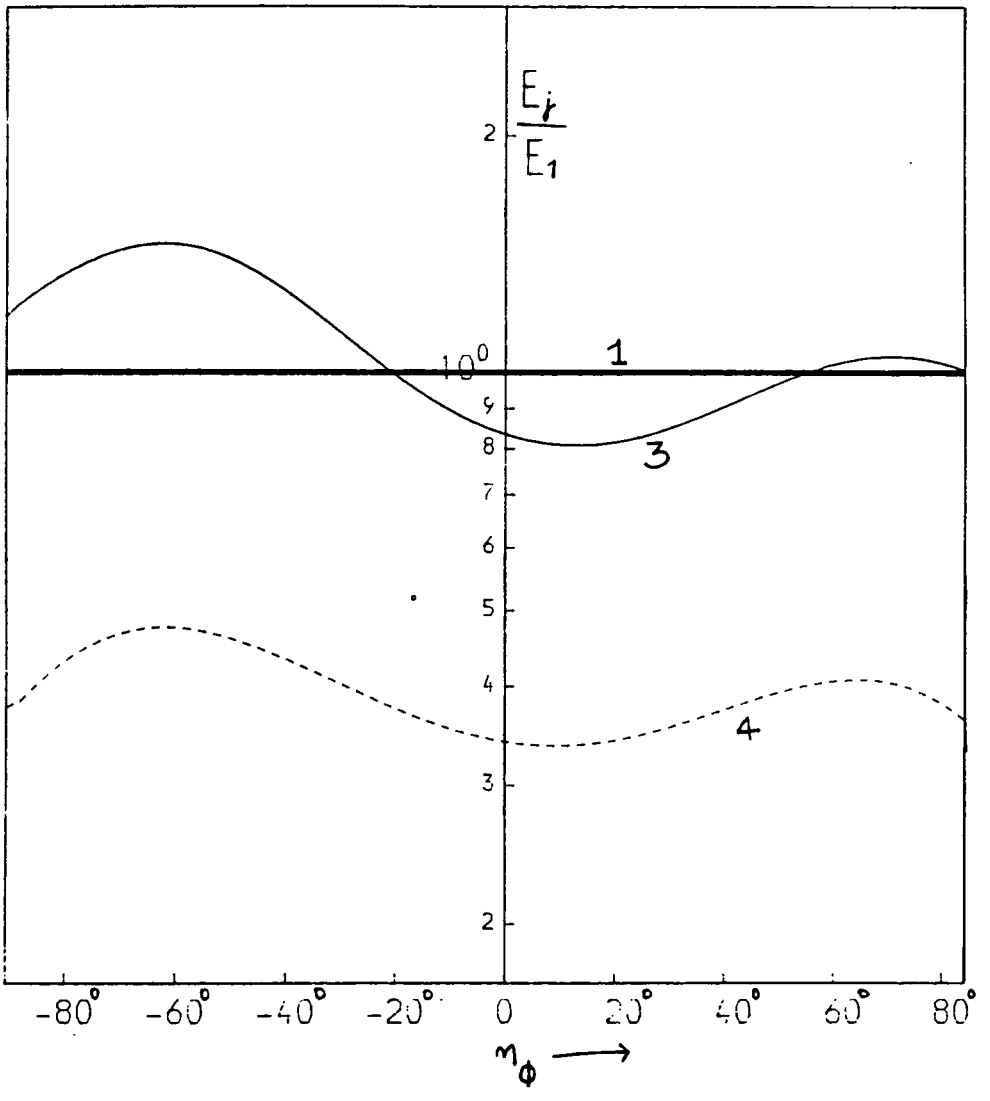

Figure 5.7(b) Same as figure 5.7(a) except that the reflections are from an insulating boundary. Notice the much lower energy densities of the magnetic mode in this case. ω = 1.21 units for all these waves and $m_\theta = 55^0$.

where α_j is the angle the wave packet j (incident or reflected) makes with the normal to the boundary. By the help of (5.47) this equation can be written as

$$F_{nl} = \bar{F}_l.\hat{n} = \sum_{\gamma} \bar{F}_r.\hat{n} = \sum_{\gamma} F_{nr} \text{ (say)} \qquad \ldots(5.49)$$

where F_{nj} is the normal component of the energy flux vector $\bar{F}_j$ of wave j. These (as fractions of the incident normal flux) are shown in Figures 5.8(a) and (b) for the case of conducting and insulating boundaries and point out that quite large proportions of the incident energy (up to 37% from a conducting boundary and up to 15% from an insulating boundary) are captured by the magnetic mode. Figures 5.9(a) and (b) show the phases, ϵ_j, of the incident and reflected waves and are seen to be highly dependent on the orientation of the boundary.

Figures 5.10 to 5.16 repeat the same experiment but keeping the orientation of the boundary as measured in the x-y plane constant this time and varying the tilt of the boundary around the incident wave [ie n_ϕ is taken as constant at $n_\phi = C_{g\phi}$ but $C_{g\theta} - \pi/2 < n_\theta < C_{g\theta} + \pi/2$]. It is seen that when n_θ is small ie when the rigid boundary is almost vertical, an incident inertial IMHD wave on reflection generates three reflected IMHD waves, one of which is a magnetic mode and the other two are inertial modes. For larger n_θ the wave represented by $\bar{K}_2$ (ie small wavenumber inertial mode) becomes a non-propagating leaking mode and does not partake of the energy flux. Figure 5.10 shows the wavenumbers $|K|$ of the incident and reflected waves and it can be seen that $|K_2| < |K_3| < |K_4|$ and $|K_4| \to \infty$ when $n_\theta \to \pi/2$ ie

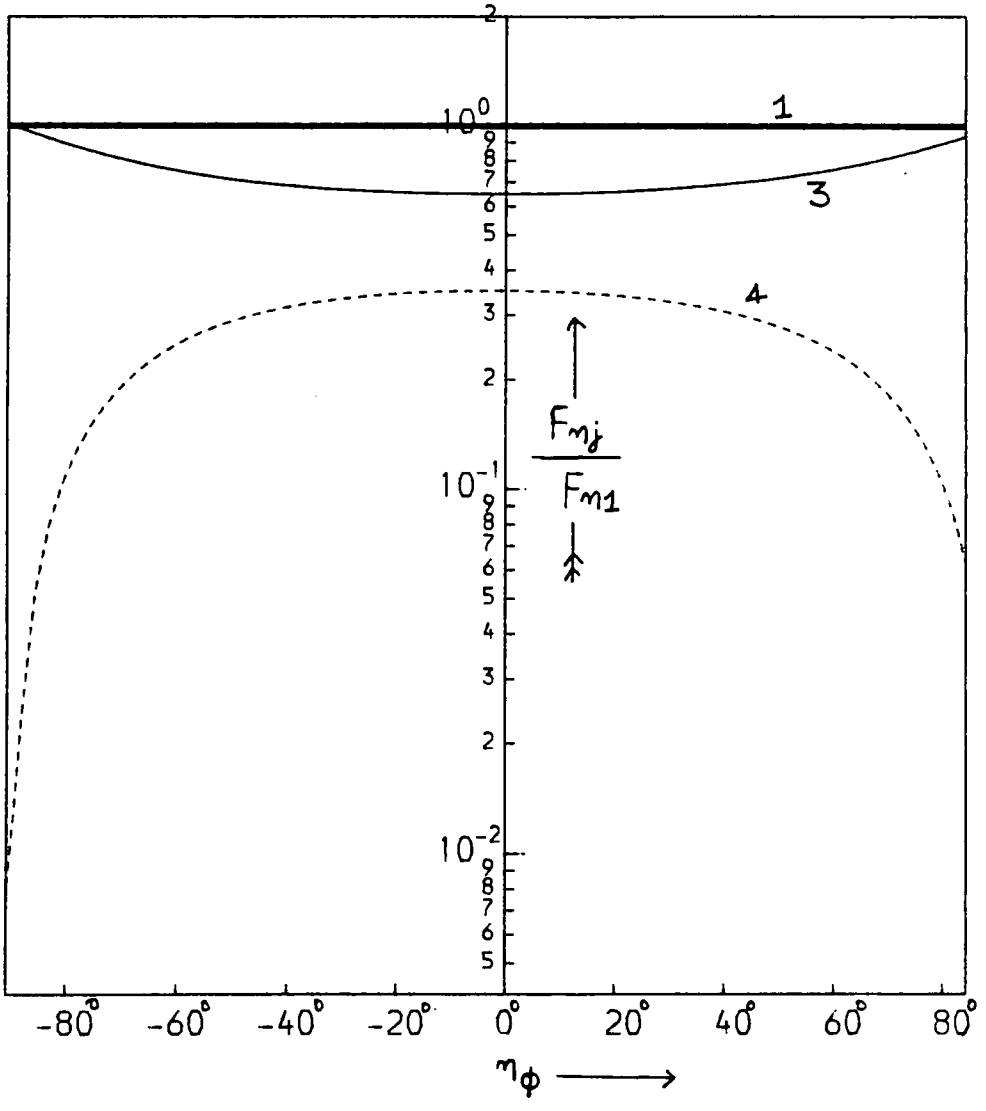

Figure 5.8(a) F_n, the average energy flux crossing a unit area of the rigid boundary for incident and reflected waves for various orientations of the boundary. The rigid boundary is assumed to be highly conducting. ω = 1.21 units for all these waves and $\eta_\theta = 55^0$.

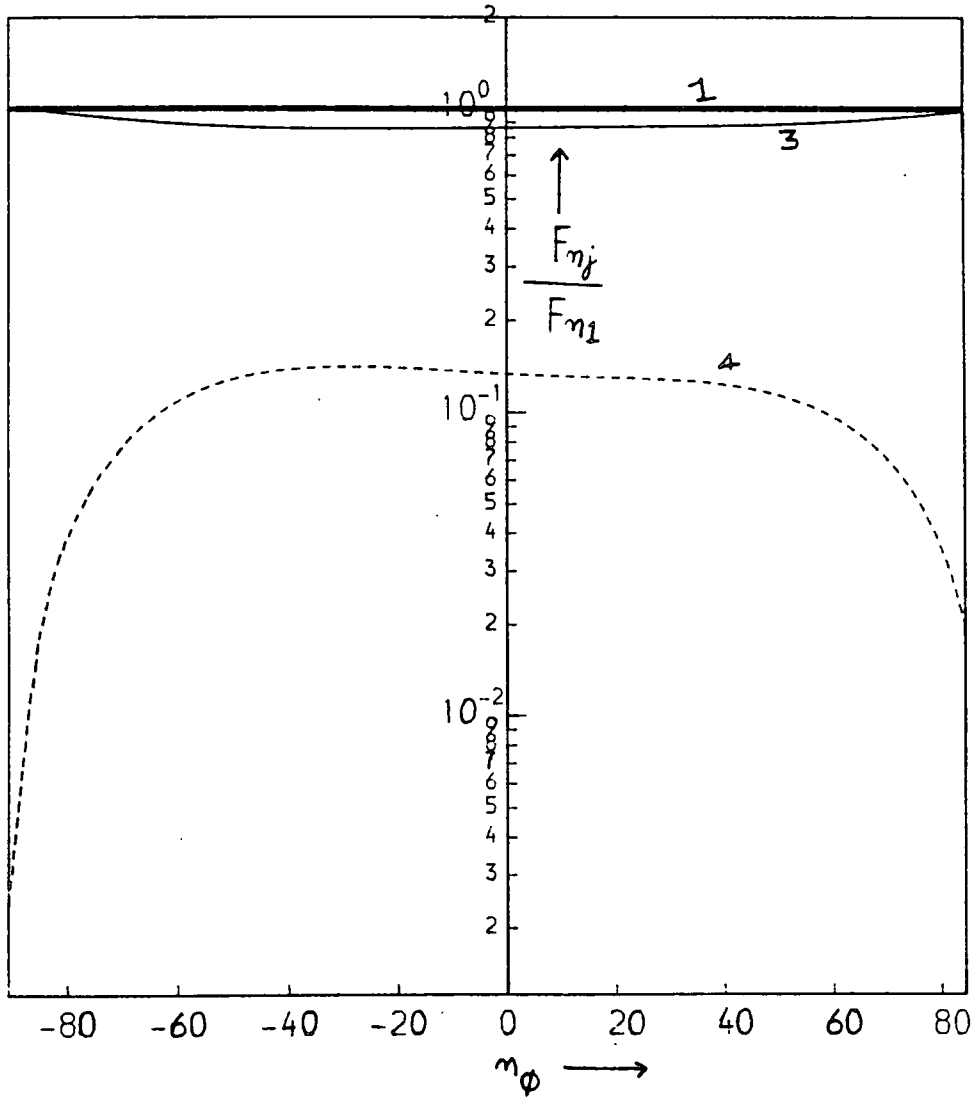

Figure 5.8(b) Same as Figure 5.8(a) except that the reflections are from an insulating boundary. ω = 1.21 units for all these waves and $\eta_\theta = 55^\circ$.

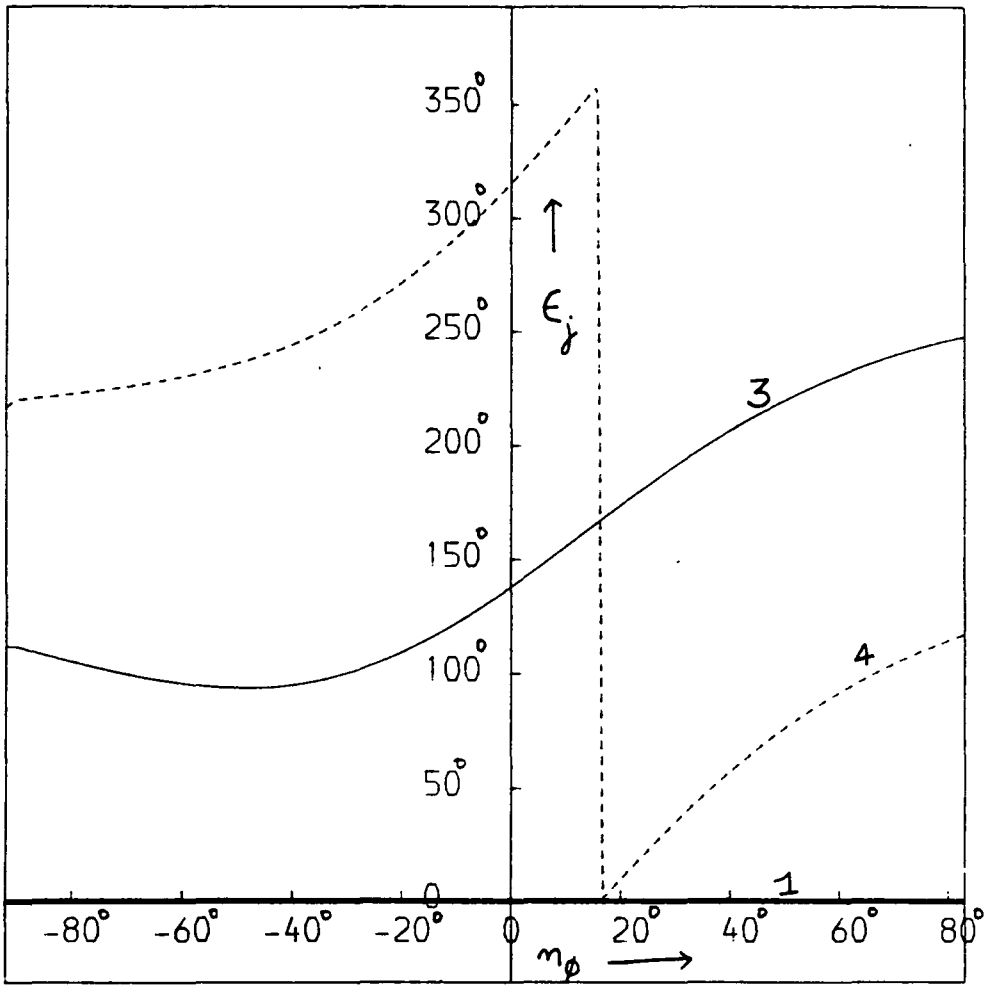

Figure 5.9(a) The phases of the incident and reflected waves as functions of n_ϕ. The case of a conducting boundary. ω = 1.21 units for all these waves and $\eta_\theta = 55^\circ$.

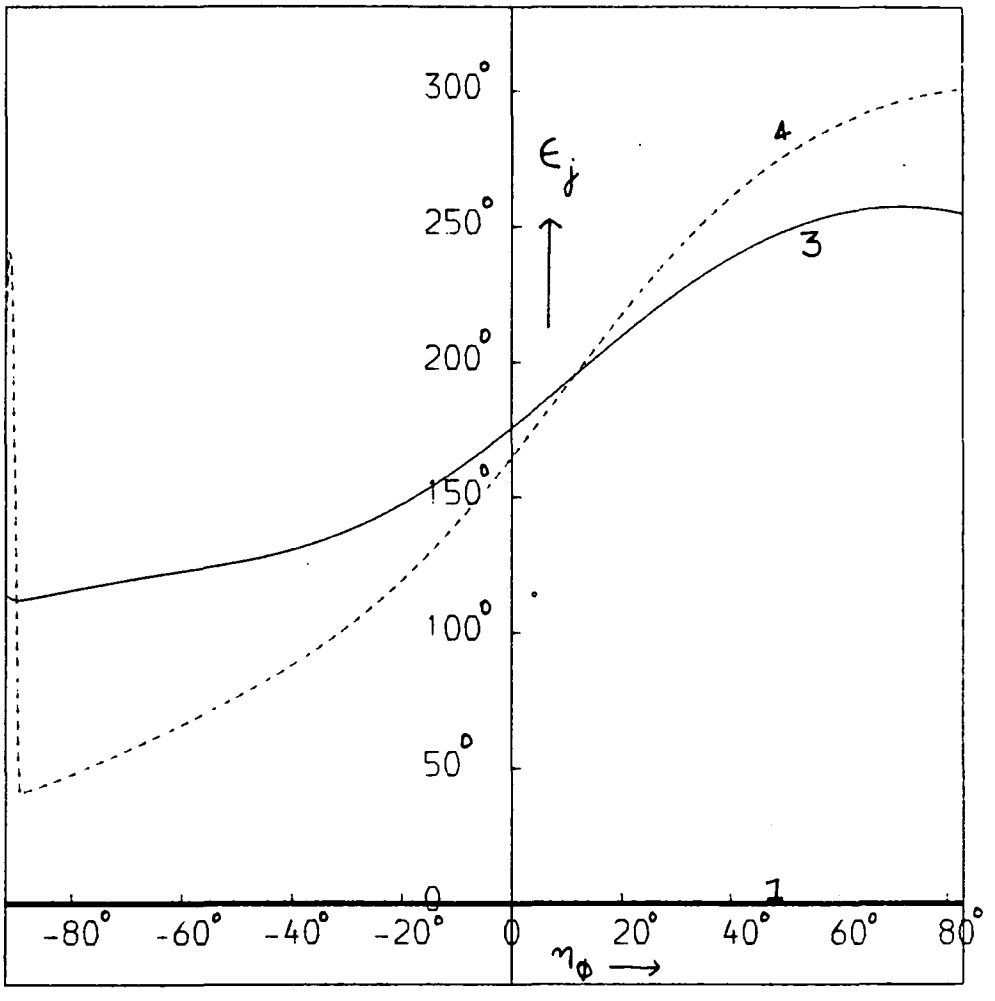

Figure 5.9(b) Same as Figure 5.9(a) when the rigid boundary is assumed to be non-conducting. ω = 1.21 units for all these waves and $\eta_\theta = 55^\circ$.

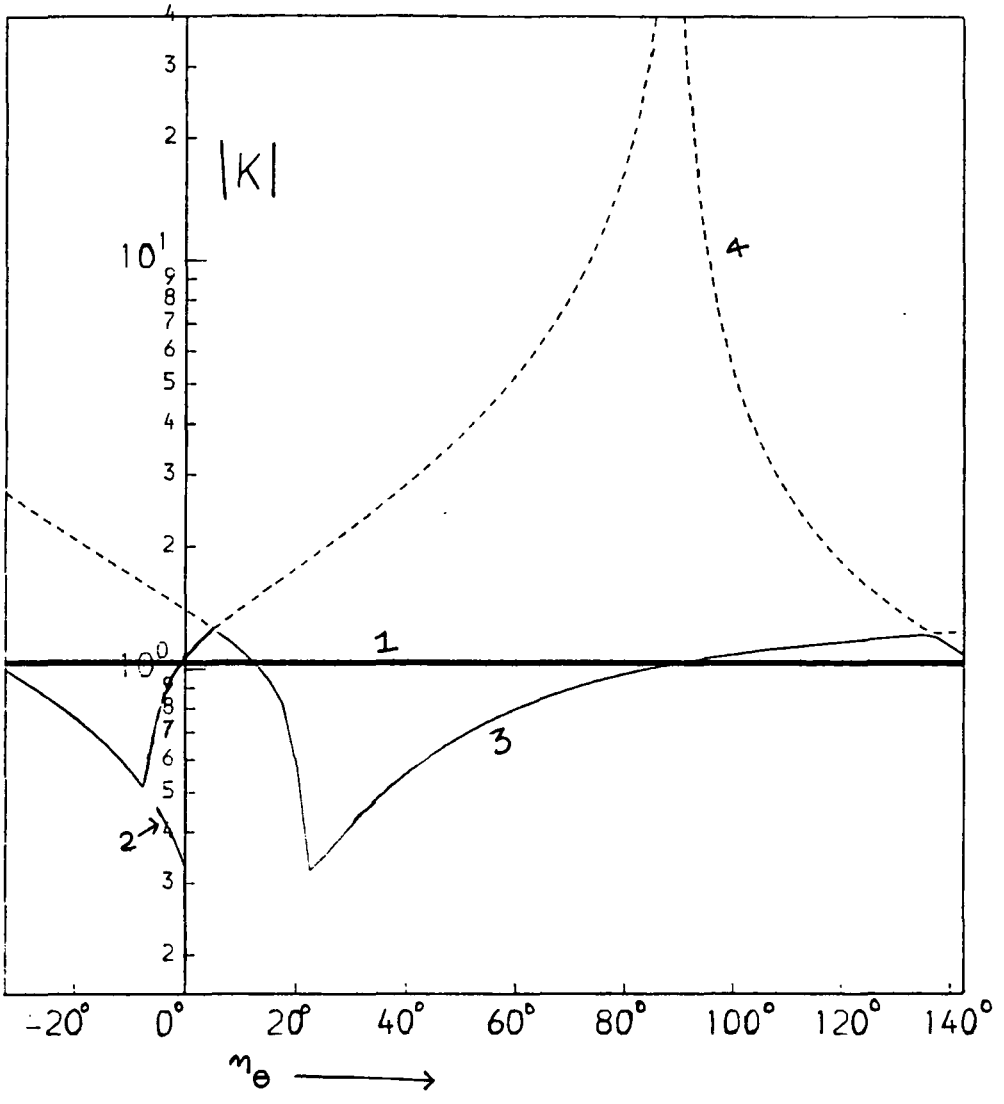

Figure 5.10 The wavenumbers |K| of the incident and reflected waves as function of n_θ . For a very small range (-7° to 0°) of n_θ, three reflected waves are produced for each reflection. For other tilts only one inertial and one magnetic mode are generated. ω = 1.21 units for all these waves and $n_\phi = -3.15^\circ$.

when the rigid boundry is horizontal. Figures 5.11 and 5.12 show the magnetic/kinetic energy ratios and group velocities of these waves respectively, confirming the fact that $\bar{K}_4$ is indeed a magnetic mode whereas $\bar{K}_1$, $\bar{K}_2$, and $\bar{K}_3$ are inertial. A steep dip for a particular value of n_θ in the normal component of the group velocity of a reflected wave (see Figure 5.13) shows that $C_{gn} \rightarrow 0$ for that n_θ indicating that the reflected wave emerges parallel to the boundary and will be dissipated quickly by the boundary. Such dips are seen around $n_\theta = -5^\circ$, and $= 16^\circ$ for wave $\bar{K}_3$ and at 90° for the magnetic mode. Though the dips in the C_{gn} curve of $\bar{K}_3$ are real, the dip in the magnetic mode is pathological because for $n_\theta = 90^\circ$, $\bar{K}_4 \rightarrow \infty$ and will be subject to large viscous and ohmic dissipation anyway. Figures 5.14(a) and (b) show the energy densities of the reflected waves relative to that of the incident wave. Both figures present qualitatively similar results though the magnetic mode has much higher energy density when reflections are from conducting boundaries. The normal flux vector diagrams of 5.15(a) and (b) present a highly intriguing and complex picture. For very small values of n_θ, (-5° to 5°), ie, when the rigid boundary is approximately vertical, most of the wave energy from the incident inertial mode is captured by the emerging magnetic mode. For n_θ out of this range, the energy captured by magnetic modes falls dramatically, though it recovers to about 30% of the incoming flux for conducting boundaries and 10% of the incoming flux for insulating boundaries in the region $n_\theta = 20^\circ$ to 80°. When the rigid boundary is horizontal, (ie $n_\theta = 90^\circ$) only inertial mode $\bar{K}_3$ is

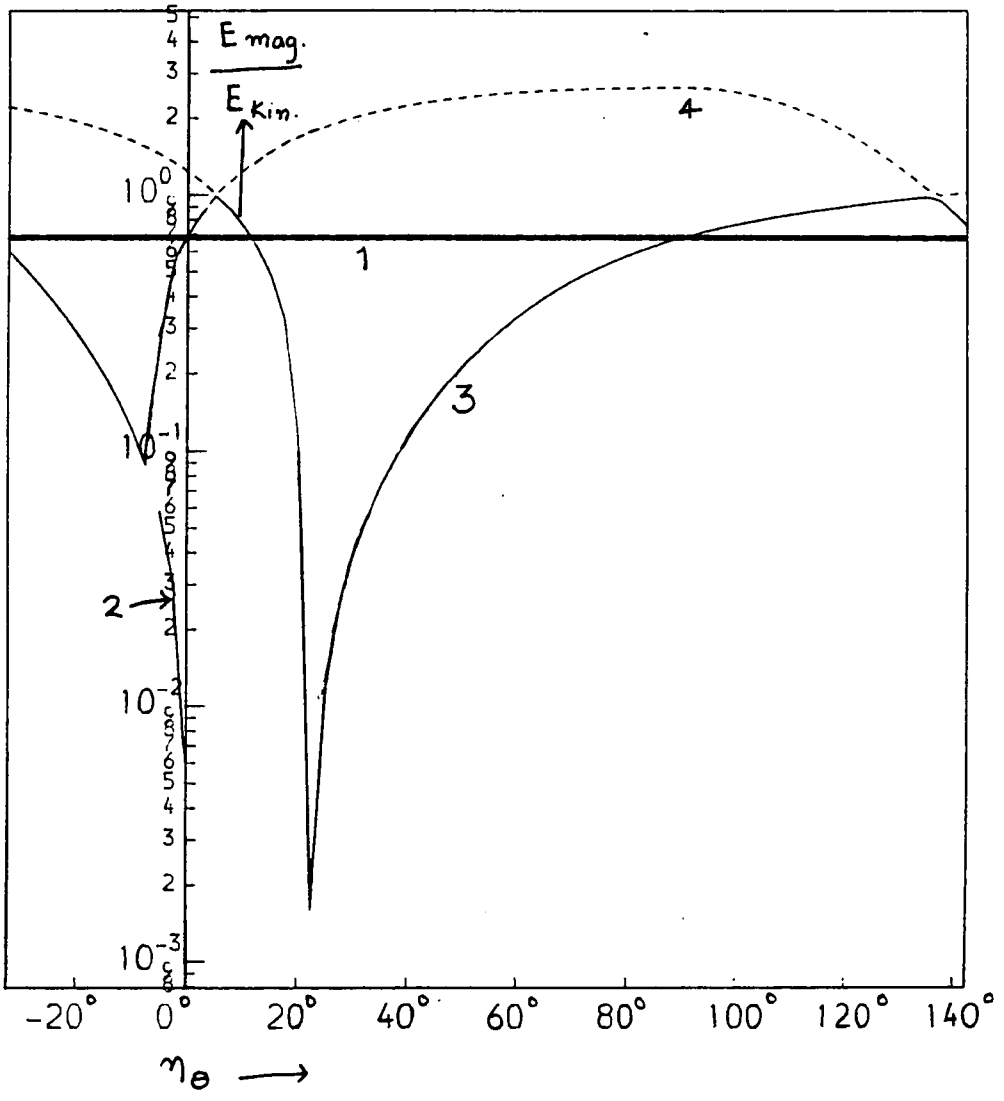

Figure 5.11 The magnetic to kinetic energy ratios of the incident and reflected waves as functions of η_θ. $\omega = 1.21$ units for all these waves and $\eta_\phi = -3.15^\circ$.

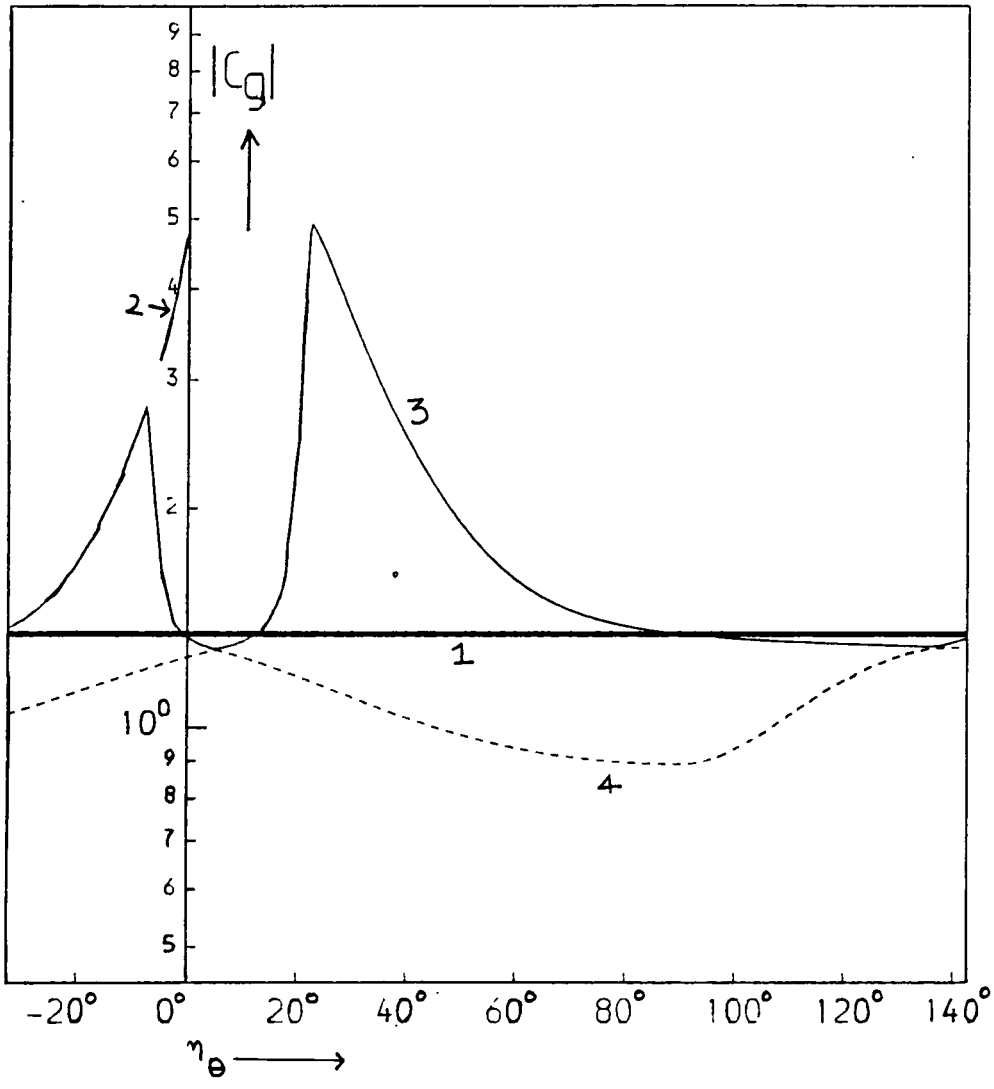

Figure 5.12 The group velocities of the incident inertial and other reflected waves as functions of n_θ. $\omega = 1.21$ units for all these waves and $n_\phi = -3.15^0$.

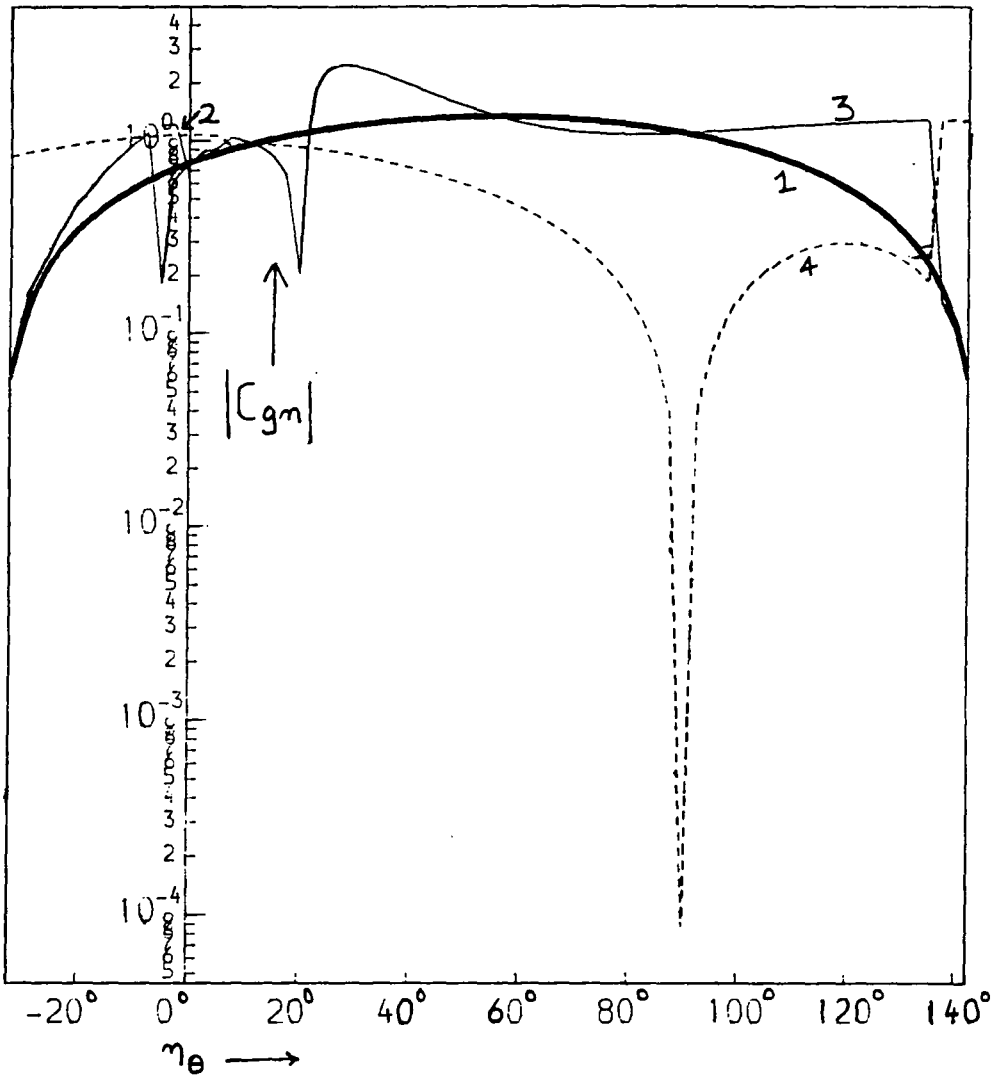

Figure 5.13 $|C_{gn}|$ the normal components of the group velocities of the incident and reflected waves as function of n_θ. Notice the two dips in the curve of wave 3 and a single dip in the curve of wave 4. $\omega = 1.21$ units for all these waves and $n_\phi = -3.15^\circ$.

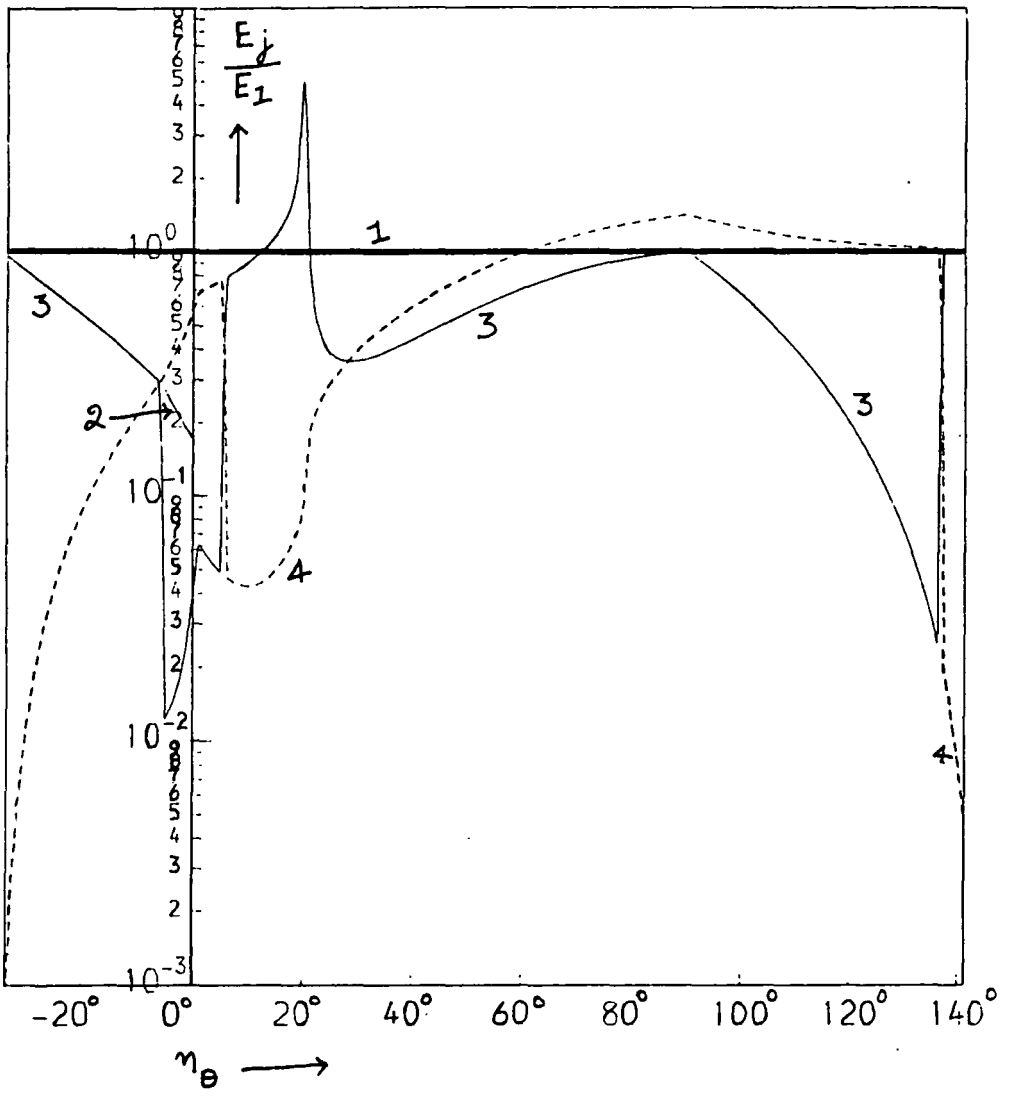

Figure 5.14(a) The normalised energy densities of the incident and reflected waves as functions of n_θ for the case of the reflection from a conducting rigid boundary. $\omega = 1.21$ units for all these waves and $n_\phi = -3.15^\circ$.

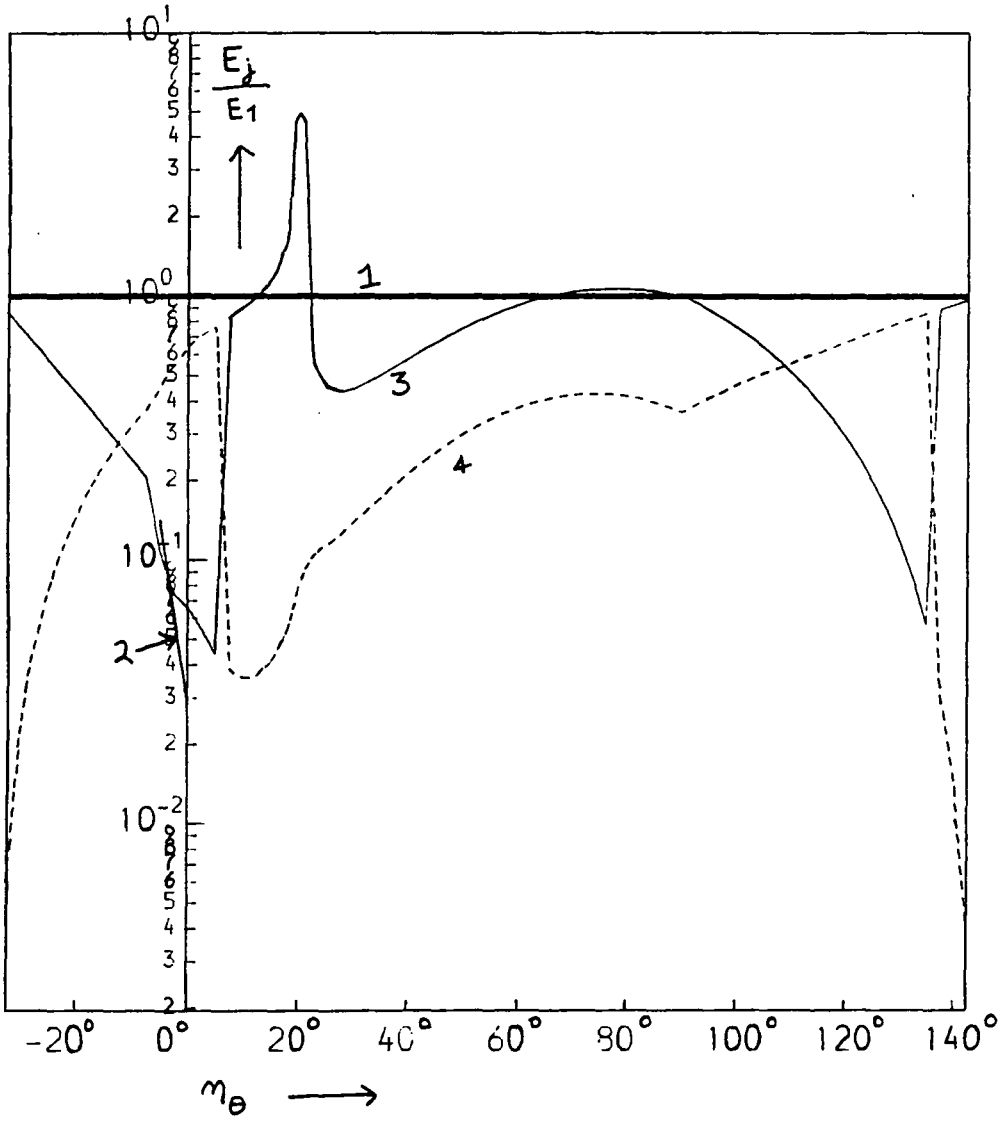

Figure 5.14(b) Same as Figure 5.14(a) except that the reflections are from an insulating boundary. ω = 1.21 units for all these waves and $n_\phi = -3.15^\circ$.

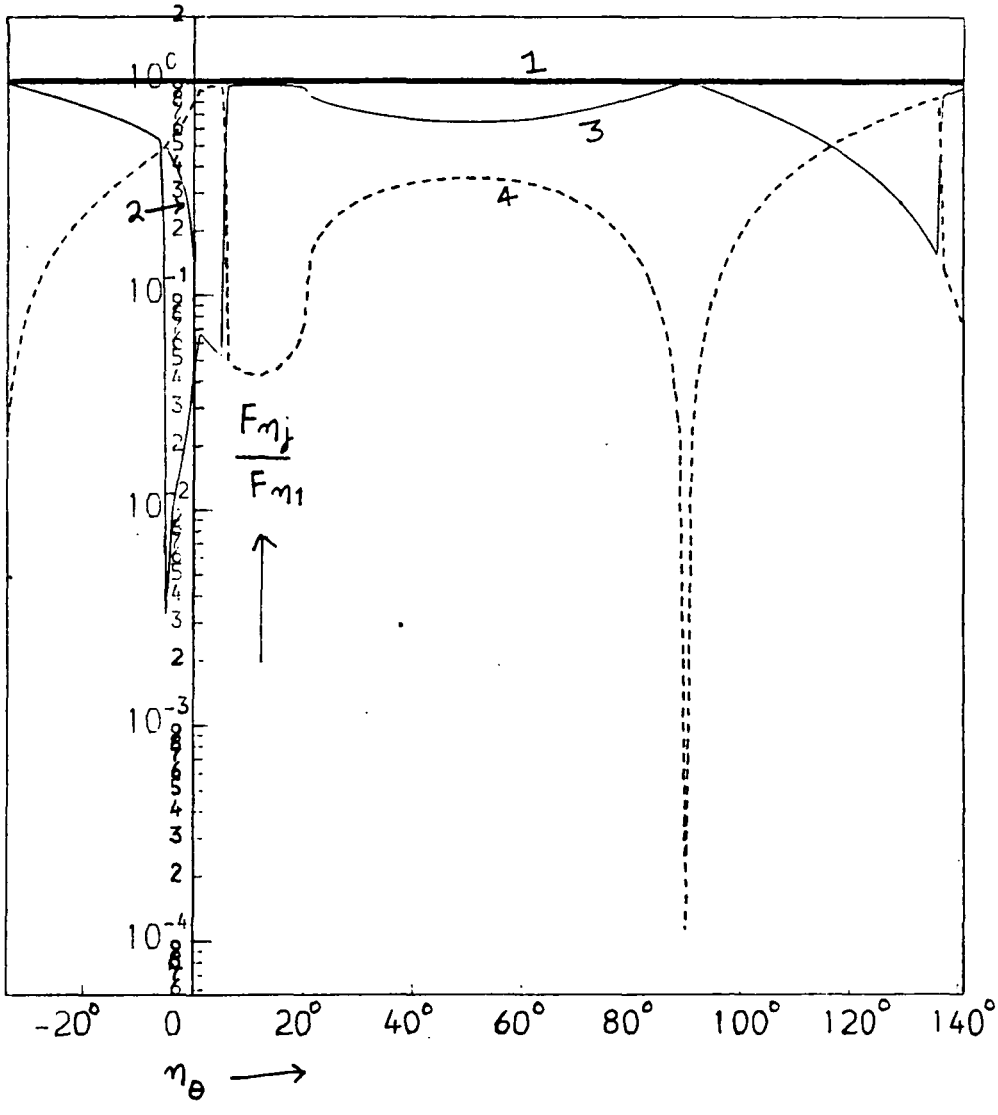

Figure 5.15(a) The normal component of the energy flux vectors. The reflections are from a conducting rigid boundary. Notice that most of the energy is captured by wave 3 except when the boundary is almost vertical. ω = 1.21 units for all these waves and $n_\phi = -3.15^\circ$.

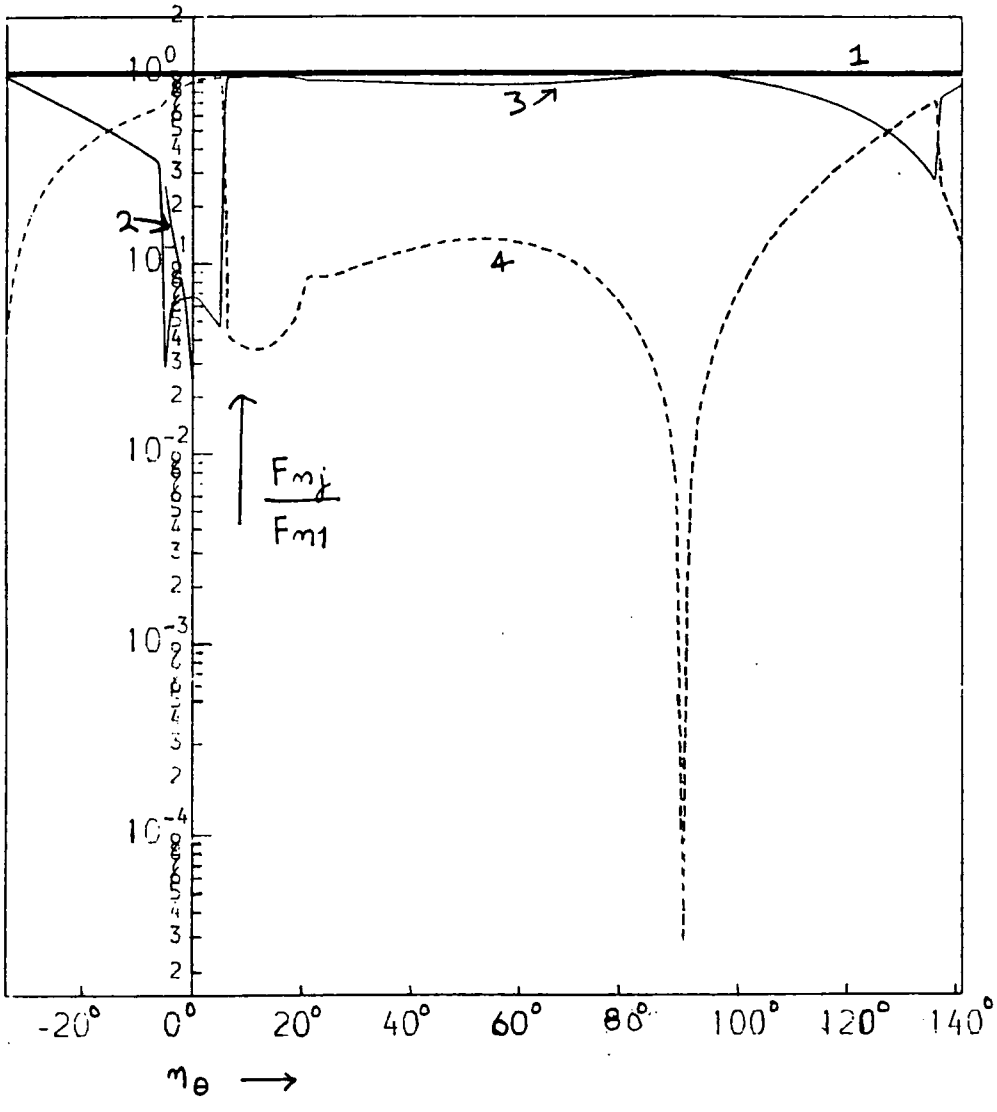

Figure 5.15(b) Same as Figure 5.15(a) except that the reflections are from an insulating rigid boundary. $\omega = 1.21$ units for all these waves and $n_\phi = -3.15°$.

generated. For even larger n_θ (say between 115° to 135° for conducting boundaries and 125° to 135° for insulating boundaries) the magnetic mode captures most of the energy, though its share drops sharply beyond $n_\theta = 135^\circ$. Figures 5.16(a) and (b) show the phases ϵ_j of the incident and reflected waves and are seen to depend greatly on the tilt of the boundary.

5.3.2. Wave 2. Reflection of a magnetic mode. In this section we study the reflection of the second wave which has frequency $\omega = 0.012$ and wavenumber $\bar{K} = (0.1, 0.05, 0.05)$, mentioned earlier. This low frequency magnetic mode travels with a group velocity of 0.37 units with its energy flux vector making an angle $C_{g\theta} = -31.52^\circ$ with the horizontal and $C_{g\phi} = 7.05^\circ$ with the x axis. Obviously, this is a downwards propagating wave whose horizontal group velocity component is in the positive x-y quadrant. Once again we will first look at the case $n_\theta = C_{g\theta} =$ constant and $C_{g\phi} - \pi/2 < n_\phi < C_{g\phi} + \pi/2$. This corresponds to studying the reflection of the wave for the complete range of orientations of the boundary in the x-y plane for a fixed value of tilt. It is seen that except for $102^\circ < n_\phi < 107^\circ$, for each incident wave only one reflected mode ($\bar{K}_4$, which is magnetic) is generated. In the interval $102^\circ < n_\phi < 107^\circ$ another magnetic mode $\bar{K}_3$ is also generated. The wavenumbers $|\bar{K}|$ for the incident and reflected waves depicted in Figure 5.17 show that for most of the region, $|K_4| > |K_1|$ and whenever mode 3 is present $|K_3| > |K_4| > |K_1|$. The magnetic/kinetic energy ratios of the incident & reflected magnetic modes sketched in Figure 5.18 show that these

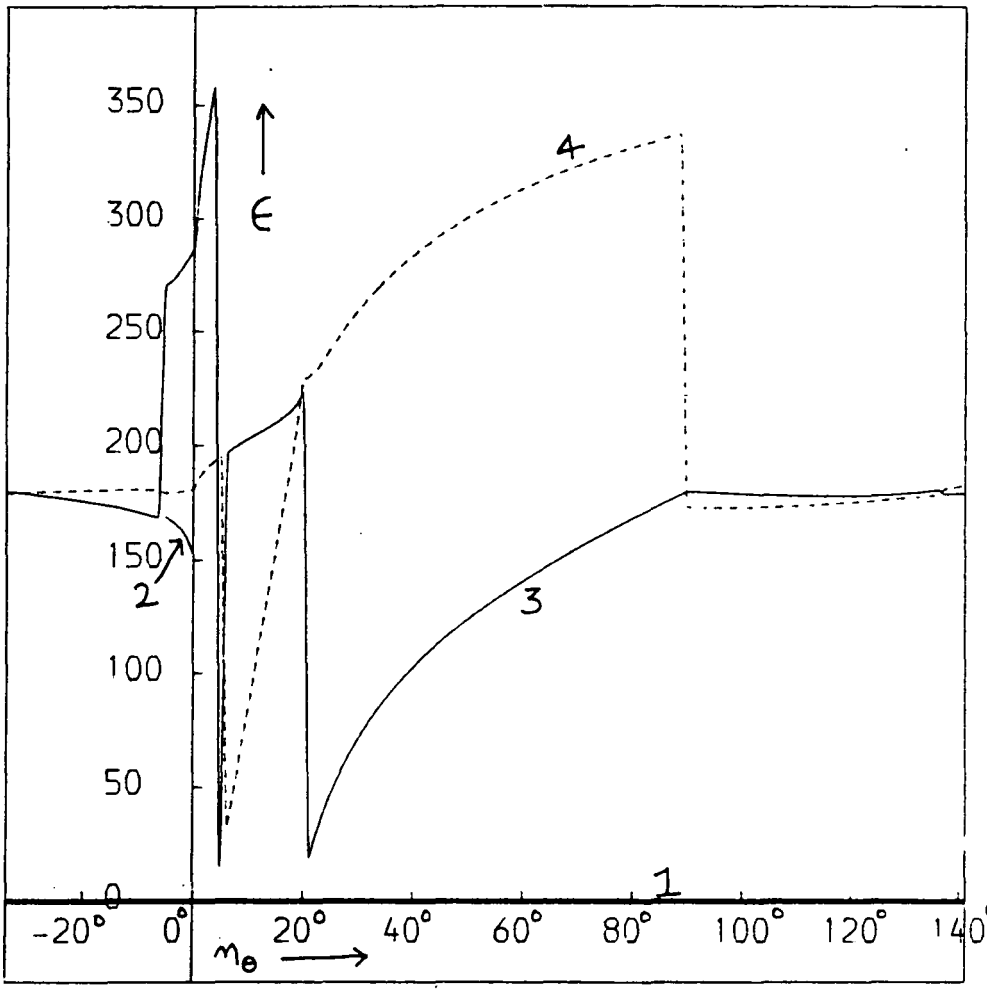

Figure 5.16(a) The phases of the incident and reflected waves as functions of n_θ for reflections from a conducting boundary. ω = 1.21 units for all these waves and $n_\phi = -3.15^\circ$.

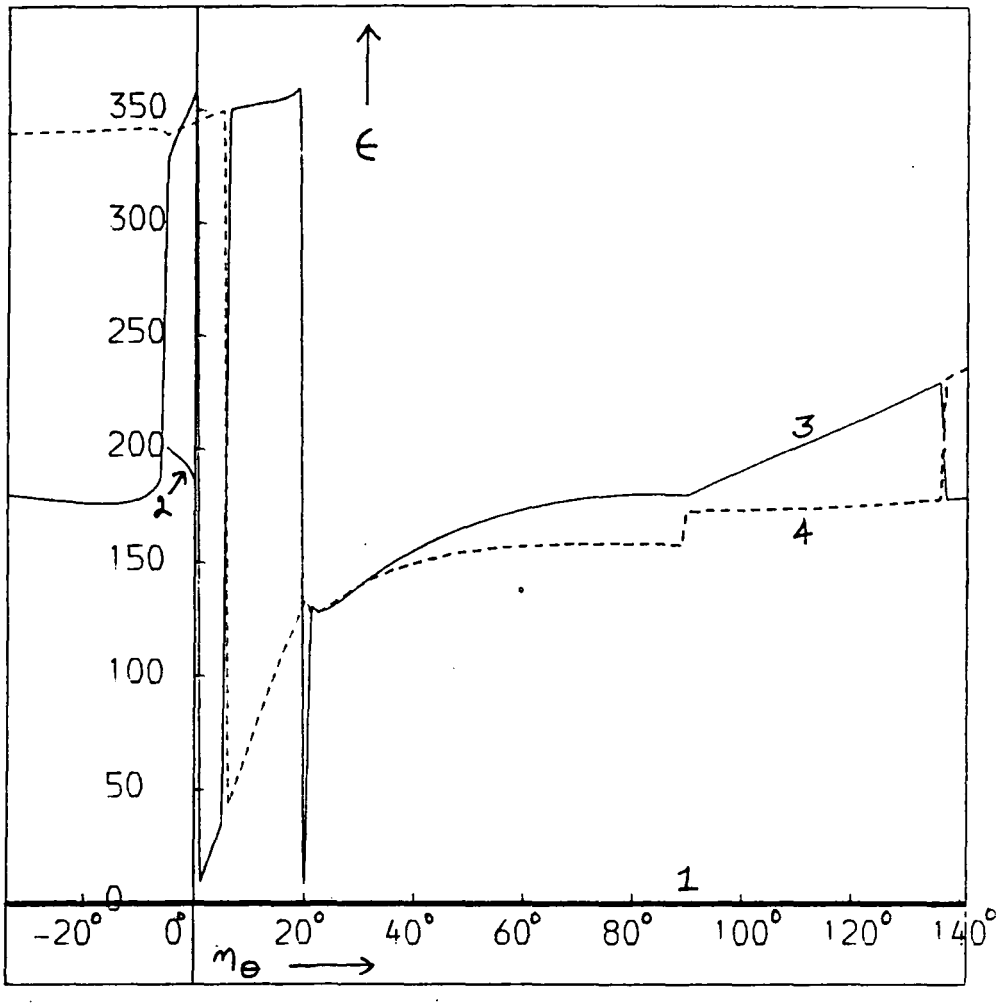

Figure 5.16(b) Same as Figure 5.16(a) except that the reflections are from an insulating boundary. ω= 1.21 units for these waves and $n_\phi = -3.15^\circ$.

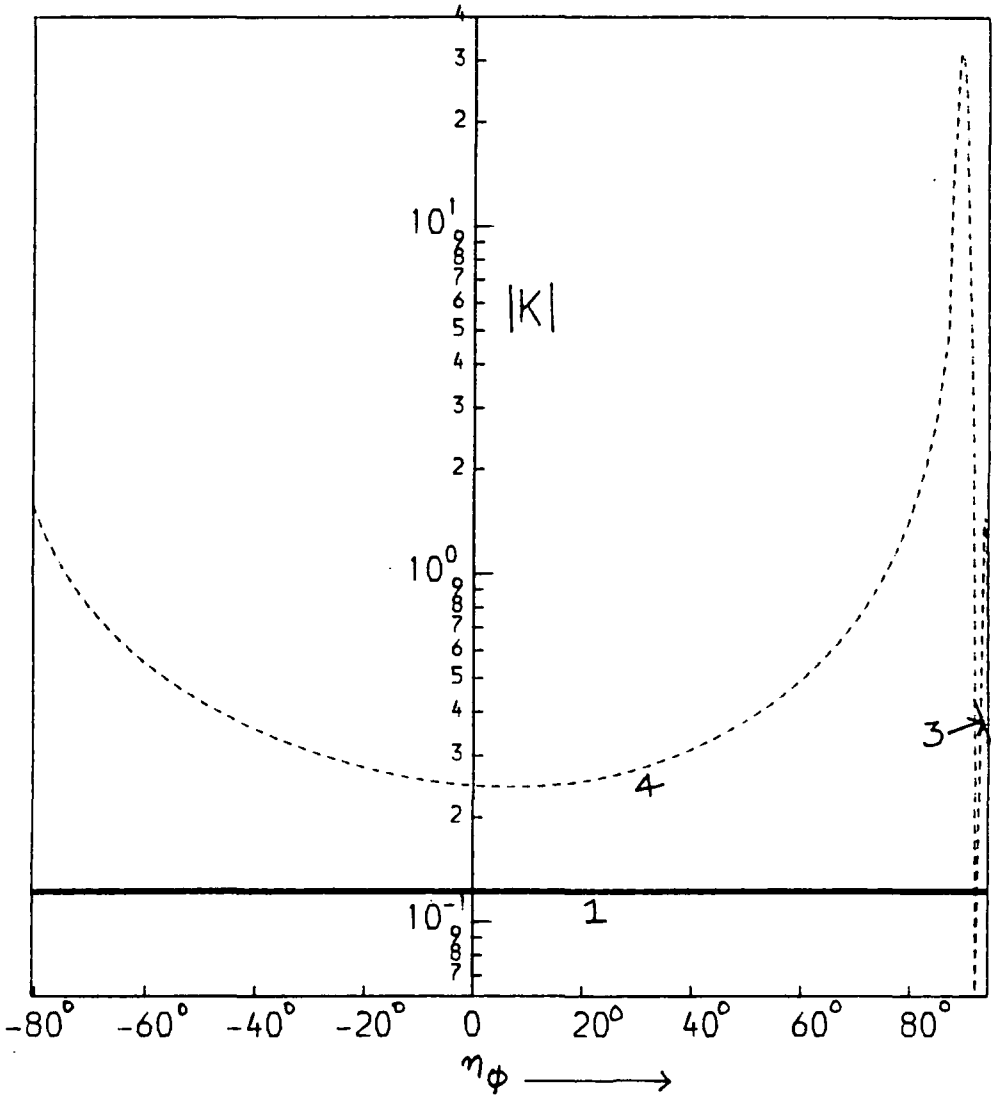

Figure 5.17 The wavenumbers of the incident (magnetic) and reflected(also magnetic) waves as functions of n_ϕ which defines the orientation of the rigid boundary in the x-y plane. ω = 0.012 units for all these waves and $n_\theta = -31.52^\circ$.

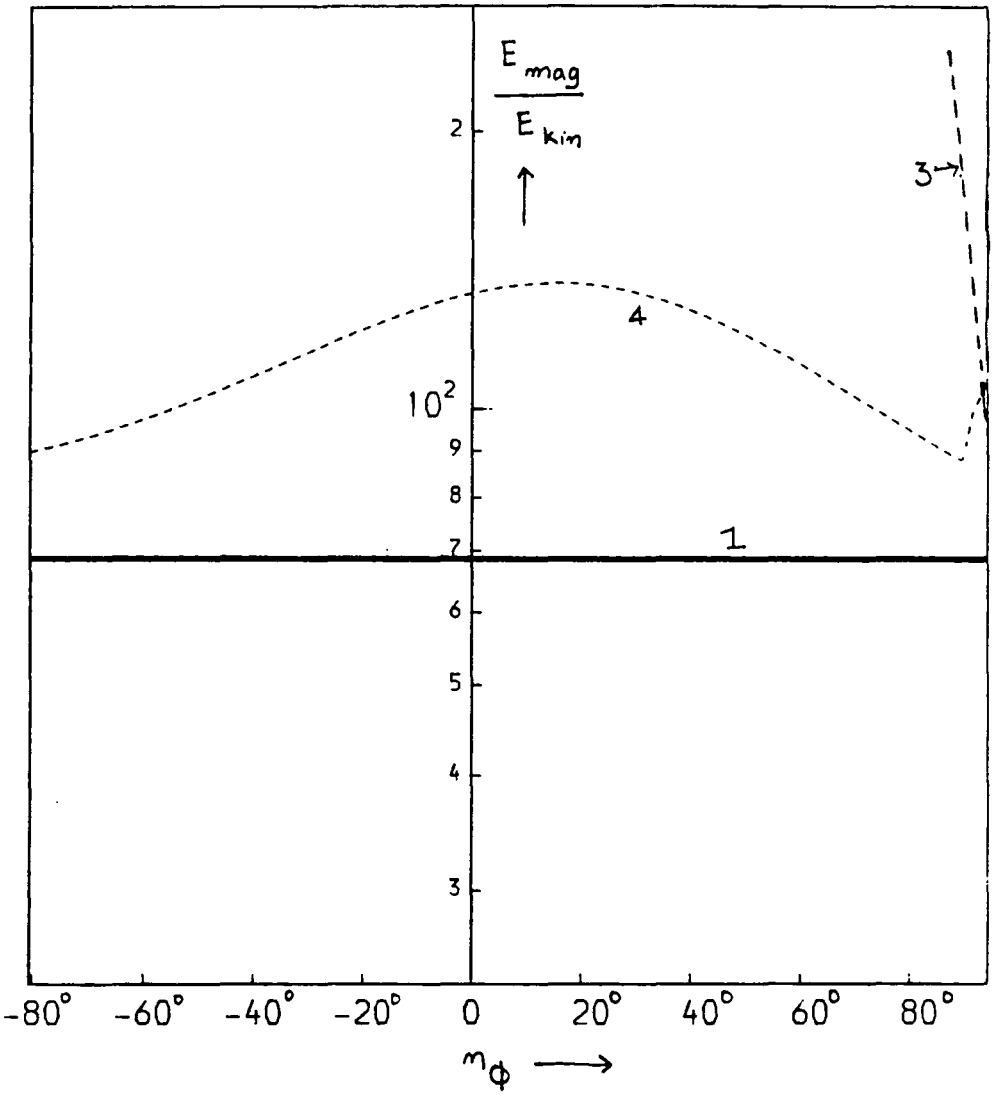

Figure 5.18 The ratio of magnetic to kinetic energy of the incident and refected waves as functions of n_ϕ. ω = 0.012 units for all these waves and n_θ = -31.52°.

modes have most of their energy in the form of associated magnetic field. Such waves will be expected to have very small group velocities as actually evident from Figure 5.19. The normal components of the group velocities of these waves show (Figure 5.20) that except for $n_\phi = 90^\circ$ [at which wave 4 has a pathological dip ($|K_4| \rightarrow \infty$ there)], the reflected waves in general do not emerge parallel to the boundary. The energy densities of the reflected waves [Figures 5.21(a) and (b)] are higher than that of the incident wave, mainly because of the low group velocities of the reflected waves, their wave packets have their lengths compressed along their propagational direction. The flux of energy per unit area of the boundary, is the same for incoming and reflected waves for conducting and insulating boundaries as Figures 5.22(a) and (b) illustrate. Figures 5.23(a) and (b) show the phases ϵ of the incident and reflected waves from conducting and insulating boundaries and are seen to vary between 0 to 2π for reflected waves. A much more interesting picture emerges when we study the reflection of the same incident wave for varying values of the tilts of the boundary (Figure 5.24). We assume boundaries for which $n_\phi = C_{g\phi} = 7.05^\circ$ and $-121.5^\circ < n_\theta < 58.5^\circ$. For $-121.5^\circ < n_\theta < -82^\circ$, two reflected waves are generated both of which turn out to be magnetic. For $-82^\circ < n_\theta < 20^\circ$, only one wave is generated which is a magnetic mode. For $20^\circ < n_\theta < 58.5^\circ$ in addition to the magnetic mode another wave is generated, which is rather hard to classify. For most values of n_θ for which it is present, it has its energy mainly in the magnetic form but in a very narrow region around

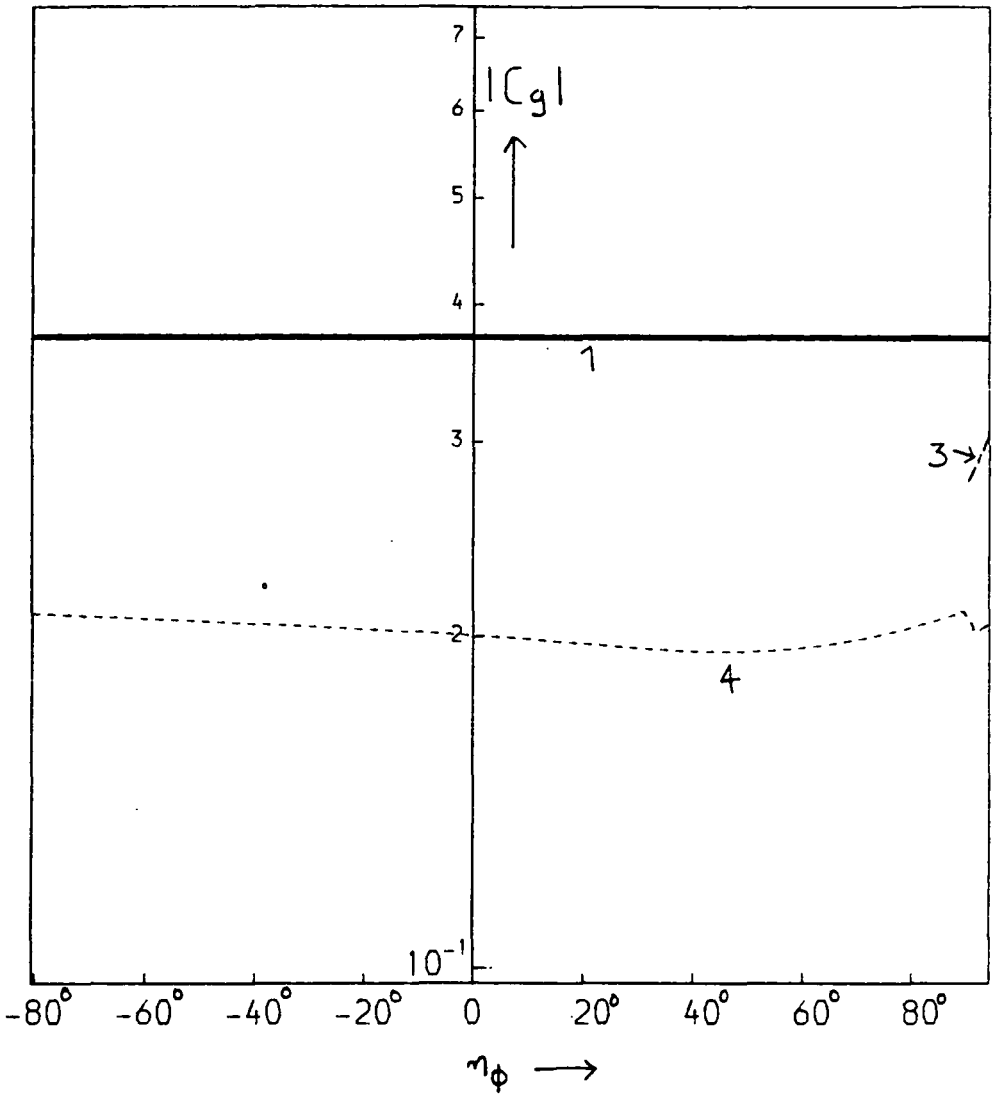

Figure 5.19 The group velocities $|C_g|$ of the incident and reflected waves as functions of n_ϕ. $\omega = 0.012$ units for all these waves and $n_\theta = -31.52^0$.

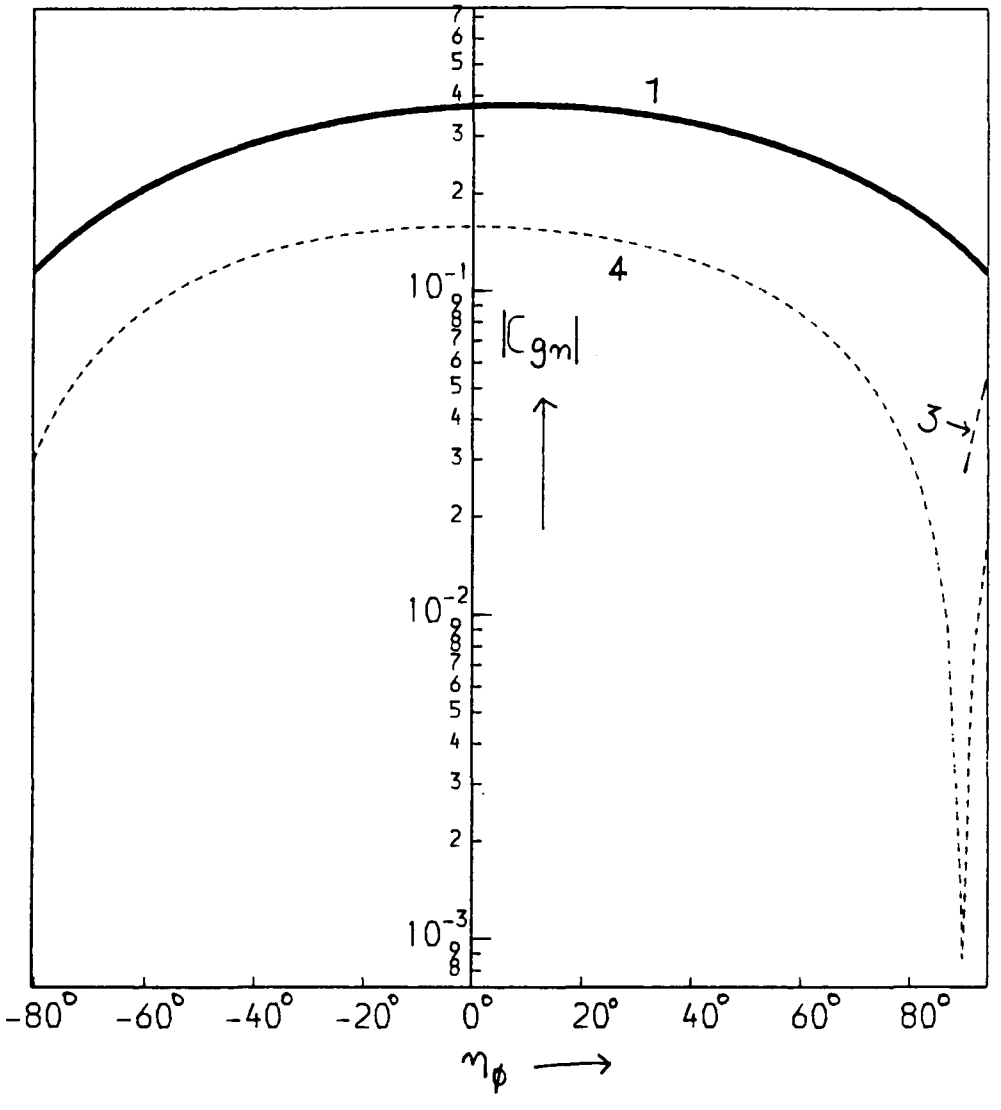

Figure 5.20 The normal components of the group velocities of the incident and reflected waves as functions of n_ϕ. $\omega = 0.012$ units for all these waves and $n_\theta = -31.52°$.

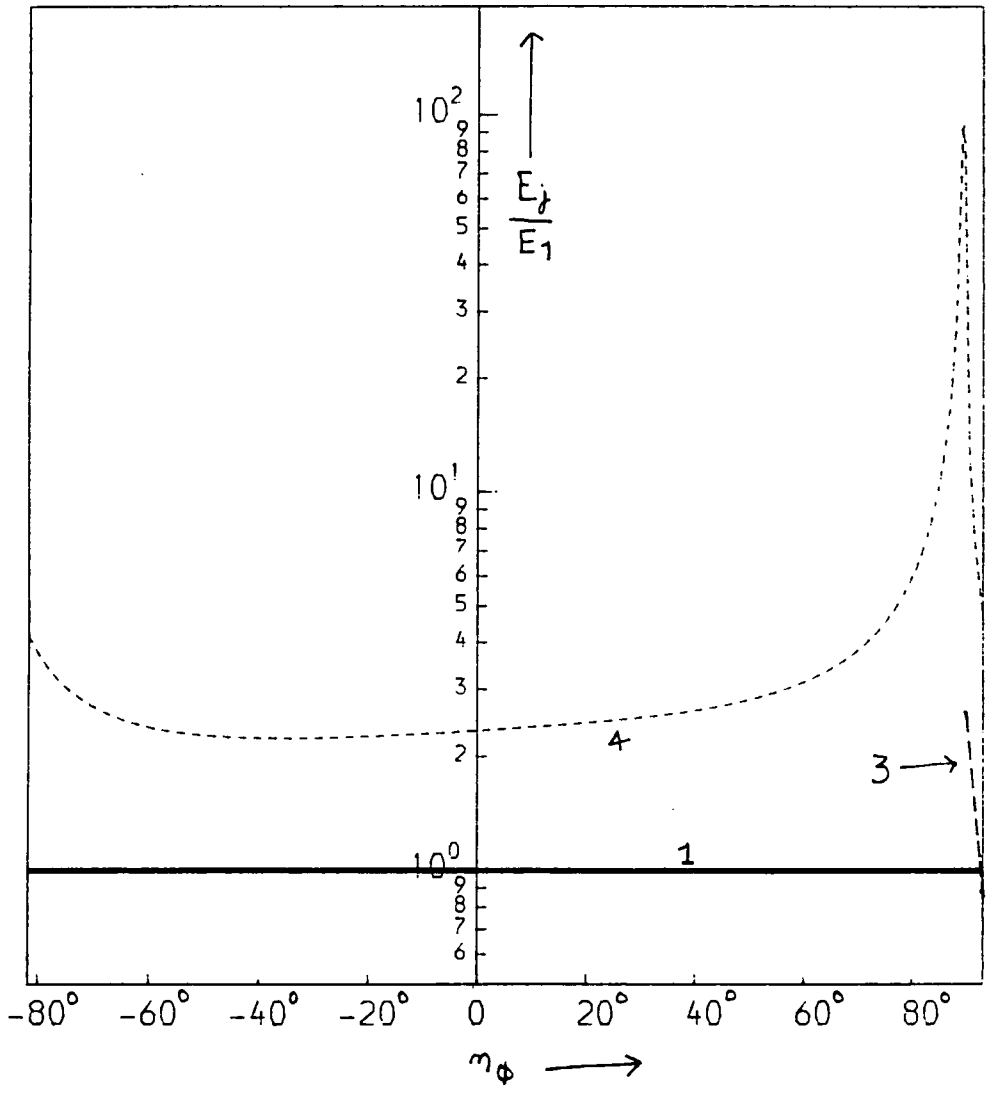

Figure 5.21(a) Normalised energy densities of the incident and reflected waves as functions of n_ϕ for the case of the reflections from conducting boundaries. $\omega = 0.012$ units for all these waves and $n_\theta = -31.52^\circ$.

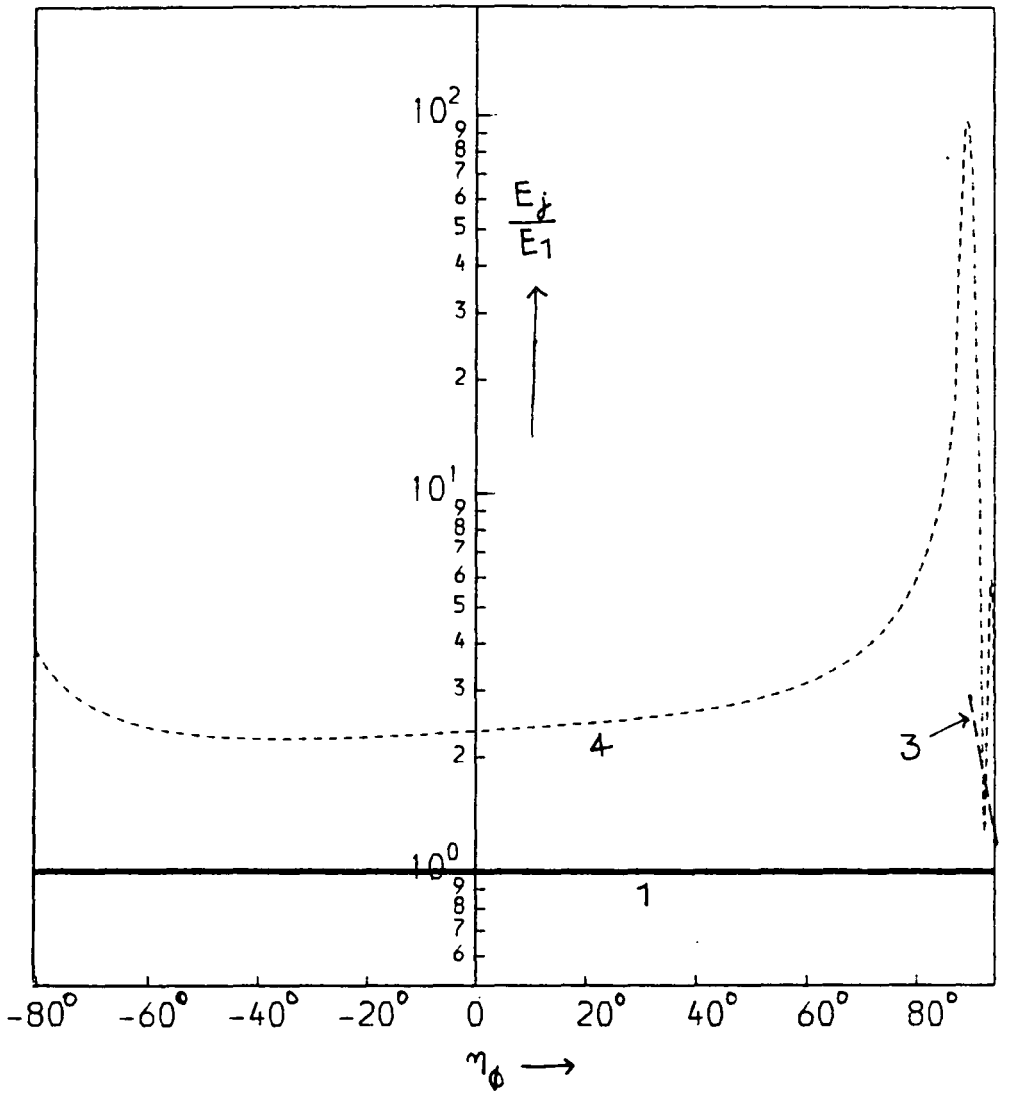

Figure 5.21(b) Same as Figure 5.21(a) except that the reflections are from insulating boundaries. The frequency of all these waves is = 0.012 units and $n_\theta = -31.52^0$.

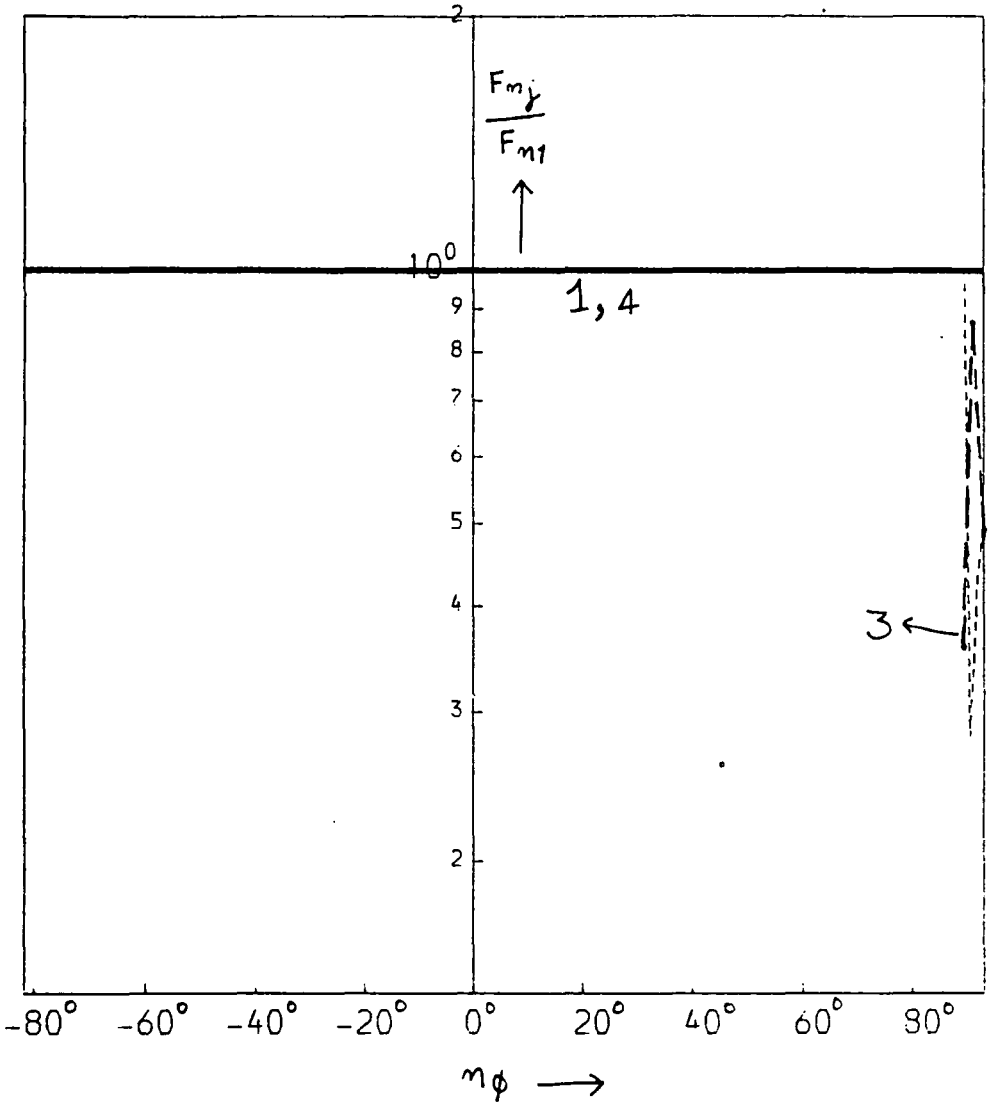

Figure 5.22(a) $|Fn|$, the normal component of the energy flux vetor for the incident and reflected waves as fractions of the incident wave's normal flux plotted for various n_ϕ. The case of reflections from conducting boundaries. ω = 0.012 units for all these waves and $n_\theta = -31.52^\circ$.

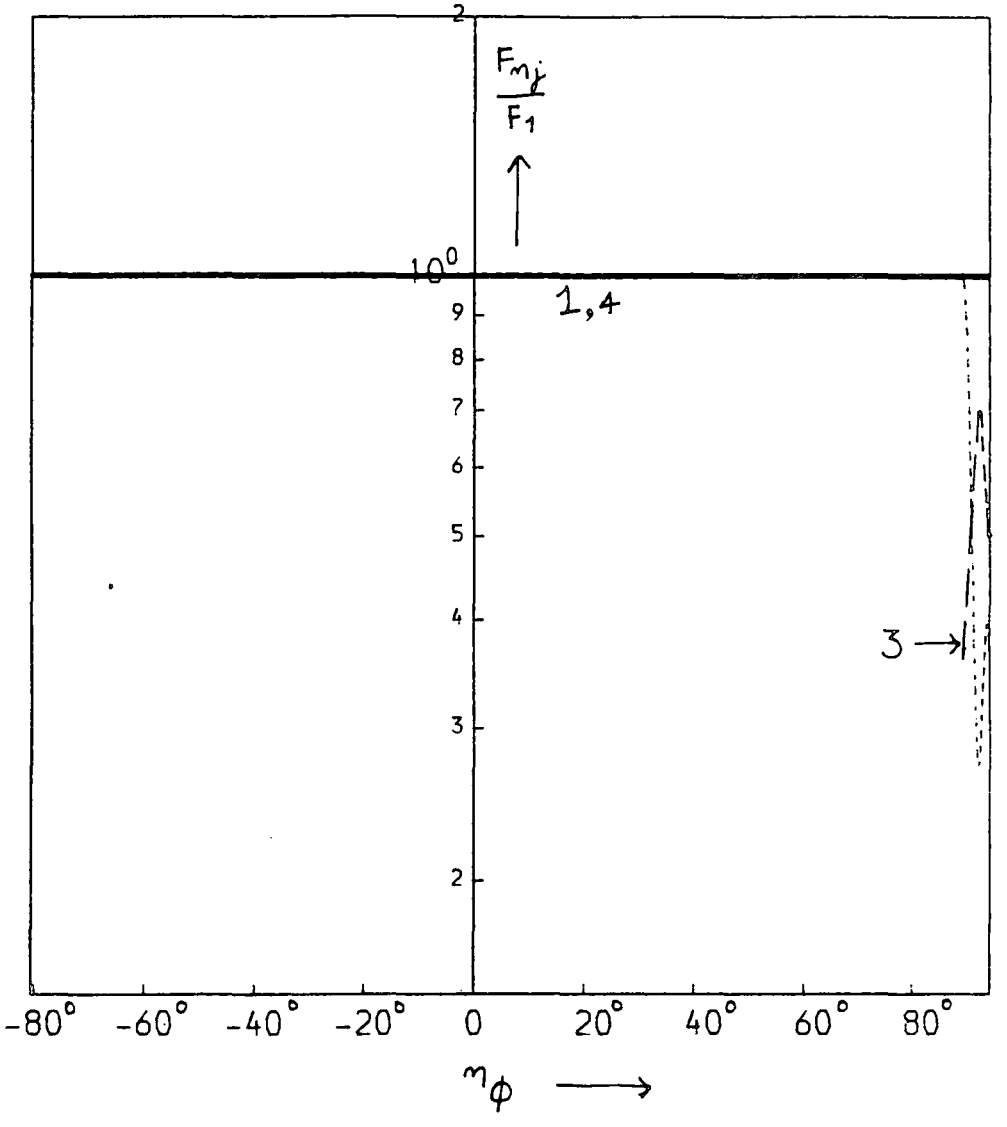

Figure 5.22(b) Same as Figure 5.22(a) except that the reflections are from insulating boundaries. ω = 0.012 units for all these waves and $n_\theta = -31.52^\circ$.

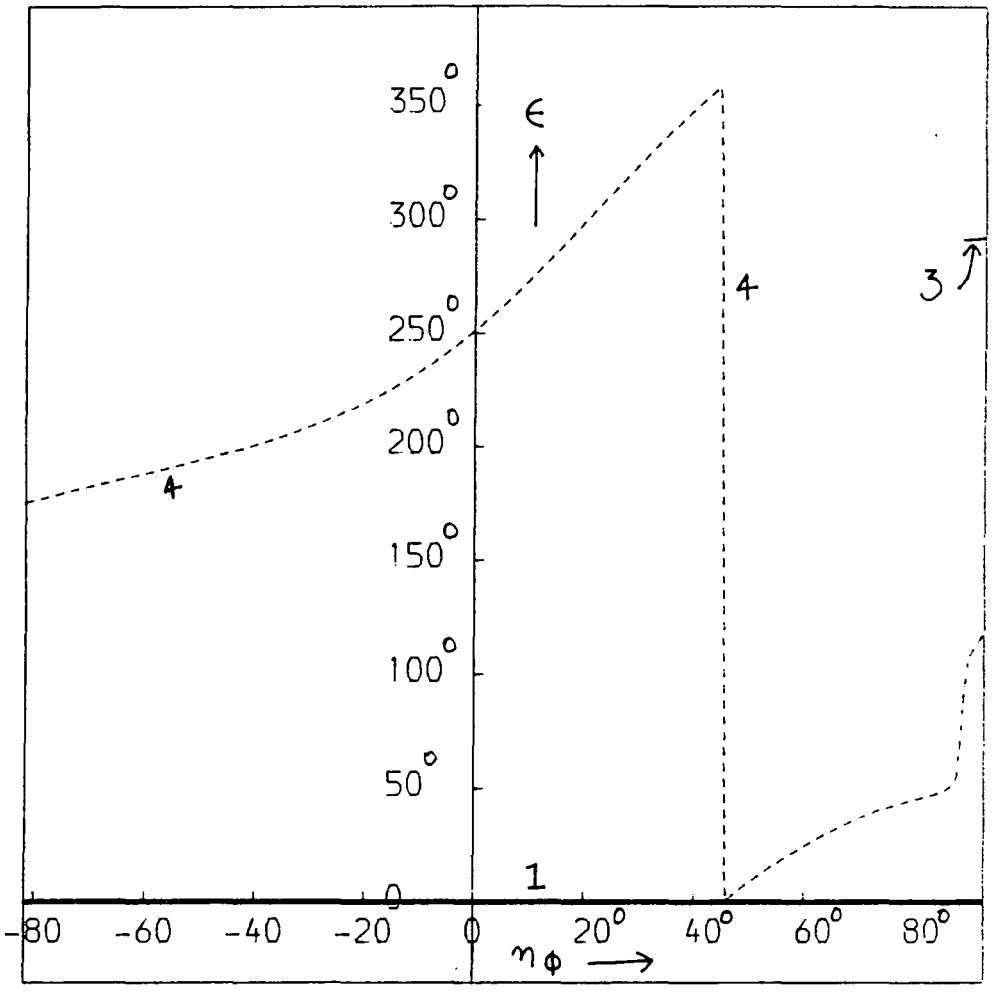

Figure 5.23(a) The phases of incident and reflected waves as function of n_ϕ for reflections from conducting rigid boundaries. ω = 0.012 units for all these waves and $n_\theta = -31.52^\circ$.

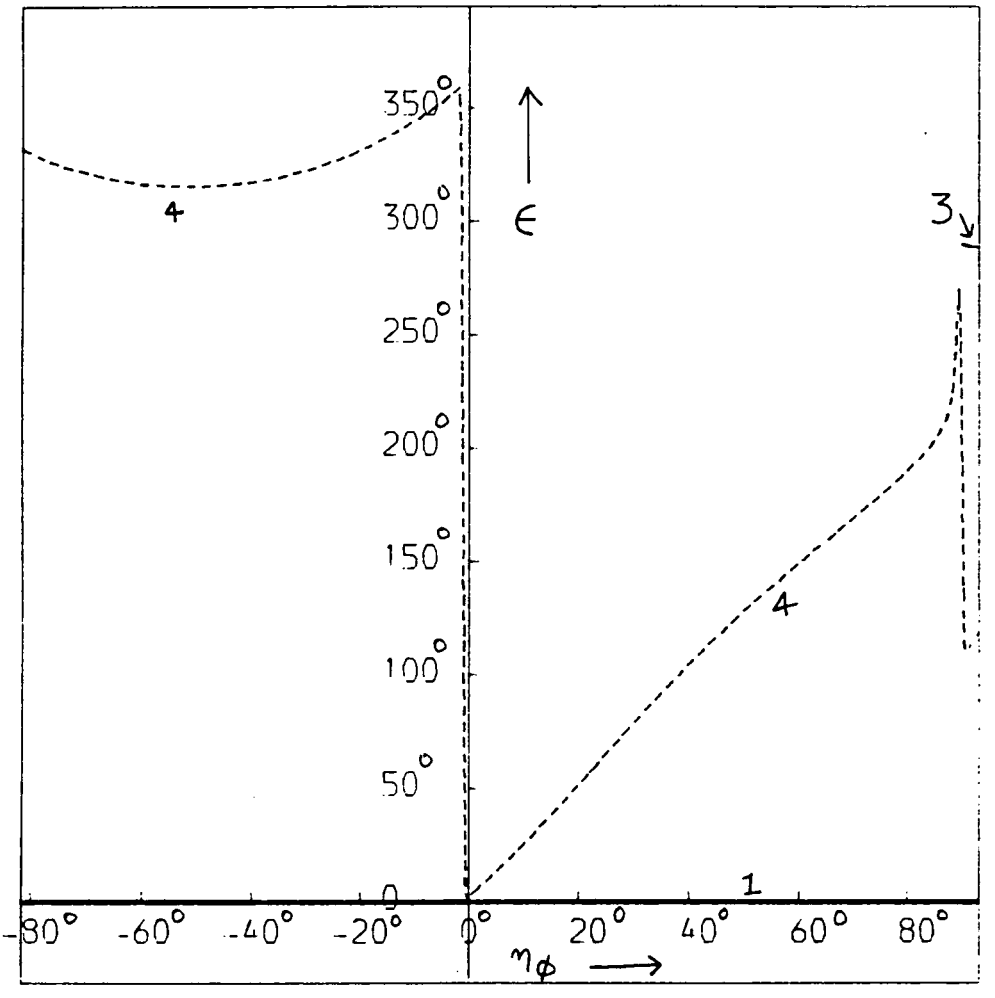

Figure 5.23(b) Same as Figure 5.23(a) except that the reflections are from insulating rigid boundaries. ω = 0.012 units for all these waves and $n_\theta = -31.52^\circ$.

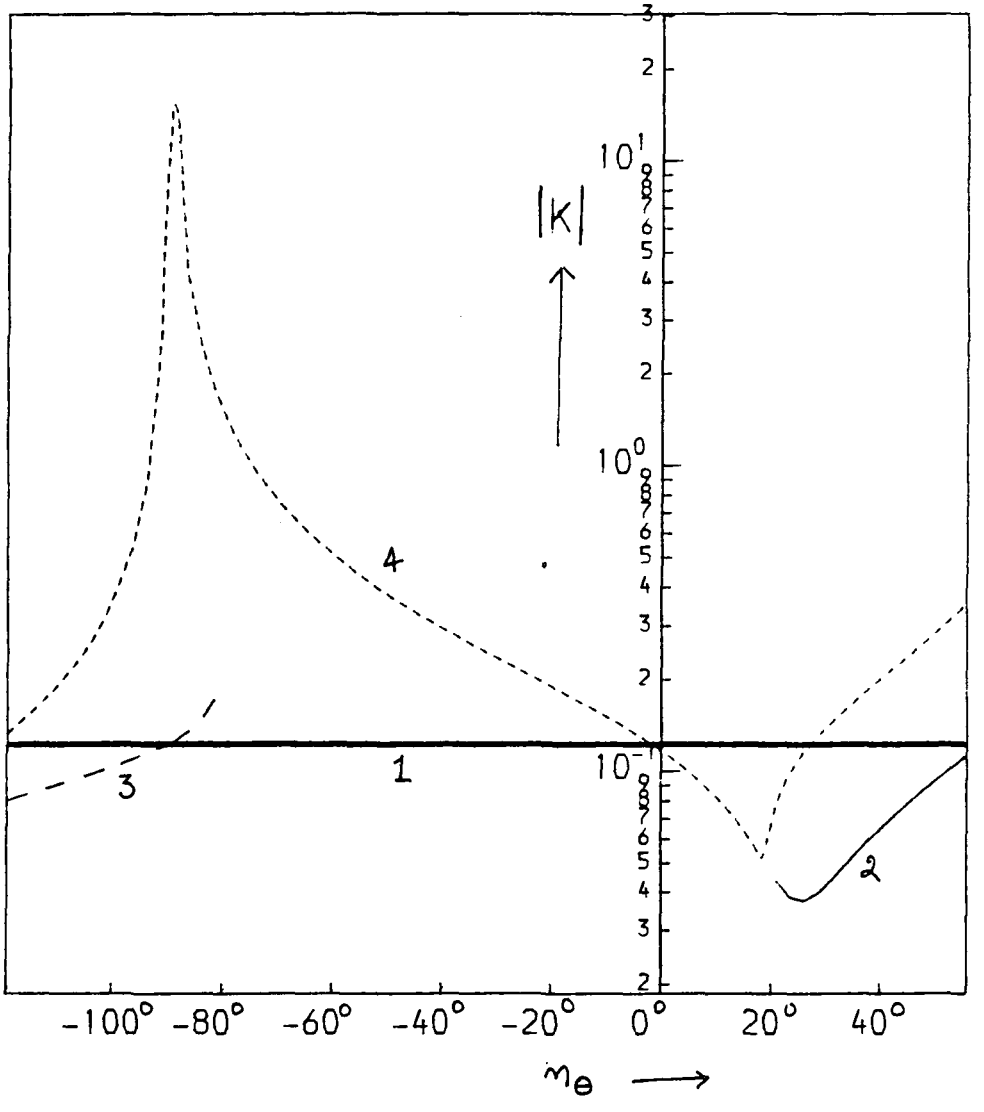

Figure 5.24 The wavenumbers |K| of the incident and reflected waves for various tilts of the boundary. The incident wave is a magnetic IMHD mode. ω = 0.012 units for all these waves and $n_\phi = 7.05^\circ$.

$n \simeq 25^{\circ}$, its energy is predominantly kinetic. Figure 5.25 showing the magnetic/kinetic energy ratios and Figure 5.26 illustrating the group velocities of these modes basically confirm this picture. Except for $n_\theta = 90^{\circ}$ when the wave $\bar{K}_4$ has a steep dip in its normal velocity plot (Figure 5.27); no other reflected waves emerge parallel to the boundary in this case. The energy densities [Figures 5.28(a) and (b)] of the reflected modes K_2 and K_3 are far below that of the incident wave due to their rather large group velocities. Figures 5.29(a) and (b) show that most of the energy of the incident magnetic mode is captured by the outgoing magnetic modes except at $n_\theta \simeq 25^{\circ}$ when the inertial mode captures about 50% of the incoming energy flux, for reflection from conducting boundaries and up to 20% of the energy flux for reflection from insulating boundaries. Figures 5.30 (a) and (b) depict the phases of the reflected waves which once again are very complicated functions of n_θ and n_ϕ.

To sum up, an IMHD wave on reflection splits into 3 reflected waves out of which all three, only two, or only one, wave may be of the propagating kind and the rest may be non-propagating 'leaking' modes which do not share any energy from the incident wave. In general, the wavenumbers, group velocities and energy densities of the reflected waves are different from that of the incident wave though their frequency and the wavenumber component tangential to the boundary are conserved. Most of the energy of an incident wave is captured by a reflected mode which is of the same type as the incident mode. A very important feature of the reflection of IMHD waves by rigid

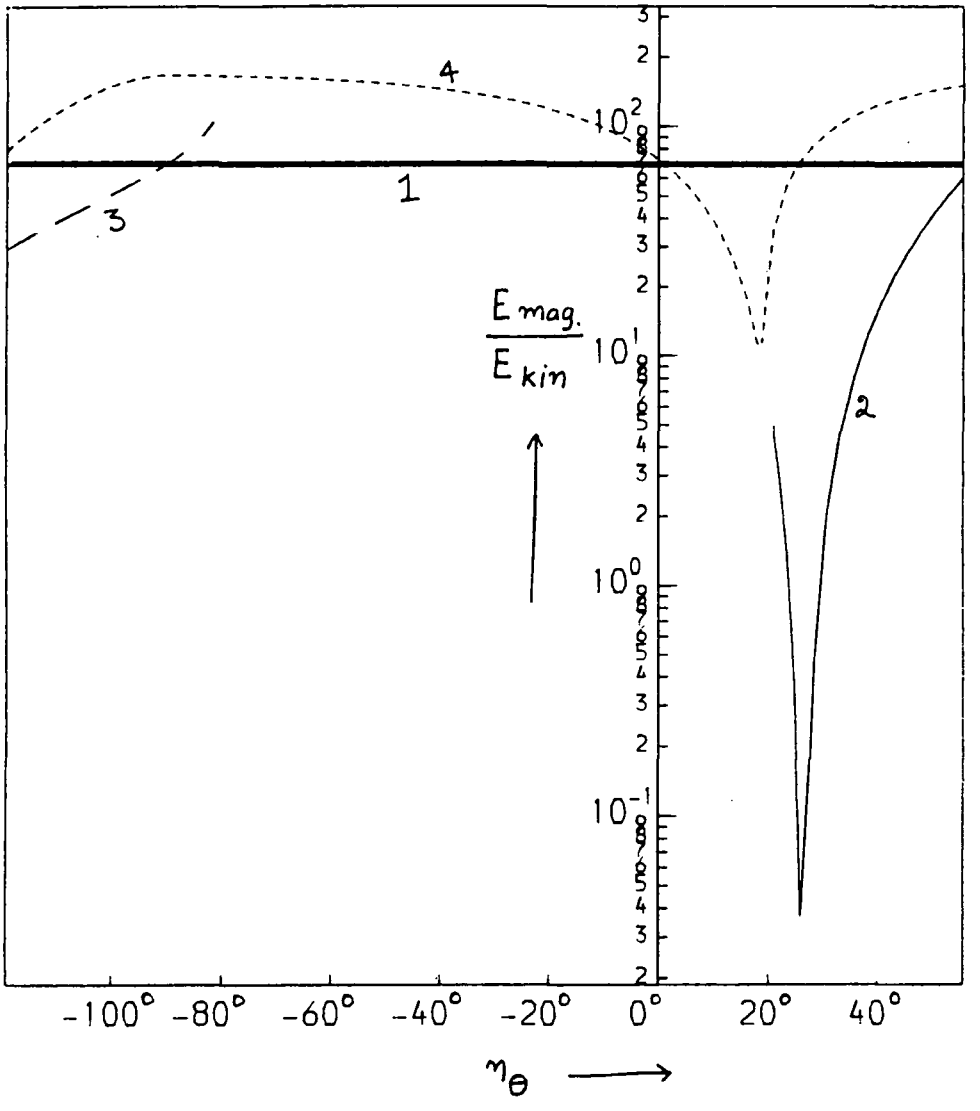

Figure 5.25 The magnetic to kinetic energy ratios of the incident ad reflected waves as functions of n_θ. ω = 0.012 units for all these waves and $n_\phi = 7.05^\circ$.

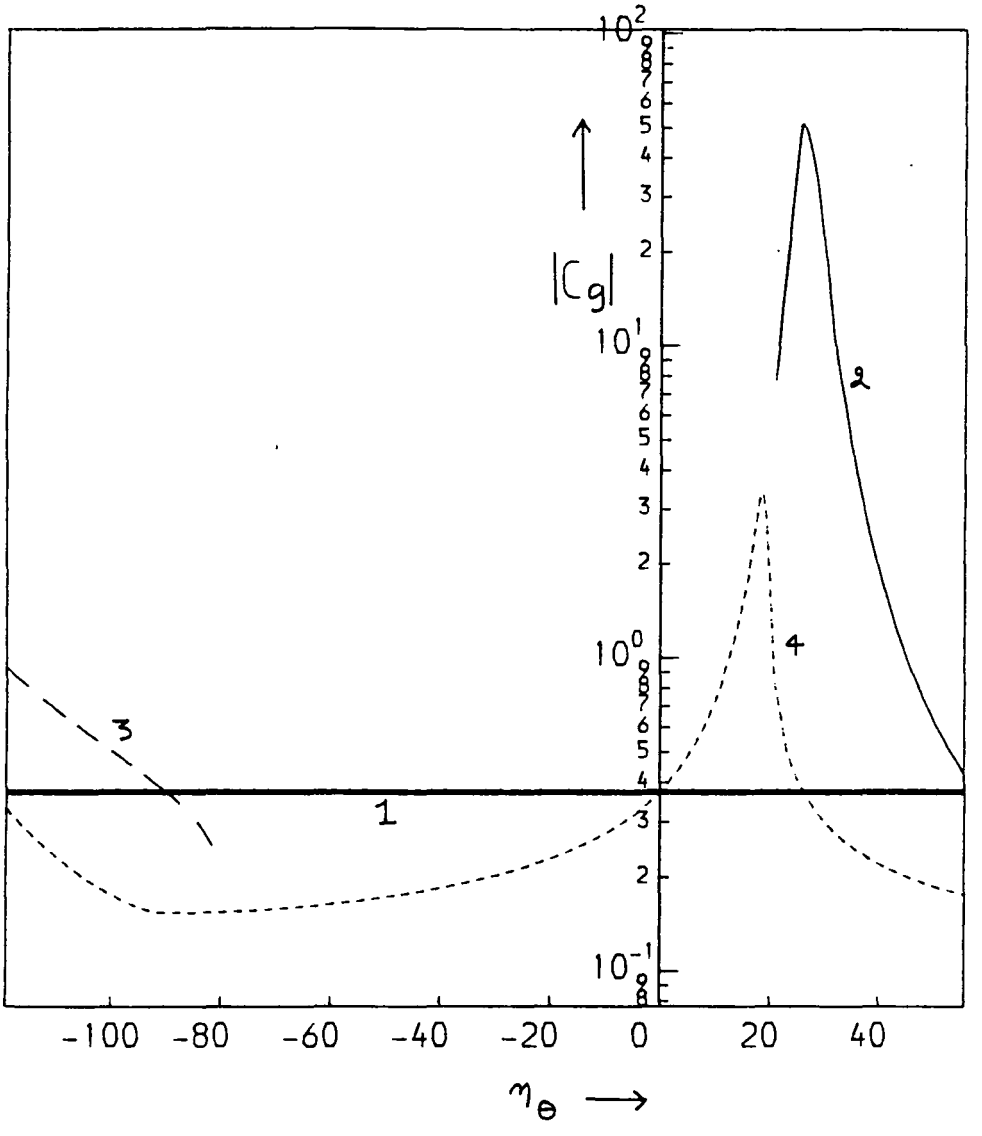

Figure 5.26 The group velocities $|C_g|$ of the incident and reflected waves as functions of n_θ. ω = 0.012 units for all these waves and $n_\phi = 7.05^\circ$.

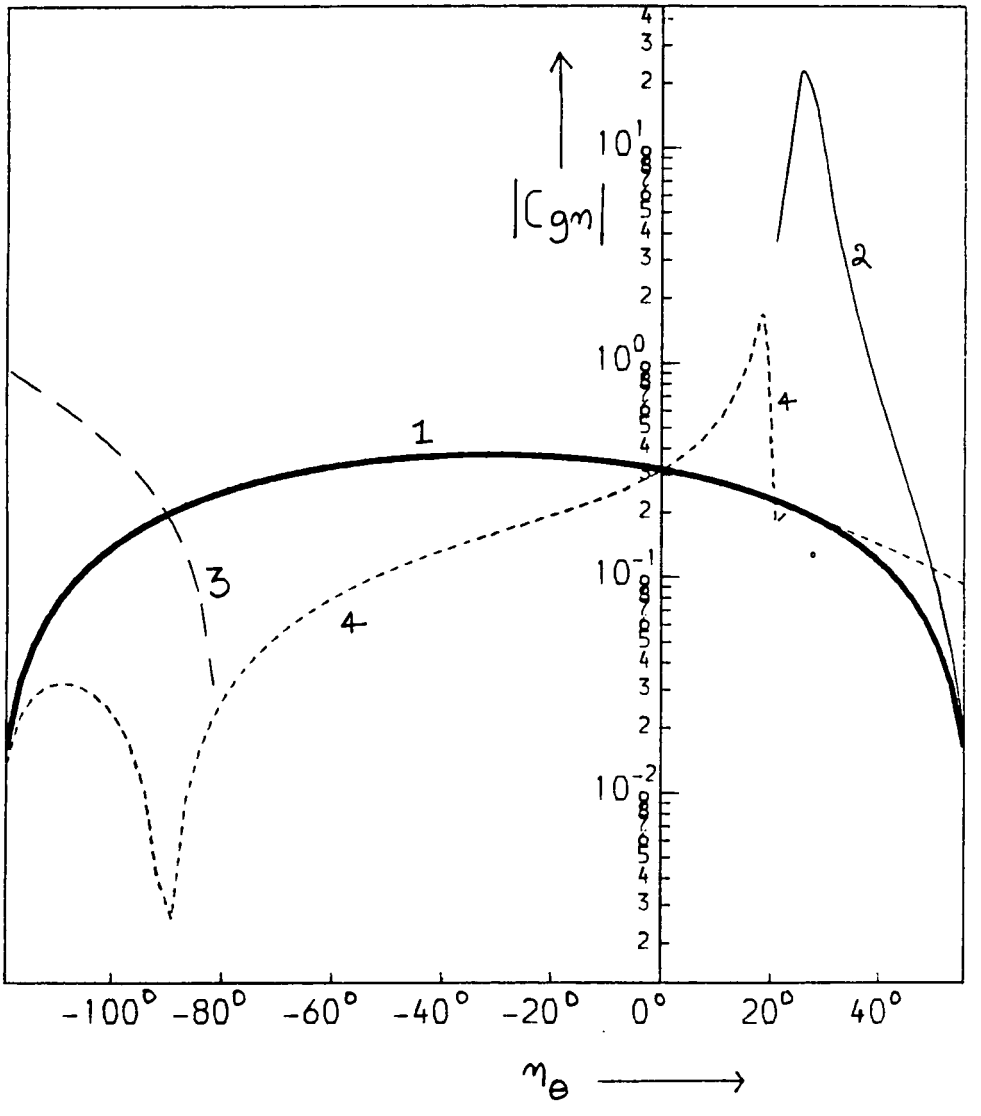

Figure 5.27 The normal component of the group velocities of theincident and reflected wave as functions of n_θ. ω = 0.012 units for all these waves and $n_\phi = 7.05^\circ$.

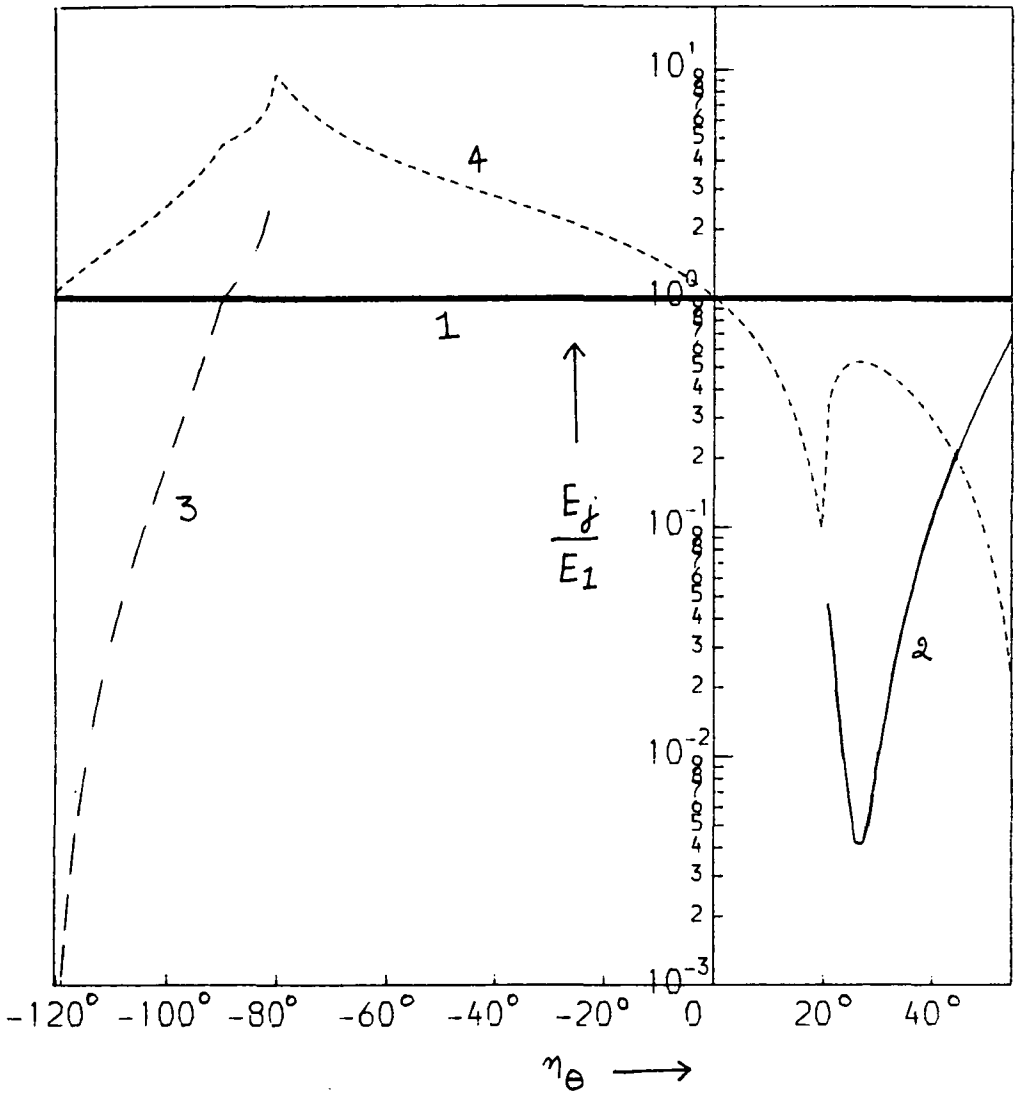

Figure 5.28(a) The normalised energy densities of the incident and reflected waves as functions of n_θ for the case of the reflections from a conducting boundary. ω = 0.012 units for all these waves and $n_\phi = 7.05^\circ$.

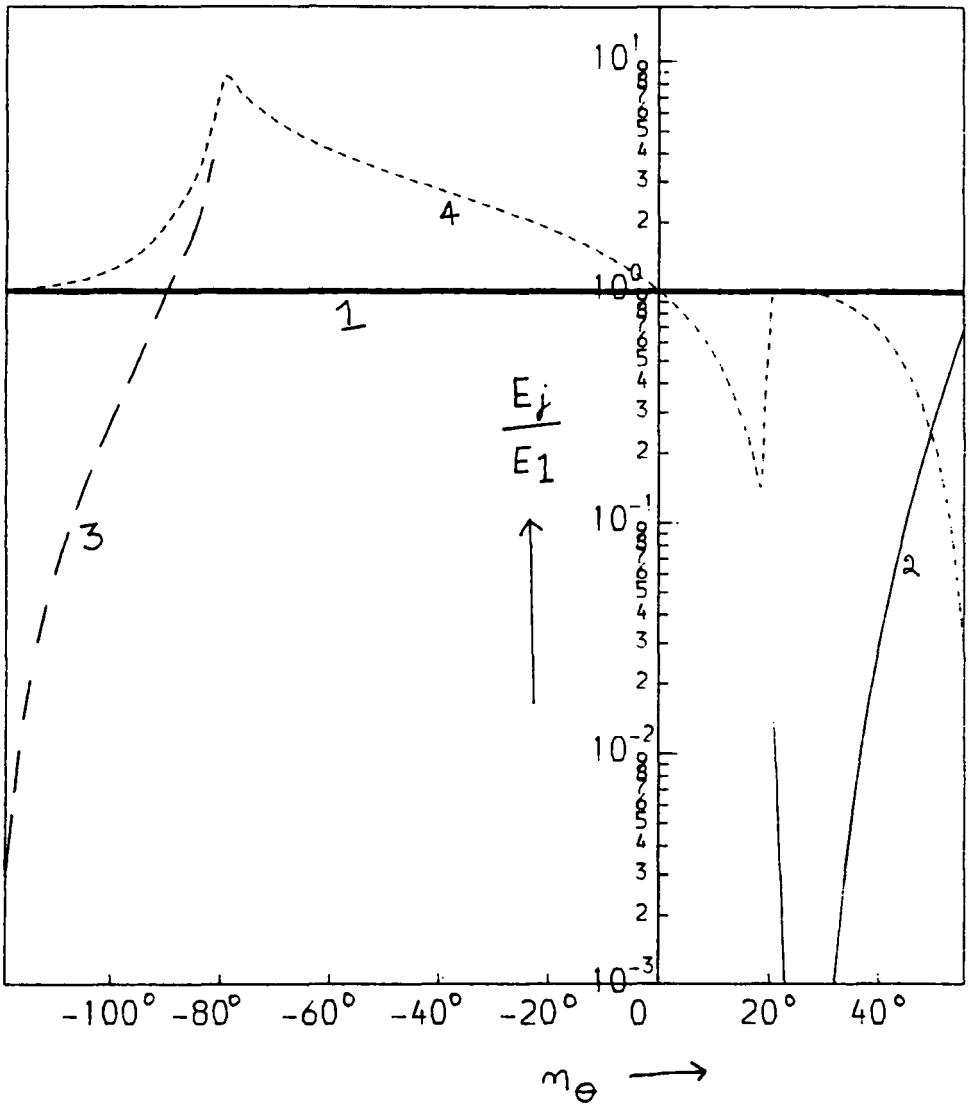

Figure 5.28(b) Same as Figure 5.28(a) except that the reflections take place from an insulating boundary. ω = 0.012 units for all these waves and $n_\phi = 7.05°$.

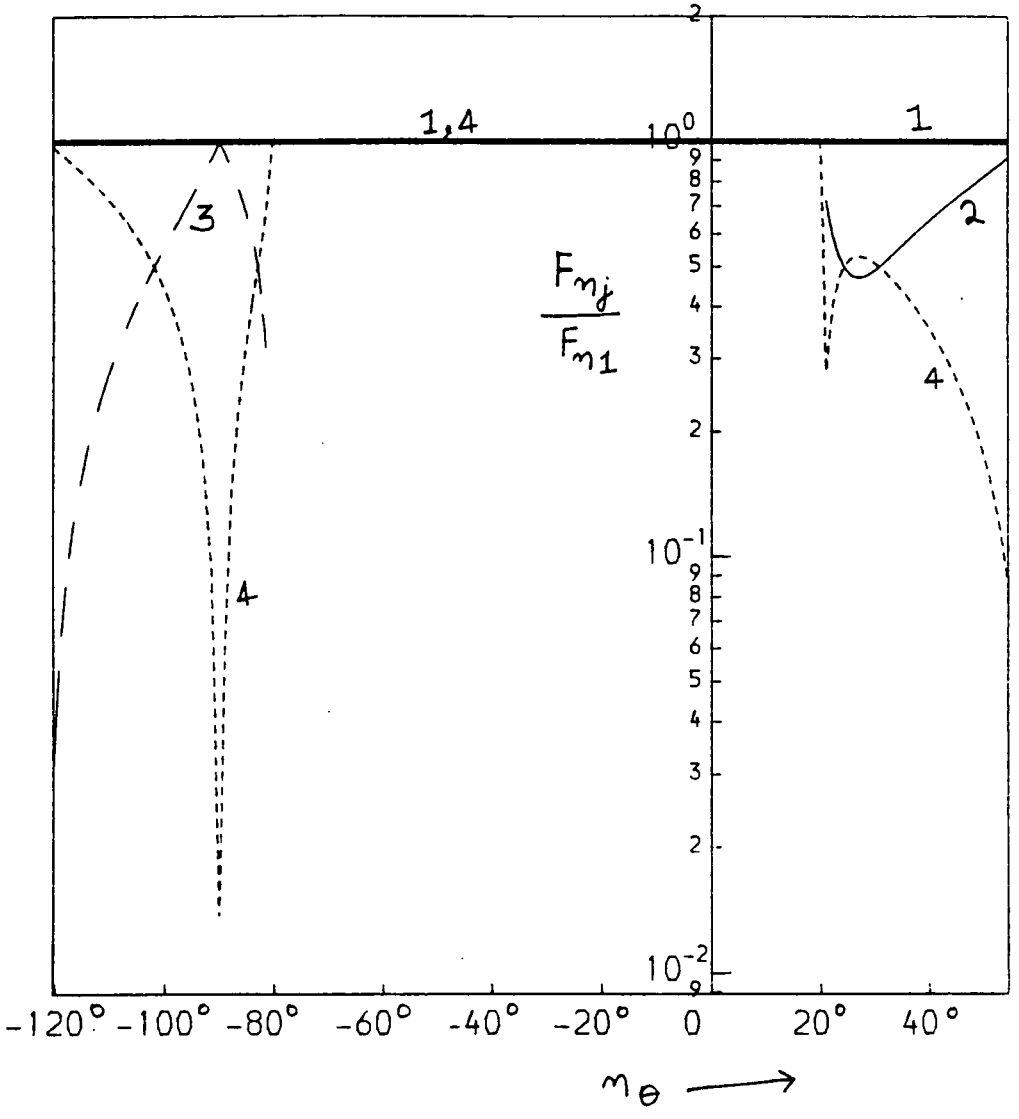

Figure 5.29(a) |Fn| the normal components of the energy flux vectors of the incident and reflected waves as functions of n_θ for the case of reflection from conducting boundaries. Notice that for almost complete range of n_θ shown here, all the energy is captured by magnetic modes. $\omega = 0.012$ units for all these waves and $n_\phi = 7.05^\circ$.

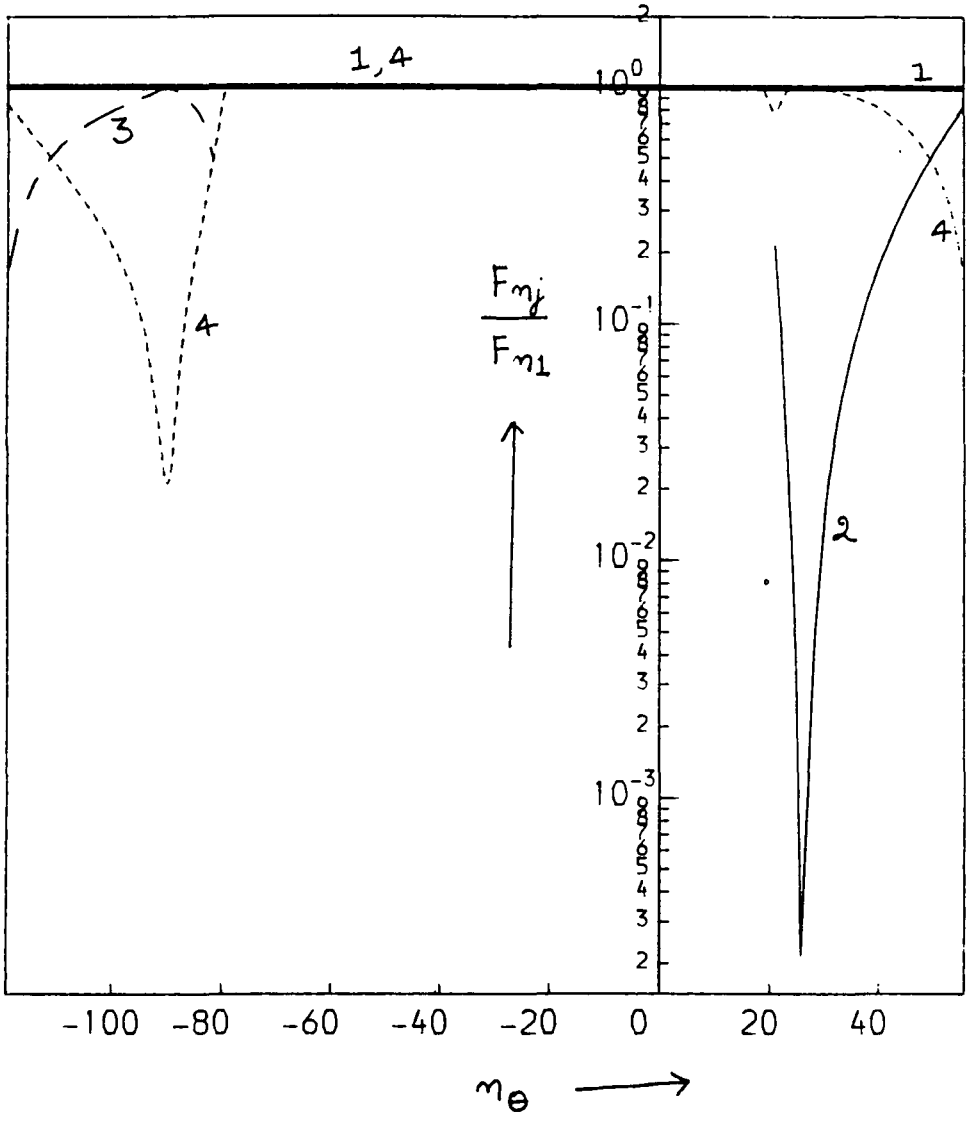

Figure 5.29(b) Same as Figure 5.29(a) except that the reflections take place from insulating boundaries. ω = 0.012 units for all these waves and $n_\phi = 7.05^{\circ}$.

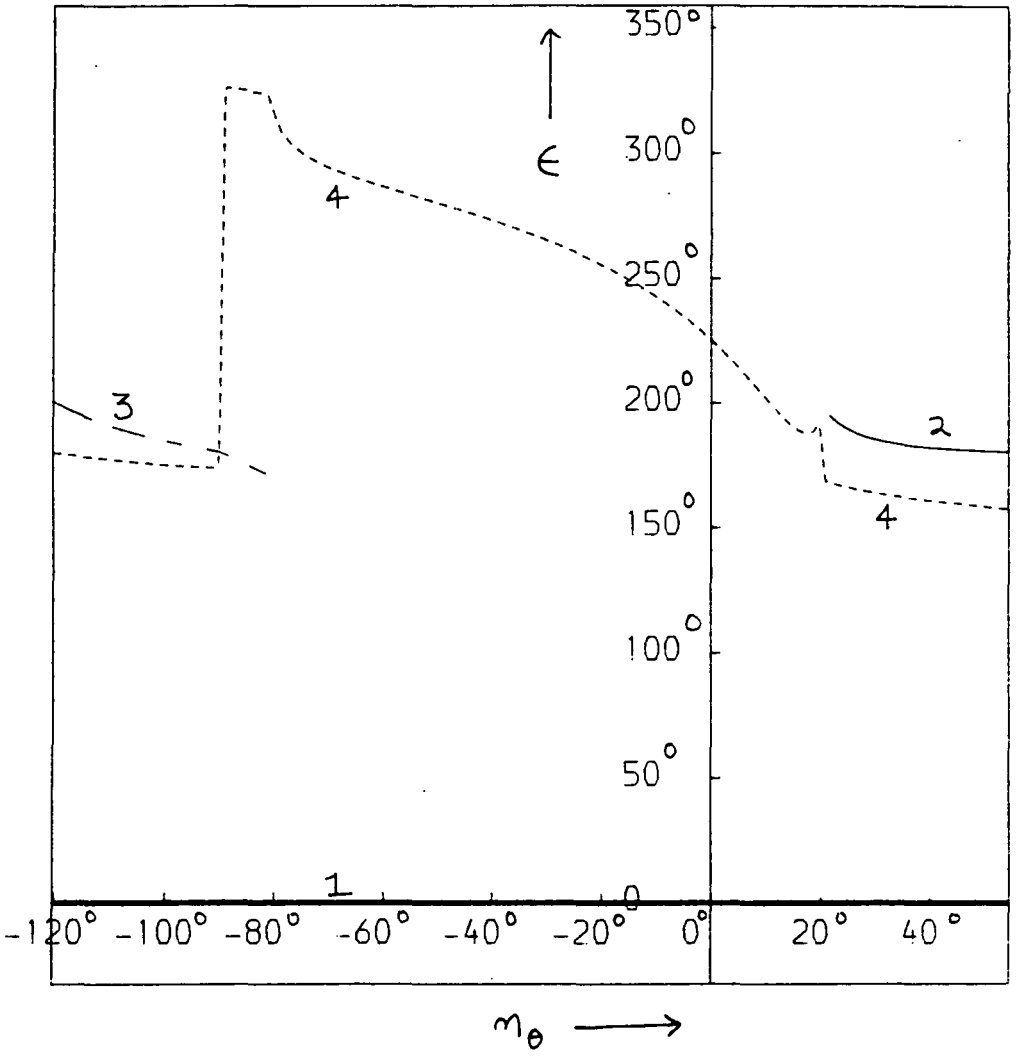

Figure 5.30(a) The phases of the incident and reflected waves as functionsof n_θ for the case of conducting boundary. ω = 0.012 units for allthese waves and $n_\phi = 7.05^\circ$.

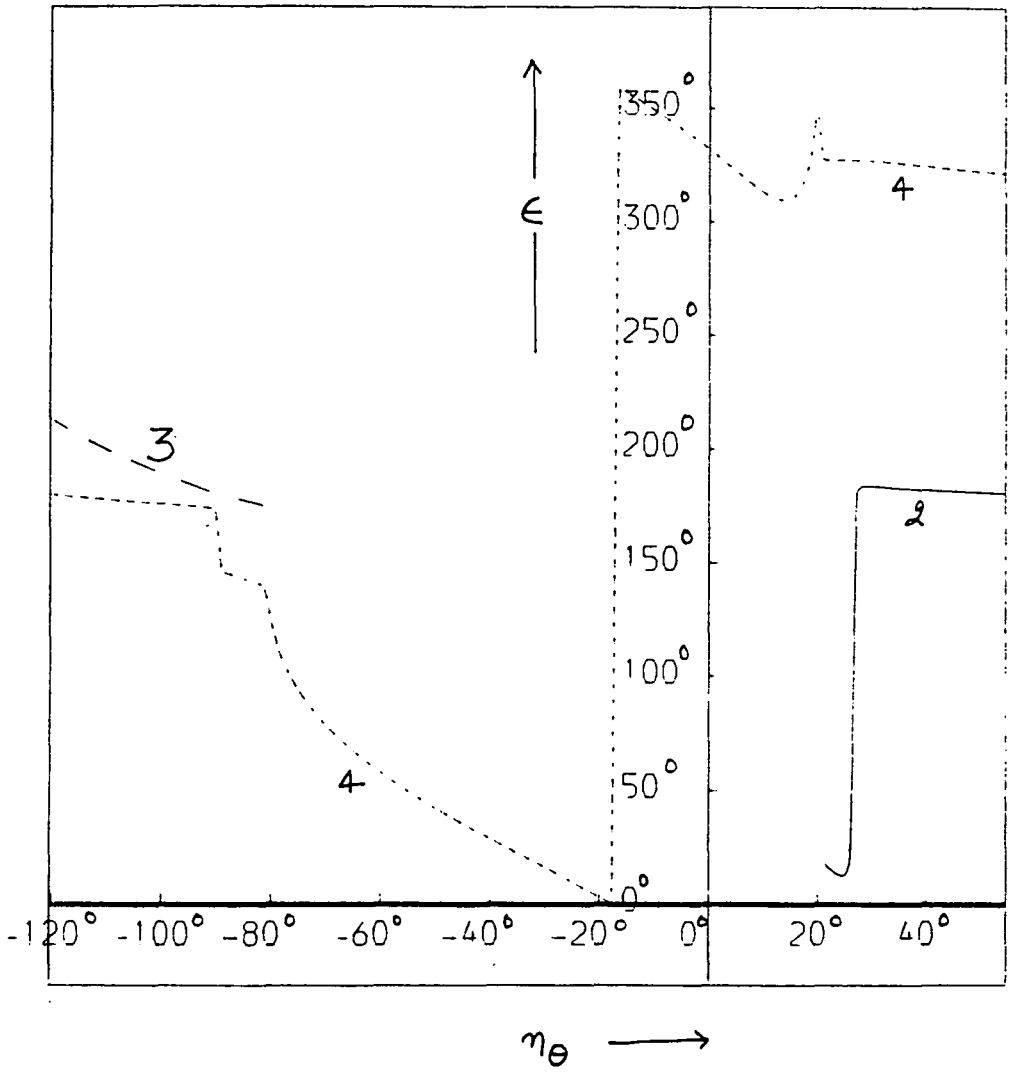

Figure 5.30(b) Same as Figure 6.30(a) except that the incident wave reflects from an insulating boundary. ω = 0.012 units for all these waves and n_ϕ = 7.05°.

boundaries is that even when the incident wave is of the inertial type, one of the reflected waves is always a magnetic mode. On the other hand, when the incident IMHD wave is a magnetic mode, for a very large range of the orientations and tilts of the boundaries only magnetic modes are generated. Thus, in a random superposition of IMHD waves the long term effect of this reluctance of the magnetic modes to share their energies on reflection with inertial modes will be to increase the share of the energy of the magnetic modes at the expense of the inertial modes. However, as our observations are based on the study of a very few waves in idealised conditions (eg. no effort has been made to include the effect of finite conductivity and viscosity of the fluid) what effect such a phenomenon may eventually have on the partitioning of energy between the magnetic and kinetic energy fields of a rotating system, is hard to judge yet.

CHAPTER SIX

SUMMARY AND CONCLUDING REMARKS

6.1 A Summary of the present work

Three studies of the propagation and reflection of magnetohydrodynamic waves in rotating fluids with implications to the dynamics and magnetic fields of the earth's core-like fluid bodies have been presented. The salient features of these studies are summarised as follows.

The asymptotic form of an initial MHD disturbance on the beta-plane is obtained by the method of stationary phase in Chapter 3. It is seen that due to the dispersive nature of these waves the contribution to the disturbance at a point (x,y) at a large time (t) comes from only those waves which have a group velocity given by $\bar{C}_g = (x/t, y/t)$. For magnetic modes of continental to global size this is possible only in roughly a triangular region enclosed by the lines $x = +\sqrt{3}y$, $x = -\sqrt{3}y$, and $x = t\,C_{gm}$, where C_{gm} is the group velocity of the fastest waves in the wave packet. Inside this region at any point two waves contribute dominantly to the waveform whereas outside this region no waves have stationary phases. The wavenumber K_s and l_s which form stationary phases have an inverse relationship; l_s is small when k_s is large and vice-versa. The amplitudes of these planetary size waves diminishes due to dispersion, as t^{-1} inside the triangular region and as $t^{-5/6}$ near the caustics, $x=\pm\sqrt{3}y$. The geometrical spreading factor is very small, being $(x^2-3y^2)^{-1/4}$ for the region where stationary phases are possible and the waves

decay exponentially as Airy's function near the caustics. The perturbations in the vorticity, the velocity and the magnetic field associated with the propagation of an initial symmetric disturbance when studied for $t \simeq 16$ years and $x = 1600$ kms and above, show perturbation wavelengths of several hundred kilometers and waveperiods of several decades when a magnetic field of 50 Oe is assumed.

Some insight into how a magnetic Rossby-MHD wave may transform partially or completely into an inertial mode by reflection is provided by the study of reflection of these waves by rigid boundaries (Chapter 4). The mechanical boundary condition for any flow at rigid boundaries dictates that the normal component of the fluid velocity at the boundary must vanish. For Rossby-MHD waves this condition implies that the frequency and the wavenumber component tangential to the boundary should be preserved for reflected waves. For frequencies larger than a critical frequency ω^*, for each magnetic mode incident on a N-S boundary, three such waves are possible, out of which only two waves possess the appropriate (away from the boundary) group velocities to qualify as reflected waves. When $\omega < \omega^*$ or $l > l^*(\omega)$, a critical wavenumber, one of these reflected waves may become a non-propagating leaking mode, which does not share any energy from the incident wave. To obtain the amplitudes of both of these reflected waves, one more boundary condition is required, which is provided by the continuity of magnetic field across conducting and insulating boundaries. A numerical investigation of the process of reflection of these waves shows

that in general the group velocities, magnetic to kinetic energy ratios, energy densities and the phases of the reflected waves are different from those of incident waves; though the flux of energy through a unit area of the rigid boundary for incident and reflected waves is equal. For waves of planetary dimensions, an eastward propagating magnetic mode (ie. $\beta > 0$) on reflection from such a boundary will be entirely transformed into a long wavelength inertial mode and a large conversion of magnetic energy into kinetic energy will be observed. A reverse process, involving the conversion of kinetic energy into magnetic energy, will take place if an inertial mode is reflected by a N-S boundary. The conductivity of the wall does not determine the wavenumbers or the group velocities of the reflected waves but certainly influences their energy densities and phases. For example an insulating boundary returns more energy in the form of a magnetic mode than a conducting wall does. The conducting boundaries in general produce larger phase shifts between the incident and reflected waves.

The reflection of full three-dimensional inertial-magnetohydrodynamic (IMHD) waves by rigid boundaries in the presence of a magnetic field that is normal to the rotation axis is studied in Chapter 5. The constraint on the normal component of fluid velocity once again specifies that the frequencies and the tangential component $\bar{K}_t$ of the wavenumber should be conserved on reflection. When ω and $\bar{K}_t$ are fixed in the dispersion relation of the waves, a sixth order polynomial in the normal component K_n of the wavenumber results. The six roots of this

polynomial when combined with $\bar{K}_t$, yield six waves that are possible which have the same frequency and the tangential component and satisfy the original dispersion relationship. Out of these waves one of the waves will be the incident wave we started with, and an examination of the normal curves and normal surfaces reveals that two of the other waves have incorrect group velocities (pointing towards the boundary) and therefore cannot exist at the boundary. This leaves us with three reflected waves, out of which at least one will always be of the propagating kind. As there are three unknowns (the amplitudes of the reflected waves, which are complex quantities because the reflected waves suffer phase shifts), we need two more complex equations to evaluate them. These are provided by the constraints on the tangential component of the velocity, and continuity of the magnetic field lines across the boundary. In addition, inside an insulating boundary, the magnetic field is expressible in terms of a potential. Numerical evaluation of these amplitudes for an incident inertial mode and an incident magnetic mode for various orientations of the boundary shows that the wavenumbers, group velocities, magnetic to kinetic energy ratios and energy densities of the incident and reflected waves are, ingeneral, different. The reflection process thus provides an interchange of energy between different wavenumbers and can also transform one type of energy into another. Generally, most of the energy of the incident wave is captured by a reflected mode which is of the same type as the incident mode. A novel result of this analysis is that, even when the incident wave is an inertial mode, one of

the reflected waves is always a magnetic mode. On the other hand when the incident wave is a magnetic mode, for a very large range of the orientations and tilts of the rigid boundary only magnetic modes are generated. Thus in a container of arbitrary shape, in the long term, the reflection process will tend to increase the share of the magnetic modes at the expense of the inertial modes.

6.2 Some Remarks on Chapter 3

It will be noted that though a very detailed analysis of the propagation of Rossby-MHD waves has been made in this chapter, no attempt was made to actually compare the calculated maps of the disturbance with the maps of the geomagnetic secular variation. There are several reasons for this. First of all the beta-plane approximation is valid for wavelengths that are much smaller than the circumference of the earth, whereas the geomagnetic secular variation has most of its energy in the first few spherical harmonics. Secondly, the calculated disturbance is a function of the initial conditions about which no information is available. (Admittedly, this dependence on initial conditions decreases with time, but for the range of time in geomagnetic context, we expect it to affect the final results substantially.) Finally, the procedure of extending the thin shell results to a thick shell model, though perhaps justified, is inexact. All these factors compell us to deduce that the results of the present analysis can only be suggestive of what might be expected in a real situation. Nevertheless, besides shedding valuable light on the propagational behaviour of these waves, this analysis confirms

the finding of Hide, that these waves possess the right wavelengths, time periods and drift velocities to be able to cause the secular variations in the geomagnetic field. This analysis also makes it clear that the group velocity, and not the phase velocity, of these waves should be compared with the westward drift of the geomagnetic field. As a consequence, an ambient magnetic field of only 30 to 50 Oe, will be required to explain the observed drift.

6.3 Some Remarks on Chapter 4

We studied the reflection of Rossby-MHD waves by rigid boundaries on a beta-plane in chapter 4, without in any way suggesting, what could act as a boundary in this system. In oceanography, the edges of the ocean form the natural barrier from which Rossby waves are reflected. In a rotating thin shell, unless there are some large scale protrusions on the boundaries of the container, this will hardly be the case. The situation is somewhat different for a thick rotating shell, like the earth's outer core. In such a system, due to Taylor-Proudman constraint, there is no change in the fluid velocities in the direction of the rotation vector, and the individual vertical filaments are constrained to move as coherent units. The beta-planes for this system will then be parallel to the equatorial plane and the z axis will be in the direction of the rotation vector. The bounding surfaces of this shell can then easily act as reflecting surfaces. The exercise presented in this chapter, therefore, is not just a theoretical curiosity.

6.4 Some Remarks on Chapter 5

An interesting experiment as a sequel to the work in this chapter will be to assume a known superposition of IMHD waves in a large box (in the sense that its dimensions are much larger than the typical wavelengths of the waves), which for simplicity can be a large cube or a rhombohedron and observe the magnetic and kinetic energy contents of the system at various time intervals, as the waves propagate and get multiply reflected from the boundaries of the box. As we are interested in the long term behaviour of the system, we will have to include the effects of the finite viscosity and conductivity of the fluid, as well as the finite conductivity of the reflecting walls. The author's contention is that for certain geometries of the container and some suitable initial conditions, there can be a gradual increase of the magnetic energy of the system at the expense of its kinetic energy.

APPENDIX I

ELECTRODYNAMIC BOUNDARY CONDITIONS AT AN INSULATING RIGID BOUNDING SURFACE OF A CONDUCTING ROTATING FLUID

The 'jump' conditions for u and B at the boundary of a conducting fluid in contact with a rigid surface in the case of $\Omega = 0, \omega = 0$ (ie. no rotation and steady flow) are easily obtained from the theory of Hartmann layer (see for example Roberts, 1967; chapter 6). However when one is dealing with non-steady flows like the wave motions in fast rotating fluids (Hide and Roberts, 1960; Hide, 1969b) Ekman-Hartmann layer theory may need certain modifications to be applicable in this context.

Following Hide (1969b) assume a conducting, rotating fluid in a magnetic field in the z direction bounded by a rigid surface (normal $\bar{n}$) in the x-y plane. Separate $\bar{B}$ and $\bar{u}$ into their interior parts $\bar{B}_i$, $\bar{u}_i$ and their boundary layer parts $\bar{B}_b$, $\bar{u}_b$ such that

$$\bar{B} = \bar{B}_i + \bar{B}_b \qquad \ldots(I.1)$$

$$\bar{u} = \bar{u}_i + \bar{u}_b \qquad \ldots(I.2)$$

The gradients of $\bar{B}.\bar{n}$ and p will be small within the boundary layer so that

$$p_b = \bar{B}_b.\bar{n} = 0 \qquad \ldots(I.3)$$

Hide and Roberts (1960) showed that the variables B_{xb}, B_{yb}, u_b and v_b satisfy a partial differential equation of the form

$$\left[\left(\frac{\partial}{\partial t} - \lambda D^2\right)\left(\frac{\partial}{\partial t} - \nu D^2\right) - V_a^2 D^2\right] \phi_b + f^2 \left(\frac{\partial}{\partial t} - \lambda D^2\right) \phi_b = 0 \qquad \ldots(I.4)$$

where $\lambda = 1/(\sigma\mu)$, σ is the conductivity of the fluid, ν is its viscosity, f is the component of $\bar{\Omega}$ in the z direction and $D = \partial/\partial z$. This equation has solutions of the form

$$\phi_b \propto \hat{\phi} \exp i[\omega t + mz)] \qquad ...(I.5)$$

provided

$$[(i\omega - \lambda m^2)(i\omega - \nu m^2) - V_a{}^2 m^2]^2 + f^2(i\omega - \lambda m^2)^2 = 0 \quad ..(I.6)$$

In our problems of reflection of Rossby-hydromagnetic and IMHD waves we are generally concerned with waves for which $\omega << f$, so that steady solutions are acceptable. Then (I.6) yields

$$m = -(f/\nu)^{1/2}(1+\alpha^2)^{1/4}[\cos\vartheta \mp i \sin\vartheta] \qquad ...(I.7)$$

where $\alpha = V_a{}^2/(f\lambda)$ is a dimensionless parameter measuring the relative importance of the magnetic field to the rotation and $\vartheta = 0.5\cot^{-1}\alpha$. Thus from (I.5) and (I.7)

$$u_b + iv_b = -\tilde{u} \exp[-(1+\alpha^2)^{1/4}(\cos\vartheta + i \sin\vartheta)\xi] \qquad ...(I.8)$$

and $$B_{xb} + i B_{yb} = (-u/\lambda)\ (\nu/f)^{1/2}\ \bar{B}_i.\bar{n}/(1+\alpha^2)^{1/4} *$$
$$\exp-[(1+\alpha^2)^{1/4}(\cos\vartheta + i \sin\vartheta)\xi + i\vartheta] \quad ...(I.9)$$

where $\xi = z/(\nu/f)^{1/2}$

The changes in $\bar{B}_b$ and $\bar{u}_b$ across the boundary layer will represent the jumps in $\bar{B}$ and $\bar{u}$. (I.8) and (I.9) give this jump in $\bar{B}$ in terms of jump in $\bar{u}$ as

$$\langle B_x + iB_y\rangle = \langle u + iv\rangle(\mu\vartheta)^{1/2}\mathrm{sgn}(\bar{B}_i.\bar{n})(\mu\sigma\nu)^{1/2} *$$
$$[H(\alpha) - iK(\alpha)] \qquad ...(I.10)$$

where

$$G(\alpha) = H(\alpha) - iK(\alpha) = \alpha^{1/2}/(1+\alpha^2)^{1/4} \exp[(-i/2)\cot^{-1}\alpha] \quad ...(I.11)$$

In planetary situations $\alpha \gtrsim 1$ for which $1 > G(\alpha) > 0.4$ (see Hide, 1969b; Figure 2) therefore

$$\langle B_x+iB_y\rangle \simeq 0.4 \langle u+iv\rangle(\mu\rho)^{1/2}\mathrm{sgn}(B_i.n)(\mu\sigma\nu)^{1/2} \quad ...(I.12)$$

For the case of the earth's core, taking $\mu = 10^{-6}$ H/m^{-1}, $\rho = 10^4$ Kg/m^{-3} and $\sigma \simeq 3X10^5$ mho/m (Roberts and Soward, 1972) and a viscosity of the order of 10^{-7} m^2/s (Bullard 1949). Thus the R.H.S. of (I.12) is infinitesimal for any reasonable values of $\langle u+iv\rangle$. This will suggest that atleast for the earth's core-mantle interface we can confidently assume that in boundary layer problems the strength of the current sheet is negligible compared to the strength of the vortex sheet there.

APPENDIX II

AMBIGUITY IN THE DEFINITION OF WAVE ENERGY FLUX

For dispersive waves there are two separate methods by which their mean energy fluxes can be calculated. The first one depends on the energy propagation velocity to define the energy flux as the product of the mean energy density E of the wave with its group velocity $\bar{C}_g$. The other relies on an energy flux vector derived from the equations of motion from the first principles. In most cases the two fluxes are equal but for Rossby waves and now we show here for Rossby-MHD waves the two fluxes disagree. This paradox is resolved in this appendix by proving that the disagreement between the two quantities is equal to a non-divergent vector field and occurs because the equations defining the energy flux vector from the first priciples are insensitive to the addition of divergenceless quantities. The implication of this exercise is that while dealing with problems like the reflection of Rossby-MHD waves at a plane boundary the first definition ($\bar{F} = E\ \bar{C}_g$) should be preferred because it will correctly predict the conservation of total energy flux through and from an insulating boundary. We will first calculate the energy flux vector from the equations of motion from the first principles.

For a homogeneous inviscid fluid rotating with angular velocity $\bar{\Omega}$, the equation of motion can be written as

$$\rho(d\bar{u}/dt + 2\bar{\Omega} \times \bar{u}) = -\nabla p + 1/\mu(\nabla \times \bar{B}) \times \bar{B} + \bar{g}\rho \qquad ...(II.1)$$

Let us linearise this equation by writing

$$\bar{u} = \bar{u}$$

$$\bar{B} = \bar{B}_0 + \bar{b}$$

$$p = p_0 + p$$

Where ρ has been assumed constant, as the fluid is homogeneous. Then

$$\rho(\partial\bar{u}/\partial t + 2\bar{\Omega}\times\bar{u}) = -\nabla p + 1/\mu(\nabla\times\bar{B}_0)\times\bar{b} + 1/\mu(\nabla\times\bar{b})\times\bar{B}_0 + [-\nabla p_0 + 1/\mu(\nabla\times\bar{B}_0)\times\bar{B}_0 + \bar{g}\rho] \quad ...(II.2)$$

where squares and products of small perturbation variables have been neglected. Notice that the terms in the square bracket on R.H.S. represent the basic magnetohydrostatic balance and are equal to zero if we assume that the fluid was initially in hydrostatic equilibrium. In addition let us assume that the macroscopic variable $\bar{B}_0$ varies on a length scale D which is very large compered to the length scale d of the variable $\bar{b}$. Then the second term on the R.H.S. of (A2) can also be neglected in comparison with the third. Thus

$$(\partial u/\partial t + 2\bar{\Omega}\times\bar{u}) = -\nabla p + 1/\mu(\nabla\times\bar{b})\times\bar{B}_0 \quad ...(II.3)$$

Multiply (II.3) scalarly with $\bar{u}$.

$$\partial/\partial t(1/2\rho u^2) = -\bar{u}.\nabla p + 1/\mu[(\nabla\times\bar{b})\times\bar{B}_0].\bar{u} \quad ...(II.4)$$

Now the linerarised form of the induction equation for a perfectly conducting fluid is written as

$$\partial b/\partial t = \nabla\times(\bar{u}\times\bar{B}_0) \quad ...(II.5)$$

which when multiplied scalarly with $\bar{b}$ yields

$$\bar{b}\cdot\partial b/\partial t = [(\bar{B}_0\cdot\nabla)\bar{u} - \bar{B}_0(\nabla\cdot\bar{u})]\cdot\bar{b} \qquad \ldots(II.6)$$

where once again terms involving derivatives of $\bar{B}_0$ have been neglected. Add (II.4) and (II.6) to obtain

$$\partial/\partial t[\rho u^2/2 + b^2/(2\mu_0)] = -\bar{u}\cdot\nabla p + 1/\mu[(\bar{B}_0\cdot\nabla)\bar{b} - \bar{B}_0(\nabla\cdot\bar{b})]\cdot\bar{u}$$

$$+ [(\bar{B}_0\cdot\nabla)\bar{u} - \bar{B}_0(\nabla\cdot\bar{u})\cdot\bar{b}$$

$$= -\nabla\cdot[(p+\bar{B}_0\bar{b}/\mu)\bar{u}] + \nabla\cdot[B_0(\bar{b}\cdot\bar{u})/\mu] \ldots(II.7)$$

Now let us focus our attention on the the second quantity on the R.H.S. of (II.7). Let us integrate this quantity over a small

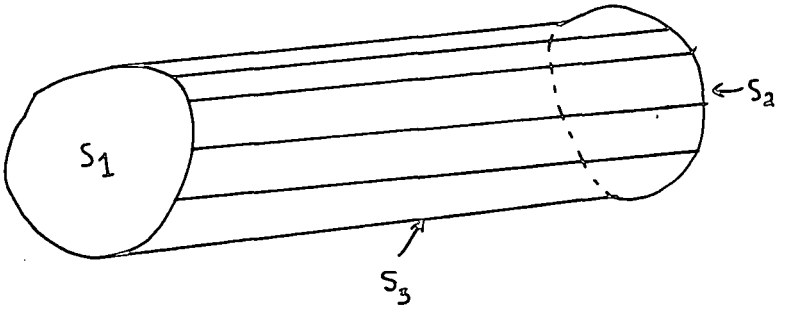

Figure II.1 Showing the geometry of field lines.

volume $\mathcal{V}$, initially undisturbed but whose boundary (S) has now been weakly distorted by waves. The boundary S can be thought to be composed of two parallel planes S1 and S2 which are initially

perpendicular to the lines of force and a simply connected surface S_3 which is initially composed of field lines (Fig. II.1) Thus by divergence theorem

$$\iiint_{\mathcal{V}} \nabla \cdot (\bar{b}.\bar{u}/\mu)\bar{B}_0 d\mathcal{V} = \iint_{S_1} (\bar{b}.\bar{u}/\mu)\bar{B}_0.d\bar{S}_1 + \iint_{S_2} (\bar{b}.\bar{u}/\mu)\bar{B}_0.d\bar{S}_2 + \iint_{S_3} (\bar{b}.\bar{u}/\mu)\bar{B}_0.d\bar{S}_3 \quad \ldots(II.8)$$

where $\bar{S}_1$, $\bar{S}_2$ and $\bar{S}_3$ are the outwards normals of the surfaces S_1, S_2 and S_3. Evidently $\bar{B}_0 \cdot d\bar{S}_2 = - \bar{B}_0.d\bar{S}_1$. Now if we further assume that the distance between S_1 and S_2 is much smaller than the typical wavelength of the disturbance, the quantity $(\bar{b}.\bar{u})\bar{B}_0$ can be assumed to have the same value on S_1 and S_2.

Then

$$\iint_{S_1} (\bar{b}.\bar{u}/\mu)\bar{B}_0.d\bar{S}_1 + \iint_{S_2} (\bar{b}.\bar{u}/\mu)\bar{B}_0.d\bar{S}_2 = 0 \quad \ldots(II.9)$$

and

$$\iiint_{\mathcal{V}} \nabla.(\bar{b}.\bar{u}/\mu)B_0 = \iint_{S_3} (\bar{b}.\bar{u}/\mu)\bar{B}_0.d\bar{S}_3 \quad \ldots(II.10)$$

Now by Alfven's theorem a surface initially composed of field lines will continue to consist of the same field lines. Thus

$(\bar{B}_0 + \bar{b}).d\bar{S}_3 = 0$ or $\bar{B}_0.d\bar{S}_3 = -\bar{b}.d\bar{S}_3$.

Thus $\iiint_{\mathcal{V}} \nabla.(\bar{b}.\bar{u}/\mu)\bar{B}_0 d\mathcal{V} = -1/\mu \iint_{S_3} (\bar{b}.\bar{u})\bar{b}.d\bar{S}_3$

Also integrate other terms of (II.7)to obtain

$$\iiint_{\mathcal{V}} \partial/\partial t[1/2\, \rho u^2 + b^2/2\mu]d\mathcal{V} = -\iint_{S}(p + \bar{B}_0\bar{b}/\mu)\bar{u}.d\bar{s} \quad \ldots(II.11)$$

where the quantity

$$\left| \iint_{S_3} (\bar{b}.\bar{u})\bar{b}.d\bar{S}_3 \right| << \left| \iint_{S} (\bar{B}_0.\bar{b})\bar{u}.d\bar{S} \right|$$

and is neglected. Thus (II.12), can be written as

$$\partial/\partial t \iiint_{\mathcal{V}} E d\mathcal{V} = \bar{F}' d\bar{S} \qquad \ldots(II.12)$$

where $E = 1/2\rho u^2 + b^2/2\mu_0$ is the total energy density per unit volume and

$$\bar{F}' = (p + B_0 b/\mu)\bar{u} \qquad \ldots(II.13)$$

can be defined as the energy flux vector. By the help of divergence theorem (II.12) can be written as

$$\partial/\partial t [\iiint_{\mathcal{V}} E \, d\mathcal{V}] = - \iiint_{\mathcal{V}} \nabla . \bar{F}' d$$

which can be integrated over $\mathcal{V}$ to yield

$$\partial/\partial t (E) + \nabla . \bar{F}' = 0 \qquad \ldots(II.14)$$

For any general system energy is propagated at group velocity (see eg Lighthill 1965, 1978 or Whitham 1974) and energy conservation considerations give us another definition of the energy flux vector:

$$\bar{F} = \langle E \rangle \bar{C}_g$$

where $\langle E \rangle$ is the average energy density of the wave and $\bar{C}_g$ its group velocity.

Now we will first show that $F \neq F'$ for the case of Rossby-hydromagnetic waves and that $F'' = F - \bar{F}'$ is a divergenceless quantity which we need to add to F' to bring the two forms of flux vector to the same value. The difference arises from the fact that any divergenceless quantity can be added to the R.H.S. of (II.13) with impunity, without affecting the equation.

Now for the sake of simplicifation we assume that $\bar{B}_0$ = (B,0,0), so that

$$\langle E \rangle = 1/4 \left[\frac{\omega^2 + V_a^2 k^2}{\omega^2 (k^2+l^2)} \right] \rho A^2 \qquad \ldots(II.15)$$

(See 4.34 which gives this result in non-dimensionalised form.) where A is the amplitude of the vorticity associated with this wave, which is assumed to be constant for neighbouring waves. And from (4.30) and (4.31)

$$C_{gx} = \frac{1}{2\omega + \frac{\beta k}{k^2+l^2}} \left[2 V_a^2 k + \beta\omega \frac{k^2 - l^2}{(k^2+l^2)^2} \right] \qquad \ldots(II.16)$$

$$C_{gy} = \frac{1}{2\omega + \frac{\beta k}{k^2+l^2}} \left[\beta\omega \frac{2kl}{(k^2+l^2)^2} \right] \qquad \ldots(II.17)$$

But $2\omega + \beta k/(k^2+l^2) = \omega + [\omega^2 + \beta k\omega/(k^2+l^2)]/\omega$

$$= \omega + V_a{}^2 k^2/\omega = (\omega^2 + V_a{}^2 k^2)/\omega$$

so that

$$F_x = \left[\frac{2 V_a^2 k}{(k^2+l^2)} + \beta\omega \frac{k^2 - l^2}{(k^2+l^2)^3} \right] \frac{A^2 \rho}{4\omega}$$

and $$F_y = \left[\beta\omega \frac{2kl}{(k^2+l^2)^3} \right] \frac{A^2 \rho}{4\omega}$$

Now $F'_x = \langle \tilde{u} \tilde{p} \rangle + \langle \tilde{u} \bar{B}_0 \tilde{b}_x / \mu \rangle$

where $p = \rho/(k^2+l^2)\ [i\omega l/k - f]\ A \exp[i(kx+ly-\omega t)]$

From the linearised form of (1.47) and (1.65)

$$u = il/(k^2+l^2)\ A \exp[i(kx+ly-\omega t)]$$

$$v = -ik/(k^2+l^2)\ A \exp[i(kx+ly-\omega t)]$$

and $b_x = -iB_0 kl/[\omega(k^2+l^2)]\ A \exp[i(kx+ly-\omega t)]$

Therefore $F'_x = \frac{1}{2}\rho\omega A^2 l^2/(k(k^2+l^2)^2) - \frac{1}{2}\frac{B_0^2}{\mu}\frac{l^2 k}{\omega(k^2+l^2)^2}A^2$ ...(II.20)

and $F'_y = -\frac{1}{2}\rho\omega A^2 \frac{l}{(k^2+l^2)^2} + \frac{1}{2}\frac{B_0^2}{\mu}\frac{lk^2}{\omega(k^2+l^2)^2}$ ...(II.21)

which by the help of dispersion relation (2.66) can be further simplified to

$$F'_x = (-A^2\rho\beta/2)\ l^2/(k^2+l^2)^3 \qquad ...(II.22)$$

and $F'_y = (A^2\rho\beta/2)\ kl/(k^2+l^2)^3$ ...(II.23)

Thus $F''_x = F_x - F'_x = \{A/(K^2+l^2)\}^2\rho/4\ [2V_a^2 k(k^2+l^2)/\omega + \beta]$

$$= a^2\rho/4\ [(2V_a^2/\omega)(k^2+l^2)/ + \beta] \qquad ...(II.24)$$

where a is the amplitude of the stream function associated with the wave and

$$F''_y = 0$$

Now if we were dealing with an inertial mode, for all frequencies $\omega >> (V_a^2/\beta)\ k(k^2+l^2)$ and thus the first term in (II. 24) is negligible. ie.

$$\bar{F}'' = (\beta A^2\rho/4,\ 0)$$

which is equivalent to the expression obtained by Longuet-Higgins (1964). Instead if we were dealing with the flux of a magnetic mode, for small frequencies

$$\omega = V_a^2/\beta \ [k(k^2+l^2)] \qquad \ldots(II.27)$$

so that $\bar{F}'' = (3\beta a^2 \mathcal{f}/4, \ 0)$ $\qquad \ldots(II.28)$

(II.26) and (II.27) can be combined in a single equation as

$$\bar{F}'' = \bar{F} - \bar{F}' = \mathcal{f} a^2 c/4 \ (\partial/\partial y, \ -\partial/\partial x) f \qquad \ldots(II.29)$$

where c = 1 for Rossby waves or inertial modes

= 3 for magnetic mode.

So, we have shown that atleast for small frequency waves the two flux vectors $\bar{F}$ and $\bar{F}'$ are equivalent and differ only by the curl of a function A defined by

$$A = \mathcal{f} f a^2 c/4.$$

Such a function is generally regarded as a stream-function for the difference of energy fluxes.

Another point that emerges from this analysis is that the flux vector $\bar{F}'$ as defined by (II.13) is valid for magnetic modes for small frequencies only. At higher frequencies relation (II.27) is clearly not applicable and the difference $\bar{F} - \bar{F}'$ will be a function of V_a, k and l and will certainly be divergent. This point is understandable, as we neglect higher order terms in $\bar{b}$ and $\bar{u}$ in the derivation of $\bar{F}'$ from the first principles.

Which of the two flux vectors is more appropriate in the study of reflections of these waves is clear from (II.29). If the amplitude a of the reflected wave r is different from that of the incident wave i, the differences $\bar{F}''_i$ and $\bar{F}''_r$ will not be equal

because of the ambiguity in the definition of $\bar{F}'$. $\bar{F}$, on the other hand correctly predicts the conservation of energy flux in reflection of these waves from rigid insulating or perfectly conducting boundaries.

APPENDIX III

THE EXPANDED FORM OF BOUNDARY CONDITIONS EMPLOYED IN CHAPTER 5

It is a common practice in fluid dynamics to seek plane wave solutions for one of the variables (u,v,w,b_x etc.) associated with a wave and express the rest of the variables in its terms. In our work we choose w, the vertical component of the fluid velocity for this purpose and the incident wave can then be represented by

$$w_1 = A_1 \exp[i(\bar{K}_1.\bar{X} - \omega t)] \qquad ...(III.1)$$

where A_1 is assumed to be real, as the choice of the origin of the time scale is at our disposal.

A reflection will produce three waves (out of which atleast one will be a travelling wave) whose vertical fluid velocities can be written as

$$w_2 = (A_{2R} + iA_{2I}) \exp[i(\bar{K}_2.\bar{X} - \omega t)] \qquad ...(III.2)$$

$$w_3 = (A_{3R} + iA_{3I}) \exp[i(\bar{K}_3.\bar{X} - \omega t)] \qquad ...(III.3)$$

$$w_4 = (A_{4R} + iA_{4I}) \exp[i(\bar{K}_4.\bar{X} - \omega t)] \qquad ...(III.4)$$

where A_{jR} and A_{jI} are the real and imaginary parts of the wave amplitude of a wave j. Then the other variables associated with any of these waves can be written in terms of w_j as (see equations 5.6 to 5.10)

$$u_j = \frac{-(k_j^2-\omega^2)\, m_j k_j + 2i l_j m_j \omega}{(k_j^2-\omega^2)(k_j^2+l_j^2)} W_j \qquad \ldots(III.5)$$

$$v_j = \frac{-(k_j^2-\omega^2) m_j l_j - 2i k_j m_j \omega}{(k_j^2-\omega^2)(k_j^2+l_j^2)} W_j \qquad \ldots(III.6)$$

$$b_{xj} = \frac{(k_j^2-\omega^2) m_j k_j - 2i l_j m_j \omega}{\omega (k_j^2-\omega^2)(k_j^2+l_j^2)} k_j W_j \qquad \ldots(III.7)$$

$$b_{yj} = \frac{(k_j^2-\omega^2) m_j l_j + 2i k_j m_j \omega}{\omega (k_j^2-\omega^2)(k_j^2+l_j^2)} k_j W_j \qquad \ldots(III.8)$$

and

$$b_{zj} = -k_j/\omega \; W_j \qquad \ldots(III.9)$$

When we substitute for variables u_j, v_j and w_j in the boundary condition (5.13) [specifying that the normal component of the velocity should vanish], its real and imaginary parts can be written in their full form as

$$\sum_{j=1}^{4}\left[\left[\frac{-m_j k_j}{k_j^2+l_j^2} n_x - \frac{m_j l_j}{k_j^2+l_j^2} n_y + n_z\right] A_{jR}\right] + \sum_{j=1}^{4}\left[\left[\frac{-2 l_j m_j \omega}{(k_j^2-\omega^2)(k_j^2+l_j^2)} n_x + \frac{2 k_j m_j \omega}{(k_j^2-\omega^2)(k_j^2+l_j^2)} n_y\right] A_{jI}\right] = 0 \qquad \ldots(III.10)$$

and

$$i\sum_{j=1}^{4}\left[\left(\frac{2l_j m_j \omega}{(k_j^2-\omega^2)(k_j^2+\omega^2)} n_x - \frac{2k_j m_j \omega}{(k_j^2-\omega^2)(k_j^2+l_j^2)} n_y\right) A_{jR}\right]$$

$$+ i\sum_{j=1}^{4}\left[\left(\frac{-m_j k_j}{k_j^2+l_j^2} n_x - \frac{m_j l_j}{k_j^2+l_j^2} n_y + \lambda n_z\right) A_{jI}\right] = 0 \qquad \ldots(III.11)$$

where $\lambda = 0$ for $j=1$ and

$= 1$ for $j=2,3,4$

and $\hat{n} = (n_x, n_y, n_z)$ is a unit vector in the direction of the normal to the boundary. For a conducting rigid boundary the second boundary condition is (see 5.33)

$$\bar{b}_1.\hat{n} + \bar{b}_2.\hat{n} + \bar{b}_3.\hat{n} + \bar{b}_4.\hat{n} = 0 \qquad \ldots(III.12)$$

which by the help of (III.5) to (III.9) can be split into its real and imaginary parts as

$$\sum_{j=1}^{4}\left[\left(\frac{-m_j k_j}{k_j^2+l_j^2} n_x - \frac{m_j l_j}{k_j^2+l_j^2} n_y + n_z\right) k_j A_{jR}\right] +$$

$$\sum_{j=1}^{4}\left[\left(\frac{-2l_j m_j \omega}{(k_j^2-\omega^2)(k_j^2+l_j^2)} n_x + \frac{2k_j m_j \omega}{(k_j^2-\omega^2)(k_j^2+l_j^2)} n_y\right) k_j A_{jI}\right] = 0 \qquad \ldots(III.13)$$

and

$$i\sum_{j=1}^{4}\left[\left(\frac{2l_j m_j \omega}{(k_j^2-\omega^2)(k_j^2+l_j^2)} n_x - \frac{2k_j m_j \omega}{(k_j^2-\omega^2)(k_j^2+l_j^2)} n_y\right) k_j A_{jR}\right]$$

$$+ i\sum_{j=1}^{4}\left[\left(\frac{-m_j k_j}{k_j^2+l_j^2} n_x - \frac{m_j l_j}{k_j^2+l_j^2} n_y + \lambda n_z\right) k_j A_{jI}\right] \qquad \ldots(III.14)$$

Similarly if $\hat{t}(t_x,t_y,t_z)$ represents a unit vector in the plane of the boundary, the boundary condition (5.35) on the tangential component of the fluid velocity can be rewritten as

$$\bar{u}_1.\hat{t} + \bar{u}_2\hat{t} + \bar{u}_3.\hat{t} + \bar{u}_4.\hat{t} = 0 \qquad \ldots(III.15)$$

Substitute for u,v and w from (III.1) to (III.6) to obtain

$$\sum_{j=1}^{4}\left[\left(\frac{-m_j k_j}{k_j^2+l_j^2}t_x - \frac{m_j l_j}{k_j^2+l_j^2}t_y + t_z\right)A_{jR}\right] +$$

$$\sum_{j=1}^{4}\left[\left(\frac{-2 l_j m_j \omega}{(k_j^2-\omega^2)(k_j^2+l_j^2)}t_x + \frac{2 k_j m_j \omega}{(k_j^2-\omega^2)(k_j^2+l_j^2)}t_y\right)A_{jI}\right] = 0$$

$$\ldots(III.16)$$

$$i\sum_{j=1}^{4}\left[\left(\frac{2 l_j m_j \omega}{(k_j^2-\omega^2)(k_j^2+l_j^2)}t_x - \frac{-2 k_j m_j \omega}{(k_j^2-\omega^2)(k_j^2+l_j^2)}t_y\right)A_{jR}\right]$$

$$+ i\sum_{j=1}^{4}\left[\left(\frac{-m_j k_j}{k_j^2+l_j^2}t_x - \frac{m_j l_j}{k_j^2+l_j^2}t_y + \lambda t_z\right)\right] = 0$$

$$\ldots(III.17)$$

In the case of an insulating rigid boundary, the second boundary condition is given by [see equation (5.43)]

$$(K_{t2}\hat{t}_1 - K_{t2}\hat{t}_2).[k_1\bar{u}_1 + k_2\bar{u}_2 + k_3\bar{u}_3 + k_4\bar{u}_4] = 0 \quad \ldots(III.18)$$

where $\hat{t}_1$ and $\hat{t}_2$ are two unit vectors in any two orthogonal directions in the plane of the boundary and K_{t1} and K_{t2} are the wavenumbers in those directions. If we denote the components of

the quantity in the first square brackets in (III.18) by P_x, P_y and P_z, by the help of above equations, it can be separated in its real and imaginary parts as

$$\sum_{j=1}^{4}\left[\left(\frac{-m_j k_j}{k_j^2+l_j^2}P_x - \frac{m_j l_j}{k_j^2+l_j^2}P_y + P_z\right)A_{jR}\right] = 0 \qquad \cdots(III.19)$$

$$\text{and } i\sum_{j=1}^{4}\left[\left(\frac{2 l_j m_j \omega}{(k_j^2-\omega^2)(k_j^2+l_j^2)}P_x - \frac{2 k_j m_j \omega}{(k_j^2-\omega^2)(k_j^2+l_j^2)}P_y\right)A_{jR}\right]$$

$$+\sum_{j=1}^{4}\left[\left(\frac{-m_j k_j}{k_j^2+l_j^2}P_x - \frac{m_j l_j}{k_j^2+l_j^2}P_y + \lambda P_z\right)A_{jI}\right] = 0 \qquad \cdots(III.20)$$

The final boundary condition for an insulating boundary is given by (5.44) and can be expanded to

$$\sum_{j=1}^{4}\Big[\Big[\left(\frac{-m_j l_j}{k_j^2+l_j^2}t_{1x} - \frac{-m_j l_j}{k_j^2+l_j^2}t_{1y} + t_{1z}\right)|k_t|$$

$$-\left(\frac{2 l_j m_j \omega}{(k_j^2-\omega^2)(k_j^2+l_j^2)}n_x - \frac{2 k_j m_j \omega}{(k_j^2-\omega^2)(k_j^2+l_j^2)}n_y\right)k_{t1}\Big]A_{jR}\Big]$$

$$+\sum\Big[\Big[\left(\frac{-2 l_j m_j \omega}{(k_j^2-\omega^2)(k_j^2+l_j^2)}t_{1x} + \frac{2 k_j m_j \omega}{(k_j^2-\omega^2)(k_j^2+l_j^2)}t_{1y}\right)|k_t|$$

$$-\left(\frac{-m_j k_j}{k_j^2+l_j^2}n_x - \frac{m_j l_j}{k_j^2+l_j^2}n_y + \lambda n_z\right)k_{t1}\Big]\Big] = 0 \qquad \cdots(III.21)$$

$$i\sum_{j=1}^{4}\Big[\Big[\left(\frac{2 l_j m_j \omega}{(k_j^2-\omega^2)(k_j^2+l_j^2)}t_{1x} - \frac{2 k_j m_j \omega}{(k_j^2-\omega^2)(k_j^2+l_j^2)}t_{1y}\right)|k_t|$$

$$+\left(\frac{-m_j k_j}{k_j^2+l_j^2}n_x - \frac{m_j l_j}{k_j^2+l_j^2}n_y + n_z\right)k_{t1}\Big]A_{jR}\Big]$$

$$+\sum_{j=1}^{4}\Big[\Big[\left(\frac{-m_j k_j}{k_j^2+l_j^2}t_{1x} - \frac{m_j l_j}{k_j^2+l_j^2}t_{1y} + \lambda t_{1z}\right)|k_t|$$

$$+\left(\frac{-2 l_j m_j \omega}{(k_j^2-\omega^2)(k_j^2+l_j^2)}n_x + \frac{2 k_j m_j \omega}{(k_j^2-\omega^2)(k_j^2+l_j^2)}n_y\right)k_{t1}\Big]A_{jI}\Big] = 0 \cdots(III.22)$$

When one of the roots of equation (5.19) [say K_{n2}] becomes complex, it marks the presence of a non propagating wave at the boundary. In this case k_2,m_2 and l_2 will also have imaginary parts with the consequence that equations (III.10) to (III.22) will no longer be either purely real or imaginary. For this special case, the two parts of each boundary conditions are added (through complex additon) and then split again into their real and imaginary parts.

APPENDIX IV

LIST OF SYMBOLS

Unless specifically mentioned, the symbols used and the quantities they represent in this thesis are as follows.

a	the x component of the fluid displacement
A	amplitude of a wave
b	the y component of the fluid displacement
$\bar{B}(B_x,B_y,B_z)$	ambient magnetic field
$\bar{b}(b_x,b_y,b_z)$	perturbation magnetic field
$\bar{C}$	the velocity of light
$\bar{C}_g(C_{gx},C_{gy},C_{gz})$	group velocity
C_p	specific heat at constant pressure
$\bar{C}_p$	phase velocity
$\bar{C}_s$	the velocity of sound
C_v	specific heat at constant volume
$\bar{D}$	electric displacement vector
E	energy density
$\bar{E}$	electric field
f	coriolis parameter
$\bar{f}$	buoyancy forces
$\bar{F}(F_x,F_y,F_z)$	energy flux vector
$\bar{g}$	acceleration due to gravity
I	imaginary part
$\bar{J}$	current density vector
$\bar{K}(k,l,m)$	wave vector
$\bar{K}_n$	component of $\bar{K}$ normal to the boundary

$\bar{K}_t(K_{tx}, K_{ty}, K_{tz})$	component of $\bar{K}$ parallel to the boundary
k_s, l_s	stationary wavenumber components
$\bar{n}$	normal vector
$\hat{n}$	unit normal vector
n_θ	angle between normal to the boundary and z axis
n_ϕ	angle between normal to the boundary and x axis
$\bar{N}$	Brunt-Väisälä frequency
p	fluid pressure
$\bar{r}$, $\bar{R}$	position vectors
R	real part
t	time
T	temperature
$\bar{U}(U, V, W)$	ambient fluid velocity
$\bar{u}(u, v, w)$	perturbation fluid velocity
$\bar{V}_a$	Alfven velocity
$\bar{X}(x,y,z)$	position vector in cartesian coordinates
α	angle of incidence or reflection
β	rate of change of coriolis parameter with latitude
γ	C_p/C_v
Λ	Lagrangian invariant
ϵ	dielectric constant of the medium, phase of a wave
η	magnetic diffusivity
θ	polar coordinate, angle between $\bar{B}_0$ and x axis, angle between $\bar{K}$ and $\bar{B}_0$
μ	permeability of free space
ν	kinematic viscosity
ρ	density of fluid

ρ_o	average density of fluid
σ	electrical conductivity
ϕ	longitudinal coordinate, electric charge density, angle between $\bar{K}$ and $\bar{\Omega}$, scalar potential field
ψ	stream function
ω	angular frequency
$\bar{\Omega}$	angular velocity
ζ	local vorticity

In addition, subscripts '0' and '1' denote respectively the ambient and perturbation-associated values of a variable. < > denotes average over a period, or jump across the boundary layer.

REFERENCES

Acheson, D.J. 1971, The Magnetohydrodynamics of Rotating Fluids. Ph. D. thesis. Univ. of East Anglia.

---------- 1972a, The critical level for hydromagnetic waves in a rotating fluid. J. Fluid Mech. 53, 401-415.

---------- 1972b, On the hydromagnetic stability of a rotating fluid annulus. J. Fluid Mech. 52, Part 3 pp. 529-541.

---------- 1973, Hydromagnetic wavelike instabilities in a rapidly rotating stratified fluid. J. Fluid Mech.61, 609-624.

---------- 1976, On over reflection. J. Fluid Mech. 77, 433-472.

---------- 1978, Magnetohydrodynamic waves and instabilities in rotating fluids. In, Rotating Fluids in Geophysics, Ed. Roberts, P.H. and Soward, A.M. Academic Press. London pp. 315-349.

Acheson, D.J. and Hide, R. 1973, Hydromagnetics of rotating fluids. Rep. Prog. Phys. 36, 159-221.

Aldridge, K.D. and Toomre, A. 1969, Axis-symmetric inertial oscillations of a fluid in a rotating spherical container. J. Fluid Mech. 37, 307-323.

Alfven, H. 1942, On the existence of electromagnetic-hydromagnetic waves. Arkiv. f. Mat. 29b, 1-7.

Alfven, H. and Falthammar, C.G. 1963, Cosmical Electrodynamics. Oxford University Press, London 228 pp.

Andrews, D.G. and McIntyre, M.E. 1978, On wave action and its relatives. J. Fluid Mech. 89, 647-664.

Backus, G.E. 1958, A class of self-sustaining dissipative spherical dynamos. Ann. Phys., 4, 372-447.

Baines, P.G. 1971a, The reflexion of internal/inertial waves from bumpy surfaces. J. Fluid Mech. 46, 273-291.

---------- 1971b, The reflexion of internal/inertial waves from bumpy surfaces. Part 2. Split reflexion and diffraction. J. Fluid Mech., 49, 113-131.

---------- 1976, The stability of planetary waves on a sphere. J. Fluid Mech. 73, 193-213.

Barraclough, D.R. 1978, Spherical harmonic models of the geomagnetic field. Geomagnetic Bulletin 8. Instt. of Geol. Sci. NERC, England, 66 pp.

Batchelor, G.K. 1967, An introduction to Fluid Dynamics. Cambridge University Press, 615 pp.

Bland, J.A. 1976, Rotating Hydromagnetic Wave Interactions. Ph.D thesis. Univ. of East Anglia.

Booker J.R. and Bretherton, F.P. 1967, The critical layer for internal gravity waves in a shear flow. J. Fluid Mech. 27, 513-539.

Bott, M.H.P. 1982, The Interior of the Earth. Edward Arnold, London. 403 pp.

Braginsky, S.I. 1967, Magnetic waves in the earth's core. Geomag. Aeronomy 7, 851-859.

Bretherton, F.P. 1966, The propagation of groups of internal gravity waves in a shear flow. Quart. J. Roy. Met. Soc. 92 466-480.

Bullard, E.C. 1949, The magnetic field within the earth. Proc. Roy. Soc. A197, 433-453.

Bullard, E.C., Freedman C., Gellman H., and Nixon J. 1950, The westward drift of the earth's magnetic field. Proc. R. Soc. Lond. A243, 67-92.

Bullard, E.C., and Gellman, H. 1954, Homogeneous dynamos and terrestrial magnetism. Phil. Trans. R. Soc.,A247, 213-278.

Cain, J.C., Hendricks, S.H., Langel, R.A., and Hudson, W.V. 1967, A proposed model for the international geomagnetic reference field. 1965. J. Geomag. Geolect. 19, 335-355.

Chandrasekhar, S. 1961, Hydrodynamic and Hydromagnetic Stability. Oxford University Press. London. pp.652.

Coaker, S.A. 1977, The stability of a Rossby wave. Geophys. Astrophys. Fluid Dynamics. 9, 1-17.

Cowling, T.G. 1976, Magnetohydrodynamics. Adam-Hilger, London. 136 pp.

Dillon, R. 1975, On the Correlation between the Earth's Gravitational and Magnetic Fields. PhD thesis. Univ. of Cambridge.

El Mekki, P., Eltayeb, I.A., and McKenzie, J.F. 1978, Hydromagnetic-gravity wave critical levels in the solar atmosphere. Solar Physics. 57, 261-266.

El Sawi, M., and Eltayeb, I.A. 1978, On the propagation of hydromagnetic inertial gravity waves in magnetic-velocity shear. Geophys. Astrophys. Fluid Dynamics. 10, 289-309.

---------- 1981, Wave action and critical surfaces for hydromagnetic-inertial gravity waves. Quart. J. Mech. Appl. Math. 34, 187-202.

Eltayeb, I.A. 1977, On linear wave motions in magnetic-velocity shears. Phil. Trans. 285, 607-636.

Eltayeb, I.A., and McKenzie, J.F. 1977, Propagation of hydromagnetic planetary waves on a beta-plane through magnetic and velocity shear. J. Fluid Mech. 81, 1-23.

Fejer, J.A. 1963, Hydromagnetic reflection and refraction at a fluid velocity discontinuity. The Physics of Fluid. 6, 508-512.

Ferraro, V.C.A. 1954, On the reflection and refraction of Alfven waves. Astrophys. J. 119, 393-406.

Ferraro, V.C.A. and Plumpton, C. 1961, Magneto-Fluid Mechanics. Oxford University Press. London. 181 pp.

Gill, A.E. 1974, The stability of planetary waves on an infinite beta-plane. Geophys. Fluid Dynamics. 6, 29-47.

Gradshteyn, I.S. and Ryzhik, I.M. 1965, Tables of integrals, series and transforms. Academic Press. New York.

Greenspan, H.P. 1968, The Theory of Rotating Fluids. Cambridge Univ. Press. 327 pp.

Grimshaw, R. 1980, A general theory of critical level absorption and valve effects for linear wave propagation. Geophys. Astrophys. Fluid Dynamics. 14, 303-326.

Hasselmann, K. 1967, A criterion for non-linear wave stability. J. Fluid Mech. 30, 737-739.

Herlofson, N., 1950, Magneto-hydrodynamic waves in a compressible fluid conductor. Nature, 165, 1020-1021.

Herzenberg, A. 1958, Geomagnetic dynamos. Phil. Trans. Roy. Soc. Lond. A250, 543-583.

Hide, R. 1966, Free hydromagnetic oscillations of the Earth's core and the theory of the geomagnetism secular variation. Phil. Trans. of Roy. Soc. A 259, 615-647.

Hide, R. 1969a, On hydromagnetic waves in a stratified rotating incompressible fluid. J. Fluid Mech. 39, 283-287.

Hide, R. 1969b, Dynamics of the atmospheres of the major planets with an appendix on the viscous boundary layer at the rigid bounding surface of an electrically-conducting rotating fluid in the presence of a magnetic field. J. Atmos. Sci. 26, 841-853.

-------- 1970, On the earth's core-mantle interface. Quart. J. Roy Met. Soc. 96, 579-590.

-------- 1977, Dynamics of rotating fluids. Quart. J. Roy. Met. Soc. 103, 1,28.

-------- 1983a, The magnetic analogue of Ertel's potential vorticity theorem. Ann. Geophys. 1, 59-60.

-------- 1983b, On the analogy between the dynamics and electrodynamics of a moving fluid. Preprint of a paper. pp. 1-20.

-------- 1984, Potential magnetic field invariants as Lagrangian tracers for infinite magnetic Reynold number flows. Preprint of a paper. pp.1-19.

Hide, R. and Jones, M.V. 1972, Hydromagnetic waves on a beta-plane: A numerical study of the dispersion relationship. Scientific paper No. 33, Meteorological Office. London.

Hide, R. and Roberts P.H. 1960, Hydromagnetic flow due to an oscillating plane. Rev. Mod. Phys. 32, 799-806.

Hilderbrand, F.B. 1974, Introduction to numerical-analysis. 2nd Edition. Mc-Graw Hill Book Company. New York.

Hoskins B.J. 1973, The stability of Rossby-Haurwitz wave. Quart. J. Roy. Met. Soc. 99, 723-745.

Hurley, D.G. 1970, Internal waves in a wedge-shaped region. J. Fluid Mech., 43, 97-120.

Ibbetson, A., and Philips, N.A. 1967, Some laboratory experiments on Rossby waves with application to the ocean. Tellus, 19, 81-88.

Jacobs, J.A. 1963, The Earth's Core and Geomagnetism. Pergamon Press. Oxford. 138 pp.

Jeffreys, H. and Jeffreys, B.S. 1956, Methods of Mathematical Physics. 3rd. edition. Cambridge Univ. Press. Cambridge. 718 pp.

Kelvin, Lord (W. Thomson) 1877, On the precessional motion of a liquid. Nature, 15, 297-298.

Kudlick, M.D. 1966, On Transient Motions in a Contained Rotating Fluid. PhD thesis. Maths. Dept. M.I.T.

Lehnert, B. 1954a, Magnetohydrodynamic waves under the action of the coriolis force - I. Astrophys. J. 119, 647-654.

Lehnert, B. 1954b, Magneto-hydrodynamic waves in liquid sodium. Phys. Rev. 94, 815-824.

Lighthill, M.J. 1960, Studies on Magneto-hydrodynamic waves and other anisotropic wave motions. Phil. Trans. R. Soc. 252, 397-430.

---------- 1965, Group velocity, J. Inst. Maths. Applic. 1, 1-28.

---------- 1978, Waves in Fluids. Cambridge Univ. Press. Cambridge. 504 pp.

Longuet-Higgins, M.S. 1964a, Planetary waves on a rotating sphere. Proc. R. Soc. A279, 446-473.

---------- 1964b, On group velocity and energy flux in planetary wave motions. Deep Sea Research.11, 35-42.

Longuet-Higgins, M.S. and Gill A.E. 1967, Resonant interactions between planetary waves. Proc. Roy. Soc. Lond. 299 120-140.

Lorenz, E.N. 1972, Barotropic instability of Rossby wave motion. J. Atmos. Sci. 29, 258-264.

Lundquist, S. 1949a, Experimental demonstration of magneto-hydrodynamic waves. Nature 164, 145-146.

---------- 1949b, Experimental investigations of magneto-hydrodynamic waves. Phys. Rev. 76, 1805-1809.

---------- 1952, Studies in magneto-hydrodynamics. Ark. f. fys. 5, 297-347.

Malkus, W.V.R. 1967, Hydromagnetic planetary waves. J. Fluid Mech. 28 793-802.

McKenzie, J.F. 1972, Reflection and amplification of acoustic-gravity waves at a density and velocity discontinuity. J. Geophys. Res. 77, 2915-2926.

Moffat, H.K. 1970, Dynamo action associated with random inertial waves in a rotating conducting fluid. J. Fluid Mech. 44, 705-719.

Negi, J.G., Singh, R.N. 1974, A similarity solution of Hide's magnetic wave equation. Geophys. J. Roy. Astr. Soc. 39, 407-409.

Nigam, S.D. and Nigam, P.D. 1962, Wave propagation in rotating liquids. Proc. Roy. Soc. London. 266A, 247-256.

Officer, C.B. 1974, Introduction to Theoretical Geophysics, Springer Verlag. Berlin. 385 pp.

Pedlosky, J. 1971, Geophysical fluid dynamics. In, Mathematical Problems in the Geophysical Sciences. Ed., W.H. Reid. Amer. Math. Soc. pp 1-66.

---------- 1979, Geophysical Fluid Dynamics. Springer Verlag. New York. 624 pp.

Phillips, O.M. 1960, Centrifugal waves. J. Fluid Mech., 7, 340-352.

---------- 1963, Energy transfer in rotating fluids by reflection of inertial waves. Phys. Fluids, 6, 513-20.

Pilant, W.L. 1979, Elastic waves in the Earth. In, Developments in Solid Earth Geophysics. Elsevier. Amsterdam. 493 pp.

Poincare, H. 1910, Sur la precession des corps deformables. Bulletin Astronomique, 27, 321-56.

Roberts, P.H. 1954, Some Applications of Electromagnetic Theory to the Problem of the Main Geomagnetic Field. PhD Thesis. University of Cambridge.

---------- 1967. An Introduction to Magnetohydrodynamics. Longmans. London. 264 pp.

Roberts, P.H. and Soward, A.M. 1972, Magnetohydrodynamics of the earth's core. Annual Review of Fluid Mech. 4, 117-54.

Rossby, C.G. et al, 1939, Relation between variations in the intensity of the zonal circulation of the atmosphere and the displacement of the semi-permanent centres of action. J. Mar. Res.2, 38-55.

Rudraiah, N. and Venkatachalappa, M. 1972, Propagation of internal gravity waves in perfectly conducting fluids with shear flow, rotation and transverse magnetic field. J. Fluid Mech. 52, 193-206.

Shercliff, J.A. 1965, A Textbook of Magnetohydrodynamics. Pergamon Press. Oxford. 265 pp.

Simon, R. 1958, On the reflection and refraction of hydromagnetic waves at the boundary of two compressible gaseous media. Astrophys. J. 128, 392-397.

Soward, A.M. and Roberts, P.H. 1976, Recent developments in dynamo theory. Magnitnaya Gidrodinamika 1, 3-51.

Stewartson, K. 1956, Motion of a sphere through a conducting fluid in the presence of a strong magnetic field. Proc. Camb. Phil. Soc.52, 301-316.

---------- 1957, The dispersion of a current on the surface of a highly conducting fluid. Proc. Camb. Phil. Soc. 53, 774-775.

---------- 1959, On the stability of a spinning top containing liquid. J. Fluid Mech., 5, 577-592.

---------- 1960, On the motion of a non-conducting body through a perfectly conducting fluid. J. Fluid Mech. 8, 82-96.

---------- 1967, Slow oscillations of fluid in a rotating cavity in the presence of a toroidal magnetic field. Proc. Roy. Soc. Lond. Ser. 299A, 173-187.

---------- 1978, Waves in rotating fluids. In, Rotating Fluids in Geophysics, Ed. P.H. Roberts and A.M. Soward. Academic Press. London. pp. 67-103.

Suffolk, G. and Allan, D.W. 1969, Planetary magnetohydrodynamic waves as a perturbation of dynamo solutions. In, The Application of Modern Physics to the Earth and Planetary Interiors. Ed. S. K. Rurncorn. Wiley Intersciences. London. pp. 653-656.

Vestine, E.M., Laporte, L., Cooper, C., Lange, I. and Hendrix, W.C. 1947, Description of the Earth's main magnetic field and its secular change, 1905-1945. Carnegie. Inst. Wash,. Publ. No.578.

Walen, C. 1944, On the theory of sunspots. Ark. f. mat. astr. o. fys. 30A, No.15.

--------- 1946, On the distribution of the solar general magnetic field. Ark. f. mat. astr. o. fys. 33A, No.18.

Whitham, G.B. 1960 A note on group velocity. J Fluid Mech. 9, 347-352.

---------- 1965. A general approach to linear and non-linear waves using a Lagrangian, J. Fluid Mech. 22, 273-283.

Whitham, G.B. 1974. Linear and Non-Linear Waves. John Wiley and Sons. New York. 636 pp.

Williams, W.E. 1960, Reflection and refraction of hydromagnetic waves at the boundary of two compressible media. Astrophys. J. 131, 438-441.

Wood, W.W. 1977, A note on the westward drift of the earth's magnetic field. J. Fluid Mech. 82, 389-400.